國立中央大學天文研究所
鹿林天文台年報

2023

No.21

國立中央大學天文研究所 編

Contents

I
SCI 期刊論文

歷年 SCI 期刊論文統計 (2003-2023)

鹿林天文台於 1999 年建立第一個天文台 (SLT)，建台初期無水無電、沒有人員常駐、望遠鏡等研究設施尚未完善、觀測研究工作進行困難。2002 年天文台控制中心落成、一米望遠鏡 (LOT) 開光、水電等基礎設施完成、人員開始常駐，觀測研究工作正式上軌道，2003 年 LOT 望遠鏡開放申請，此後每年都有鹿林天文台相關 SCI 期刊論文產出。自 2003 年至 2023 年底共計 232 篇，按「年別」及「期刊別」分別統計如下:

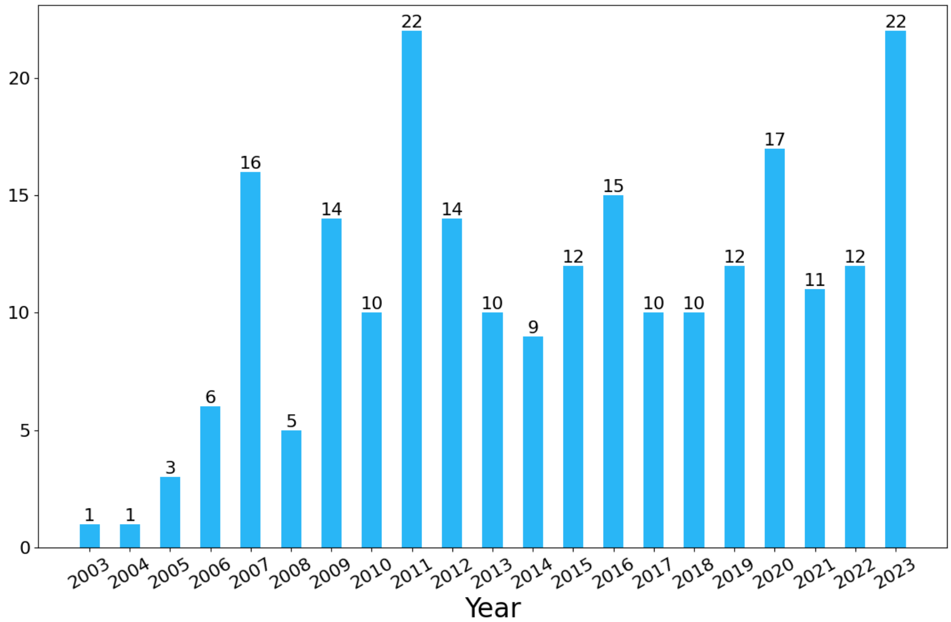

Figure 1: 鹿林天文台相關 SCI 期刊論文統計 (2003-2023) - 按年別

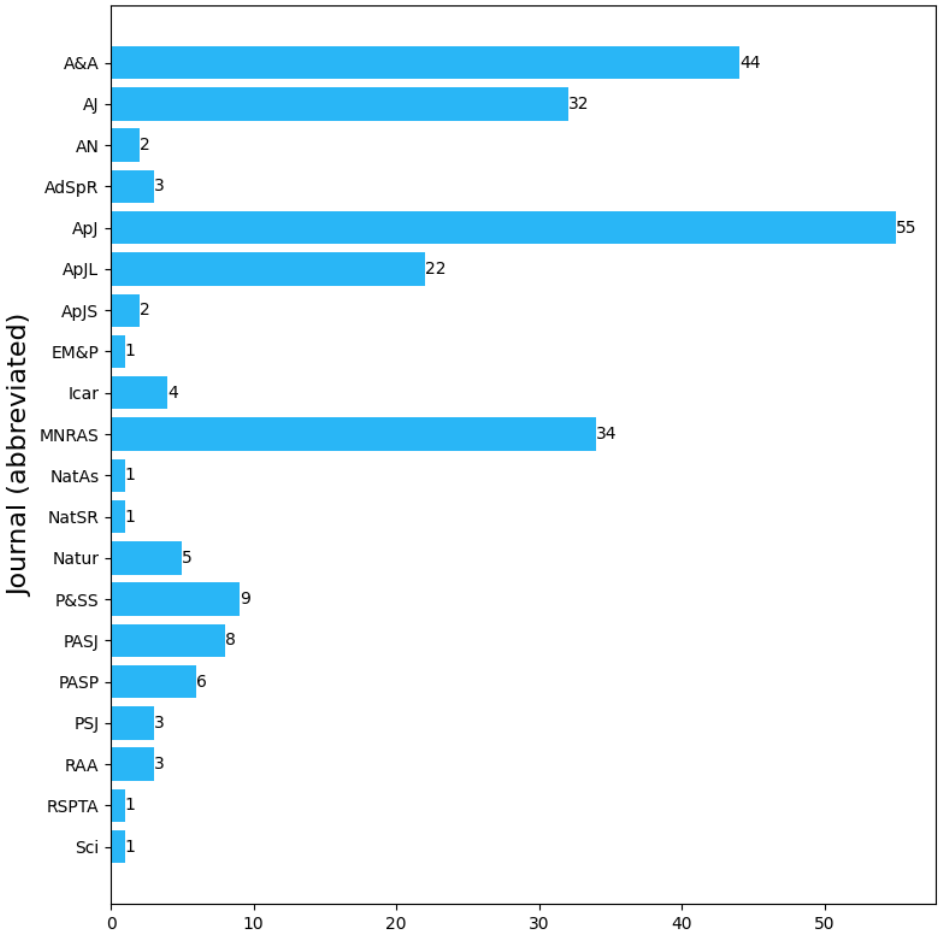

Figure 2: 鹿林天文台相關 SCI 期刊論文統計 (2003-2023) - 按期刊別

Table 1: 期刊全名、簡稱對照表

A&A : Astronomy and Astrophysics
AJ : The Astronomical Journal
AN : Astronomische Nachrichten
AdSpR : Advances in Space Research
ApJ : The Astrophysical Journal
ApJL : The Astrophysical Journal Letters
ApJS : The Astrophysical Journal Supplement Series
EM&P : Earth, Moon, and Planets
Icar : Icarus
MNRAS : Monthly Notices of the Royal Astronomical Society
NatAs : Nature Astronomy
NatSR : Nature Scientific Reports
Natur : Nature
P&SS : Planetary and Space Science
PASJ : Publications of the Astronomical Society of Japan
PASP : Publications of the Astronomical Society of the Pacific
PSJ : The Planetary Science Journal
RAA : Research in Astronomy and Astrophysics
RSPTA : Philosophical Transactions of the Royal Society A
Sci : Science

A&A 672, A70 (2023)
https://doi.org/10.1051/0004-6361/202245440

Astronomy & Astrophysics

A super-Earth and a mini-Neptune near the 2:1 MMR straddling the radius valley around the nearby mid-M dwarf TOI-2096

F. J. Pozuelos[1,2,3], M. Timmermans[1], B. V. Rackham[15,7,⋆], L. J. Garcia[1], A. J. Burgasser[11], S. R. Kane[14], M. N. Günther[28,⋆⋆], K. G. Stassun[17], V. Van Grootel[3], M. Dévora-Pajares[29], R. Luque[10,2], B. Edwards[6,8,⋆⋆⋆], P. Niraula[15], N. Schanche[26,23,22], R. D. Wells[26], E. Ducrot[6,⋆⋆⋆], S. Howell[21], D. Sebastian[24], K. Barkaoui[1,15,5], W. Waalkes[13], C. Cadieux[18], R. Doyon[18,19], R. P. Boyle[34], J. Dietrich[32], A. Burdanov[15], L. Delrez[1,3], B.-O. Demory[26], J. de Wit[15], G. Dransfield[24], M. Gillon[1], Y. Gómez Maqueo Chew[27], M. J. Hooton[4], E. Jehin[3], C. A. Murray[13,4], P. P. Pedersen[4], D. Queloz[4], S. J. Thompson[4], A. H. M. J. Triaud[24], S. Zúñiga-Fernández[1], K. A. Collins[25], M. M Fausnaugh[16], C. Hedges[22], K. M. Hesse[16], J. M. Jenkins[21], M. Kunimoto[16], D. W. Latham[25], A. Shporer[16], E. B. Ting[21], G. Torres[25], P. Amado[2], J. R. Rodón[2], C. Rodríguez-López[2], J.C. Suárez[29], R. Alonso[5,9], Z. Benkhaldoun[30], Z. K. Berta-Thompson[13], P. Chinchilla[1,5], M. Ghachoui[1,30], M. A. Gómez-Muñoz[27], R. Rebolo[5,9], L. Sabin[27], U. Schroffenegger[26], E. Furlan[20], C. Gnilka[21,20], K. Lester[21], N. Scott[31], C. Aganze[11], R. Gerasimov[11], C. Hsu[12], C. Theissen[11,⋆⋆⋆⋆], D. Apai[32,33], W. P. Chen[35], P. Gabor[34], T. Henning[36], and L. Mancini[37,36,38,39]

(Affiliations can be found after the references)

Received 11 November 2022 / Accepted 6 February 2023

ABSTRACT

Context. Several planetary formation models have been proposed to explain the observed abundance and variety of compositions of super-Earths and mini-Neptunes. In this context, multitransiting systems orbiting low-mass stars whose planets are close to the radius valley are benchmark systems, which help to elucidate which formation model dominates.

Aims. We report the discovery, validation, and initial characterization of one such system, TOI-2096 (TIC 142748283), a two-planet system composed of a super-Earth and a mini-Neptune hosted by a mid-type M dwarf located 48 pc away.

Methods. We characterized the host star by combining optical spectra, analyzing its broadband spectral energy distribution, and using evolutionary models for low-mass stars. Then, we derived the planetary properties by modeling the photometric data from TESS and ground-based facilities. In addition, we used archival data, high-resolution imaging, and statistical validation to support our planetary interpretation.

Results. We found that the stellar properties of TOI-2096 correspond to a dwarf star of spectral type M4±0.5. It harbors a super-Earth ($R = 1.24 \pm 0.07\ R_\oplus$) and a mini-Neptune ($R = 1.90 \pm 0.09\ R_\oplus$) in likely slightly eccentric orbits with orbital periods of 3.12 d and 6.39 d, respectively. These orbital periods are close to the first-order 2:1 mean-motion resonance (MMR), a configuration that may lead to measurable transit timing variations (TTVs). We computed the expected TTVs amplitude for each planet and found that they might be measurable with high-precision photometry delivering mid-transit times with accuracies of $\lesssim$2 min. Moreover, we conclude that measuring the planetary masses via radial velocities (RVs) could also be possible. Lastly, we found that these planets are among the best in their class to conduct atmospheric studies using the NIRSpec/Prism onboard the *James Webb* Space Telescope (JWST).

Conclusions. The properties of this system make it a suitable candidate for further studies, particularly for mass determination using RVs and/or TTVs, decreasing the scarcity of systems that can be used to test planetary formation models around low-mass stars.

Key words. techniques: photometric – stars: low-mass – planets and satellites: individual: TOI-2096

1. Introduction

The discovery of a large abundance of small transiting exoplanets with sizes ranging from slightly larger than the Earth to 4 $R_\oplus$ was one of the most relevant results of NASA's Kepler mission (Howard et al. 2012; Fressin et al. 2013). It is worth mentioning that the first exoplanet discovered with its size in this range was found by the CoRoT mission (Baglin et al. 2006), named CoRoT-7b (Léger et al. 2009), which was also the first small exoplanet with both measured radius and mass and, consequently, the first constraint on the bulk composition of a planet of this class (Queloz et al. 2009). With additional discoveries by K2 and TESS, these worlds have reached >3000 out of the >5000 confirmed planets that exist to date[1].

This category of planets has become the most abundant of the known planets in our Galaxy, seeming to exist around roughly 30–50% of all main-sequence stars (see, e.g., Raymond & Morbidelli 2022, and references therein). As these planets are not present in our Solar System, their abundance has challenged past planetary formation models (Ida & Lin 2004; Mordasini et al. 2009), and the mechanisms that form them are still hotly debated (Howard et al. 2010;

⋆ 51 Pegasi b Fellow.
⋆⋆ ESA Research Fellow.
⋆⋆⋆ Paris Region Fellow, Marie Sklodowska-Curie Action.
⋆⋆⋆⋆ NASA Sagan Fellow.

[1] Based on the NASA Exoplanet Archive in October 2022; https://exoplanetarchive.ipac.caltech.edu/

The Astronomical Journal, 165:149 (18pp), 2023 April https://doi.org/10.3847/1538-3881/acba0b

EDEN Survey: Small Transiting Planet Detection Limits and Constraints on the Occurrence Rates of Planets around Late-M Dwarfs within 15 pc

Jeremy Dietrich[1], Dániel Apai[1,2], Martin Schlecker[1,3], Kevin K. Hardegree-Ullman[1], Benjamin V. Rackham[4,5,16], Nicolas Kurtovic[3], Karan Molaverdikhani[3,6,7,8], Paul Gabor[9], Thomas Henning[3], Wen-Ping Chen[10], Luigi Mancini[3,11,12,13], Alex Bixel[1], Aidan Gibbs[14], Richard P. Boyle[9], Samantha Brown-Sevilla[3], Remo Burn[3], Timmy N. Delage[3], Lizxandra Flores-Rivera[3], Riccardo Franceschi[3], Gabriele Pichierri[3], Sofia Savvidou[3], Jonas Syed[3], Ivan Bruni[15], Wing-Huen Ip[10], Chow-Choong Ngeow[10], An-Li Tsai[10], Chia-Lung Lin[10], Wei-Jie Hou[10], Hsiang-Yao Hsiao[10], Chi-Sheng Lin[10], Hung-Chin Lin[10], and Ritvik Basant[1]
Project EDEN

[1] Steward Observatory and Department of Astronomy, The University of Arizona, Tucson, AZ 85721, USA; jdietrich1@arizona.edu
[2] Lunar and Planetary Laboratory and Department of Planetary Sciences, The University of Arizona, Tucson, AZ 85721, USA
[3] Max-Planck-Institut für Astronomie, Königstuhl 17, D-69117 Heidelberg, Germany
[4] Department of Physics and Kavli Institute for Astrophysics and Space Research, Massachusetts Institute of Technology, Cambridge, MA 02139, USA
[5] Department of Earth, Atmospheric and Planetary Science, Massachusetts Institute of Technology, 77 Massachusetts Avenue, Cambridge, MA 02139, USA
[6] Universitäts-Sternwarte, Ludwig-Maximilians-Universität München, Scheinerstrasse 1, D-81679 München, Germany
[7] Exzellenzcluster Origins, Boltzmannstrasse 2, D-85748 Garching, Germany
[8] Landessternwarte, Zentrum für Astronomie der Universität Heidelberg, Königstuhl 12, D-69117 Heidelberg, Germany
[9] Vatican Observatory, I-00120 Città del Vaticano, Italy
[10] Graduate Institute of Astronomy, National Central University, Zhongli, Taoyuan 32001, Taiwan
[11] Department of Physics, University of Rome "Tor Vergata", Via della Ricerca Scientifica 1, I-00133, Rome, Italy
[12] INAF–Turin Astrophysical Observatory, via Osservatorio 20, I-10025, Pino Torinese, Italy
[13] International Institute for Advanced Scientific Studies (IIASS), Via G. Pellegrino 19, I-84019, Vietri sul Mare (SA), Italy
[14] Department of Physics & Astronomy, University of California, Los Angeles, CA 90095, USA
[15] INAF–OAS, Osservatorio di Astrofisica e Scienza dello Spazio di Bologna, Via P. Gobetti 93/3, I-40129–Bologna, Italy
Received 2022 August 29; revised 2023 February 2; accepted 2023 February 6; published 2023 March 8

Abstract

Earth-sized exoplanets that transit nearby, late-spectral-type red dwarfs will be prime targets for atmospheric characterization in the coming decade. Such systems, however, are difficult to find via widefield transit surveys like Kepler or TESS. Consequently, the presence of such transiting planets is unexplored and the occurrence rates of short-period Earth-sized planets around late-M dwarfs remain poorly constrained. Here, we present the deepest photometric monitoring campaign of 22 nearby late-M dwarf stars, using data from over 500 nights on seven 1–2 m class telescopes. Our survey includes all known single quiescent northern late-M dwarfs within 15 pc. We use transit injection-and-recovery tests to quantify the completeness of our survey, successfully identify most (>80%) transiting short-period (0.5–1 days) super-Earths ($R > 1.9\,R_{\oplus}$), and are sensitive (∼50%) to transiting Earth-sized planets (1.0–1.2 $R_{\oplus}$). Our high sensitivity to transits with a near-zero false-positive rate demonstrates an efficient survey strategy. Our survey does not yield a transiting planet detection, yet it provides the most sensitive upper limits on transiting planets orbiting our target stars. Finally, we explore multiple hypotheses about the occurrence rates of short-period planets (from Earth-sized planets to giant planets) around late-M dwarfs. We show, for example, that giant planets with short periods (<1 day) are uncommon around our target stars. Our data set provides some insight into the occurrence rates of short-period planets around TRAPPIST-1-like stars, and our results can help test planetary formation and system evolution models, as well as guide future observations of nearby late-M dwarfs.

Unified Astronomy Thesaurus concepts: Exoplanets (498); Surveys (1671); Stellar photometry (1620); Ground-based astronomy (686)

1. Introduction

Due to their intrinsic faintness, the in-depth characterization (beyond transit spectroscopy) of Earth-sized exoplanets will remain, for the foreseeable future, limited to the closest of planets—those that are within approximately 15 pc (e.g., Apai et al. 2019; Quanz 2019; The LUVOIR Team 2019; Gaudi et al. 2020). Although there are about 1000 stars in that volume (Gaia Collaboration et al. 2021) and likely at least one planet per star (e.g., Hardegree-Ullman et al. 2019), as of 2022 July only 175 planets have been confirmed, mostly via radial velocity (RV) measurements.[17] Even in this small volume of the Milky Way surrounding us, a large fraction of planets remains undiscovered. Of the planets known, a rarely found type stands out: small planets ($R_p < 1.8\,R_{\oplus}$) transiting small host stars ($R_* < 0.4\,R_{\odot}$), which are ideal targets for transmission spectroscopic studies due to the deeper transits

[16] 51 Pegasi b Fellow.

[17] https://exoplanetarchive.ipac.caltech.edu/

variety of future studies (e.g., stellar activity and rotation measurements), we make the reduced and calibrated light curves available to the community as an online data set accompanying this paper. The non-EDEN targets observed in our survey (Tables 3 and 4) represent a less homogeneous data set. Those light curves and the ensemble of images obtained are available on a collaborative basis and will be made fully available in the near future.

7.2. A Possible Signal for EIC 9 (2MASS J04195212+4233304)

During observation runs in fall–winter 2020, we identified transit-like features in the light curves of EIC 9 (2MASS J04195212+4233304), i.e., a 0.5%–1% dip with a duration of ∼45 minutes. Similar features occurred twice on the same day of 2020 November 18 (UT), once observed by the Lulin One-meter Telescope (LOT) in Taiwan and again about 14 hr later by the Kuiper 61″ Telescope in Arizona. The Vatican Advanced Technology Telescope (VATT) in Arizona observed another feature on 2020 December 22 (UT). The VATT and Kuiper features were both 1% depths, whereas the LOT feature was 0.5%, and the LOT and Kuiper features were both ∼40–45 minutes in duration, whereas the VATT feature was ∼60 minutes (see Figures 5 and 6). The weather at the sites for all three events was nominal—no clouds during the LOT and VATT events, and light cirrus at the Kuiper site in the east as the target was setting. Our observations are done with intra-exposure guiding every few seconds on a bright star near the target, and there were no guiding errors during the observations so the target and reference star centroids remained consistent.

This star was also observed by TESS in Sector 19, and was found to have stellar variability with an amplitude of ∼1% on a 0.99 day period. Once that trend was removed, a low-confidence recurring event (S/N = 4.9, and signal detection efficiency ∼ 6.5) was found with a period of 2.883 days and a transit depth of 0.7%. Notably, the ephemerides aligned with both the LOT and VATT detections—12 orbits of separation with a period of 2.883 days between the two sets of data. However, additional observations from Lulin and Calar Alto ruled out additional transits during those observation windows, casting doubt on the veracity of the original transit observations.

Additional analysis of the light curves from the LOT and VATT events found both to be highly dependent on systematics, as the VATT event was at high airmass and the LOT event is canceled out by the detrending procedure (compare the top panel of Figure 5 with the top panel of Figure 6 and the middle panel of Figure 7). The event in the Kuiper telescope light curve remained even through additional detrending. Previous observations by the Bok telescope in 2019 were not sensitive enough to rule out a transit of the given depth, but new data from the Calar Alto 1.23 m telescope in 2021 January ruled out the ∼2.883 day period for the candidate (see Figure 7). Transit fitting of the signal from the Kuiper event put the period at 3.003 days with a 68% confidence interval of [1.735, 3.781] days. Based on our observing coverage of the target, we likely would have seen multiple transits of any planets within a 5 day period.

Eventually, we determined that our effective phase coverage was providing diminishing returns on continued observations beyond ∼40 nights of data, so with no further transit signals we suspended the follow up of this target and returned to the standard survey monitoring procedures. The event could be a transit, but we would likely have seen an additional transit in our observations unless the data quality was consistently poor. At this point the origin of the detected signal remains unexplained. It may have been caused by telluric contamination such as variable PWV (see the discussion in Section 3.3), which we shall estimate qualitatively here. Typical amounts of water vapor in the Santa Catalina Mountains of 2 mm have been measured (Warner 1977). For a bandpass similar to GG495, this was estimated to cause a ∼3% flux difference due to PWV for an M8 target star (Murray et al. 2020; Pedersen et al. 2023). According to these data, a PWV variation on the order of 1 mm would be consistent with a 1%-level flux change, making PWV variations a potentially viable source of the observed signal.

The `TLS` results from the full set of light curves of this target confirm our analysis of the potential signal. There was no strong event matching the period or any multiples of the expected transit from the TESS data, and the best transit model that `TLS` found had too short of a duration to be a physical transit of an exoplanet. In addition, none of the best-fit models from any of the precision cuts included the Kuiper event as a possible transit match.

7.3. Light-curve Analysis

Our observations were collected with seven telescopes located on three different continents. We developed a uniform observing protocol and data reduction and analysis approach that provided uniform final products, where differences are primarily due to the sensitivity of the instrument (a combination of the telescopes' light-collecting area and the quantum efficiency of the detectors). Our data reduction and analysis approach was developed to maximize sensitivity (finding many possible transit candidates and following up on them) and efficiency (observing many targets where follow-up monitoring requires a substantial amount of telescope time) simultaneously.

The EDEN survey's sensitivity is demonstrated by the injection-and-retrieval tests we performed (see Section 4.2). Its efficiency is, perhaps counterintuitively, reflected in the overall scarcity of possible detections: our sensitivity analysis shows that our observations can very efficiently detect short-period planets (P <1.5 days), even if they are relatively small ($R_p < 1.5\,R_\oplus$). Yet, during our survey of over 2450 hr, we detected only one target with a potential single transit (see Section 7.2). The combination of high sensitivity and the very low number of false positives demonstrates high efficiency and reliability, as well as robust approaches to the data reduction and analysis, which are particularly important for any targeted survey. In order to support future surveys, we commit to making the complete EDEN data analysis package available on a collaborative basis.

7.4. No Planets Detected

Project EDEN survey's extensive data set yielded multiple possible detections, but only EIC 9 was not identified immediately as a false positive. Further observations successfully eliminated it as a potential planet candidate, leaving no detected transit in our survey. Translating nondetections into constraints on the exoplanet demographics and occurrence rates is nontrivial, and requires a careful sensitivity analysis (see,

Publ. Astron. Soc. Japan (2023) 75 (2), 462–475
https://doi.org/10.1093/pasj/psad012
Advance Access Publication Date: 2023 March 2

Long-term monitoring of comet 29P/Schwassmann–Wachmann from the Lulin Observatory

Zhong-Yi Lin*

Institute of Astronomy, National Central University, No. 300, Zhongda Rd., Zhongli Dist., Taoyuan City 320317, Taiwan

*E-mail: zylin@astro.ncu.edu.tw

Received 2022 April 21; Accepted 2023 February 7

Abstract

Multi-band photometric monitoring of comet 29P/Schwassmann–Wachmann 1 was conducted with the standard Johnson–Cousins filter set. Observations extended from 2018 July to 2021 December. The comet was detected to show at least 12 relatively large outbursts, during which its brightness increased by 1.5 to 5 mag as measured through a 5″ aperture. The outbursts resulted in a clear variation of the cometary brightness profile. The derived slopes of the surface brightness profiles showed a significant variation with time from a shallower slope to a steeper one at the beginning of each outburst and then slowly returning to pre-outburst values. There did not seem to be any obvious change in the color indices as the outbursts occurred. However, for the quadruple outbursts in late September of 2021, we could confidently spot a change in the color of the comet, indicating that the color indices seem to be less than the mean values, especially in the $B - V$ term. Dust production derived by using the dust production rate parameter, $Af\rho$, from the R-band photometry measurements shows the outburst to be accompanied by a large increasing trend. Using a simple model and the derived outflow velocity of 0.11 km s^{-1} from the expanding shell features, an estimated lower limit of 1.0×10^8 kg up to 2.7×10^9 kg of dust was released during the quadruple outbursts by using a specific dust size of 1 μm.

Key words: comets: individual (29P/Schwassmann–Wachmann 1) — dust — outburst

1 Introduction

Comets are some of the most easily observable astronomical phenomena, but we understand little about them, especially some comet outbursts. Many comets have outbursts, but 29P/Schwassmann–Wachmann 1, hereafter P/SW 1, is unique because it averages 7.3 outbursts a year (Trigo-Rodríguez et al. 2010). Therefore, this makes comet P/SW 1 the second most active body in our solar system, after Jupiter's moon, Io, whose level of volcanism is engendered by tidal interactions with the planet. Comet P/SW 1 was discovered on 1925 November 15 by A. Schwassmann and A. A. Wachmann. Soon after its discovery, comet P/SW 1 was assigned to the Centaur population because of its orbital properties (Jewitt 2009). It is located at a mean heliocentric distance of 6.0 au (a perihelion distance of 5.7 au and an aphelion of 6.3 au) and moves along a near-circular orbit with an orbital period of 14.9 yr. Frankly, to see any active comet at such an incredible distance, a fair bit beyond Jupiter, is not a rare event. Some

The Planetary Science Journal, 4:56 (17pp), 2023 March https://doi.org/10.3847/PSJ/acc1e7

OPEN ACCESS

Implications for the Formation of (155140) 2005 UD from a New Convex Shape Model

Jay K. Kueny[1,2,3,19], Colin Orion Chandler[4,5,19], Maxime Devogéle[6], Nicholas Moskovitz[1], Petr Pravec[7], Hana Kučáková[7,8,9], Kamil Hornoch[7], Peter Kušnirák[7], Mikael Granvik[10,11], Christina Konstantopoulou[12,13], Nicholas E. Jannsen[13,14], Shane Moran[13,15], Lauri Siltala[10], Grigori Fedorets[10,16], Marin Ferrais[17,18], Emmanuel Jehin[17], Theodore Kareta[1], and Josef Hanuš[8]

[1] Lowell Observatory, 1400 W. Mars Hill Rd., Flagstaff, AZ 86001, USA
[2] Steward Observatory, University of Arizona, Tucson, 933 N. Cherry Avenue, Tucson, AZ 85721, USA
[3] Wyant College of Optical Sciences, University of Arizona, 1630 E. University Boulevard, Tucson, AZ 85721, USA
[4] Department of Astronomy and Planetary Science, Northern Arizona University, PO Box 6010, Flagstaff, AZ 86011, USA
[5] Dept. of Astronomy & the DiRAC Institute, University of Washington, 3910 15th Avenue NE, Seattle, WA 98195, USA
[6] Arecibo Observatory, University of Central Florida, HC-3 Box 53995, Arecibo, PR 00612, USA
[7] Astronomical Institute, Academy of Sciences of the Czech Republic, Fričova 1, CZ-25165 Ondřejov, Czech Republic
[8] Institute of Astronomy, Faculty of Mathematics and Physics, Charles University, V Holešovickách 2, 18000 Prague, Czech Republic
[9] Research Centre for Theoretical Physics and Astrophysics, Institute of Physics, Silesian University in Opava, Bezručovo nám. 13, 74601 Opava, Czech Republic
[10] Department of Physics, P.O. Box 64, FI-00014 University of Helsinki, Finland
[11] Asteroid Engineering Laboratory, Luleå University of Technology, Box 848, SE-98128 Kiruna, Sweden
[12] Department of Astronomy, University of Geneva, Chemin Pegasi 51, 1290 Versoix, Switzerland
[13] Nordic Optical Telescope, Apartado 474, E-38700 Santa Cruz de La Palma, Spain
[14] Institute of Astronomy, Celestijnenlaan 200D bus 2401, B-3001 Leuven, Belgium
[15] Department of Physics and Astronomy, University of Turku, Vesilinnantie 5, FI-20500, Finland
[16] Astrophysics Research Centre, School of Mathematics and Physics, Queen's University Belfast, Belfast BT7 1NN, UK
[17] Space sciences, Technologies & Astrophysics Research (STAR) Institute University of Liège Allée du 6 Août 19, B-4000 Liège, Belgium
[18] Aix Marseille Univ, CNRS, LAM, Laboratoire d'Astrophysique de Marseille, Marseille, France
Received 2022 September 1; revised 2023 February 27; accepted 2023 March 1; published 2023 March 31

Abstract

(155140) 2005 UD has a similar orbit to (3200) Phaethon, an active asteroid in a highly eccentric orbit thought to be the source of the Geminid meteor shower. Evidence points to a genetic relationship between these two objects, but we have yet to fully understand how 2005 UD and Phaethon could have separated into this associated pair. Presented herein are new observations of 2005 UD from five observatories that were carried out during the 2018, 2019, and 2021 apparitions. We implemented light curve inversion using our new data, as well as dense and sparse archival data from epochs in 2005–2021, to better constrain the rotational period and derive a convex shape model of 2005 UD. We discuss two equally well-fitting pole solutions ($\lambda = 116^\circ.6$, $\beta = -53^\circ.6$) and ($\lambda = 300^\circ.3$, $\beta = -55^\circ.4$), the former largely in agreement with previous thermophysical analyses and the latter interesting due to its proximity to Phaethon's pole orientation. We also present a refined sidereal period of $P_{\rm sid} = 5.234246 \pm 0.000097$ hr. A search for surface color heterogeneity showed no significant rotational variation. An activity search using the deepest stacked image available of 2005 UD near aphelion did not reveal a coma or tail but allowed modeling of an upper limit of 0.04–0.37 kg s^{-1} for dust production. We then leveraged our spin solutions to help limit the range of formation scenarios and the link to Phaethon in the context of nongravitational forces and timescales associated with the physical evolution of the system.

Unified Astronomy Thesaurus concepts: Near-Earth objects (1092); CCD photometry (208); Light curves (918)

Supporting material: data behind figure

1. Introduction

Near-Earth asteroid (NEA) 2005 UD is a kilometer-class object and is a potential flyby target of JAXA's DESTINY$^+$ mission,[20] scheduled to launch within the next decade. It was discovered in 2005 by the Catalina Sky Survey (Christensen et al. 2005) and was revealed to have an orbit similar to (3200) Phaethon and the Geminid meteor stream. A subsequent observational campaign revealed surface color variations as a function of rotational phase (Kinoshita et al. 2007). Previous studies on the visible reflectance spectrum suggest that 2005 UD is a B-type asteroid (Jewitt & Hsieh 2006; Devogèle et al. 2020), though recent findings regarding the near-infrared spectrum by Kareta et al. (2021) and a phase curve analysis by Huang et al. (2021) contest this. It is in the Apollo dynamical class with a semimajor axis of 1.275 au, an eccentricity of 0.87, and an orbital inclination of $28^\circ.7$ (see Appendix A for a comprehensive reference table). Light curve inversion by Huang et al. (2021) using the Lommel–Seeliger ellipsoid method yielded a 2005 UD spin pole solution of ($285^\circ.8^{+1.1}_{-5.3}$, $-25^\circ.8^{+5.3}_{-12.5}$), which is comparable to that of Phaethon (Hanuš et al. 2018, Kim et al. 2018). A common origin with Phaethon continues to be extensively investigated (see, e.g., Devogèle et al. 2020; Kareta et al. 2021; MacLennan et al. 2021).

Asteroid (3200) Phaethon is a B-type NEA (Licandro et al. 2007) and exhibits short bursts of activity at perihelion

[19] National Science Foundation Graduate Research Fellow.
[20] https://destiny.isas.jaxa.jp/science/

Appendix B
2005 UD Observations

Tables B1, B2, and B3 describe all observations used in this work including those rejected from the shape modeling procedure.

Table B1
Observational Circumstances

#	Date/Time (UT)	Span (hr)	Telescope	Filter	N_p	m_V (au)	r (au)	Δ (au)	$\angle_{STO}$ (deg)	Reference
1	2005-Nov-2 11:54:32	3.26	LOT	R	6	18.3	1.37	0.55	36.7	1
2	2005-Nov-3 12:11:24	3.22	LOT	R	5	18.4	1.39	0.57	36.7	1
3	2005-Nov-4 12:05:20	3.00	LOT	R	13	18.5	1.4	0.59	36.7	1
4	2005-Nov-5 11:52:45	1.78	LOT	R	16	18.6	1.41	0.61	36.6	1
5	2005-Nov-19 08:50:19	0.56	UH88	R	15	19.6	1.57	0.91	35.9	2
6	2005-Nov-20 07:23:39	0.79	UH88	R	16	19.7	1.58	0.93	35.9	2
7	2005-Nov-21 05:48:28	3.19	UH88	R	17	19.8	1.59	0.95	35.8	2
8	2005-Nov-22 05:31:34	3.53	UH88	R	9	19.9	1.61	0.99	35.7	2
9	2018-Sep-27 00:49:29	1.97	LCO-fl16	r	92	16.6	1.09	0.23	62.5	4
10[a]	2018-Sep-27 07:09:27	5.23	31in	⋯	87	16.5	1.1	0.22	58.2	4
11	2018-Sep-27 16:35:01	1.97	LCO-fl11	r	114	16.5	1.1	0.22	58.2	4
12	2018-Oct-1 15:55:45	2.47	LCO-fl11	r	115	16.1	1.16	0.23	40.6	4
13	2018-Oct-1 23:39:44	2.45	LCO-fl16	r	122	16.1	1.16	0.23	40.6	4
14	2018-Oct-3 05:41:52	2.45	LCO-fa15	r	142	16	1.18	0.23	36.3	4
15	2018-Oct-3 21:57:50	0.29	Ondřejov	R	17	15.9	1.2	0.24	28.0	5
16	2018-Oct-3 23:22:49	1.46	Ondřejov	R	134	15.9	1.2	0.24	28.0	5
17	2018-Oct-3 23:50:50	2.98	LCO-fl16	r	146	15.9	1.2	0.24	28.0	4
18	2018-Oct-4 00:51:58	0.96	Ondřejov	R	86	15.9	1.2	0.24	28.0	5
19	2018-Oct-4 02:20:05	1.63	Ondřejov	R	110	15.9	1.2	0.24	28.0	5
20	2018-Oct-5 21:17:57	2.18	Ondřejov	R	158	15.9	1.22	0.24	24.1	5
21	2018-Oct-5 23:32:08	1.97	Ondřejov	R	140	15.9	1.22	0.24	24.1	5
22	2018-Oct-5 01:31:54	2.23	Ondřejov	R	160	15.9	1.22	0.24	24.1	5
23*	2018-Oct-6 04:07:48	8.38	31in	r	32	15.9	1.23	0.25	20.4	4
24	2018-Oct-6 02:59:19	6.29	TRAPPIST-S	R	348	15.9	1.23	0.25	20.4	4
25	2018-Oct-9 20:40:28	1.30	Ondřejov	R	80	15.8	1.27	0.28	10.6	5
26	2018-Oct-9 22:00:18	2.26	Ondřejov	R	154	15.8	1.27	0.28	10.6	5
27	2018-Oct-9 00:17:27	1.92	Ondřejov	R	125	15.8	1.27	0.28	10.6	5
28	2018-Oct-9 02:17:16	0.46	Ondřejov	R	28	15.8	1.27	0.28	10.6	5
29	2018-Oct-9 13:45:09	3.46	LCO-fl11	r	155	15.8	1.27	0.28	10.6	4
30	2018-Oct-9 20:30:22	3.55	LCO-fl06	r	168	15.8	1.27	0.28	10.6	4

Note. Date/Time: start of observations; Span: duration of observations; N_P: number of points; m_V: 2005 UD apparent V-band magnitude; r: Sun−target distance; Δ: Earth−target distance; $\angle_{STO}$: Sun−target−observer (phase) angle; LOT: Lulin One-meter Telescope; UH88: University of Hawaii 88-inch Telescope; LCO: Las Cumbres Observatory; 31in: Lowell Observatory NURO 31-inch Telescope; Ondřejov: Ondřejov Observatory 0.65 m Telescope; TRAPPIST-S: South TRAnsiting Planets and PlanetesImals Small Telescope.

References. (1) Kinoshita et al. 2007; (2) Jewitt & Hsieh 2006; (3) Warner & Stephens 2019; (4) Devogèle et al. 2020; (5) this work.

[a] Rejected from the inversion process due to excessive photometric noise or temporal overlap with other data.

The Planetary Science Journal, 4:138 (18pp), 2023 August https://doi.org/10.3847/PSJ/ace827

Characterization of the Ejecta from the NASA/DART Impact on Dimorphos: Observations and Monte Carlo Models

Fernando Moreno[1], Adriano Campo Bagatin[2,3], Gonzalo Tancredi[4], Jian-Yang Li[5], Alessandro Rossi[6], Fabio Ferrari[7], Masatoshi Hirabayashi[8], Eugene Fahnestock[9], Alain Maury[10], Robert Sandness[10], Andrew S. Rivkin[11], Andy Cheng[11], Tony L. Farnham[12], Stefania Soldini[13], Carmine Giordano[7], Gianmario Merisio[7], Paolo Panicucci[7], Mattia Pugliatti[7], Alberto J. Castro-Tirado[1,14], Emilio Fernández-García[1], ignacio Pérez-García[1], Stavro Ivanovski[15], Antti Penttila[16], Ludmilla Kolokolova[17], Javier Licandro[18,19], Olga Muñoz[1], Zuri Gray[20,21], Jose L. Ortiz[1], and Zhong-Yi Lin[22]

[1] Instituto de Astrofísica de Andalucía, CSIC Glorieta de la Astronomía, s/n, E-18008 Granada, Spain
[2] Instituto de Fìsica Aplicada a las Ciencias y las Tecnologías (IUFACyT), Universidad de Alicante, San Vicent del Raspeig, E-03690 Alicante, Spain
[3] Departamento de Física, Ingeniería de Sistemas y Teoría de la Señal Universidad de Alicante, San Vicent del Raspeig, E-03690 Alicante, Spain
[4] Departamento de Astronomía, Facultad de Ciencias, Iguá 4225, 11400 Montevideo, Uruguay
[5] Planetary Science Institute, Tucson, AZ, USA
[6] FAC-CNR, Via Madonna del Piano 10, I-50142, Sesto Fiorentino, Italy
[7] Department of Aerospace Science and Technology, Politecnico di Milano, Milano, Italy
[8] Auburn University, Auburn, AL, USA
[9] Jet Propulsion Laboratory, California Institute of Technology, Pasadena, CA, USA
[10] SPACEOBS, San Pedro de Atacama, Chile
[11] Johns Hopkins University Applied Physics Laboratory, Laurel, MD, USA
[12] University of Maryland, Department of Astronomy, College Park, MD, USA
[13] Department of Mechanical, Materials and Aerospace Engineering, University of Liverpool, Liverpool, UK
[14] Unidad Asociada al CSIC, Departamento de Ingeniería de Sistemas y Automática, Escuela de Ingenierías, Universidad de Málaga, Málaga, Spain
[15] INAF—Osservatorio Astronomico di Trieste, Via G.B. Tiepolo, 11, Trieste, Italy
[16] Department of Physics, P.O. Box 64, FI-00014, University of Helsinki, Finland
[17] Department of Astronomy, University of Maryland, College Park, MD, USA
[18] Instituto de Astrofísica de Canarias C/Vía Láctea s/n, E-38205 La Laguna, Spain
[19] Departamento de Astrofísica, Universidad de La Laguna, E-38206 La Laguna, Tenerife, Spain
[20] Armagh Observatory & Planetarium, College Hill, Armagh, BT61 9DG, UK
[21] Mullard Space Science Laboratory, Department of Space and Climate Physics, University College London, Holmbury St. Mary, Dorking, Surrey RH5 6NT, UK
[22] Institute of Astronomy, National Central University, No. 300, Zhongda Road, Zhongli Dist., Taoyuan City 32001, Taiwan
Received 2023 June 2; revised 2023 July 7; accepted 2023 July 16; published 2023 August 7

Abstract

The NASA Double Asteroid Redirection Test (DART) spacecraft successfully crashed on Dimorphos, the secondary component of the binary (65803) Didymos system. Following the impact, a large dust cloud was released, and a long-lasting dust tail developed. We have extensively monitored the dust tail from the ground and the Hubble Space Telescope. We provide a characterization of the ejecta dust properties, i.e., particle size distribution and ejection speeds, ejection geometric parameters, and mass, by combining both observational data sets and using Monte Carlo models of the observed dust tail. The size distribution function that best fits the imaging data is a broken power law having a power index of –2.5 for particles of $r \leqslant 3$ mm and –3.7 for larger particles. The particles range in size from 1 μm up to 5 cm. The ejecta is characterized by two components, depending on velocity and ejection direction. The northern component of the double tail, observed since 2022 October 8, might be associated with a secondary ejection event from impacting debris on Didymos, although is also possible that this feature results from the binary system dynamics alone. The lower limit to the total dust mass ejected is estimated at $\sim 6 \times 10^6$ kg, half of this mass being ejected to interplanetary space.

Unified Astronomy Thesaurus concepts: Asteroid dynamics (2210)

1. Introduction

The Double Asteroid Redirection Test (DART) is a NASA mission that impacted a spacecraft on the surface of Dimorphos, the satellite of the primary asteroid (65803) Didymos (Cheng et al. 2018). On 2022 September 26, 23:14 UT, DART impacted in a nearly head-on configuration on Dimorphos's surface, giving rise to a fast ejected material (plume; speed of ≈ 2 km s^{-1}) whose spectrum consists of emission lines of ionized alkali metals (Na I, K I, and Li I; Shestakova et al. 2023). This plume was clearly observed in images obtained from Les Makes Observatory (Graykowski et al. 2023) right after impact time and was also seen in the earliest images during the Hubble Space Telescope (HST) monitoring (Li et al. 2023). A wide ejection cone of dust particles and meter-sized boulders was monitored by the Light Italian CubeSat for Imaging of Asteroid (LICIACube; Dotto et al. 2021; Farnham et al. 2023), which performed a fast flyby of the system.

Apart from the plume, a fraction of the ejected mass was emitted at significantly lower speeds, forming the ejecta pattern and tail that could be seen on the earliest images acquired from ground-based observatories (Bagnulo et al. 2023; Opitom et al. 2023) and the HST (Li et al. 2023). Our purpose is to characterize the dust properties of this mostly slow-moving ejecta, the ejection velocities, the size distribution, and the

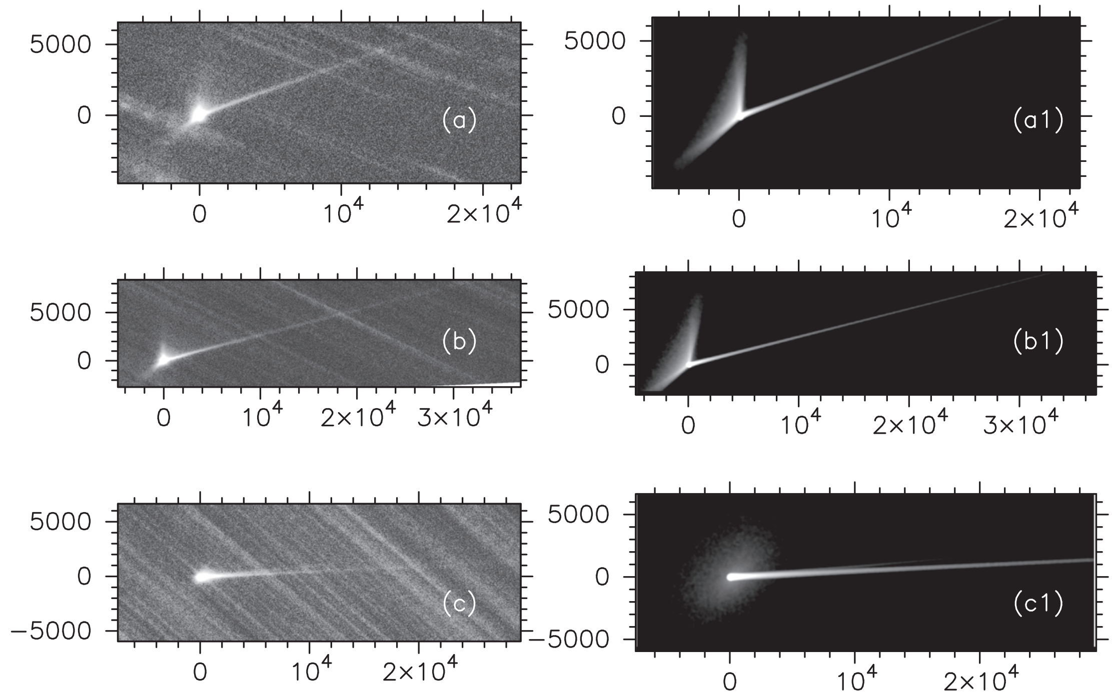

Figure 5. Panels (a), (b), and (c) display the SPACEOBS images at the corresponding dates in Table 2, and panels (a1), (b1), and (c1) display the corresponding synthetic images generated with the simple Monte Carlo model. All images are stretched between 28 and 22 mag arcsec^{-2}. Axes are labeled in kilometers projected on the sky plane. North is up and east is to the left in all images.

Table 4
Parameters of the Best-fit Models

Ejecta Component	Speed (m s^{-1})	Ejected Mass (kg)	Ejection Mode	Total Unbound[a] Ejected Mass (kg)
Simple Monte Carlo Model				
Slow	$0.05(1+\xi)$	2.8×10^6	Hemispherical	
Fast	$0.375\chi r^{-0.5}$	9.2×10^5	Conical	4.2×10^6
Late	$0.05(1+\xi)$	4.6×10^5	Isotropic	
Detailed Dynamical Monte Carlo Model				
Slow	0.09	4.3×10^6	Hemispherical	
Fast	$0.225\chi r^{-0.5}$	2.1×10^6	Conical	4.9×10^6
Late	0.09	3.0×10^6	Isotropic	

Note.
[a] Delivered to interplanetary space. Note that in the case of the detailed dynamical Monte Carlo model, this mass is not the sum of the total masses ejected due to intervening dynamical stirring and collision of a sizable fraction of the ejecta with Didymos and Dimorphos.

undetectable in the images. In that respect, it is convenient to mention the findings by Farnham et al. (2023), who detected a boulder population after DART impact by analyzing LICIACube LUKE images. Those authors found a population of some 100 meter-sized boulders, so that, assuming a density of 3500 kg m^{-3}, they would give a total mass of $\approx 1.5 \times 10^6$ kg. Those boulders are moving at speeds of 20–50 m s^{-1}, so that they carry a momentum that might be comparable to that of the DART spacecraft (Farnham et al. 2023). Let us assume that the actual boulder population was a factor of 100 higher, i.e., a total mass of 10^8 kg, and that this population is distributed following a power law of index –3.7 (as in our model) with ejection speeds of 20 m s^{-1}. This would result in a unrealistic momentum balance, but we would like to remark that even in this case, the boulder population would add a negligible increase in the integrated flux of only 0.06% relative to the corresponding model results on the dates shown in Table 2. Even if we reduce the speed of those boulders to the much smaller speeds used in the modeling (see Table 4), that will tend to concentrate the boulders much closer to the optocenter at all epochs, the contribution to the total flux coming from the boulders would be of only 7% compared with the flux computed with the best-fit model parameters.

The synthetic images generated are convolved with a Gaussian function of FWHM consistent with the average seeing point-spread function. The modeled images are then compared to the observed images in Figures 5–7 using the same gray scale. As shown, the modeled images capture well many of the features displayed in the observed images.

The model image showing the double tail in comparison with the SPACEOBS observation is given in more detail in Figure 8. For purposes of comparison only, an additional image, taken at the LULIN Observatory 1 m aperture telescope in Taiwan on October 12, i.e., 4 days before the SPACEOBS image on October 16, also displays the feature, with a slightly higher signal-to-noise ratio than the SPACEOBS image in Figure 8, see Lin et al. (2023; Figure 9). By November 2,

A&A 676, A116 (2023)
https://doi.org/10.1051/0004-6361/202245629

Astronomy & Astrophysics

Physical properties of the Didymos system before and after the DART impact

Zhong-Yi Lin[1], Jean-Baptiste Vincent[2], and Wing-Huen Ip[1]

[1] Institute of Astronomy, National Central University, No. 300, Zhongda Rd., Zhongli Dist., Taoyuan City 32001, Taiwan
e-mail: zylin@astro.ncu.edu.tw
[2] DLR Institute of Planetary Research, Rutherfordstrasse 2, 12489 Berlin, Germany
e-mail: jean-baptiste.vincent@dlr.de

Received 7 December 2022 / Accepted 7 June 2023

ABSTRACT

Context. On September 26, 2022, the Double Asteroid Redirection Test (DART) successfully changed the trajectory of the asteroid Dimorphos (i.e. 65803 Didymos I), a satellite circling (65803) Didymos.

Aims. We aim to characterize the consequence of this collision and derive the physical properties of the ejecta features based on ground-based observations in East Asia.

Methods. Filtered photometric observations were made between September 21 2022 (~5 days before DART impact) and January 5 2023 using the Lulin 1-m telescope to identify the taxonomy, size, and rotational period of Didymos. The Finson-Probstein dust dynamical models were used to determine the grain sizes (mm–cm) released after the DART impact and the date of the activity.

Results. We report a rapid increase in the brightness by about one order of magnitude after the impact, to be followed by a gradual 0.07 mag decrease over the first two weeks producing a relatively shallow brightness slope at the end of October. The size and rotation period at post-impact were $0.72^{+0.12}_{-0.10}$ km and 2.27 h, respectively. The Principal Component Index (PCI), relative reflectance, and colors were all classified as S-complex. The Dydimos system became bluer after the collision before returning to its original color. The formation of a comet-like trail containing debris in the anti-sunward direction can be explained by expansion driven by the pressure of solar radiation. A Finson-Probstein modeling approach led to an estimate of the grain size in the mm-cm range. The splitting of the tail into two components is shown in the image acquired on October 12, which may possibly be interpreted as being due to the secondary impact of fallback ejecta about a week after DART.

Key words. minor planets, asteroids: individual: Didymos

1. Introduction

NASA's Double Asteroid Redirection Test (DART) mission was designed to test and validate a method to protect the Earth in the case of a future small asteroid strike. The mission's target was the binary asteroid system Didymos which consists of the near-Earth asteroid 65803 Didymos, measuring 780 meters across, and its moonlet, Dimorphos, 160 meters in diameter (Pravec et al. 2006). The aim was for DART to collide with the moonlet Dimorphos and change its orbit around the primary body Didymos. With an impact speed of 6.6 km s^{-1}, DART would transfer a huge amount of momentum to Dimorphos, and ground telescopes could be used to detect the resultant change in orbital motion over the course of weeks or months. On October 11, 2022, NASA officially announced that the DART impact has shortened Dimorphos' nearly 12-h orbit by 32 min, according to ground-based observations (Thomas et al. 2023). In other words, the "kinetic impactor" technique was successful and can feasibly be used for planetary defense in the future.

Ground-based telescopes in East Asia were not able to acquire a sequence of images showing the brightening of the asteroid. Didymos immediately after the impact of NASA's DART spacecraft due to its position in relation to Earth at the time. However, it was possible to obtain photometric observations that provided additional information on the system's physical properties before and after the impact. A dynamical model of ejecta expansion was also applied to derive the time of emission and the physical properties of the observed tail of debris. The photometric observations and data reduction are described in Sect. 2. In Sect. 3, we present the results and a discussion, including the asteroid's colors, size, period, morphology, and dust modeling of the ejecta. Our findings are summarized in Sect. 4.

2. Observations and data reduction

The asteroid Didymos was monitored by the Lulin Observatory (National Central University, Taiwan) from September 21, 2022, until January 5, 2023. Lulin's 1 m telescope is equipped with a 2 K × 2 K thermoelectrically cooled CCD camera, Andor E2V 42-40 with a field of view of 23 arcmins × 23 arcmins. Except for the night of October 25, 2 × 2 pixels binning and was carried out to obtain a resulting plate scale of 0.69 arcsecs per pixel. The observing sequence (*R*-*B*-*R*-*V*-*R*-*I*-*R* ...) for color measurements was meant to remove the effect of the magnitude variation that was due to the asteroid's rotation. Light curve measurements for the determination of the rotation period were also planned. Broadband images for a total of 22 observing nights were acquired. All asteroid observations were carried out with telescope tracking of the asteroid's non-sidereal motion. The typical mean seeing was 1.5 ~ 2.5 arcsec. Appropriate bias and flat

Monthly Notices
of the
ROYAL ASTRONOMICAL SOCIETY

MNRAS **520,** 1092–1110 (2023) https://doi.org/10.1093/mnras/stad013
Advance Access publication 2023 January 6

Photometric variable stars in the young open cluster NGC 6823

Sneh Lata,[1★] W. P. Chen,[2,3★] J. C. Pandey ,[1] Athul Dileep,[1] Zhong-Han Ai,[3] Alisher S. Hojaev,[4] Neelam Panwar,[1] Santosh Joshi,[1] Soumen Mondal ,[5] Siddhartha Biswas[5] and B. C. Bhatt[6]

[1]*Aryabhatta Research Institute of Observational Sciences, Manora Peak, Nainital 263001, Uttarakhand, India*
[2]*Graduate Institute of Astronomy, National Central University, 300 Zhongda Road, Zhongli 32001 Taoyuan, Taiwan*
[3]*Department of Physics, National Central University, 300 Zhongda Road, Zhongli 32001 Taoyuan, Taiwan*
[4]*Ulugh Beg Astronomical Institute, Uzbekistan Academy of Sciences, Tashkent, Republic of Uzbekistan*
[5]*S. N. Bose National Centre for Basic Sciences, Kolkata 700106, India*
[6]*Indian Institute of Astrophysics, Koramangala, Bangalore-560034, India*

Accepted 2022 December 22. Received 2022 December 6; in original form 2022 September 29

ABSTRACT

We present stellar variability towards the young open cluster NGC 6823. Time series *V*- and *I*-band CCD photometry led to identification and characterization of 88 variable stars, of which only 14 have been previously recognized. We ascertain the membership of each variable with optical *UBVI* and infrared photometry, and with Gaia EDR3 parallax and proper motion data. Seventy two variable stars are found to be cluster members, of which 25 are main sequence stars and 48 are pre-main-sequence stars. The probable cluster members collectively suggest an isochrone age of the cluster to be about 2 Myrs based on the GAIA photometry. With the colour and magnitude, as well as the shape of the light curve, we have classified the main sequence variables into β Cep, δ Scuti, slowly pulsating B type, and new class variables. Among the pre-main-sequence variables, eight are classical T Tauri variables, and four are Herbig Ae/Be objects, whereas the remaining belong to the weak-lined T Tauri population. The variable nature of 32 stars is validated with TESS light curves. Our work provides refined classification of variability of pre-main-sequence and main-sequence cluster members of the active star-forming complex, Sharpless 86. Despite no strong evidence of the disc-locking mechanism in the present sample of TTSs, one TTS with larger $\Delta(I-K)$ is found to be a slow rotator.

Key words: open clusters and associations: individual NGC 6823 – Hertzsprung-Russell and colour-magnitude diagram – stars: pre-main-sequence – stars: variables: T Tauri – Herbig Ae/Be.

1 INTRODUCTION

Young open clusters serve as useful tools for the study of the star formation mechanism and early stellar evolution. For example, young star clusters are used to trace the Galactic spiral structure. In particular, variability of young stellar members provides diagnostics on the sporadic (accretion or occultation) or periodical (rotation) properties of the stars, and of their relation to the circumstellar environments (Morales-Calderon et al. 2011).

Pre-main-sequence (PMS) objects are categorized on the basis of the spectral energy distribution in the infrared wavelengths: Class 0, Class I, Class II, and Class III (Lada 1987; Andre, Ward-Thompson & Barsony 1993) with the classification sequence roughly corresponding to the evolutionary status. Namely, a Class 0 object signifies a clump of dust and gas heavily enshrouded in the molecular envelope, and is detected only in far-infrared wavelengths or longer. A Class I object is more evolved, now emerging from the cloud to become visible in near-infrared (NIR) and mid-infrared (MIR). A Class I object is in the protostellar stage and derives the luminosity from mass accretion.

A Class II object, corresponding to a classical T Tauri star (TTS), has dispersed much of the envelope of gas and dust but retains a circumstellar disc within which planets may condense or are being formed. Inside the optically thick but geometrically thin disc, the dust grains absorb the starlight and re-emit in the infrared, manifest as infrared excess seen typically in a classical TTS. Accretion from the disc onto the star, while matter is partly lost as bipolar jets/outflows, leads to strong emission lines in the spectrum. As the inner disc is dissipated (or going into planet formation), the PMS object then evolves to Class III, now with negligible infrared excess and with weak emission lines, if any, due to surface chromospheric activity. A Class III object hence is called a weak-lined TTS (Joy 1945; Appenzeller & Mundt 1989). Variability of PMS objects hence serves as an important diagnosis to understand the earliest PMS stellar evolution, e.g. the accretion (Johnstone et al. 2018), rotation (Herbst et al. 1994), or dust properties (Huang et al. 2019).

Here we report the variability study of the Galactic young open cluster NGC 6823. At a distance of about 2 kpc, the cluster is associated with the prominent H II region, Sharpless 86. This cluster has been investigated by several authors (Turner 1979; Sagar and Joshi 1981; Stone 1988; Guetter 1992; Massey et al. 1995; Pigulski, Kolaczkowski & Kopacki 2000; Hojaev, Chen & Lee 2003; Bica, Bonatto & Dutra 2008; Zahajkiewicz 2012). Using optical and *JHK* photometric observations, Riaz et al. (2012) found a large population of young stellar sources in the region, including two δ Scuti variables of PMS nature, and 13 other variables such as eclipsing binaries, slowly pulsating B type (SPB) candidates, and UX Ori type variables. In the

★ E-mail: sneh@aries.res.in (SL); wchen@astro.ncu.edu.tw (WPC)

The Astrophysical Journal Letters, 953:L17 (7pp), 2023 August 20 https://doi.org/10.3847/2041-8213/acec4c

Evidence of Stellar Oscillations in the Post-common-envelope Binary Candidate ASASSN-V J205543.90+240033.5

J. Takata[1], A. K. H. Kong[2], X. F. Wang[1], F. F. Song[3,4,5], J. Mao[3,4,6], X. Hou[3,4], C.-P. Hu[7], L. C.-C. Lin[8], K. L. Li[8], and C. Y. Hui[9]

[1] Department of Astronomy, School of Physics, Huazhong University of Science and Technology, Wuhan 430074, People's Republic of China; takata@hust.edu.cn
[2] Institute of Astronomy, National Tsing Hua University, Hsinchu 30013, Taiwan; akong@gapp.nthu.edu.tw
[3] Yunnan Observatories, Chinese Academy of Sciences, 650011 Kunming, Yunnan Province, People's Republic of China
[4] Key Laboratory for the Structure and Evolution of Celestial Objects, Chinese Academy of Sciences, 650011 Kunming, People's Republic of China
[5] University of Chinese Academy of Sciences, 100049 Beijing, People's Republic of China
[6] Center for Astronomical Mega-Science, Chinese Academy of Sciences, 20A Datun Road, Chaoyang District, 100012 Beijing, People's Republic China
[7] Department of Physics, National Changhua University of Education, Changhua 50007, Taiwan
[8] Department of Physics, National Cheng Kung University, Tainan 701401, Taiwan
[9] Department of Astronomy and Space Science, Chungnam National University, Daejeon 305-764, Republic of Korea
Received 2023 May 18; revised 2023 July 31; accepted 2023 August 1; published 2023 August 16

Abstract

ASASSN-V J205543.90+240033.5 (ASJ2055) is a possible post-common-envelope binary system. Its optical photometric data show an orbital variation of about 0.52 days and a fast period modulation of $P_0 \sim 9.77$ minutes, whose origin is unknown. In this Letter, we report evidence of the stellar oscillation of the companion star as the origin of the fast period modulation. We analyze the photometric data taken by the Transiting Exoplanet Survey Satellite, the Liverpool Telescope, and the Lulin One-meter Telescope. It is found that the period of the 9.77 minutes signal measured in 2022 August is significantly shorter than that in 2021 July/August, and the magnitude of the change is of the order of $|\triangle P_0|/P_0 \sim 0.0008(4)$. Such a large variation will be incompatible with the scenario of the white dwarf (WD) spin as the origin of the 9.77 minutes periodic modulation. We suggest that the fast periodic signal is related to the emission from the irradiated companion star rather than that of the WD. Using existing photometric data covering a wide wavelength range, we estimate that the hot WD in ASJ2055 has a temperature of $T_{\rm eff} \sim 80{,}000$ K and is heating the oscillating M-type main-sequence star with $T_{\rm eff} \sim 3500$ K on its unirradiated surface. The stellar oscillation of the M-type main-sequence star has been predicted in theoretical studies, but no observational confirmation has been done. ASJ2055, therefore, has the potential to be a unique laboratory for investigating the stellar oscillation of an M-type main-sequence star and the heating effect on stellar oscillation.

Unified Astronomy Thesaurus concepts: Binary stars (154); White dwarf stars (1799)

1. Introduction

ASASSN-V J205543.90+240033.5 (hereafter, ASJ2055) is a binary system, which is composed of a hot white dwarf (WD) and a cool main-sequence star that is detached from the Roche lobe. The information about the binary nature of ASJ2055 is reported by Kato (2021) and Kato et al. (2021), who find two periodic modulations with ~0.5 days and ~9.77 minutes in the optical data taken by the Zwicky Transient Facility (ZTF; Masci et al. 2019). The former is thought to be the orbital period ($P_{\rm orb}$), while the origin of the latter (P_0) is not yet understood. An interesting property of ASJ2005 is that the orbital light curve in the optical bands shows a single broad peak with a large amplitude of $\triangle m \sim 1.5$ mag (Figure 1). This orbital modulation is interpreted as a result of the irradiation on the dayside of the companion star by the WD (Kato 2021; Wagner et al. 2021), with the rate of energy deposited on the companion star being of the order of $\sim 10^{32}$ erg s^{-1}.

If the periodic signal with the 9.77 minutes modulation represents a spin period of the WD, ASJ2055 may be a binary system similar to AR Scorpii (Marsh et al. 2016; Pelisoli et al. 2022), as suggested by Kato (2021). AR Scorpii comprises a WD and a low-mass (M-type) companion star, and its orbital period is $P_{\rm orb} \sim 3.56$ hr. It also shows a large orbital variation ($\triangle m \sim 2$ mag) in the optical light curve and contains a rapidly spinning WD with a spin period of $P_s \sim 118$ s. The signature of the nonthermal emission in the broad energy bands from radio to X-ray (Marsh et al. 2016; Buckley et al. 2017; Takata et al. 2018; du Plessis et al. 2022) of AR Scorpii suggests a particle acceleration process in the WD binary system.

Although the optical properties of the two binary systems are similar to each other, the heating process of the companion star in ASJ2055 may be different from that in AR Scorpii. For AR Scorpii, the temperature of the WD's surface is ~11,500 K, indicating that the WD luminosity level, $L_{\rm WD} \sim 10^{31}$ erg s^{-1}, is lower than the luminosity $\sim 10^{32}$ erg s^{-1} of the companion star (Marsh et al. 2016; Garnavich et al. 2021). It is therefore suggested that AR Scorpii contains a fast-spinning magnetized WD with a surface magnetic field of $B_s \sim 10^{7-8}$ Gauss, and the WD's magnetic field or rotation will be the energy source of the irradiation and nonthermal activities (Geng et al. 2016; Marsh et al. 2016; Buckley et al. 2017; Takata et al. 2017; Bednarek 2018; Lyutikov et al. 2020). For ASJ2055, Wagner et al. (2021) measure the spectrum in ~300–1000 nm bands and find that the flux is rising steeply toward the UV bands (see Figure 1). With the properties of the spectrum, they suggest that ASJ2055 is a post-common-envelope binary (PCEB) and contains a hot WD that heats up the companion star, which is

The Astronomical Journal, 166:143 (8pp), 2023 October https://doi.org/10.3847/1538-3881/acedb0

Monitoring Hα Emission from the Wide-orbit Brown-dwarf Companion FU Tau B

Ya-Lin Wu[1,2], Yu-Chi Cheng[1,2], Li-Ching Huang[1,2], Brendan P. Bowler[3], Laird M. Close[4], Wei-Ling Tseng[2,5], Ning Chen[1], and Da-Wei Chen[6]

[1] Department of Physics, National Taiwan Normal University, Taipei 116, Taiwan; yalinwu@ntnu.edu.tw
[2] Center of Astronomy and Gravitation, National Taiwan Normal University, Taipei 116, Taiwan
[3] Department of Astronomy, The University of Texas at Austin, Austin, TX 78712, USA
[4] Steward Observatory, University of Arizona, Tucson, AZ 85721, USA
[5] Department of Earth Sciences, National Taiwan Normal University, Taipei 116, Taiwan
[6] Graduate Institute of Physics, National Taiwan University, Taipei 106, Taiwan
Received 2023 March 30; revised 2023 August 5; accepted 2023 August 6; published 2023 September 5

Abstract

Monitoring mass accretion onto substellar objects provides insights into the geometry of the accretion flows. We use the Lulin One-meter Telescope to monitor Hα emission from FU Tau B, a $\sim$19 $M_{\rm Jup}$ brown-dwarf companion at 5$''$.7 (719 au) from the host star, for six consecutive nights. This is the longest continuous Hα monitoring for a substellar companion near the deuterium-burning limit. We aim to investigate if accretion near the planetary regime could be rotationally modulated as suggested by magnetospheric accretion models. We find tentative evidence that Hα mildly varies on hourly and daily timescales, though our sensitivity is not sufficient to definitively establish any rotational modulation. No burst-like events are detected, implying that accretion onto FU Tau B is overall stable during the time baseline and sampling windows over which it was observed. The primary star FU Tau A also exhibits Hα variations over timescales from minutes to days. This program highlights the potential of monitoring accretion onto substellar objects with small telescopes.

Unified Astronomy Thesaurus concepts: Accretion (14); Brown dwarfs (185); Stellar accretion (1578); Time series analysis (1916); Lomb-Scargle periodogram (1959)

Supporting material: machine-readable tables

1. Introduction

Variability of mass accretion onto giant planets provides clues to their formation timescales and the geometry of the accretion flow. In magnetospheric accretion models (e.g., Königl 1991; Batygin 2018; Thanathibodee et al. 2019), mass inflow along the nearly pole-on magnetic field lines could form hot spots that corotate with the planet, making the shock-induced emission lines potentially variable over the rotation period. On the other hand, unsteady inflow and obscuration from the tilted or puffed inner disk could add stochastic bursts and dips to the rotational modulation (e.g., Bouvier et al. 1999; Cody et al. 2014). It is thus desirable to measure accretion variability on timescales relevant to these phenomena and mechanisms.

While there has been accretion monitoring for T Tauri stars (e.g., Nguyen et al. 2009; Biazzo et al. 2012; Pouilly et al. 2020; Sousa et al. 2021; Zsidi et al. 2022) and young isolated brown dwarfs (e.g., Natta et al. 2004; Scholz & Jayawardhana 2006; Stelzer et al. 2007; Herczeg et al. 2009), such efforts near the planetary regime have been rare. Among the dozens of young substellar companions and protoplanets discovered in direct-imaging surveys, very few of them have multiepoch accretion-rate measurements (e.g., GQ Lup B and GSC 06214–00210 B; Demars et al. 2023; PDS 70 b, Zhou et al. 2021). Moreover, many of these studies were carried out at different observatories, further complicating the interpretations. A monitoring program with identical instrumentation and data reduction is beneficial to measure the mean accretion rate and variability and reduce systematics. This is important to constrain the slope and scatter of the relationship between object mass and accretion rate in the substellar regime, which may reflect the formation mechanism for these wide companions. For instance, Stamatellos & Herczeg (2015) suggested that companions formed via disk fragmentation should tend to be more actively accreting than those formed in collapsing prestellar cores. Constraining mass accretion also helps estimate the dissipation timescale of circumsubstellar disks and therefore the growth timescale of these wide companions and their satellites (e.g., Benisty et al. 2021; Wu et al. 2022).

At optical wavelengths, the Hα emission at 6563 Å is arguably the best accretion tracer as it is the most prominent hydrogen recombination line—often $\mathcal{O}(10^2)$ brighter than the photosphere and the shock-induced continuum excess. Indeed, several young brown-dwarf companions and protoplanets have strong Hα emission indicative of active accretion (e.g., Zhou et al. 2014, 2021; Santamaría-Miranda et al. 2018; Wagner et al. 2018; Eriksson et al. 2020). Follow-up Hα monitoring opens the possibility of probing the variability amplitude and periodicity. As wide substellar companions are typically hundreds to thousands of au from their hosts, it is possible to resolve the widest pairs under moderate seeing without resorting to adaptive optics systems. Small telescopes can play an important and complementary role in monitoring accretion in these systems alongside large ground-based and space facilities.

Here we present our six-night Hα imaging of the FU Tau system with the Lulin One-meter Telescope (LOT) at Lulin Observatory in Taiwan. This is the longest continuous monitoring of an accretion-tracing emission line for a brown-

nature astronomy

Article https://doi.org/10.1038/s41550-022-01820-x

The Birth of a Relativistic Jet Following the Disruption of a Star by a Cosmological Black Hole

Received: 27 May 2022

Accepted: 30 September 2022

Published online: 30 November 2022

Check for updates

A list of authors and their affiliations appears at the end of the paper

A black hole can launch a powerful relativistic jet after it tidally disrupts a star. If this jet fortuitously aligns with our line of sight, the overall brightness is Doppler boosted by several orders of magnitude. Consequently, such on-axis relativistic tidal disruption events have the potential to unveil cosmological (redshift $z > 1$) quiescent black holes and are ideal test beds for understanding the radiative mechanisms operating in super-Eddington jets. Here we present multiwavelength (X-ray, UV, optical and radio) observations of the optically discovered transient AT 2022cmc at $z = 1.193$. Its unusual X-ray properties, including a peak observed luminosity of $\gtrsim 10^{48}$ erg s^{-1}, systematic variability on timescales as short as 1,000 s and overall duration lasting more than 30 days in the rest frame, are traits associated with relativistic tidal disruption events. The X-ray to radio spectral energy distributions spanning 5–50 days after discovery can be explained as synchrotron emission from a relativistic jet (radio), synchrotron self-Compton (X-rays) and thermal emission similar to that seen in low-redshift tidal disruption events (UV/optical). Our modelling implies a beamed, highly relativistic jet akin to blazars but requires extreme matter domination (that is, a high ratio of electron-to-magnetic-field energy densities in the jet) and challenges our theoretical understanding of jets.

AT 2022cmc was discovered in the optical waveband by the Zwicky Transient Facility (ZTF)[1] on 11 February 2022 as a fast-evolving transient, and was publicly reported to the Gamma-ray Coordinates Network on 14 February 2022[2]. We confirmed the rapid evolution of this transient in the Asteroid Terrestrial-impact Last Alert System (ATLAS) survey data with a non-detection 24 h before the ZTF discovery and a subsequent decline of 0.6 mag d^{-1} (ref. [3]). A radio counterpart was identified in Karl G. Jansky Very Large Array (VLA) observations on 15 February 2022[4]. Although the optical spectrum taken on 16 February 2022 revealed a featureless continuum[5], spectral features were detected in subsequent spectra taken 1 d later with the European Southern Observatory's (ESO) Very Large Telescope (VLT)[6] and Keck/DEIMOS[7]. In particular, the detection of [O III] λ5007 emission and Ca II, Mg II and Fe II absorption lines yielded a redshift measurement of $z = 1.193$, or a luminosity distance of 8.45 Gpc (refs. [6,7]). The source did not have a neutrino counterpart[8]. Our follow-up X-ray (0.3–5 keV) observations with the Neutron star Interior Composition ExploreR (NICER) on 16 February 2022 revealed a luminous X-ray counterpart[9]. We also triggered additional multiwavelength observations with numerous facilities, including AstroSat, NICER and The Neil Gehrels Swift Observatory (Swift) in the X-ray and the UV wavebands (Extended Data Figs. 1–3). We obtained an optical spectrum with ESO/VLT (Extended Data Fig. 4) and imaging with several optical telescopes (for example, see Extended Data Fig. 5 and Supplementary Data 1). In the radio band, we acquired multifrequency data with the VLA, the Arcminute Microkelvin Imager-Large Array (AMI-LA) and the European Very Long Baseline Interferometry Network (EVN; see 'Observations and data analysis' in the Methods for details of these observations). We adopted modified Julian date (MJD) 59621.4458 (the

e-mail: drreddy@mit.edu

the photon-counting mode. We only used events with grades between 0 and 12 in the energy range of 0.3–5 keV to match NICER's bandpass. We extracted the source and background counts using a circular aperture of 47 arcsec and an annulus with an inner and outer radii of 80 arcsec and 200 arcsec, respectively. XRT count rates were extracted on a per-obsID basis and these values are provided in Supplementary Data 2.

To convert Swift/XRT count rates to fluxes, we extracted an average energy spectrum by combining all the XRT exposures. We fitted the 0.3–5.0 keV spectra with a power-law model, modified by AT 2022cmc's host-galaxy neutral hydrogen column and Milky Way, the same as the model used for the NICER data mentioned above. Because the signal-to-noise ratio of the Swift XRT spectrum is low, the host-galaxy hydrogen column was fixed at 9.8×10^{20} cm^{-2} as derived from NICER fits. We left the power-law photon index free, which yielded a best-fit value of 1.45 ± 0.06. This value was consistent with the NICER spectral fits. From this fit we estimated the observed 0.3–5 keV flux and a count rate-to-flux scaling factor of 3.6×10^{-11} erg cm^{-2} counts^{-1} to convert from the 0.3–5 keV background-subtracted XRT count rate to the observed flux in the 0.3–5 keV band (Fig. 2). The uncertainties on the count rates and, consequently, the scaled fluxes, were computed using the formulae for small number statistics described in ref. [61].

GRB and TDE comparison data. To compare the X-ray light curve of AT 2022cmc with other relativistic transients, we compiled a sample of X-ray light curves of the three known relativistic TDEs, together with the bright GRBs from ref. [62]. For the GRBs in our comparison sample, we downloaded the 0.3–10 keV count-rate light curves from the UK Swift Science Data Centre (UKSSDC)[63,64] and corrected them for absorption using the ratio of time-averaged unabsorbed flux to time-averaged observed flux per burst provided in the UKSSDC catalogue (https://www.swift.ac.uk/xrt_live_cat/). We k-corrected the light curves to rest-frame 0.3–10 keV luminosity following ref. [65], assuming a power-law spectrum with photon index given by the time-averaged photon-counting mode photon index from the UKSSDC catalogue.

We extracted X-ray light curves of the three relativistic TDEs using the UKSSDC XRT products builder (https://www.swift.ac.uk/user_objects/)[63,64]. We used a time bin size of 1 d. We converted the 0.3–10 keV count-rate light curves to unabsorbed flux using the counts-to-flux ratio of the time-averaged spectral fits, and k-corrected them to rest-frame 0.3–10 keV luminosity as described above. The X-ray spectral indices for Sw J1644+57 and Sw J2058+0516 varied between 1.2 and 1.8 (ref. [41]). This range is similar to AT 2022cmc (see Table 1). Here we used the following fiducial values: Sw J1644+57: counts:flux = 9.32 $\times 10^{-11}$ erg cm^{-2} count^{-1}, photon index = 1.58 ± 0.01; Sw J1112.2-8238: counts:flux = 6.13×10^{-11} erg cm^{-2} count^{-1}, photon index = 1.35 ± 0.08; Sw J2058.4+0516: counts:flux = 5.36×10^{-11} erg cm^{-2} count^{-1}, photon index = 1.55 ± 0.08. We plot these light curves, together with the GRB X-ray light curves extracted above, in Fig. 1.

UV/optical observations. ZTF. AT 2022cmc was discovered and reported by the ZTF[1] and released as a transient candidate ZTF22aaajecp in the public stream to brokers and the Transient Name Server, with data available in Lasair (https://lasair.roe.ac.uk/object/ZTF22aaajecp)[66]. We performed point spread function (PSF) photometry on all publicly available ZTF data using the ZTF forced-photometry service[67] in the g and r bands. We report our photometry corrected for Galactic extinction of $A_V = 0.0348$ mag (ref. [68]) and converted to flux density in millijansky. A_V is the total photometric extinction in the V (550 nm) band.

ATLAS. ATLAS (ref. [69]) is a 4 × 0.5 m telescope system that provides all-sky nightly cadence at typical limiting magnitudes of ~19.5 in cyan (g + r) and orange (r + i) filters. The data were processed in real time and the transients were identified by the ATLAS Transient Science Server[70]. We stacked individual nightly exposures and used the ATLAS forced-photometry server[71] to obtain the light curves of AT 2022cmc in both filters. Photometry was produced with standard PSF fitting techniques on the difference images and we initially reported the fast-declining optical flux in ref. [3].

Follow-up optical imaging. Follow-up observations of AT 2022cmc were conducted as part of the 'advanced' extended Public ESO Spectroscopic Survey of Transient Objects (ePESSTO+)[72] using the EFOSC2 imaging spectrograph at the ESO New Technology Telescope to obtain images in the g, r and i bands. Images were reduced using the custom PESSTO pipeline (https://github.com/svalenti/pessto), and the PSF photometry was measured without template subtraction using photometry-sans-frustration; an interactive Python wrapper that uses the Astropy and Photutils packages[73]. Aperture photometry was applied to the few images in which the target PSF was slightly elongated, otherwise the magnitudes were derived from PSF fitting. All photometry was calibrated against Pan-STARRS field stars.

AT 2022cmc was also followed up in the r, i, z and w bands with the 1.8 m Pan-STARRS2 telescope in Hawaii[74]. Pan-STARRS2 operates in survey mode, searching for near-Earth objects, but the survey can be interrupted for photometry of specific targets. Pan-STARRS2 is equipped with a 1.4 gigapixel camera with a pixel scale of 0.26 arcsec. The images were processed with the image processing pipeline[75] and difference imaging was performed using the PS1 Science Consortium[74] 3π survey data as reference. PSF photometry was used to compute instrumental magnitudes, and zero points were calculated from PS1 reference stars in the field.

AT 2022cmc was also observed as part of the Kinder (kilonova finder) survey[76] in the g, r and i bands with the 0.4 m SLT at Lulin Observatory, Taiwan. The images were reduced using a standard IRAF routine with bias, dark and flat calibrations. We used the automated photometry of transients pipeline[77] to perform PSF photometry and calibrate against SDSS field stars[78]. We used the Lulin one-metre telescope for deeper imaging in the g, r, i and z bands over four nights spanning 13.4–16.2 d post discovery. The images were also reduced using the standard charged-coupled device (CCD) processing techniques in IRAF. We performed aperture photometry calibrated against SDSS field stars. In a combined stack of the images from the Lulin one-metre telescope, AT 2022cmc was clearly detected in the g, r and i bands, with magnitudes of 21.76 ± 0.14, 21.71 ± 0.18 and 21.93 ± 0.31 mag, respectively, and undetected in the z band with an upper limit of >20.69 mag. We list the photometry from our individual observations in Supplementary Data 1.

We compiled additional optical photometry from the Gamma-ray Coordinates Network circulars[79–89] and corrected for extinction. These are also included in Supplementary Data 1.

Swift/UVOT. We performed photometry on Swift/UVOT[90] observations of AT 2022cmc with the uvotsource task in HEAsoft package v6.29 using a 5 arcsec aperture on the source position. Another region of 40 arcsec located at a nearby position was used to estimate the background emission. Because the host galaxy was not detected in the GALEX[91] co-added UV images and AT 2022cmc's UVOT detections are ~2 mag brighter then host upper limits (see 'Constraints on host luminosity'), we did not attempt any type of host subtraction.

AstroSat/Ultra-Violet Imaging Telescope. The AstroSat Ultra-Violet Imaging Telescope[92,93] onboard AstroSat[94] also observed the source, simultaneous with the SXT, with its far-UV channel using the F148W (λ_{mean} = 1,481 Å; $\Delta\lambda$ = 500 Å) and F154W (λ_{mean} = 1,541 Å; $\Delta\lambda$ = 380 Å) filters for exposures of 6,024 s and 9,674 s, respectively. We processed the level-1 data using the CCDLAB pipeline[95] and constructed broadband images. We extracted source counts using a circular aperture of radius 10 arcsec centred at the source position. We also extracted background counts from nearby source-free regions, and corrected for the background contribution. We then converted the net count rates to

The Astrophysical Journal Letters, 946:L22 (12pp), 2023 March 20 https://doi.org/10.3847/2041-8213/acc101

The Optical Light Curve of GRB 221009A: The Afterglow and the Emerging Supernova

M. D. Fulton[1], S. J. Smartt[1,2], L. Rhodes[2], M. E. Huber[3], V. A. Villar[4,5,6], T. Moore[1], S. Srivastav[1], A. S. B. Schultz[3], K. C. Chambers[3], L. Izzo[7], J. Hjorth[7], T.-W. Chen[8,9], M. Nicholl[10], R. J. Foley[11], A. Rest[12,13], K. W. Smith[1], D. R. Young[1], S. A. Sim[1], J. Bright[2], Y. Zenati[13], T. de Boer[3], J. Bulger[3], J. Fairlamb[3], H. Gao[3], C.-C. Lin[3], T. Lowe[3], E. A. Magnier[3], I. A. Smith[14], R. Wainscoat[3], D. A. Coulter[11], D. O. Jones[15], C. D. Kilpatrick[16], P. McGill[11], E. Ramirez-Ruiz[11], K.-S. Lee[17], G. Narayan[18,19], V. Ramakrishnan[17], R. Ridden-Harper[20], A. Singh[21], Q. Wang[13], A. K. H. Kong[22], C.-C. Ngeow[23], Y.-C. Pan[23], S. Yang[24], K. W. Davis[11], A. L. Piro[25], C. Rojas-Bravo[11], J. Sommer[1,26], and S. K. Yadavalli[4,5,6]

[1] Astrophysics Research Centre, School of Mathematics and Physics, Queen's University Belfast, BT7 1NN, UK; mfulton07@qub.ac.uk
[2] Department of Physics, University of Oxford, Denys Wilkinson Building, Keble Road, Oxford OX1 3RH, UK
[3] Institute for Astronomy, University of Hawai'i, 2680 Woodlawn Drive, Honolulu, HI 96822, USA
[4] Department of Astronomy and Astrophysics, Pennsylvania State University, 525 Davey Laboratory, University Park, PA 16802, USA
[5] Institute for Computational & Data Sciences, The Pennsylvania State University, University Park, PA 16802, USA
[6] Institute for Gravitation and the Cosmos, The Pennsylvania State University, University Park, PA 16802, USA
[7] DARK, Niels Bohr Institute, University of Copenhagen, Jagtvej 128, DK-2200 Copenhagen, Denmark
[8] Technische Universität München, TUM School of Natural Sciences, Physik-Department, James-Franck-Straße 1, D-85748 Garching, Germany
[9] Max-Planck-Institut für Astrophysik, Karl-Schwarzschild Straße 1, D-85748 Garching, Germany
[10] Birmingham Institute for Gravitational Wave Astronomy and School of Physics and Astronomy, University of Birmingham, Birmingham B15 2TT, UK
[11] Department of Astronomy and Astrophysics, University of California Santa Cruz, 1156 High St., Santa Cruz, CA 95060, USA
[12] Space Telescope Science Institute, 3700 San Martin Drive, Baltimore, MD 21218, USA
[13] Department of Physics and Astronomy, The Johns Hopkins University, Baltimore, MD 21218, USA
[14] Institute for Astronomy, University of Hawai'i, 34 Ohia Ku St., Pukalani, HI 96768-8288, USA
[15] Gemini Observatory, NSF's NOIRLab, 670 N. A'ohoku Place, Hilo, Hawai'i, 96720, USA
[16] Center for Interdisciplinary Exploration and Research in Astrophysics (CIERA), Northwestern University, 1800 Sherman Ave, Evanston, IL 60201, USA
[17] Department of Physics and Astronomy, Purdue University, 525 Northwestern Avenue, West Lafayette, Indiana 47907, USA
[18] Department of Astronomy, University of Illinois at Urbana-Champaign, 1002 W. Green St., IL 61801, USA
[19] Center for Astrophysical Surveys, National Center for Supercomputing Applications, Urbana, IL 61801, USA
[20] School of Physical and Chemical Sciences—Te Kura Matū, University of Canterbury, Private Bag 4800, Christchurch 8140, New Zealand
[21] Departamento de Ciencias Fisicas, Facultad de Ciencias Exactas, Universidad Andres Bello, Fernandez Concha 700, Las Condes, Santiago, Chile
[22] Institute of Astronomy, National Tsing Hua University, Hsinchu 30013, Taiwan
[23] Graduate Institute of Astronomy, National Central University, 300 Jhongda Road, 32001 Jhongli, Taiwan
[24] Department of Astronomy, The Oskar Klein Center, Stockholm University, AlbaNova, SE-10691 Stockholm, Sweden
[25] The Observatories of the Carnegie Institution for Science, 813 Santa Barbara St., Pasadena, CA 91101, USA
[26] Universitäts-Sternwarte München, Fakultät für Physik, Ludwig-Maximilians Universität München, Scheinerstr. 1, D-81679 Munich, Germany
Received 2023 January 23; revised 2023 February 28; accepted 2023 March 2; published 2023 March 28

Abstract

We present extensive optical photometry of the afterglow of GRB 221009A. Our data cover 0.9–59.9 days from the time of Swift and Fermi gamma-ray burst (GRB) detections. Photometry in *rizy*-band filters was collected primarily with Pan-STARRS and supplemented by multiple 1–4 m imaging facilities. We analyzed the Swift X-ray data of the afterglow and found a single decline rate power law $f(t) \propto t^{-1.556\pm0.002}$ best describes the light curve. In addition to the high foreground Milky Way dust extinction along this line of sight, the data favor additional extinction to consistently model the optical to X-ray flux with optically thin synchrotron emission. We fit the X-ray-derived power law to the optical light curve and find good agreement with the measured data up to 5−6 days. Thereafter we find a flux excess in the *riy* bands that peaks in the observer frame at ~20 days. This excess shares similar light-curve profiles to the Type Ic broad-lined supernovae SN 2016jca and SN 2017iuk once corrected for the GRB redshift of $z = 0.151$ and arbitrarily scaled. This may be representative of an SN emerging from the declining afterglow. We measure rest-frame absolute peak AB magnitudes of $M_g = -19.8 \pm 0.6$ and $M_r = -19.4 \pm 0.3$ and $M_z = -20.1 \pm 0.3$. If this is an SN component, then Bayesian modeling of the excess flux would imply explosion parameters of $M_{\rm ej} = 7.1^{+2.4}_{-1.7}\,M_\odot$, $M_{\rm Ni} = 1.0^{+0.6}_{-0.4}\,M_\odot$, and $v_{\rm ej} = 33{,}900^{+5900}_{-5700}$ km s^{-1}, for the ejecta mass, nickel mass, and ejecta velocity respectively, inferring an explosion energy of $E_{\rm kin} \simeq 2.6$–9.0×10^{52} erg.

Unified Astronomy Thesaurus concepts: Gamma-ray bursts (629); Type Ic supernovae (1730); Light curves (918); X-ray photometry (1820); Optical astronomy (1776)

Supporting material: data behind figure

1. Introduction

Long-duration gamma-ray bursts (lGRBs) are typically associated with the signature of a broad-lined Type Ic supernova (SN) in their light curves and spectra, as the afterglow fades and an SN rises within 10–20 days. Since the at R.A. = 288°.26459 decl. = +19°.77341) are listed in Table 1. The photometric zero points on the PS2 target images were set with the Pan-STARRS1 3π catalog (Flewelling et al. 2020). We typically used 100–200 s exposures and stacked images on any one night (from 1 to 12 images, depending on target magnitude and sky brightness).

Two methods were used to measure the flux on the difference images. A difference image was created from each individual exposure, and a point-spread function (PSF) was forced at the GRB 221009A afterglow position (measured from the early, bright epochs). We statistically combined the measured PSF flux from each difference image through a weighted average, using a temporal bin size of 1 day. For the later Pan-STARRS epochs ($t - T_0 > 34$ days) we increased the bin size to 4 days in the zy filters to enhance the signal-to-noise. Alternatively, an image stack on each night was created, and a difference image produced from the stack. Again, a PSF was forced at the GRB afterglow position and flux measurement used. All fluxes and magnitudes quoted here are in microjanskys (μJy) and AB magnitudes. The results from image stacking were used instead of the weighted average of fluxes only when the object fell on a masked chip within the camera CCD, which prevented the typical pipeline processing of target images described in Chambers et al. (2016). Regardless of the method, the resulting flux measurements were calibrated carefully to the Pan-STARRS1 DR2 3π reference catalog (Flewelling et al. 2020) using approximately 1000 field stars visible within the target frames.

While most of the data here are provided by PS2, we gathered other important photometric data with the 0.4 m Ritchey–Chrétien Super Light Telescope (SLT; Chen et al. 2022) and Cassegrain Lulin One-meter Telescope (LOT) at the Lulin Observatory, Taiwan; the Dark Energy Camera (DECam) on the 4 m Telescope at the Cerro Tololo Inter-American Observatory, Chile; the 4.1 m Southern Astrophysical Research (SOAR) Telescope, Chile; the 1 m Swope Telescope, Chile; the IO:O on the 2.2 m Liverpool Telescope (LT), La Palma; and MegaCam on the 3.6 m Canada–France–Hawaii Telescope, Hawaii.

Eight epochs of DECam observations were conducted between 2022 October 16 (MJD 59,868.01) and 2022 October 31 (MJD 59,883.011) taking between 2 and 5×100 s exposures in the filters r and i. The data were reduced and photometrically calibrated with the `photpipe` package (Rest et al. 2014) using the images from 2022 October 16 as templates. These were subtracted from all subsequent images and a PSF was forced at the afterglow position on the difference images. Since the template contains transient flux and we were not able to get a final set of templates in which the afterglow had faded, we applied an offset to match the DECam r-filter flux measured on MJD 59,880.01 to the SOAR epoch on MJD 59,880.02, and the DECam i-filter flux measured on MJD 59,875.01 to the PS2 epoch on MJD 59,875.23. These offsets were subsequently applied to all the DECam difference images in the respective filters. Data from Swope were subjected to difference imaging, using the Pan-STARRS1 3π references as templates and forced photometry was implemented thereafter.

We used the three epochs of Hubble Space Telescope (HST) data that are publicly available through the DDT program of Levan et al. (2022). The WFC3 passbands of the F625W, F775W, and F098M filters are similar to that of the $r_{\rm PS}$, $i_{\rm PS}$, and $y_{\rm PS}$ filters respectively (see Section 4). PSF magnitudes were measured on the HST target images using the DOLPHOT package (Dolphin 2016). Observations conducted by SLT, LOT, SOAR, LT, and MegaCam between October 10 and November 8 were not subjected to any form of image subtraction; instead, a PSF was forced onto the target images using python packages, *Astropy* and *Photutils*,[27] and the resulting flux measurements were calibrated against Pan-STARRS1 3π survey field stars.

Since no difference imaging was applied to the SLT, LOT, SOAR, or LT one may be concerned by late-time host-galaxy flux contamination. This is particularly concerning when the measured flux of the transient is comparable to, or fainter than, the limits we can put on the host galaxy from the Pan-STARRS1 3π data (see Table 1). However, the photometry between different instruments (with and without difference imaging) is consistent within the statistical uncertainties. A probable faint host galaxy is visible in the deepest F625W and F775W HST images, approximately 0″.5 offset to the northeast. However, this is too faint to contribute significantly to the r and i photometry and our $y_{\rm PS}$ data are all image subtracted. Hence we make the assumption that there is no host-galaxy flux contributing to the nondifferenced images in the filters r, i, or z. This can only be confirmed with deep observations in the next observing season. We list our measurements also in fluxes (microjanskys) within Appendix A so that a future correction can be applied should that be necessary.

3. Analysis of the X-Ray and Optical Afterglow

The X-ray counterpart to GRB 221009A was observed by the Neil Gehrels Swift Observatory X-ray telescope (XRT) starting 0.9 hr after the Fermi trigger (Veres et al. 2022), and is still observing at the time of writing. We downloaded the Swift XRT data to date from the Swift Burst Analyser (Evans et al. 2007, 2009, 2010). A single decaying power law can best describe the XRT light curve. We fit a power-law component to the first 60 days of flux data, using the fluxes and not flux densities so as not to introduce any spectral bias, and found the light curve is described with $f(t) \propto t^{-1.556 \pm 0.002}$. There is no evidence of any breaks in the light curve that could result from either a spectral break (e.g., the cooling break) passing through the band or a jet break. There is also no evidence of a change in the X-ray photon index (related to the spectral index), indicating no significant spectral evolution occurring over the first 60 days postburst. The Swift Burst Analyser quotes an X-ray photon index of 1.78 ± 0.01, which corresponds to a spectral index ($S(\nu) \propto \nu^{\alpha}$) of $\alpha = -0.78 \pm 0.01$. The measured X-ray light-curve decay and spectral index indicate the X-ray emission originates from optically thin synchrotron radiation, where the synchrotron cooling break has a frequency that is higher than that of the observing band.

Given that the optical light curve is also showing a decay, and that only optically thin synchrotron radiation produces a decaying light curve within the fireball model, the optical emission should be on the same branch of the afterglow spectrum as the X-ray band and thus the decay rates should be identical (Sari et al. 1998; Granot & Sari 2002). A power-law decay also best describes the measured optical decay. However, the difference between the optical and X-ray decay rates is not

[27] Python tool used to measure PSF photometry can be found on GitHub. https://github.com/mnicholl/photometry-sans-frustration.

The Astrophysical Journal Supplement Series, 266:37 (43pp), 2023 June https://doi.org/10.3847/1538-4365/acc181

Multimessenger Characterization of Markarian 501 during Historically Low X-Ray and γ-Ray Activity

H. Abe[1], S. Abe[1], V. A. Acciari[2], I. Agudo[3], T. Aniello[4], S. Ansoldi[5,98], L. A. Antonelli[4], A. Arbet-Engels[6], C. Arcaro[7], M. Artero[8], K. Asano[1], D. Baack[9], A. Babić[10], A. Baquero[11], U. Barres de Almeida[12], J. A. Barrio[11], I. Batković[7], J. Baxter[1], J. Becerra González[2], W. Bednarek[13], E. Bernardini[7], M. Bernardos[3], A. Berti[6], J. Besenrieder[6], W. Bhattacharyya[14], C. Bigongiari[4], A. Biland[15], O. Blanch[8], G. Bonnoli[4], Ž. Bošnjak[10], I. Burelli[5], G. Busetto[7], R. Carosi[16], M. Carretero-Castrillo[17], A. J. Castro-Tirado[3], G. Ceribella[1], Y. Chai[6], A. Chilingarian[18], S. Cikota[10], E. Colombo[2], J. L. Contreras[11], J. Cortina[19], S. Covino[4], G. D'Amico[20], V. D'Elia[4], P. Da Vela[16,99], F. Dazzi[4], A. De Angelis[7], B. De Lotto[5], A. Del Popolo[21], M. Delfino[8,100], J. Delgado[8,100], C. Delgado Mendez[19], D. Depaoli[22], F. Di Pierro[22], L. Di Venere[23], E. Do Souto Espiñeira[8], D. Dominis Prester[24], A. Donini[4], D. Dorner[25], M. Doro[7], D. Elsaesser[9,26], G. Emery[27], J. Escudero[3], V. Fallah Ramazani[28,101], L. Fariña[8], A. Fattorini[9], L. Foffano[4], L. Font[29], C. Fruck[6], S. Fukami[15], Y. Fukazawa[30], R. J. García López[2], M. Garczarczyk[14], S. Gasparyan[31,97], M. Gaug[29], J. G. Giesbrecht Paiva[12], N. Giglietto[23], F. Giordano[23], P. Gliwny[13], N. Godinović[32], R. Grau[8], D. Green[6], J. G. Green[6], D. Hadasch[1], A. Hahn[6], T. Hassan[19], L. Heckmann[6,97,102], J. Herrera[2], D. Hrupec[33], M. Hütten[1], R. Imazawa[30], T. Inada[1], R. Iotov[25], K. Ishio[13], I. Jiménez Martínez[19], J. Jormanainen[28], D. Kerszberg[8], Y. Kobayashi[1], H. Kubo[1], J. Kushida[34], A. Lamastra[4], D. Lelas[32], F. Leone[4], E. Lindfors[28], L. Linhoff[9], S. Lombardi[4], F. Longo[5,103], R. López-Coto[3], M. López-Moya[11], A. López-Oramas[2], S. Loporchio[23], A. Lorini[35], E. Lyard[27], B. Machado de Oliveira Fraga[12], P. Majumdar[36,104], M. Makariev[37], G. Maneva[37], N. Mang[9], M. Manganaro[24], S. Mangano[19], K. Mannheim[25,26], M. Mariotti[7], M. Martínez[8], A. Mas-Aguilar[11], D. Mazin[1,6], S. Menchiari[35], S. Mender[9], S. Mićanović[24], D. Miceli[7], T. Miener[11], J. M. Miranda[35], R. Mirzoyan[6], E. Molina[17], H. A. Mondal[36], A. Moralejo[8], D. Morcuende[11], V. Moreno[29], T. Nakamori[38], C. Nanci[4], L. Nava[4], V. Neustroev[39], M. Nievas Rosillo[2], C. Nigro[8], K. Nilsson[28], K. Nishijima[34], T. Njoh Ekoume[2], K. Noda[1], S. Nozaki[6], Y. Ohtani[1], T. Oka[40], A. Okumura[41], J. Otero-Santos[2], S. Paiano[4], M. Palatiello[5], D. Paneque[6,97], R. Paoletti[35], J. M. Paredes[17], L. Pavletić[24], M. Persic[5,105], M. Pihet[6], G. Pirola[6], F. Podobnik[35], P. G. Prada Moroni[16], E. Prandini[7], G. Principe[5], C. Priyadarshi[8], W. Rhode[9], M. Ribó[17], J. Rico[8], C. Righi[4], A. Rugliancich[16], N. Sahakyan[31,97], T. Saito[1], S. Sakurai[1], K. Satalecka[28], F. G. Saturni[4], B. Schleicher[25], K. Schmidt[9], F. Schmuckermaier[6], J. L. Schubert[9], T. Schweizer[6], J. Sitarek[13], V. Sliusar[27], D. Sobczynska[13], A. Spolon[7], A. Stamerra[4], J. Strišković[33], D. Strom[6], M. Strzys[1], Y. Suda[30], T. Surić[42], H. Tajima[41], M. Takahashi[41], R. Takeishi[1], F. Tavecchio[4], P. Temnikov[37], K. Terauchi[40], T. Terzić[24], M. Teshima[1,6], L. Tosti[43], S. Truzzi[35], A. Tutone[4], S. Ubach[29], J. van Scherpenberg[6], M. Vazquez Acosta[2], S. Ventura[35], V. Verguilov[37], I. Viale[7], C. F. Vigorito[22], V. Vitale[44], I. Vovk[1], R. Walter[27], M. Will[6], C. Wunderlich[35], T. Yamamoto[45], D. Zarić[32]

(The MAGIC Collaboration),

M. Cerruti[17,46,97], J. A. Acosta-Pulido[47], G. Apolonio[48], R. Bachev[49], M. Baloković[50,51], E. Benítez[52], I. Björklund[53,54], V. Bozhilov[55], L. F. Brown[56], A. Bugg[48], W. Carbonell[56], M. I. Carnerero[57], D. Carosati[58,59], C. Casadio[60,61], W. Chamani[53,54], W. P. Chen[62], R. A. Chigladze[63], G. Damljanovic[64], K. Epps[48], A. Erkenov[65], M. Feige[26], J. Finke[66], A. Fuentes[3], K. Gazeas[67], M. Giroletti[68], T. S. Grishina[69], A. C. Gupta[70], M. A. Gurwell,[71], E. Heidemann[26], D. Hiriart[72], W. J. Hou[62], T. Hovatta[53,73], S. Ibryamov[74], M. D. Joner[48], S. G. Jorstad[75,76], J. Kania[26], S. Kiehlmann[77,78], G. N. Kimeridze[63], E. N. Kopatskaya[69], M. Kopp[26], M. Korte[26], B. Kotas[26], S. Koyama[79,80], J. A. Kramer[81], L. Kunkel[26], S. O. Kurtanidze[63,82], O. M. Kurtanidze[63,82,83], A. Lähteenmäki[53,54], J. M. López[84], V. M. Larionov[69,85], E. G. Larionova[69], L. V. Larionova[69], C. Leto[86,87], C. Lorey[26], R. Mújica[88], G. M. Madejski[89], N. Marchili[68], A. P. Marscher[75], M. Minev[55], A. Modaressi[56], D. A. Morozova[69], T. Mufakharov[65,90], I. Myserlis[91], A. A. Nikiforova[69,85], M. G. Nikolashvili[63,82], E. Ovcharov[55], M. Perri[86,92], C. M. Raiteri[57], A. C. S. Readhead[93], A. Reimer[94], D. Reinhart[26], S. Righini[68], K. Rosenlehner[26], A. C. Sadun[95], S. S. Savchenko[69,85], A. Scherbantin[26], L. Schneider[26], K. Schoch[26], D. Seifert[26], E. Semkov[49], L. A. Sigua[63], C. Singh[56], P. Sola[47], Y. Sotnikova[65], M. Spencer[48], R. Steineke[26], M. Stojanovic[64], A. Strigachev[49], M. Tornikoski[53], E. Traianou[3], A. Tramacere[96], Yu. V. Troitskaya[69], I. S. Troitskiy[69], J. B. Trump[48], A. Tsai[62], A. Valcheva[55], A. A. Vasilyev[69], F. Verrecchia[86,92], M. Villata[57], O. Vince[64], K. Vrontaki[67], Z. R. Weaver[75], E. Zaharieva[55], and N. Zottmann[26]

[1] Japanese MAGIC Group: Institute for Cosmic Ray Research (ICRR), The University of Tokyo, Kashiwa, 277-8582 Chiba, Japan
[2] Instituto de Astrofísica de Canarias and Departamento de Astrofísica, Universidad de La Laguna, E-38200, La Laguna, Tenerife, Spain
[3] Instituto de Astrofísica de Andalucía-CSIC, Glorieta de la Astronomía s/n, E-18008, Granada, Spain
[4] National Institute for Astrophysics (INAF), I-00136 Rome, Italy
[5] Università di Udine and INFN Trieste, I-33100 Udine, Italy
[6] Max-Planck-Institut für Physik, D-80805 München, Germany
[7] Università di Padova and INFN, I-35131 Padova, Italy

simple power-law model, absorbed by intervening material with solar abundances and the Galactic column of 1.55×10^{20} cm^{-2} (Kalberla et al. 2005). In all cases, the spectra are adequately described by such a simple model, but in all three cases, we see a modest improvement to the spectral fit when we attempt a more complex model, such as log parabola. While this is not significant in any of the three pointings reported here, this spectral behavior is fully consistent with that reported in Furniss et al. (2015).

2.4. Swift

The study reported in this paper makes use of two instruments on board the Neil Gehrels Swift Gamma-Ray Burst Observatory (Gehrels et al. 2004); namely, XRT (Burrows et al. 2005) and the Ultraviolet/Optical Telescope (UVOT; Roming et al. 2005). The related observations were organized and performed within the framework of planned extensive multi-instrument campaigns on Mrk 501, which occur yearly since 2008 (Aleksić et al. 2015a). In this study we consider all observations within the years 2017 and 2020 for both the UVOT and XRT instruments with an extension using the all data from 2005 to 2020 for the long-term studies on the XRT light curve.

The Swift-XRT observations are performed in the Windowed Timing (WT) and Photon Counting (PC) readout modes, and the data are processed using the XRTDAS software package (v.3.5.0) developed by the ASI Space Science Data Center (SSDC), and released by the NASA High Energy Astrophysics Archive Research Center (HEASARC) in the HEASoft package (v.6.26.1). The calibration files from Swift-XRT CALDB (version 20190910) are used within the `xrtpipeline` to calibrate and clean the events. The X-ray spectrum from each observation is extracted from the summed cleaned event file. For WT readout mode data, events for the spectral analysis are selected within a circle of 20 pixel (∼46″) radius, which contains about 90% of the point-spread function (PSF), centered at the source position. For PC readout mode data, the source count rate is above ∼0.5 counts s^{-1} and data are significantly affected by pileup in the inner part of the PSF. We remove pileup effects by excluding events within a 4–6 pixel radius circles centered on the source position and use an outer radius of 30 pixels. The background is estimated from a nearby circular region with a radius of 20 and 40 pixels for WT and PC data, respectively. The ancillary response files (ARFs) are generated with the `xrtmkarf` task applying corrections for PSF losses and CCD defects using the cumulative exposure map. The 0.3–10 keV source spectra are binned using the `grppha` task to ensure a minimum of 20 counts per bin, and then are modeled in XSPEC using power-law and log-parabola models (with a pivot energy fixed at 1 keV) that include photoelectric absorption due to a neutral-hydrogen column density fixed to the Galactic 21 cm value in the direction of Mrk 501, namely, 1.55×10^{20} cm^{-2} (Kalberla et al. 2005).

The Swift-UVOT data analysis reported here relates only to all the observations with the UV filters (namely, W1, M2, and W2) performed during the Swift pointings to Mrk 501, 259 exposures. Differently to the optical bands, the emission in the UV is not affected by the emission from the host galaxy, which is very low at these frequencies. We perform aperture photometry for all filters using the standard UVOT software within the HEAsoft package (v6.23) and the calibration included in the latest release of the CALDB (20201026). The source photometry is evaluated following the recipe in Poole et al. (2008), extracting source counts from a circular aperture of 5″ radius, and the background ones from an annular aperture of 26″ and 34″ for the inner and outer radii in all filters. The count rates are converted to fluxes using the standard zero-points (Breeveld et al. 2011) and finally dereddened considering an $E(B-V)$ value of 0.017 (Schlegel et al. 1998; Schlafly & Finkbeiner 2011) for the UVOT filters effective wavelengths and the mean galactic interstellar extinction curve from Fitzpatrick (1999).

2.5. Optical

We focus on the R band for the optical wave band, as it is often done in previous studies of Mrk 501, and HSPs, in general. The optical data are collected within the GLAST and AGILE program (GASP) of the Whole Earth Blazar Telescope (WEBT; Villata et al. 2008, 2009; Gazeas 2016; Carnerero et al. 2017; Raiteri et al. 2017) including the instruments: West Mountain (91 cm), Vidojevica (140 cm), Vidojevica (60 cm), University of Athens Observatory (UOAO), Tijarafe (40 cm), Teide (STELLA-I), Teide (IAC80), St. Petersburg, Skinakas, San Pedro Martir (84 cm), Rozhen (200 cm), Rozhen (50/70 cm), Perkins (1.8 m), New Mexico Skies (T21), New Mexico Skies (T11), Lulin (SLT), Hans Haffner, Crimean (70 cm; ST-7; pol), Crimean (70 cm; ST-7), Crimean (70 cm; AP7), Connecticut (51 cm), Burke-Gaffney, Belogradchik, Astro-Camp (T7), and Abastumani (70 cm). Additional data were provided by AAVSO and by the Tuorla observatory using the Kungliga Vetenskapsakademien (KVA) telescope.

The data analysis is performed using standard prescriptions. The host galaxy contribution is subtracted according to the Nilsson et al. (2007) recipe for an aperture of 7.″5, which was adopted by the participating instruments. The R-band flux is then corrected for Galactic extinction assuming the values reported by Schlafly & Finkbeiner (2011). In order to account for instrumental (systematic) differences among the analyses related to the various telescopes (i.e., due to different filter spectral responses and analysis procedures, combined with the strong host galaxy contribution), offsets of a few mJy have to be applied. To calculate the corresponding offsets, KVA is used as a reference due to its good time coverage taking simultaneous data within two days into account. For data sets containing majorly data collected in 2020, when KVA was not operational anymore, Hans Haffner is used as the reference. The corresponding offsets can be found in Table 11. To further account for instrumental (systematic) uncertainties, a relative error of 2% is added in quadrature to the statistical uncertainties of all the flux values, as done in previous works (Ahnen et al. 2018). Afterward, the data sets from all the instruments are combined into a single R-band light curve and binned in 1 day time intervals.

2.6. Radio

We report here radio observations from the single-dish telescopes at the Owens Valley Radio Observatory (OVRO) operating at 15 GHz; the Medicina observatory operating at 8 GHz and 24 GHz; RATAN-600 at 4.7 GHz, 11.2 GHz, and 22 GHz; the Metsähovi Radio Observatory at 37 GHz; IRAM at 100 GHz and 230 GHz; the interferometry observations from the Very Long Baseline Array (VLBA) at 43 GHz; and the Submillimeter Array (SMA) at 230 GHz and 345 GHz.

Monthly Notices of the ROYAL ASTRONOMICAL SOCIETY

MNRAS **522,** 102–116 (2023) https://doi.org/10.1093/mnras/stad942
Advance Access publication 2023 March 29

The optical behaviour of BL Lacertae at its maximum brightness levels: a blend of geometry and energetics

C. M. Raiteri,[1★] M. Villata,[1] S. G. Jorstad,[2,3] A. P. Marscher,[2] J. A. Acosta Pulido,[4,5] D. Carosati,[6,7] W. P. Chen,[8] M. D. Joner,[9] S. O. Kurtanidze,[10] C. Lorey,[11] A. Marchini,[12] K. Matsumoto,[13] D. O. Mirzaqulov,[14] S. S. Savchenko,[3,15,16] A. Strigachev,[17] O. Vince,[18] P. Aceti,[19,20] G. Apolonio,[9] C. Arena,[21] A. Arkharov,[16] R. Bachev,[17] N. Bader,[11] M. Banfi,[19] G. Bonnoli,[22] G. A. Borman,[23] V. Bozhilov,[24] L. F. Brown,[25] W. Carbonell,[25] M. I. Carnerero,[1] G. Damljanovic,[18] V. Dhiman,[26,27] S. A. Ehgamberdiev,[14,28] D. Elsaesser,[11,29] M. Feige,[11] D. Gabellini,[30] D. Galán,[5] G. Galli,[31] H. Gaur,[26] K. Gazeas,[32] T. S. Grishina,[3] A. C. Gupta,[26,33,34] V. A. Hagen-Thorn,[3] M. K. Hallum,[2] M. Hart,[2] K. Hasuda,[35] K. Heidemann,[11] B. Horst,[11] W.-J. Hou,[8] S. Ibryamov,[36] R. Z. Ivanidze,[10] M. D. Jovanovic,[18] G. N. Kimeridze,[10] S. Kishore,[26,37] S. Klimanov,[16] E. N. Kopatskaya,[3] O. M. Kurtanidze,[10,38,39] P. Kushwaha,[26,40] D. J. Lane,[41] E. G. Larionova,[3] S. Leonini,[42] H. C. Lin,[8] K. Mannheim,[11,43] G. Marino,[21,44] M. Minev,[17,24] A. Modaressi,[25] D. A. Morozova,[3] F. Mortari,[30] S. V. Nazarov,[23] M. G. Nikolashvili,[10] J. Otero Santos,[4,5] E. Ovcharov,[24] R. Papini,[44] V. Pinter,[45,46,47] C. A. Privitera,[12] T. Pursimo,[45,46] D. Reinhart,[11] J. Roberts,[9] F. D. Romanov,[48,49] K. Rosenlehner,[11] T. Sakamoto,[35] F. Salvaggio,[21,44] K. Schoch,[11] E. Semkov,[17] J. Seufert,[11] D. Shakhovskoy,[23] L. A. Sigua,[10] C. Singh,[25] R. Steineke,[11] M. Stojanovic,[18] T. Tripathi,[26,37] Y. V. Troitskaya,[3] I. S. Troitskiy,[3] A. Tsai,[8] A. Valcheva,[24] A. A. Vasilyev,[3] K. Vrontaki,[32] Z. R. Weaver,[2] J. H. F. Wooley,[9] E. Zaharieva[24] and A. V. Zhovtan[23]

Affiliations are listed at the end of the paper

Accepted 2023 March 27. Received 2023 March 27; in original form 2023 January 14

ABSTRACT

In 2021 BL Lacertae underwent an extraordinary activity phase, which was intensively followed by the Whole Earth Blazar Telescope (WEBT) Collaboration. We present the WEBT optical data in the *BVRI* bands acquired at 36 observatories around the world. In mid-2021 the source showed its historical maximum, with $R = 11.14$. The light curves display many episodes of intraday variability, whose amplitude increases with source brightness, in agreement with a geometrical interpretation of the long-term flux behaviour. This is also supported by the long-term spectral variability, with an almost achromatic trend with brightness. In contrast, short-term variations are found to be strongly chromatic and are ascribed to energetic processes in the jet. We also analyse the optical polarimetric behaviour, finding evidence of a strong correlation between the intrinsic fast variations in flux density and those in polarization degree, with a time delay of about 13 h. This suggests a common physical origin. The overall behaviour of the source can be interpreted as the result of two mechanisms: variability on time-scales greater than several days is likely produced by orientation effects, while either shock waves propagating in the jet, or magnetic reconnection, possibly induced by kink instabilities in the jet, can explain variability on shorter time-scales. The latter scenario could also account for the appearance of quasi-periodic oscillations, with periods from a few days to a few hours, during outbursts, when the jet is more closely aligned with our line of sight and the time-scales are shortened by relativistic effects.

Key words: galaxies: active – BL Lacertae objects: general – BL Lacertae objects: individual: BL Lacertae – galaxies: jets.

1 INTRODUCTION

Active galactic nuclei (AGNs) are among the most powerful sources in the Universe. Their central engine is a supermassive black hole fed by an accretion disc. Some AGNs exhibit two plasma jets launched roughly perpendicularly to the accretion disc. In blazars, one relativistic jet is directed towards us, so that the jet emission undergoes Doppler boosting. This implies a series of effects, among which are an enhancement of the flux, a blueshift of the emitted frequencies, and a shortening of the variability time-scales (e.g. Urry & Padovani 1995; Blandford, Meier & Readhead 2019).

★ E-mail: claudia.raiteri@inaf.it

Table 1. Details of the 43 optical data sets contributing to this paper.

Data set	Country	Diameter	Filters	N_{obs}	Symbol	Colour
Abastumani	Georgia	70	*R*	671	◇	Dark green
Abbey Ridge	Canada	35	*BVRI*	268	▷	Orange
Aoyama Gakuin	Japan	35	*BVRI*	18	□	Cyan
ARIES	India	104	*BVRI*	19	□	Blue
ARIES	India	130	*BVRI*	27	□	Green
Athens[a]	Greece	40	*R*	141	◇	Cyan
Beli Brezi	Bulgaria	20	*VR*	152	*	Blue
Belogradchik[b]	Bulgaria	60	*BVRI*	191	+	Cyan
Burke-Gaffney	Canada	61	*VR*	660	▷	Dark green
Catania (Arena)	Italy	20	*BVR*	40	×	Cyan
Catania (GAC)	Italy	25	*VRI*	61	△	Cyan
Connecticut	USA	51	*VR*	434	*	Grey
Crimean (AP7p)	Russia	70	*BVRI*	368	×	Magenta
Crimean (ST-7)	Russia	70	*BVRI*	432	+	Magenta
Crimean (ST-7; pol)[b]	Russia	70	*R*	535	×	Dark green
Crimean (ZTSh)[c]	Russia	260	*R*	223	△	Red
Felizzano	Italy	20	*R*	14	*	Magenta
GiaGa	Italy	36	*BVR*	62	*	Black
Haleakala (LCO)	USA	40	*VR*	50	+	Blue
Hans Haffner	Germany	50	*BVR*	1254	◦	Red
Hypatia	Italy	25	*R*	827	◇	Red
Lowell (LDT)	USA	430	*VR*	18	◦	Magenta
Lulin (SLT)	Taiwan	40	*R*	592	×	Violet
McDonald (LCO)	USA	40	*VR*	117	×	Blue
Montarrenti	Italy	53	*BVRI*	434	◦	Dark green
Monte San Lorenzo	Italy	53	*R*	165	◦	Green
Mt. Maidanak	Uzbekistan	60	*BVRI*	2961	◇	Green
Osaka Kyoiku	Japan	51	*BR*	569	□	Orange
Perkins[b]	USA	180	*BVRI*	824	◦	Blue
Roque (NOT; e2v)[b]	Spain	256	*BVRI*	124	+	Green
Rozhen	Bulgaria	200	*BVRI*	51	□	Red
Rozhen	Bulgaria	50/70	*BVRI*	181	×	Orange
Seveso	Italy	30	*VR*	69	+	Violet
Siena	Italy	30	*VRI*	2367	◇	Blue
Skinakas	Greece	130	*BVRI*	1976	×	Black
St. Petersburg[b]	Russia	40	*BVRI*	347	+	Orange
Teide (IAC80)	Spain	80	*VR*	308	*	Green
Teide (LCO)	Spain	40	*VR*	76	+	Black
Tijarafe	Spain	40	*BR*	2946	*	Red
Vidojevica[d]	Serbia	140	*BVRI*	647	□	Black
Vidojevica[d]	Serbia	60	*BVRI*	37	△	Black
West Mountain	USA	91	*BVR*	2152	△	Magenta
Wild Boar	Italy	24	*VR*	28	△	Green

Note. 'LCO' refers to telescopes belonging to the Las Cumbres Observatory global telescope network.
[a]University of Athens Observatory (UOAO).
[b]Also polarimetry.
[c]Only polarimetry.
[d]Astronomical Station Vidojevica.

in Fig. 1, where the time difference between subsequent data points is plotted for all bands in bins of 1 h each. In the case of the best-sampled *R* bands, more than 90 per cent of data pairs are contained in the first bin.

The resulting cleaned light curves are shown in Fig. 2 in observed magnitudes. The peak of the mid-2021 outburst represents the observed historical maximum, with $B = 12.75 \pm 0.02$, $V = 11.75 \pm 0.02$, $R = 11.14 \pm 0.03$, and $I = 10.47 \pm 0.01$ on August 6–7. The overall variation amplitude, defined as the maximum minus minimum magnitude, is 2.40, 2.36, 2.31, and 2.17 in the *B*, *V*, *R*, and *I* filters, respectively. Although the light curves have different sampling, the increasing amplitude variation with increasing frequency is typical of BL Lac objects. An enlargement of the *R*-band light curve of Fig. 2 is shown in Fig. 3 to better appreciate the source short-term variability.

In the following analysis we will also use flux densities in mJy. They were obtained from the observed magnitudes using the zero-mag flux densities by Bessell, Castelli & Plez (1998), after correcting for the Galactic extinction values given by the NASA/IPAC Extragalactic Database[2] (NED): 1.192, 0.901, 0.713, and 0.495 mag in the *B*, *V*, *R*, and *I* bands, respectively. We also corrected for the emission contribution of the host galaxy according to Raiteri et al. (2009, 2010), i.e. we adopted a host galaxy flux density of 1.297,

[2]https://ned.ipac.caltech.edu/

The Astrophysical Journal, 952:86 (17pp), 2023 July 20 https://doi.org/10.3847/1538-4357/acd5d5

SN2019wxt: An Ultrastripped Supernova Candidate Discovered in the Electromagnetic Follow-up of a Gravitational Wave Trigger

Hinna Shivkumar[1], Amruta D. Jaodand[2], Arvind Balasubramanian[3], Christoffer Fremling[2], Alessandra Corsi[3], Anastasios Tzanidakis[4], Samaya Nissanke[5,6], Mansi Kasliwal[2], Murray Brightman[2], Geert Raaijmakers[5], Kristin Kruse Madsen[7], Fiona Harrison[2], Dario Carbone[8], Nayana A. J.[9], Jean-Michel Désert[1], and Igor Andreoni[10,11,12]

[1] Anton Pannekoek Institute for Astronomy, University of Amsterdam, Science Park 904, 1098 XH Amsterdam, The Netherlands; h.shivkumar@uva.nl
[2] California Institute of Technology, 1200 E. California Boulevard, Pasadena, CA 91125, USA; ajaodand@caltech.edu
[3] Department of Physics and Astronomy, Texas Tech University, Box 1051, Lubbock, TX 79409-1051, USA
[4] University of Washington, 3910 15th Avenue NE, Seattle, WA 98195, USA
[5] GRAPPA, Anton Pannekoek Institute for Astronomy and Institute of High-Energy Physics, University of Amsterdam, Science Park 904,1098 XH Amsterdam, The Netherlands
[6] Nikhef, Science Park 105, 1098 XG Amsterdam, The Netherlands
[7] CRESST and X-ray Astrophysics Laboratory, NASA Goddard Space Flight Center, Greenbelt, MD 20771, USA
[8] University of the Virgin Islands, 2 Brewers Bay Road, Charlotte Amalie, USVI 00802, USA
[9] Indian Institute of Astrophysics, II Block, Koramangala, Bangalore 560034, India
[10] Joint Space-Science Institute, University of Maryland, College Park, MD 20742, USA
[11] Department of Astronomy, University of Maryland, College Park, MD 20742, USA
[12] Astrophysics Science Division, NASA Goddard Space Flight Center, Mail Code 661, Greenbelt, MD 20771, USA
Received 2022 August 19; revised 2023 March 29; accepted 2023 April 12; published 2023 July 19

Abstract

We present optical, radio, and X-ray observations of a rapidly evolving transient SN2019wxt (PS19hgw), discovered during the search for an electromagnetic counterpart to the gravitational-wave (GW) trigger S191213g. Although S191213g was not confirmed as a significant GW event in the off-line analysis of LIGO-Virgo data, SN2019wxt remained an interesting transient due to its peculiar nature. The optical/near-infrared (NIR) light curve of SN2019wxt displayed a double-peaked structure evolving rapidly in a manner analogous to currently known ultrastripped supernovae (USSNe) candidates. This double-peaked structure suggests the presence of an extended envelope around the progenitor, best modeled with two components: (i) early-time shock-cooling emission and (ii) late-time radioactive ^{56}Ni decay. We constrain the ejecta mass of SN2019wxt at $M_{\rm ej} \approx 0.20 M_\odot$, which indicates a significantly stripped progenitor that was possibly in a binary system. We also followed up SN2019wxt with long-term Chandra and Jansky Very Large Array observations spanning ∼260 days. We detected no definitive counterparts at the location of SN2019wxt in these long-term X-ray and radio observational campaigns. We establish the X-ray upper limit at 9.93×10^{-17} erg cm^{-2} s^{-1} and detect an excess radio emission from the region of SN2019wxt. However, there is little evidence for SN1993J- or GW170817-like variability of the radio flux over the course of our observations. A substantial host-galaxy contribution to the measured radio flux is likely. The discovery and early-time peak capture of SN2019wxt in optical/NIR observations during EMGW follow-up observations highlight the need for dedicated early, multiband photometric observations to identify USSNe.

Unified Astronomy Thesaurus concepts: Core-collapse supernovae (304); Supernovae (1668); Ejecta (453); Stellar remnants (1627); Gravitational wave sources (677); X-ray sources (1822); X-ray astronomy (1810); Radio interferometry (1346); Extragalactic radio sources (508); Spectral line identification (2073); Transient detection (1957); Transient sources (1851)

Supporting material: data behind figure

1. Introduction

Massive stars at the endpoints of their lives undergo mass loss through the ejection of some or all of their hydrogen (and possibly helium) envelopes, eventually collapsing in what are known as stripped-envelope core-collapse supernovae (SESNe; Clocchiatti et al. 1996; Filippenko 1997; Gal-Yam et al. 2014). The extent to which the outer layers of massive stars are stripped dictates their spectroscopic classification into their various subclasses. Partial stripping in Type IIb supernovae (SNe) is supported by the presence of Balmer lines, while strong stripping in Type Ic SNe is evident by the absence of both hydrogen and helium lines. The current population of SESNe suggests that the ejection of the progenitor envelopes can be driven by (a) mass loss via stellar wind (Begelman & Sarazin 1986; Woosley & Weaver 1995; Pod 2001), or (b) mass transfer during binary interaction (Podsiadlowski et al. 1992; Yoon et al. 2010; Smith et al. 2011; Yoon 2017).

Large uncertainties currently persist in our understanding of the progenitors of SESNe. Specifically, if any links exist between the various SESNe subclasses, and if different subclasses have preferred mass-loss mechanisms. At the same time, the observational picture of SESNe has been evolving in the last few years as wide-field optical surveys have accelerated

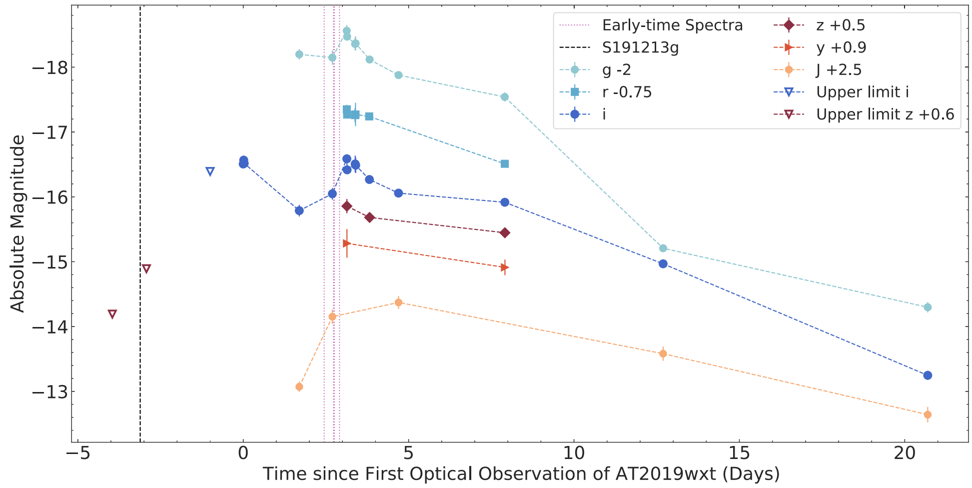

Figure 1. Galactic extinction-corrected optical and NIR light curves of the transient SN2019wxt using the data from Table 7. The cyan, light blue, blue, magenta, dark red, orange, and yellow markers represent photometric data in the *g*, *r*, *i*, *z*, y, and *J* band, respectively, and the markers for each band are connected by a dashed line to visually track the photometric evolution. The magnitudes are offset vertically for better visibility and the times displayed are relative to the first optical observation at MJD 58833.305, used as a reference epoch henceforth. The vertical black dashed line indicates the time of the GW trigger S191213g, for reference. Vertical, dotted, magenta lines indicate epochs where early-time spectroscopic observations were used in this work (see 2.2.2).

Sloan Digital Sky Survey (SDSS) images of KUG 0152+311, and the source photometry was derived in the AB magnitude system (Fremling 2019).

The GROWTH collaboration also obtained 300 s exposure images in *g*, *r*, and *i* filters with the Lulin 1 m Telescope (LOT) located in Taiwan. The LOT magnitudes, also in the AB magnitude system, are calibrated against the PS1 catalog (Kong 2019). Follow-up observations of SN2019wxt were also conducted with the Large Monolithic Imager (Bida et al. 2014) on the 4.3 m Lowell's Discovery Channel Telescope (DCT; located in Arizona) for each of the *griz* filters. The magnitudes are calibrated with the SDSS catalog and are presented in the AB system (Dichiara & a larger Collaboration 2019). Simultaneously, optical observations of SN2019wxt were also undertaken with the three-channel imager 3KK camera (Lang-Bardl et al. 2016) on the 2 m telescope at the Wendelstein Observatory. Observations were obtained on five epochs for each of the filters (*g'*, *i'*, *J*). Aperture photometry was performed using eight comparison stars within the field of view of the detector. Magnitude errors include statistical errors in the measurement of the magnitude of SN2019wxt and in the zero-point calculation (Hopp et al. 2020).

The observations and photometric measurements are summarized in Table 7 and span ≈20.7 days since the initial detection. The multiband light curves are collectively displayed in Figure 1. We corrected apparent magnitudes for Galactic extinction using the data available on the foreground galactic extinction for the host galaxy KUG 0152+311 on NED for each band. The NED calculates Galactic extinction values assuming the Fitzpatrick (1999) reddening law with $R_V \equiv A(V)/E(B-V) = 3.1$.

2.2.2. Spectroscopic Observations

Early-time spectroscopic observations of SN2019wxt were taken on 2019 December 18 and 19 (see Table 8). The initial spectroscopic observations were unable to firmly classify the transient (Dutta et al. 2019; Izzo et al. 2019; Srivastav & Smartt 2019). SN2019wxt showed narrow lines consistent with the host-galaxy redshift of $z = 0.037$, and a blue, relatively featureless continuum with a broad feature at 5400–6200 Å. Vogl et al. (2019) identified the broad feature as He I lines and suggested that SN2019wxt was either a young Type Ib or perhaps Type IIb supernova given the blue continuum. The similarities of the spectra to SN 2011fu (Kumar et al. 2013) prompted Vallely (2019) to classify SN2019wxt as a Type IIb. This supernova classification was subsequently supported by Valeev & Castro-Rodriguez (2019) and Becerra-Gonzalez & a larger Collaboration (2019).

In this work, we use early-time spectroscopic observations obtained with various telescopes, such as: (i) the 2 m Himalayan Chandra Telescope (HCT) at Indian Astronomical Observatory at Hanle; (ii) the 8.2 m Very Large Telescope (VLT) UT1 at European Southern Observatory (ESO) at Paranal Observatory, Chile; (iii) the 3.58 m New Technology Telescope (NTT) at La Silla Observatory, as part of the extended-Public ESO Spectroscopic Survey for Transient Objects (ePESSTO; PI: Smartt); and (iv) the 8.4 m Large Binocular Telescope (LBT) at LBT Observatory in Arizona, USA. The HCT observations were conducted with the Hanle Faint Object Spectrograph Camera (HFOSC2) instrument (Dutta et al. 2019). HCT/HFOSC2 provides low- to medium-resolution grism spectroscopy with a resolution of 150–4500 based on grism settings. HCT observations in this work used grism 7 to provide a resolution of 1200 for the observations in the wavelength range of 3800–7500 Å. The VLT observations were carried out with the FOcal Reducer/low dispersion Spectrograph 2 (FORS2) instrument on UT1 Cassegrain focus in long-slit mode (slit-width of 1″) to obtain spectroscopic observations of SN2019wxt (Vogl et al. 2019). The long-slit mode provides a resolution of 260–2600. ESO-NTT was used with the ESO Faint Object Spectrograph (EFOSC2) on Nasmyth B focus (Müller Bravo et al. 2019). EFOSC2 provides low-resolution spectroscopy of faint objects. The

The Astrophysical Journal, 951:34 (26pp), 2023 July 1 https://doi.org/10.3847/1538-4357/acc6c3

Supernova 2020wnt: An Atypical Superluminous Supernova with a Hidden Central Engine

Samaporn Tinyanont[1,2], Stan E. Woosley[1], Kirsty Taggart[1], Ryan J. Foley[1], Lin Yan[3], Ragnhild Lunnan[4], Kyle W. Davis[1], Charles D. Kilpatrick[5], Matthew R. Siebert[6], Steve Schulze[7], Chris Ashall[8], Ting-Wan Chen[4], Kishalay De[9], Georgios Dimitriadis[10], Dillon Z. Dong[3], Christoffer Fremling[3], Alexander Gagliano[11], Saurabh W. Jha[12], David O. Jones[13], Mansi M. Kasliwal[3], Hao-Yu Miao[14], Yen-Chen Pan[14], Daniel A. Perley[15], Vikram Ravi[3], César Rojas-Bravo[1], Itai Sfaradi[16], Jesper Sollerman[4], Vanessa Alarcon[1], Rodrigo Angulo[17], Karoli E. Clever[18], Payton Crawford[1], Cirilla Couch[1], Srujan Dandu[1], Atirath Dhara[1], Jessica Johnson[1], Zhisen Lai[1], and Carli Smith[19]

[1] Department of Astronomy and Astrophysics, University of California, Santa Cruz, CA 95064, USA; samaporn@narit.or.th
[2] National Astronomical Research Institute of Thailand, 260 Moo 4, Donkaew, Maerim, Chiang Mai, 50180, Thailand
[3] Division of Physics, Mathematics and Astronomy, California Institute of Technology, Pasadena, CA 91125, USA
[4] The Oskar Klein Centre, Department of Astronomy, Stockholm University, AlbaNova, SE-106 91 Stockholm, Sweden
[5] Center for Interdisciplinary Exploration and Research in Astrophysics (CIERA) and Department of Physics and Astronomy, Northwestern University, Evanston, IL 60208, USA
[6] Space Telescope Science Institute, 3700 San Martin Drive, Baltimore, MD 21218, USA
[7] The Oskar Klein Centre, Department of Physics, Stockholm University, AlbaNova, SE-106 91 Stockholm, Sweden
[8] Department of Physics, Virginia Tech, Blacksburg, VA 24061, USA
[9] MIT-Kavli Institute for Astrophysics and Space Research, 77 Massachusetts Avenue, Cambridge, MA 02139, USA
[10] School of Physics, Trinity College Dublin, The University of Dublin, Dublin 2, Ireland
[11] Department of Astronomy, University of Illinois at Urbana-Champaign, 1002 W. Green Street, IL 61801, USA
[12] Department of Physics and Astronomy, Rutgers, the State University of New Jersey, Piscataway, NJ 08854-8019, USA
[13] Gemini Observatory, NSF's NOIRLab, 670 N. A'ohoku Place, Hilo, HI 96720, USA
[14] Graduate Institute of Astronomy, National Central University, 300 Zhongda Road, Zhongli, Taoyuan 32001, Taiwan
[15] Astrophysics Research Institute, Liverpool John Moores University, IC2, Liverpool Science Park, 146 Brownlow Hill, Liverpool, L3 5RF, UK
[16] Racah Institute of Physics, The Hebrew University of Jerusalem, Jerusalem 91904, Israel
[17] Department of Physics and Astronomy, The Johns Hopkins University, Baltimore, MD 21218, USA
[18] Department of Biomolecular Engineering and Bioinformatics, Baskin School of Engineering, University of California, Santa Cruz, CA 95064, USA
[19] Ken and Mary Alice Lindquist Department of Nuclear Engineering, The Pennsylvania State University, University Park, PA 16802, USA
Received 2022 November 4; revised 2023 March 17; accepted 2023 March 17; published 2023 June 29

Abstract

We present observations of a peculiar hydrogen- and helium-poor stripped-envelope (SE) supernova (SN) 2020wnt, primarily in the optical and near-infrared (near-IR). Its peak absolute bolometric magnitude of -20.9 mag ($L_{\rm bol,\ peak} = (6.8 \pm 0.3) \times 10^{43}$ erg s^{-1}) and a rise time of 69 days are reminiscent of hydrogen-poor superluminous SNe (SLSNe I), luminous transients potentially powered by spinning-down magnetars. Before the main peak, there is a brief peak lasting <10 days post explosion, likely caused by interaction with circumstellar medium (CSM) ejected ∼years before the SN explosion. The optical spectra near peak lack a hot continuum and O II absorptions, which are signs of heating from a central engine; they quantitatively resemble those of radioactivity-powered hydrogen/helium-poor Type Ic SESNe. At ∼1 yr after peak, nebular spectra reveal a blue pseudo-continuum and narrow O I recombination lines associated with magnetar heating. Radio observations rule out strong CSM interactions as the dominant energy source at +266 days post peak. Near-IR observations at +200–300 days reveal carbon monoxide and dust formation, which causes a dramatic optical light-curve dip. Pair-instability explosion models predict slow light curve and spectral features incompatible with observations. SN 2020wnt is best explained as a magnetar-powered core-collapse explosion of a 28 $M_\odot$ pre-SN star. The explosion kinetic energy is significantly larger than the magnetar energy at peak, effectively concealing the magnetar-heated inner ejecta until well after peak. SN 2020wnt falls into a continuum between normal SNe Ic and SLSNe I, and demonstrates that optical spectra at peak alone cannot rule out the presence of a central engine.

Unified Astronomy Thesaurus concepts: Core-collapse supernovae (304); Massive stars (732); Dust formation (2269)

Supporting material: data behind figures

1. Introduction

Massive stars, $\gtrsim 8\,M_\odot$, conclude their evolution in many different variants of core-collapse supernovae (CCSNe). Stars that have lost their hydrogen envelope throughout their evolution, either via winds or binary interaction, produce a stripped-envelope (SE) supernova (SN), which shows little (Type IIb) to no sign of hydrogen (Type Ib) or helium (Type Ic) in their spectra around peak. Rapidly rotating stars may also undergo chemically homogeneous evolution (CHE), and lose hydrogen through nuclear burning. In the past two decades, a subclass of CCSNe, superluminous (SL) SNe, with a total this vast range of SESN properties are still routinely being discovered.

Here, we present observations of SN 2020wnt, a hydrogen- and helium-poor SN with distinct photometric and spectroscopic properties. Its light-curve shape resembles that of SESNe, showing a relatively symmetric peak falling onto an exponential decline tail. However, the peak luminosity is much larger and the rise time is much longer than those of SESNe. Its spectroscopic evolution closely resembles that of SNe Ic up to about 1 year post peak with many marked differences compared to SLSNe. Late-time optical spectra, however, reveal features similar to magnetar-powered SLSNe. Late-time near-infrared (IR) observations reveal the formation of carbon monoxide (CO) and dust, similar to what is observed in SESNe and relatively novel for SLSNe. We recognize that while preparing this paper, Gutiérrez et al. (2022) posted their paper on the same SN on arXiv, presenting some similar observations and analysis; this work should be treated as an independent analysis on a largely independent data set (with only shared public ATLAS and ZTF photometry). In Section 2, we summarize the discovery and follow-up observations of SN 2020wnt. In Section 3, we analyze photometric data and compute explosion properties. In Section 4, we discuss the optical to near-IR spectroscopic evolution of SN 2020wnt, quantitatively comparing it to SESNe and SLSNe. In Section 6, we compare our bolometric luminosity to various models to discern the nature of SN 2020wnt. In Section 7, we compare our nebular spectra to model spectra to measure the properties of the ejecta. In Section 8, we discuss the stellar mass, star formation rate, and metallicity of the host galaxy. We provide a discussion and conclusion in Section 9.

2. Observations

2.1. Supernova Discovery and Classification

SN 2020wnt (ZTF20acjeflr) was discovered by the ZTF (Bellm et al. 2019; Graham et al. 2019; Masci et al. 2019) through the event broker Automatic Learning for the Rapid Classification of Events (Förster et al. 2021) on 2020 October 14 UT (Förster et al. 2020) (UT dates used hereafter). The discovery magnitude was $g = 19.7$. We decided to start following up this SN based on public light curves gathered by YSE-PZ, our Target and Observation Management System (Coulter et al. 2022). We classified SN 2020wnt as a Type I SN on 2020 November 16 using an optical spectrum obtained with the Kast spectrograph on the 3 m Shane Telescope at Lick Observatory (Tinyanont et al. 2020). All subsequent photometric and spectroscopic observations are also organized using YSE-PZ. The classification spectrum contained a narrow Hα emission from the host galaxy, putting the SN at $z = 0.0323 \pm 0.0001$. The corresponding luminosity distance is 141.8 Mpc, assuming a standard Lambda cold dark matter cosmology with $H_0 = 70\ \mathrm{km\ s^{-1}\ Mpc^{-1}}$, $\Omega_M = 0.3$, and $\Omega_\Lambda = 0.7$. At the time of classification, the transient had been brightening for a month. The Galactic extinction along the line of sight toward SN 2020wnt is $E(B - V) = 0.42$ mag (Schlafly & Finkbeiner 2011). We use this value for extinction correction throughout the paper, assuming $R_V = 3.1$ (Cardelli et al. 1989) and the extinction law of Fitzpatrick (1999). We assume that the host extinction is negligible owing to the lack of Na I D absorption at the host redshift.

2.2. Photometry

We obtained public forced photometry of SN 2020wnt from ZTF in the g and r bands, and from the Asteroid Terrestrial-impact Last Alert System (ATLAS; Tonry et al. 2018; Smith et al. 2020) in the cyan and orange bands. The SN was observed by these public surveys at a cadence of a few days.

These regularly scheduled photometry were supplemented by observations in the *griz* bands from the 2 m Liverpool Telescope on La Palma; *BVgriz* bands from the Lulin One-meter Telescope (LOT) at the Lulin Observatory in Taiwan; and *BVri* bands from the 1 m Nickel telescope at Lick Observatory in California. These observations were reduced using standard optical imaging procedures: bias and flat-field correction and photometric calibration using stars observed in the same field of view.

We analyzed the *griz* imaging from the LOT and the *ri* imaging from the Nickel telescope using image frames from the Pan-STARRS 3π survey (Flewelling et al. 2020) as templates. After registering and estimating a zero point for each LOT image in photpipe (Rest et al. 2005), we performed digital image subtraction between each LOT and Pan-STARRS image using hotpants (Becker 2015). We then performed forced photometry at the location of SN 2020wnt using a custom version of DoPhot (Schechter et al. 1993).

We obtained ground-based near-IR imaging of SN 2020wnt on 2021 August 19 using the slit-viewing camera of the SpeX spectrograph (Rayner et al. 2003) on the NASA InfraRed Telescope Facility (IRTF) in the J, H, and K bands. The data were reduced using a custom python script that constructed the sky flat image from the dithered observations, performed flat-fielding and background subtraction, then shifted and coadded observations in each band. We obtained another epoch of near-IR photometry on 2021 December 10 using the Near-InfraRed Imager (NIRI) on Gemini North in the J, H, and Ks bands as part of the fast-turnaround program GN-2021B-FT-109 (PI: Tinyanont). We used DRAGONS v.3.0.1 to reduce NIRI images; the steps were similar to the script we used to reduce the IRTF images. Photometric calibration in both cases were obtained using Two Micron All Sky Survey (Milligan et al. 1996; Skrutskie et al. 2006) stars in the field of view.

In addition to ground-based observations, we observed SN 2020wnt with the Ultra-Violet and Optical Telescope (Roming et al. 2005) on board the Neil Gehrels Swift Observatory (Gehrels et al. 2004) at 46, 98, 118, 138, and 158 days post discovery in the U, B, V, $UVW1$, and $UVW2$ bands. The data were processed by the standard data-reduction pipeline and obtained via the HEASARC archive. We did not detect the SN in the UV bands. Aperture photometry was obtained using a 3″ radius aperture centered on the SN with local background subtraction.

SN 2020wnt was observed during the ongoing Near-Earth Object Wide-field Infrared Survey Explorer (NEOWISE) all-sky mid-IR survey in the W1 (3.4 μm) and W2 (4.5 μm) channels (Wright et al. 2010; Mainzer et al. 2014). We retrieved time-resolved coadded images of the field created as part of the unWISE project (Lang 2014; Meisner et al. 2018). To remove contamination from the host galaxies, we used a custom code (De et al. 2020) based on the ZOGY algorithm (Zackay et al. 2016) to perform image subtraction on the NEOWISE images using the full-depth coadds of the WISE and NEOWISE mission (obtained during 2010–2014) as reference images. Photometric measurements were obtained

Monthly Notices
of the
ROYAL ASTRONOMICAL SOCIETY

MNRAS **523,** 2530–2550 (2023) https://doi.org/10.1093/mnras/stad1433
Advance Access publication 2023 May 15

SN 2022ann: a Type Icn supernova from a dwarf galaxy that reveals helium in its circumstellar environment

K. W. Davis,[1★] K. Taggart,[1] S. Tinyanont,[1,2] R. J. Foley,[1] V. A. Villar,[3] L. Izzo,[4] C. R. Angus,[4] M. J. Bustamante-Rosell,[1] D. A. Coulter,[1] N. Earl,[5] D. Farias,[4] J. Hjorth,[4] M. E. Huber,[6] D. O. Jones,[1,7] P. L. Kelly,[8] C. D. Kilpatrick,[9] D. Langeroodi,[4] H.-Y. Miao,[10] C. M. Pellegrino,[11,12] E. Ramirez-Ruiz,[1] C. L. Ransome,[3] S. Rest,[13] M. R. Siebert,[14] G. Terreran,[11] I. M. Thornton,[3] S. K. Yadavalli,[3] G. R. Zeimann,[15] K. Auchettl,[1,16,17] C. R. Bom,[18] T. G. Brink,[19] J. Burke,[11,12] Y. Camacho-Neves,[20] K. C. Chambers,[6] T. J. L. de Boer,[6] L. DeMarchi,[9] A. V. Filippenko,[19] L. Galbany,[21,22] C. Gall,[4] H. Gao,[6] F. R. Herpich,[23] D. A. Howell,[11,12] W. V. Jacobson-Galan,[19] S. W. Jha,[20] A. Kanaan,[10] N. Khetan,[4] L. A. Kwok,[20] Z. Lai,[1] C. Larison,[20] C.-C. Lin,[6] K. C. Loertscher,[1] E. A. Magnier,[6] C. McCully,[11] P. McGill,[1] M. Newsome,[11,12] E. Padilla Gonzalez,[11,12] Y.-C. Pan,[10] A. Rest,[14,13] J. Rho,[24] T. Ribeiro,[25] A. Santos,[18] W. Schoenell,[26] S. N. Sharief,[5] K. W. Smith,[27] R. J. Wainscoat,[6] Q. Wang,[13] Y. Zenati[13†‡] and W. Zheng[19]

Affiliations are listed at the end of the paper

Accepted 2023 May 4. Received 2023 April 28; in original form 2022 November 15

ABSTRACT

We present optical and near-infrared (NIR) observations of the Type Icn supernova (SN Icn) 2022ann, the fifth member of its newly identified class of SNe. Its early optical spectra are dominated by narrow carbon and oxygen P-Cygni features with absorption velocities of ~800 km s^{-1}; slower than other SNe Icn and indicative of interaction with a dense, H/He-poor circumstellar medium (CSM) that is outflowing slower than typical Wolf–Rayet wind velocities of >1000 km s^{-1}. We identify helium in NIR spectra 2 weeks after maximum and in optical spectra at 3 weeks, demonstrating that the CSM is not fully devoid of helium. Unlike other SNe Icn, the spectra of SN 2022ann never develop broad features from SN ejecta, including in the nebular phase. Compared to other SNe Icn, SN 2022ann has a low luminosity (o-band absolute magnitude of ~−17.7), and evolves slowly. The bolometric light curve is well-modelled by 4.8 M$_\odot$ of SN ejecta interacting with 1.3 M$_\odot$ of CSM. We place an upper limit of 0.04 M$_\odot$ of ^{56}Ni synthesized in the explosion. The host galaxy is a dwarf galaxy with a stellar mass of $10^{7.34}$ M$_\odot$ (implied metallicity of $\log(Z/Z_\odot) \approx 0.10$) and integrated star-formation rate of $\log(\mathrm{SFR}) = -2.20$ M$_\odot$ yr^{-1}; both lower than 97 per cent of galaxies observed to produce core-collapse supernovae, although consistent with star-forming galaxies on the galaxy Main Sequence. The low CSM velocity, nickel and ejecta masses, and likely low-metallicity environment disfavour a single Wolf–Rayet progenitor star. Instead, a binary companion is likely required to adequately strip the progenitor and produce a low-velocity outflow.

Key words: stars: massive – binaries – transients: supernovae.

1 INTRODUCTION

Massive stars $\gtrsim$8 M$_\odot$ typically end their lives in terminal explosions known as core-collapse supernovae (CCSNe). Some massive stars, as a result of either strong stellar winds or interaction with a companion, are stripped of their hydrogen envelopes (Woosley, Langer & Weaver 1995; Eldridge, Izzard & Tout 2008; Tauris et al. 2013; Tauris, Langer & Podsiadlowski 2015), producing a stripped-envelope SN (SESN) of Type Ib. Further stripping can remove the helium envelope, exposing the remaining carbon/oxygen core. If such a star exploded, the resulting SN would lack signatures of hydrogen and helium, producing a Type Ic SN (SN Ic; for a review of spectroscopic classification; see Filippenko 1997). However, carbon burning lasts only ~100 yr for a star with a zero-age main sequence mass of ~25 M$_\odot$. If we assume that the lack of observed helium is due to the absence of helium itself, this sets a stringent time-scale of no more than decades (or perhaps a few centuries) before the explosion for the entirety of the stripping to occur. Another possible way to produce SNe Ic may be to 'hide' the helium. The excitation of helium requires high-energy photons, such as gamma-rays produced

★ E-mail: kywdavis@ucsc.edu
† Einstein Fellow.
‡ ISEF Postdoctoral Fellow.

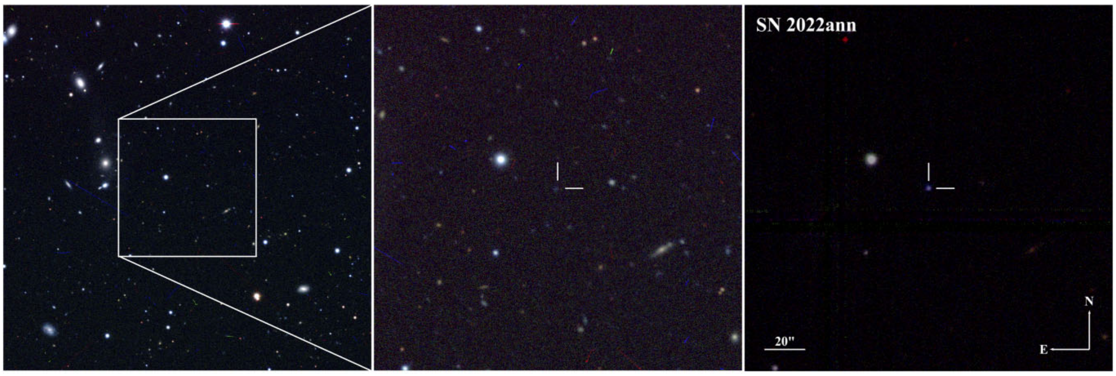

Figure 1. Finder charts of SN 2022ann (right-hand panel) and its host galaxy, SDSS J101729.72–022535.6 (centre and left). North is up and east is to the left. The left-hand panel is an 8′ × 8′ finder chart centred on the position of SN 2022ann from archival *grz* DECam images. To the east are members of the V1CG 662 galaxy group at $z = 0.0495$ (Lee et al. 2017). The DECam images were processed by the Dark Energy Spectroscopic Instrument Legacy Imaging Surveys (Dey et al. 2019). The centre panel is a 3′ × 3′ close-up view with the location of SN 2022ann marked. SN 2022ann is offset slightly to the northwest of SDSS J101729.72–022535.6. The right-hand panel is created from 3′ × 3′ Pan-STARRS *gri* images from 3 February, 30 January, and 3 February that are mapped to the blue, red, and green channels of the image, respectively.

Table 1. Basic observational parameters of SN 2022ann. Presented apparent magnitudes are not extinction-corrected. The *o* band is a wide-pass filter that covers roughly 5600–8200 Å, comparable to the combined wavelength coverage of the *r* and *i* filters. There is no indication of host-galaxy reddening at the SN location.

Time of first detection (MJD)	59604.5
Estimated time of explosion (MJD)	59600.5
Estimated time of maximum (MJD)	59613.5
RA (J2000)	$10^{h}17^{m}29.66^{s}$
Dec (J2000)	$-02°25'35''.45$
Redshift	0.04938 ± 0.0004
$E(B-V)_{MW}$	0.034 ± 0.001 mag
$E(B-V)_{host}$	0
$m_o^{discovery}$	19.22 ± 0.11 mag
$M_o^{discovery}$	-17.47 mag
m_o^{peak}	19.00 ± 0.069 mag
M_o^{peak}	-17.69 mag

be made available in electronic format online. We define the time of explosion, t_0, as the mid-point between the last pre-explosion non-detection and the first detection. For SN 2022ann, there are two relevant ATLAS non-detections with which we can estimate the time of explosion: a deeper, but earlier non-detection on 2022 January 13.5 (MJD 59592.5) and a shallower, but later non-detection on 2022 January 17.5 (MJD 59596.5) with corresponding limiting magnitudes of $o = 20.37$ mag and 19.47 mag, respectively. In our analysis, we use the later non-detection to estimate the time of explosion as 2022 January 21.5 (MJD 59600.5). Doing so results in a rise time in the *o*-band of ∼10 d, which is similar to that of other SNe Ibn/Icn, but we note that the non-detections are not particularly constraining. As we do not perform any detailed modelling that relies on a precise measurement of t_0, the current constraint is sufficient for our analysis presented here. We estimate the time of maximum brightness using the *o*-band light curve owing to its coverage at early times. The light curve is very flat around peak (see Section 3). We estimate the time of peak brightness to be the mid-point of this flat region, which yields a t_{peak} of 2022 February 03.5 (MJD 59613.5). Phases for SN 2022ann in this paper are given relative to the *o*-band time of maximum unless stated otherwise.

SN 2022ann was observed in the *c* and *o* bands by ATLAS between −8 and 21 d. We use the ATLAS forced photometry server (Tonry et al. 2018; Smith et al. 2020; Shingles et al. 2021) to recover the difference-image photometry for SN 2022ann. To remove erroneous measurements and have significant SN flux detection at the location of SN 2022ann, we apply several cuts on the total number of individual data points and nightly averaged data. Our first cut uses the χ^2 and uncertainty values of the point-spread-function (PSF) fitting to remove discrepant data. We then obtain forced photometry of eight control light curves located in a circular pattern around the location of the SN with a radius of 17″. The flux of these control light curves is expected to be consistent with zero within the uncertainties, and any deviation from zero would indicate that there are either unaccounted systematic biases or underestimated uncertainties. We search for such deviations by calculating the weighted mean of the set of control light-curve measurements for a given epoch after removing any $>3\sigma$ outliers (for a more detailed discussion, see Rest et al., in preparation[1]). If the weighted mean of these photometric measurements is inconsistent with zero, we flag and remove those epochs from the SN light curve. This method allows us to identify potentially incorrect measurements without using the SN light curve itself. We then bin the SN 2022ann light curve by calculating a 3σ-cut weighted mean for each night (ATLAS typically has four epochs per night), excluding the flagged measurements from the previous step.

We also observed SN 2022ann with the Lulin Compact Imager on the 1-m telescope at Lulin Observatory from 2022 February 11 to 2022 March 8 in the *griz* bands. The images were calibrated using bias and flat-field frames following standard procedures. To account for background emission due to its host galaxy, we subtracted Pan-STARRS 3π cutout images (Magnier et al. 2020) using the image convolution and subtraction software, HOTPANTS (Becker 2015). We then performed forced photometry in each frame using DoPhot (Schechter, Mateo & Saha 1993) within photpipe (Rest et al. 2005). The photometry was calibrated using Pan-STARRS *griz* local standard stars (Flewelling et al. 2020).

We also obtained *uBgVri*-band images of SN 2022ann using Sinistro cameras on Las Cumbres Observatory (LCO) 1.0 m telescopes

[1]https://github.com/srest2021/atlaslc

The Astrophysical Journal, 955:21 (9pp), 2023 September 20 https://doi.org/10.3847/1538-4357/acea82

A Light Redback Companion of PSR J1622–0315 and Irradiation Power in Spider Systems

Y. X. Jane Yap[1], Albert K. H. Kong[1], and Kwan-Lok Li[2]
[1] Institute of Astronomy, National Tsing Hua University, Hsinchu 30013, Taiwan R.O.C
[2] Department of Physics, National Cheng Kung University, Tainan 701, Taiwan R.O.C
Received 2022 February 3; revised 2023 July 16; accepted 2023 July 24; published 2023 September 12

Abstract

We report optical observations of the millisecond pulsar binary system PSR J1622–0315 with the Lulin 1 m telescope in Taiwan and the Lijiang 2.4 m telescope in China between 2019 and 2021. The companion of the pulsar, which is of $V \sim 19$ mag, showed ellipsoidal-distorted orbital variations in its light curves. The best-fit model to the light curves, with the binary code PHOEBE, gives a companion mass of $0.122 \pm 0.006\,M_\odot$. This places PSR J1622–0315 in the spider-system subclass. We compared the properties of PSR J1622–0315 with other spider pulsar binaries for the scalings between the spin-down luminosity derived for the pulsar, irradiation luminosity of the companion, and X-ray luminosity of the binary. We find that pulsar irradiation in PSR J1622–0315 is insignificant and the irradiation luminosity of the transitional millisecond pulsars PSR J1023+0038 and PSR J1227–4853 are the highest among the redback systems.

Unified Astronomy Thesaurus concepts: Millisecond pulsars (1062); Compact binary stars (283); Low-mass x-ray binary stars (939)

1. Introduction

Spider pulsar systems are compact binaries containing a millisecond pulsar (MSP) with a low-mass companion star orbiting around each other in a period of $P_b \lesssim 24$ hr. They are usually classified as black widows (BWs) or redbacks (RBs). The companion stars generally have masses $\lesssim 0.1\,M_\odot$ and ~ 0.1–$0.4\,M_\odot$ for BW and RB, respectively (see e.g., Chen et al. 2013; Roberts & van Leeuwen 2013). A rapid-spinning MSP is believed to be a phenomenon caused by the accretion of material from the companion star.[3] This scenario is supported by observations that showed state transition(s) between accretion-powered and rotation-powered (pulsar) states in three transitional MSPs (tMSPs): PSR J1023+0038 (Archibald et al. 2009), PSR J1227–4853 (Bassa et al. 2014) and PSR J1824–2452I (Papitto et al. 2013).

The light curve of the companion star in spider systems contains information about the irradiation of the system and the companion's stellar properties. The effect of strong irradiation is observed in a few RBs and BWs (e.g., Breton et al. 2013; Draghis et al. 2019). Pulsar irradiation also causes evaporation of the companion star and results in the mass loss of the star (van den Heuvel & van Paradijs 1988). The evolution history of a companion star in spider systems evolving from a low-mass X-ray binary (LMXB) system under ablation was discussed in Chen et al. (2013). The interaction between the magnetodipole radiation and a disk was proposed to explain the neutron star (NS) rotation properties in these systems, and the model was applied in transitional systems during the rotation-powered state. (Burderi et al. 2001; Papitto & Torres 2015).

[3] Known as the recycling scenario (Alpar et al. 1982).

In this work, we report new optical observations of PSR J1622–0315. We use Markov Chain Monte Carlo (MCMC) sampling to explore the parameter space in the models we use to fit the light curves and to estimate the uncertainties of the masses of the components and the orbital properties of the system. We constructed a table of archival values to compare the spider systems in terms of their irradiation luminosities ($L_{\rm irr}$) inferred from the light curves, X-ray luminosities ($L_{\rm x}$) of the systems, and spin-down luminosities ($\dot{E}$) of the pulsars.

We introduce our target and summarize our observations in Section 2. In Section 3, we describe our light-curve analysis using the eclipsing binary modeling code PHOEBE (Prša et al. 2016). In Section 4, we discuss the empirical relationship between $L_{\rm irr}$, $L_{\rm x}$, and $\dot{E}$ in BWs, RBs, and tMSPs. We summarize and discuss the implications of this work in Section 5.

2. Target and Observations

2.1. PSR J1622–0315

PSR J1622–0315 is a binary MSP discovered by Sanpa-Arsa (2016) using the Green Bank Telescope (GBT) and the Nançay telescope. It has a spin period of 3.845 ms, and it is located at coordinates R.A. = $16^{\rm h}22^{\rm m}59^{\rm s}.6$ and decl. = $-03°15'37''.3$ (J2000). The system has an orbital period of 3.9 hr and the dispersion measure is 21.4 pc cm^{-3} ($\sim$20% uncertainties; Sanpa-Arsa 2016). Radio flux variations, possibly caused by scattering with the interstellar medium or ejected particles from the companion were also reported (Sanpa-Arsa 2016). An optical counterpart was identified with the MDM Observatory located in Arizona, United States, and its light curve exhibits an ellipsoidal variation. From the pulsar timing, the mass function was obtained and a companion mass of $>0.1\,M_\odot$ was derived, assuming an NS mass of $1.35\,M_\odot$ and an edge-on orbit. No strong emission lines were observed in the optical spectrum of the companion of PSR J1622–0315 (Strader et al. 2019). Measurements of the companion radial velocity further allowed the NS mass to be constrained to $>1.45\,M_\odot$ for an edge-on

The Astrophysical Journal, 955:42 (17pp), 2023 September 20 https://doi.org/10.3847/1538-4357/ace965

Late-time Hubble Space Telescope Observations of AT 2018cow. I. Further Constraints on the Fading Prompt Emission and Thermal Properties 50–60 days Post-discovery

Yuyang Chen[1,2], Maria R. Drout[1,3], Anthony L. Piro[3], Charles D. Kilpatrick[4,5], Ryan J. Foley[6], César Rojas-Bravo[6], Kirsty Taggart[6], Matthew R. Siebert[7], and M. R. Magee[8]

[1] David A. Dunlap Department of Astronomy and Astrophysics, University of Toronto, 50 St. George Street, Toronto M5S 3H4, Canada; yuyangf.chen@mail.utoronto.ca
[2] Dunlap Institute for Astronomy and Astrophysics, University of Toronto, 50 St. George Street, Toronto M5S 3H4, Canada
[3] The Observatories of the Carnegie Institution for Science, 813 Santa Barbara Street, Pasadena, CA 91101, USA
[4] Department of Physics and Astronomy, Northwestern University, Evanston, IL 60208, USA
[5] Center for Interdisciplinary Exploration and Research in Astrophysics (CIERA), 1800 Sherman Avenue, Evanston, IL 60201, USA
[6] Department of Astronomy and Astrophysics, University of California, Santa Cruz, CA 95064, USA
[7] Space Telescope Science Institute, Baltimore, MD 21218, USA
[8] Department of Physics, University of Warwick, Gibbet Hill Road, Coventry CV4 7AL, UK
Received 2023 March 6; revised 2023 June 23; accepted 2023 July 19; published 2023 September 15

Abstract

The exact nature of the luminous fast blue optical transient AT 2018cow is still debated. In this first of a two-paper series, we present a detailed analysis of three Hubble Space Telescope (HST) observations of AT 2018cow covering ~50–60 days post-discovery in combination with other observations throughout the first two months and derive significantly improved constraints of the late thermal properties. By modeling the spectral energy distributions (SEDs), we confirm that the UV–optical emission over 50–60 days was still a smooth blackbody (i.e., optically thick) with a high temperature ($T_{\rm BB} \sim 15{,}000$ K) and small radius ($R_{\rm BB} \lesssim 1000\,R_\odot$). Additionally, we report for the first time a break in the bolometric light curve: the thermal luminosity initially declined at a rate of $L_{\rm BB} \propto t^{-2.40}$ but faded much faster at $t^{-3.06}$ after day 13. Reexamining possible late-time power sources, we disfavor significant contributions from radioactive decay based on the required ^{56}Ni mass and lack of UV line blanketing in the HST SEDs. We argue that the commonly proposed interaction with circumstellar material may face significant challenges in explaining the late thermal properties, particularly the effects of the optical depth. Alternatively, we find that continuous outflow/wind driven by a central engine can still reasonably explain the combination of a receding photosphere, optically thick and rapidly fading emission, and intermediate-width lines. However, the rapid fading may have further implications on the power output and structure of the system. Our findings may support the hypothesis that AT 2018cow and other "Cow-like transients" are powered mainly by accretion onto a central engine.

Unified Astronomy Thesaurus concepts: Supernovae (1668); Circumstellar matter (241); Hubble Space Telescope (761); Compact objects (288); Accretion (14)

Supporting material: data behind figure

1. Introduction

The recent advent of high-cadence, wide-field optical surveys has unveiled a new class of peculiar transients, commonly termed the fast blue optical transients (FBOTs; adopted hereafter), rapidly evolving transients (RETs), or fast-evolving luminous transients (FELTs). As the name suggests, the defining characteristics of FBOTs are the fast-evolving light curves (time above half-brightness $\lesssim$15 days) and blue color ($g - r \lesssim 0.0$) at peak (e.g., Drout et al. 2014; Arcavi et al. 2016; Tanaka et al. 2016; Pursiainen et al. 2018; Rest et al. 2018; Tampo et al. 2020; Wiseman et al. 2020; Ho et al. 2023).

FBOTs have peak magnitudes that span a wide range ($-15 \gtrsim M_{\rm peak} \gtrsim -22$) and can have vastly varying light curves and spectra, demonstrating diversity within the class itself. As a whole, FBOTs are not intrinsically rare, with an inferred volumetric rate of ~1%–10% of the core-collapse supernova (CCSN) rate (Drout et al. 2014; Pursiainen et al. 2018, although this depends on the exact definition of an FBOT). However, their extreme timescales pose a challenge to conventional supernova (SN) models that rely on radioactive decay and hydrogen recombination as the primary energy source.

As a result, a variety of alternative scenarios have been proposed to explain the characteristics of FBOTs, some of which involve interactions with circumstellar material (CSM; Ofek et al. 2010; Shivvers et al. 2016; Kleiser et al. 2018b; McDowell et al. 2018; Rest et al. 2018; Tolstov et al. 2019; Wang et al. 2019; Suzuki et al. 2020; Wang & Li 2020; Karamehmetoglu et al. 2021; Maeda & Moriya 2022; Margalit et al. 2022; Margalit 2022; Khatami & Kasen 2023; Liu et al. 2023; Mor et al. 2023), energy injection by a central engine such as a neutron star (NS; Yu et al. 2015; Hotokezaka et al. 2017; Whitesides et al. 2017; Liu et al. 2022; Wang & Gan 2022) or a black hole (BH; Kashiyama & Quataert 2015; Rest et al. 2018; Tsuna et al. 2021; Fujibayashi et al. 2022), tidal disruption events (TDEs; Kawana et al. 2020; Kremer et al. 2021), electron-capture supernovae (ECSNe; Moriya & Eldridge 2016), and SNe within extended envelopes (Brooks et al. 2017; Kleiser et al. 2018a).

A recent population study by Ho et al. (2023) revealed that most FBOTs are located in star-forming galaxies and are

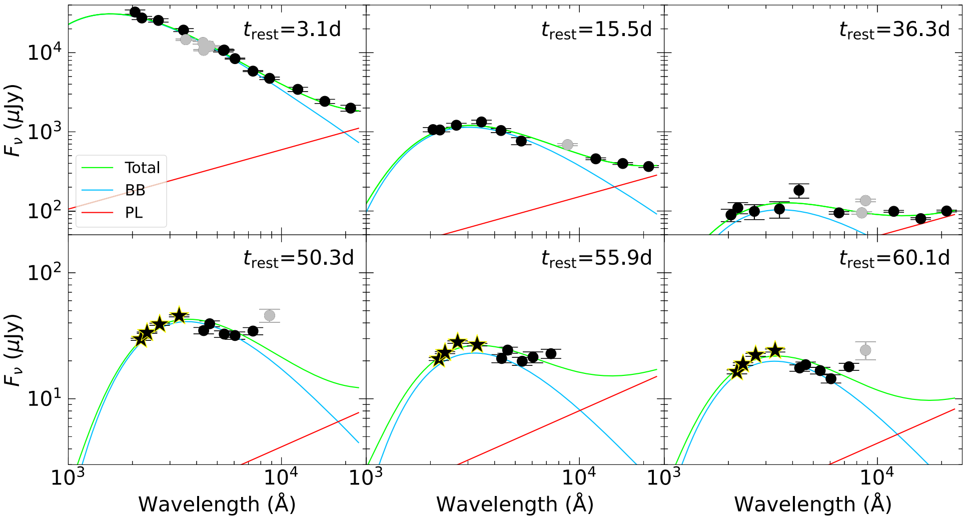

Figure 3. Observed (dereddened) SEDs (black) of AT 2018cow at six sample epochs including the three HST epochs (bottom panels). The HST measurements are marked as stars. The best-fit models (solid lines) are also shown, derived using the BLACKBODY + POWER LAW model. Photometry excluded from the fit is shown in gray (see text for reasoning). The UV–optical continuum of AT 2018cow at $t \simeq 50$–60 days is consistent with a blackbody curve peaking at $\lambda \sim 3000$ Å.

we required optical data at similar epochs. We obtained photometry from the 1 m Swope Telescope at the Las Campanas Observatory, Chile, which started observing AT 2018cow at $t \sim 3$ days and continued for ∼70 days. The observations covered the *uBgVri* bands, spanning the wavelength range $\lambda_{\rm eff} \simeq 3608$–7458 Å.

Following the reduction procedures described in Kilpatrick et al. (2018), all image processing and optical photometry on the Swope data were performed using `photpipe` (Rest et al. 2005), including bias subtraction, flat-fielding, image stitching, registration, and photometric calibration. The *BgVri* photometry was calibrated using standard sources from the Panoramic Survey Telescope and Rapid Response System Data Release 1 catalog (Flewelling et al. 2020), and the *u*-band data were calibrated using SkyMapper *u*-band standards (Onken et al. 2019), both in the same field as AT 2018cow, and transformed into the Swope natural system (Krisciunas et al. 2017) with the Supercal method (Scolnic et al. 2015).

To ensure precise measurements at late times, when background contamination from a nearby star-forming region (Figure 1) becomes significant, we obtained deep *uBgVri* observations between 2019 April 10 and 2021 April 27 with the same telescope and instrument configuration and performed image subtraction using `hotpants` (Becker 2015). Forced photometry was performed on the subtracted images to obtain the final photometry shown in Figure 2. We note that our Swope photometry is also generally consistent with previously published photometry in the *uBgVri* bands from different telescopes (e.g., Perley et al. 2019).

2.4. Near-Infrared Photometry (t ∼ *2–80 days)*

We also make use of the *RIzJHK* photometry published by Perley et al. (2019), which spans $t \sim 2$–80 days. These measurements were taken by the 2 m Liverpool Telescope (Steele et al. 2004), the 1 m telescope at the Mount Laguna Observatory (Smith & Nelson 1969), the 1.5 m telescope at the Cerro Tololo Inter-American Observatory, the 2 m Himalayan Chandra Telescope, the 0.4 m telescope at Lulin Observatory, the Palomar 200 inch Hale Telescope, and the MPG/ESO 2.2 m telescope (Greiner et al. 2008) at La Silla Observatory. For details on image processing, calibration, and host subtraction, see Section 2.2 of Perley et al. (2019).

3. Evolution of Prompt UVOIR Emission

Our final multiband UVOIR light curves from the prompt emission ($t \sim 2$–80 days) of AT 2018cow are shown in Figure 2. The addition of the HST measurements provides significantly improved constraints on the UV emission beyond the coverage of Swift. In this section, we describe our updated analysis of the prompt UVOIR emission of AT 2018cow, with an emphasis on the later epochs ($t \sim 40$–60 days).

3.1. Constructing UVOIR SEDs

To construct the SEDs, we linearly interpolated the light curves to a common set of epochs. We selected a total of 22 epochs, including the three HST epochs, that have sufficient UV–optical spectral coverage. The errors in the interpolated magnitudes were found through Monte Carlo propagation. At each epoch, we only interpolated a given light curve if the nearest measurement was within 1.0 days from the epoch. The only exception was the first HST epoch ($t = 50.3$ days), which did not have any measurements in the optical bands within 1.0 days. For this epoch, we interpolated all the optical bands regardless and added 0.03 mag (approximately 3% of flux) to the uncertainties of the interpolated magnitudes to account for deviation from linear interpolation.

3.2. SED Shape at t ≃ *50–60 days*

The precision of the HST photometry allows for the most accurate assessment to date of the UV–optical SED of AT 2018cow at $t \simeq 50$–60 days. As shown in the bottom panels of Figure 3, the HST photometry traces a smooth curve peaking at $\lambda \sim 3000$ Å with an exponential decay in the NUV. The

The Astrophysical Journal Letters, 954:L42 (15pp), 2023 September 10 https://doi.org/10.3847/2041-8213/acf2ec

SN 2023ixf in Messier 101: Photo-ionization of Dense, Close-in Circumstellar Material in a Nearby Type II Supernova

W. V. Jacobson-Galán[1,30], L. Dessart[2], R. Margutti[1,3], R. Chornock[1], R. J. Foley[4], C. D. Kilpatrick[5], D. O. Jones[6], K. Taggart[4], C. R. Angus[7], S. Bhattacharjee[8], L. A. Braff[4], D. Brethauer[1], A. J. Burgasser[9], F. Cao[10], C. M. Carlile[11], K. C. Chambers[12], D. A. Coulter[4,30], E. Dominguez-Ruiz[4], C. B. Dickinson[4], T. de Boer[12], A. Gagliano[13,14,30], C. Gall[7], H. Gao[12], E. L. Gates[15], S. Gomez[16], M. Guolo[17], M. R. J. Halford[18], J. Hjorth[7], M. E. Huber[12], M. N. Johnson[19], P. R. Karpoor[11], T. Laskar[20], N LeBaron[1], Z. Li[21], Y. Lin[22], S. D. Loch[18], P. D. Lynam[15], E. A. Magnier[12], P. Maloney[4], D. J. Matthews[1], M. McDonald[22], H.-Y. Miao[8], D. Milisavljevic[23], Y.-C. Pan[8], S. Pradyumna[22], C. L. Ransome[24], J. M. Rees[15], A. Rest[16,17], C. Rojas-Bravo[4], N. R. Sandford[1], L. Sandoval Ascencio[25], S. Sanjaripour[22], A. Savino[1], H. Sears[5], N. Sharei[22], S. J. Smartt[26,27], E. R. Softich[11], C. A. Theissen[11], S. Tinyanont[4], H. Tohfa[22], V. A. Villar[24,28,29], Q. Wang[17], R. J. Wainscoat[12], A. L. Westerling[4], E. Wiston[1], M. A. Wozniak[22], S. K. Yadavalli[24], and Y. Zenati[17,31]

[1] Department of Astronomy, University of California, Berkeley, CA 94720, USA; wynnjg@berkeley.edu
[2] Institut d'Astrophysique de Paris, CNRS-Sorbonne Université, 98 bis boulevard Arago, F-75014 Paris, France
[3] Department of Physics, University of California, Berkeley, CA 94720, USA
[4] Department of Astronomy and Astrophysics, University of California, Santa Cruz, CA 95064, USA
[5] Center for Interdisciplinary Exploration and Research in Astrophysics (CIERA), and Department of Physics and Astronomy, Northwestern University, Evanston, IL 60208, USA
[6] Gemini Observatory, NSF's NOIRLab, 670 N. A'ohoku Place, Hilo, HI 96720, USA
[7] DARK, Niels Bohr Institute, University of Copenhagen, Jagtvej 128, DK-2200 Copenhagen, Denmark
[8] Graduate Institute of Astronomy, National Central University, 300 Zhongda Road, Zhongli, Taoyuan 32001, Taiwan
[9] Department of Astronomy & Astrophysics, UC San Diego, La Jolla, CA 92093, USA
[10] Department of Statistics, University of California, Riverside, CA 92521, USA
[11] Center for Astrophysics and Space Sciences, University of California, San Diego, La Jolla, CA 92093, USA
[12] Institute for Astronomy, University of Hawaii, 2680 Woodlawn Drive, Honolulu, HI 96822, USA
[13] Department of Astronomy, University of Illinois at Urbana-Champaign, 1002 W. Green St., IL 61801, USA
[14] Center for Astrophysical Surveys, National Center for Supercomputing Applications, Urbana, IL, 61801, USA
[15] University of California Observatories/Lick Observatory, Mount Hamilton, CA 95140, USA
[16] Space Telescope Science Institute, Baltimore, MD 21218, USA
[17] Department of Physics and Astronomy, The Johns Hopkins University, Baltimore, MD 21218, USA
[18] Department of Physics, Auburn University, 380 Duncan Drive, Auburn, AL 36849, USA
[19] Department of Physics, University of California, Santa Cruz, CA 95064, USA
[20] Department of Physics & Astronomy, University of Utah, Salt Lake City, UT 84112, USA
[21] Department of Earth and Planetary Sciences, University of California, Riverside, CA 92521, USA
[22] Department of Physics & Astronomy, University of California Riverside, 900 University Ave, Riverside, CA, USA
[23] Department of Physics and Astronomy, Purdue University, 525 Northwestern Avenue, West Lafayette, IN 47907, USA
[24] Department of Astronomy and Astrophysics, Pennsylvania State University, 525 Davey Laboratory, University Park, PA 16802, USA
[25] Department of Physics and Astronomy, University of California, Irvine, California 92697-4575, USA
[26] Astrophysics Research Centre, School of Mathematics and Physics, Queen's University Belfast, Belfast BT7 1NN, UK
[27] Department of Physics, University of Oxford, Keble Road, Oxford, UK
[28] Institute for Computational & Data Sciences, The Pennsylvania State University, University Park, PA, USA
[29] Institute for Gravitation and the Cosmos, The Pennsylvania State University, University Park, PA 16802, USA
Received 2023 June 7; revised 2023 August 21; accepted 2023 August 21; published 2023 September 8

Abstract

We present UV and/or optical observations and models of SN 2023ixf, a type II supernova (SN) located in Messier 101 at 6.9 Mpc. Early time (*flash*) spectroscopy of SN 2023ixf, obtained primarily at Lick Observatory, reveals emission lines of H I, He I/II, C IV, and N III/IV/V with a narrow core and broad, symmetric wings arising from the photoionization of dense, close-in circumstellar material (CSM) located around the progenitor star prior to shock breakout. These electron-scattering broadened line profiles persist for ∼8 days with respect to first light, at which time Doppler broadened the features from the fastest SN ejecta form, suggesting a reduction in CSM density at $r \gtrsim 10^{15}$ cm. The early time light curve of SN 2023ixf shows peak absolute magnitudes (e.g., $M_u = -18.6$ mag, $M_g = -18.4$ mag) that are $\gtrsim 2$ mag brighter than typical type II SNe, this photometric boost also being consistent with the shock power supplied from CSM interaction. Comparison of SN 2023ixf to a grid of light-curve and multiepoch spectral models from the non-LTE radiative transfer code CMFGEN and the radiation-hydrodynamics code HERACLES suggests dense, solar-metallicity CSM confined to $r = (0.5–1) \times 10^{15}$ cm, and a progenitor mass-

[30] NSF Graduate Research Fellow.
[31] ISEF International Fellowship.

2023 May 21 and June 2 in *grizy* bands through the Young Supernova Experiment (YSE; Jones et al. 2021). Data storage and/or visualization and follow-up coordination was done through the YSE-PZ web broker (Coulter et al. 2022, 2023). The YSE photometric pipeline is based on `photpipe` (Rest et al. 2005), which relies on calibrations from Magnier et al. (2020), Waters et al. (2020). Each image template was taken from stacked PS1 exposures, with most of the input data from the PS1 3π survey. All images and templates were resampled and astrometrically aligned to match a skycell in the PS1 sky tessellation. An image zero-point is determined by comparing point-spread function (PSF) photometry of the stars to updated stellar catalogs of PS1 observations (Flewelling et al. 2020). The PS1 templates are convolved with a three-Gaussian kernel to match the PSF of the nightly images, and the convolved templates are subtracted from the nightly images with `HOTPANTS` (Becker 2015). Finally, a flux-weighted centroid is found for the position of the SN in each image, and PSF photometry is performed using *forced photometry*: the centroid of the PSF is forced to be at the SN position. The nightly zero-point is applied to the photometry to determine the brightness of the SN for that epoch.

We obtained *ugri* imaging of SN 2023ixf with the Las Cumbres Observatory (LCO) 1 m telescopes from 2023 May 20 to June 1 (programs NSF2023A-011 and NSF2023A-015; PIs Foley and Kilpatrick, respectively). After downloading the `BANZAI`-reduced images from the LCO data archive (McCully et al. 2018), we used `photpipe` (Rest et al. 2005) to perform `DoPhot` PSF photometry (Schechter et al. 1993). All photometry was calibrated using PS1 stellar catalogs described above with additional transformations to SDSS *u* band derived from Finkbeiner et al. (2016). For additional details on our reductions, see Kilpatrick et al. (2018). We also obtained photometry using a 0.7 m Thai Robotic Telescope at Sierra Remote Observatories and the Nickel Telescope at Lick Observatory in the *BVRI* bands. Images are bias subtracted and field flattened. Absolute photometry is obtained using stars in the $10' \times 10'$ field of view.

We also observed SN 2023ixf with the Lulin 1 m telescope in *griz* bands from 2023 May 21 to June 1. Standard calibrations for bias and flat-fielding were performed on the images using `IRAF`, and we reduced the calibrated frames in `photpipe` using the same methods described above for the LCO images.

We also observed SN 2023ixf with the Auburn 10″ telescope located in Auburn, AL from 2023 May 27 to June 3 in *BGR* bands. Following standard procedures in `python`, we corrected each frame for bias, dark current, and flat-fielding using image frames obtained in the same instrumental setup. We then registered each frame using Gaia Data Release 3 astrometric standard stars (Gaia Collaboration 2022) observed in the same field as each image. Finally, we stacked images in each filter for each night with `swarp` and performed final photometry using `DoPhot` with calibration using Pan-STARRS *gri* standard stars transformed to *BVR* bands.[32] The complete multicolor light curve of SN 2023ixf is presented in Figure 1(a).

The Milky Way (MW) *V*-band extinction and color excess along the SN line of site is $A_V = 0.025$ mag, and $E(B-V) = 0.008$ mag (Schlegel et al. 1998; Schlafly & Finkbeiner 2011), respectively, which we correct for using a standard Fitzpatrick (1999) reddening law ($R_V = 3.1$). In addition to the MW color excess, we estimate the contribution of galaxy extinction in the local SN environment. Using a high resolution Kast spectrum of SN 2023ixf at $\delta t = 2.4$ days, we calculate Na I D2 and D1 equivalent widths (EWs) of 0.16 and 0.12 Å, respectively; these values are consistent with those derived from a Keck Planet Finder spectrum (Lundquist et al. 2023). We use Equations (7) and (8) in Poznanski et al. (2012) to convert these EWs to an intrinsic $E(B-V)$ and find a host galaxy extinction of $E(B-V)_{\rm host} = 0.033 \pm 0.010$ mag, also corrected for using the Fitzpatrick (1999) reddening law.

2.2. Spectroscopic Observations

SN 2023ixf was observed with Shane/Kast (Miller & Stone 1993) between $\delta t = 2.4$ and 14.4 days. For all these spectroscopic observations, standard CCD processing and spectrum extraction were accomplished with IRAF.[33] The data were extracted using the optimal algorithm of Horne (1986). Low-order polynomial fits to calibration-lamp spectra were used to establish the wavelength scale, and small adjustments derived from night-sky lines in the object frames were applied. SN 2023ixf spectra were also obtained with the Kitt Peak Ohio State Multi-Object Spectrograph (KOSMOS; Martini et al. 2014) on the Astrophysical Research Consortium 3.5 m Telescope at Apache Point Observatory (APO). The KOSMOS spectra were reduced through the `KOSMOS`[34] pipeline. One optical spectrum (in a red and blue arm) was taken through the Low-Resolution Spectrograph 2 (LRS2) instrument on the Hobby Eberly Telescope (HET) on 2023 May 21 (blue arm) and 2023 May 22 (red arm). The LRS2 data were processed with `Panacea`,[35] the HET automated reduction pipeline for LRS2. The initial processing includes bias correction, wavelength calibration, fiber-trace evaluation, fiber normalization, and fiber extraction; moreover, there is an initial flux calibration from default response curves, an estimation of the mirror illumination, as well as the exposure throughput from guider images. After the initial reduction, we use LRS2Multi[36] in order to perform sky subtraction.

In Figure 2, we present the complete series of optical spectroscopic observations of SN 2023ixf from $\delta t = 2.4$ to 14.4 days. In this plot, we also show the classification spectrum of SN 2023ixf at +1.1 days from the Liverpool telescope (Perley et al. 2023). However, because we cannot verify the quality of this spectral reduction, we only use these data for narrow line identification. Additionally, we include Swift UV grism spectra of SN 2023ixf from $\delta t = +1.8$ to 2.8 days in Appendix Figure 7; the data were reduced using the techniques outlined in Pan et al. (2020). The complete spectral sequence is shown in Figure 2, and the log of spectroscopic observations is presented in Appendix Table A1.

[32] Note that our *G*-band filter is close to Johnson *V* band, and so we calibrate against Pan-STARRS standard stars transformed into this band. For filter functions, see https://astronomy-imaging-camera.com/product/zwo-lrgb-31mm-filters-2.

[33] https://github.com/msiebert1/UCSC_spectral_pipeline
[34] https://github.com/jradavenport/pykosmos
[35] https://github.com/grzeimann/Panacea
[36] https://github.com/grzeimann/LRS2Multi

Monthly Notices of the ROYAL ASTRONOMICAL SOCIETY

MNRAS **524**, 2161–2185 (2023) https://doi.org/10.1093/mnras/stad1954
Advance Access publication 2023 June 29

Type II-P supernova progenitor star initial masses and SN 2020jfo: direct detection, light-curve properties, nebular spectroscopy, and local environment

Charles D. Kilpatrick ,[1★†] Luca Izzo,[2] Rory O. Bentley,[3] Kenneth C. Chambers,[4] David A. Coulter,[5] Maria R. Drout,[6] Thomas de Boer,[4] Ryan J. Foley,[5] Christa Gall,[2] Melissa R. Halford,[7] David O. Jones,[5] Danial Langeroodi,[2] Chien-Cheng Lin ,[4] Eugene A. Magnier,[4] Peter McGill ,[5] Anna J. G. O'Grady,[6] Yen-Chen Pan(潘彥丞),[8] Enrico Ramirez-Ruiz,[5] Armin Rest,[9,10] Jonathan J. Swift,[11] Samaporn Tinyanont ,[5] V. Ashley Villar,[12,13,14] Richard J. Wainscoat,[4] Amanda Rose Wasserman,[15] S. Karthik Yadavalli[12] and Grace Yang[11]

Affiliations are listed at the end of the paper

Accepted 2023 June 26. Received 2023 June 20; in original form 2022 August 11

ABSTRACT

We present optical, ultraviolet, and infrared data of the type II supernova (SN II) 2020jfo at 14.5 Mpc. This wealth of multiwavelength data allows us to compare different metrics commonly used to estimate progenitor masses of SN II for the same object. Using its early light curve, we infer SN 2020jfo had a progenitor radius of ≈700 $R_{\odot}$, consistent with red supergiants of initial mass $M_{\rm ZAMS}$ =11–13 $M_{\odot}$. The decline in its late-time light curve is best fit by a ^{56}Ni mass of 0.018 ± 0.007 $M_{\odot}$ consistent with that ejected from SN II-P with ≈13 $M_{\odot}$ initial mass stars. Early spectra and photometry do not exhibit signs of interaction with circumstellar matter, implying that SN 2020jfo experienced weak mass-loss within the final years prior to explosion. Our spectra at >250 d are best fit by models from 12 $M_{\odot}$ initial mass stars. We analysed integral field unit spectroscopy of the stellar population near SN 2020jfo, finding its massive star population had a zero age main sequence mass of $9.7^{+2.5}_{-1.3}$ $M_{\odot}$. We identify a single counterpart in pre-explosion imaging and find it has an initial mass of at most $7.2^{+1.2}_{-0.6}$ $M_{\odot}$. We conclude that the inconsistency between this mass and indirect mass indicators from SN 2020jfo itself is most likely caused by extinction with A_V = 2–3 mag due to matter around the progenitor star, which lowered its observed optical luminosity. As SN 2020jfo did not exhibit extinction at this level or evidence for interaction with circumstellar matter between 1.6 and 450 d from explosion, we conclude that this material was likely confined within ≈3000 $R_{\odot}$ from the progenitor star.

Key words: stars: evolution – stars: massive – transients: supernovae.

1 INTRODUCTION

Type II supernovae (SNe II; with broad lines of hydrogen, Filippenko 1997) are the terminal explosions of stars more massive than ≈8 $M_{\odot}$ that retain massive hydrogen envelopes (Anderson & James 2008; Smartt et al. 2009; Arcavi 2017). While some peculiar SNe II are observed to explode from blue and yellow supergiants (e.g. the B3 I progenitor star of SN 1987A; Arnett 1987; Hillebrandt et al. 1987; Woosley, Pinto & Ensman 1988; Podsiadlowski, Joss & Hsu 1992), the vast majority of these transient sources are thought to be the terminal explosions of red supergiants (RSGs) that undergo nuclear burning up to the iron peak then unbind their outer layers via core-collapse and neutrino-driven explosions (Burrows, Hayes & Fryxell 1995).

In particular, the type II-P SN subclass, which is characterized by a ≈50–100 d plateau in optical light curves (Barbon, Ciatti & Rosino 1979; Kirshner 1990; Valenti et al. 2016; Arcavi 2017), requires a progenitor star that retains a massive, extended hydrogen envelope that is first ejected and ionized by the SN explosion and then slowly recombines as the ejecta expand (Falk & Arnett 1973; Chevalier 1976; Falk 1978). Although there is some diversity in peak luminosity, plateau duration, and rise times even among SNe II-P (e.g. Hillier & Dessart 2019), the overall similarity in SN II-P light-curve properties points to the explosion of RSGs with varying hydrogen-envelope and oxygen-core masses (Goldberg & Bildsten 2020; Dessart et al. 2021).

One of the most significant open questions from the population of directly detected SN II-P and II-L (a SN II subclass with linearly declining light curves; Barbon et al. 1979) progenitor stars is why they all appear consistent with having log ($L/L_{\odot}$) < 5.2 (or $M_{\rm ZAMS}$ ≲ 17 $M_{\odot}$ assuming stellar evolution tracks in Choi et al. 2016) while the overall population of RSGs extends to log ($L/L_{\odot}$) ≈ 5.6 (or $M_{\rm ZAMS}$ ≈ 25–30 $M_{\odot}$; Smartt 2009; Elias-Rosa et al. 2010;

★ E-mail: ckilpatrick@northwestern.edu
† NASA Hubble Fellow

in dophot and calibrated using *gri* Pan-STARRS1 and *u*-band SDSS photometric standards (Alam et al. 2015) observed in the same field as SN 2020jfo.

We observed SN 2020jfo with the 1 m Nickel telescope at Lick Observatory on Mt. Hamilton, California from 2020 May 10 to July 6 in *BVri* bands. Following standard procedures in photpipe as described for the LCO data, we calibrated and performed photometry on all Nickel images. The magnitudes were calibrated using PS1 *gri* photometric standards transformed into Johnson *BV* bands.

The Lulin Compact Imager on the 1 m telescope at Lulin Observatory observed SN 2020jfo from 2020 May 8 to May 11 in *BVgri* bands. These data were calibrated following standard procedures, and we performed photometry in each image following the same methods described above for the LCO data.

SN 2020jfo was observed with the Ultraviolet and Optical Telescope (UVOT; Roming et al. 2005) on the *Neil Gehrels Swift Observatory* from 2020 May 7 to 2021 February 25. We used uvotsource in HEASoft v6.26 to perform aperture photometry within a 3 arcsec aperture centred on SN 2020jfo on the UVOT data files as described in Brown et al. (2014). In order to account for background emission in each UVOT band, we measured the total flux at the site of SN 2020jfo in frames obtained from 2021 February 24–25 and subtracted this from all previous observations. We detect significant emission in all early-time ($\Delta t < 30$ d; Fig. 1) UVOT data, but in later imaging where we do not detect emission, we report the combined 3σ magnitude limit from each epoch and the later template imaging in Table A1.

We also observed SN 2020jfo in *griz* bands with the 0.7 m Thacher Observatory telescope (Swift et al. 2022) located in Ojai, CA from 2020 May 7 to December 18. We reduced these images in photpipe using bias, dark, and flat-field frames obtained in the same instrumental configuration and following procedures described in Jacobson-Galán et al. (2020). We obtained photometry of SN 2020jfo following the same procedure as the LCO imaging described above.

SN 2020jfo was observed with the Auburn 10 arcmin telescope located in Auburn, AL from 2020 May 13 to July 17 in *BGR* bands.[2] Following standard procedures in astropy, we aligned and stacked individual exposures from each date and bandpass. We then performed photometry on the stacked frames with dophot and calibrated the photometry using Pan-STARRS *griz* standard star magnitudes transformed into Johnson *BVR* magnitudes. We note that the *G* bandpass has an effective wavelength of 5290 Å, close to that of Johnson *V*-band (≈5480 Å in this photometric system), and so we calibrate our *G*-band photometry with *V*-band magnitudes.

We also used the ZTF photometry of SN 2020jfo presented in Sollerman et al. (2021).

2.2 *Swift*/XRT observations

SN 2020jfo was observed over 29 epochs with *Swift*/XRT (Burrows et al. 2005) from 2020 May 7 to 2021 February 25. Analysing these data with HEASOFT v6.28 (Nasa High Energy Astrophysics Science Archive Research Center (Heasarc) 2014), we do not detect emission at $>3\sigma$ in any of these epochs or in the total merged event file. From these data, we infer upper limits on the total count rate of 1.6×10^{-3} to 9×10^{-2} counts s^{-1} in each epoch, consistent with analysis in Sollerman et al. (2021).

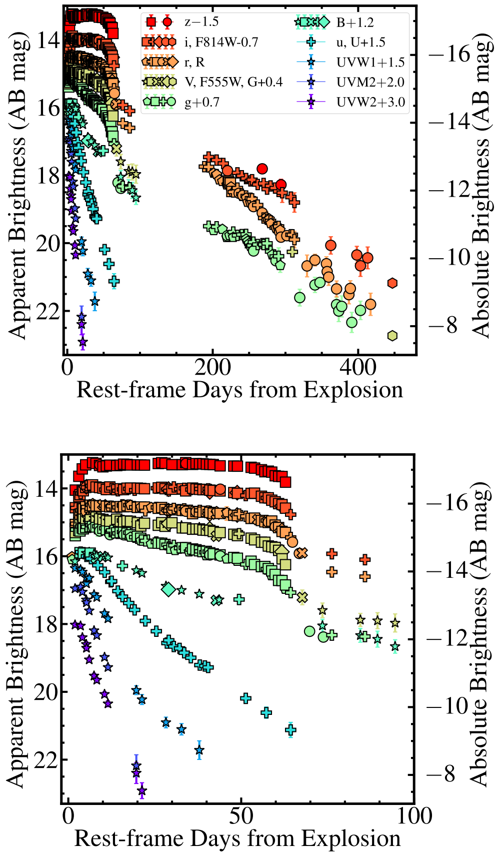

Figure 1. (Top panel): Our ultraviolet and optical light curves of SN 2020jfo. We show all Auburn (solid X), *HST* (hexagons), Las Cumbres (pluses), Nickel (diamonds), Pan-STARRS (circles), *Swift* (stars), Thacher (squares), and ZTF (pentagons) detections of the SN on the same light curve. All magnitudes are shown as observed in the AB system and before correcting for Milky Way extinction. We show absolute magnitude on the right-hand axis assuming a distance modulus of 30.81 mag (14.5 Mpc). (Bottom panel): Same as the upper panel but for the first 100 rest-frame days of data.

From our *Swift*/XRT limits, we derive an equivalent X-ray luminosity limit assuming a line-of-sight hydrogen column of $N_H = 1.4 \times 10^{20}$ cm^2 (using our Milky Way extinction and following Güver & Özel (2009) and the distance given above. Assuming a photon spectral index of $\Gamma = 2$, these limits are equivalent to 1.0–6.9×10^{39} erg s^{-1} from 0.9 to 295.3 d from discovery.

2.3 Spectroscopy

SN 2020jfo was observed with the FLOYDS spectrograph on the Faulkes-North 2 m telescope at Haleakalā, Hawaii, and the Faulkes-South 2 m telescope at Siding Spring Observatory, Australia. Both sets of spectra were processed using standard procedures for bias, flat-fielding, cosmic-ray rejection, aperture extraction, wavelength, and flux calibration in IRAF.[3] We performed telluric corrections and

[2]Filter transmission curves for the Auburn camera are available at https://astronomy-imaging-camera.com/product/zwo-lrgb-31mm-filters-2

[3]IRAF is distributed by the National Optical Astronomy Observatory, which is operated by the Association of Universities for Research in Astronomy

Article

Minutes-duration optical flares with supernova luminosities

https://doi.org/10.1038/s41586-023-06673-6

Received: 26 May 2023

Accepted: 25 September 2023

Published online: 15 November 2023

Check for updates

Anna Y. Q. Ho[1]✉, Daniel A. Perley[2], Ping Chen[3], Steve Schulze[4], Vik Dhillon[5,6], Harsh Kumar[7], Aswin Suresh[7], Vishwajeet Swain[7], Michael Bremer[8], Stephen J. Smartt[9,10], Joseph P. Anderson[11,12], G. C. Anupama[13], Supachai Awiphan[14], Sudhanshu Barway[13], Eric C. Bellm[15], Sagi Ben-Ami[3], Varun Bhalerao[7], Thomas de Boer[16], Thomas G. Brink[17], Rick Burruss[18], Poonam Chandra[19], Ting-Wan Chen[20,21], Wen-Ping Chen[22], Jeff Cooke[23,24,25], Michael W. Coughlin[26], Kaustav K. Das[27], Andrew J. Drake[27], Alexei V. Filippenko[17], James Freeburn[23,24], Christoffer Fremling[18,28], Michael D. Fulton[10], Avishay Gal-Yam[3], Lluís Galbany[29,30], Hua Gao[16], Matthew J. Graham[28], Mariusz Gromadzki[31], Claudia P. Gutiérrez[29,30], K-Ryan Hinds[2], Cosimo Inserra[32], Nayana A J[13], Viraj Karambelkar[27], Mansi M. Kasliwal[27], Shri Kulkarni[27], Tomás E. Müller-Bravo[29,30], Eugene A. Magnier[16], Ashish A. Mahabal[28,33], Thomas Moore[10], Chow-Choong Ngeow[22], Matt Nicholl[10], Eran O. Ofek[3], Conor M. B. Omand[34], Francesca Onori[35], Yen-Chen Pan[22], Priscila J. Pessi[34], Glen Petitpas[36,37], David Polishook[38], Saran Poshyachinda[14], Miika Pursiainen[39], Reed Riddle[18], Antonio C. Rodriguez[27], Ben Rusholme[40], Enrico Segre[41], Yashvi Sharma[27], Ken W. Smith[10], Jesper Sollerman[34], Shubham Srivastav[10], Nora Linn Strotjohann[3], Mark Suhr[23,25], Dmitry Svinkin[42], Yanan Wang[43,44], Philip Wiseman[44], Avery Wold[40], Sheng Yang[45], Yi Yang[17], Yuhan Yao[27], David R. Young[10] & WeiKang Zheng[17]

In recent years, certain luminous extragalactic optical transients have been observed to last only a few days[1]. Their short observed duration implies a different powering mechanism from the most common luminous extragalactic transients (supernovae), whose timescale is weeks[2]. Some short-duration transients, most notably AT2018cow (ref. 3), show blue optical colours and bright radio and X-ray emission[4]. Several AT2018cow-like transients have shown hints of a long-lived embedded energy source[5], such as X-ray variability[6,7], prolonged ultraviolet emission[8], a tentative X-ray quasiperiodic oscillation[9,10] and large energies coupled to fast (but subrelativistic) radio-emitting ejecta[11,12]. Here we report observations of minutes-duration optical flares in the aftermath of an AT2018cow-like transient, AT2022tsd (the 'Tasmanian Devil'). The flares occur over a period of months, are highly energetic and are probably nonthermal, implying that they arise from a near-relativistic outflow or jet. Our observations confirm that, in some AT2018cow-like transients, the embedded energy source is a compact object, either a magnetar or an accreting black hole.

In a 30-s exposure beginning at 11:21:22 on 7 September 2022 (UTC), the Zwicky Transient Facility (ZTF; Methods section 'Observations and data processing') detected a new optical transient (internal name ZTF22abftjko) at $r = 20.36 \pm 0.23$ mag with the position right ascension α = 03 h 20 min 10.873 s and declination $\delta = +08° 44' 55.739''$ (J2000; uncertainty 0.009″ from Methods section 'Observations and data processing') as part of its public 2-day cadence all-sky survey. The transient was reported[13] to the Transient Name Server by the Automatic Learning for the Rapid Classification of Events (ALeRCE) alert broker[14] and designated AT2022tsd. Forced photometry on ZTF images (Methods section 'Observations and data processing') revealed that the light-curve evolution was faster than that of typical supernovae (Fig. 1). The optical light curve, and the implied high peak luminosity from a nearby (1.4″) catalogued galaxy (Methods section 'Identification of AT2022tsd and redshift measurement' and Fig. 1), led AT2022tsd to be flagged as a transient of interest as part of continuing efforts to discover luminous and fast-evolving optical transients (Methods section 'Identification of AT2022tsd and redshift measurement').

We obtained two spectra of AT2022tsd with the Low Resolution Imaging Spectrometer (LRIS) on the Keck I 10-m telescope (Extended Data Fig. 1; Methods section 'Observations and data processing') and measured[15] a redshift of $z = 0.2564 \pm 0.0003$ (luminosity distance D_L = 1.34 Gpc assuming a Planck cosmology[16]) of the nearby galaxy using prominent narrow host-galaxy emission lines (Methods section 'Identification of AT2022tsd and redshift measurement'). The optical properties—the fast light-curve evolution, the implied high peak luminosity ($M_{peak} = -20.64 \pm 0.13$ at rest-frame wavelength 5,086 Å; Methods section 'Identification of AT2022tsd and redshift measurement') and the lack of prominent spectroscopic features after the transient faded by 2–3 magnitudes—were unusual for extragalactic transients but similar to AT2018cow, which motivated us to trigger further multiwavelength observations (Fig. 2; Methods section 'Multiwavelength properties of

A list of affiliations appears at the end of the paper.

Himalayan Chandra Telescope. We observed AT2022tsd with the 2-m Himalayan Chandra Telescope (HCT) on 26 December 2022 under a Director's Discretionary Time proposal. We obtained a series of 5-min exposures in the R band from 13:47 to 20:25, covering almost all of the first Chandra X-ray Observatory observing window. Seeing and focus were generally poor and vary greatly over the course of the observation. A stacked subset of the best-quality images is used as a reference and all other images are differenced relative to this one by cross-convolution of the respective PSFs. We did not detect any clear flares, with a limiting magnitude per exposure of $R \geq 22$ mag. It is possible that there are some weak flares at the detection threshold, but the detections are not robust owing to the variable PSF size and shape over the course of the observation window.

GROWTH-India telescope. We observed AT2022tsd on 26 December 2022 using the GROWTH-India Telescope (GIT[161]) located at the Indian Astronomical Observatory (IAO), Hanle, Ladakh, simultaneously with the HCT (see previous section). Images were observed in an open-filter configuration with a 300-s exposure time. Images were analysed using a method similar to that used on other facilities. We used a stacked image containing all observations from the night as the reference image to subtract host-galaxy emission in the region of the transient and performed forced aperture photometry using a 2″-radius aperture. No notable flares were detected during the observation sequence.

Magellan-Baade telescope. Starting at 04:30 on 15 December 2022, we obtained five 3-min g-band exposures of AT2022tsd using the IMACS[162] mounted on the 6.5-m Magellan-Baade telescope at Las Campanas Observatory. This sequence shows an unambiguous, high-S/N (about 70) flare detection peaking in the middle of the five-exposure sequence and is what led to our initial visual discovery of the short-timescale behaviour of this event. Image subtraction is performed using a stack of flare-free g-band images from Keck/LRIS taken in January as a reference, and forced aperture photometry is applied to the difference image.

Nordic Optical Telescope. Starting at 02:30 on 4 October 2022, we obtained an epoch of *ugri* observations of AT2022tsd using the Alhambra Faint Object Spectrograph and Camera (ALFOSC) on the 2.56-m NOT at the Observatorio del Roque de los Muchachos on La Palma in Spain. Following the discovery of flaring, we obtained two further epochs of observations, the first in g (five 60-s exposures on the night of 16 December 2022) and the second in g and r (five 90-s exposures in each) on the night of 23 December 2022. A flare was detected in the final g-band epoch. Image subtraction in g is performed using a stack of the 16 December 2022 epoch as a reference; image subtraction in r is performed using a stack of the 22 December 2022 observations. Individual flare-free exposures from the Keck/LRIS observations are used as references for i and u. Photometry is performed using a fixed aperture of 1″ radius. The NOT photometry is presented in Supplementary Table 1.

Palomar Hale 200-inch telescope. On 27 January 2023, we observed the position of AT2022tsd for 3 h using the Caltech HIgh-speed Multi-color camERA (CHIMERA[163]) on the Palomar 200-inch Hale telescope. The seeing was 2.5–3″. A total of 210 exposures of 50 s each were obtained simultaneously in the g and r filters. Images were reduced using a custom pipeline modified from that of ULTRACAM[164] and image subtraction was performed using PS1 as a reference using the same techniques as for LT and ULTRASPEC. Photometry was performed using a 2.5″-radius aperture.

Lulin Observatory. Between 14:38 and 17:27 on 26 December 2022, we obtained 27 g-band images with the Lulin One-meter Telescope and 31 r-band images with the 40-cm Super Light Telescope, coordinated with Chandra X-ray Observatory observations (Methods section titled 'Observations and data processing'). Each exposure was 300 s, with varying seeing conditions (with an average of 2.8″). The g images were subtracted from a PanSTARRS template, with no detection of AT2022tsd in any image. Combining all 27 g images results in a 3σ limit of $g > 22.0$ mag. To perform image subtraction on the r-band images, a template image was acquired with the Super Light Telescope. The 3σ upper limits for individual frames are provided in Supplementary Table 1.

European Southern Observatory New Technology Telescope. We observed AT2022tsd on two nights (18 and 19 December 2022) using ULTRACAM[164]. On 18 December, we obtained 116 i-band frames with a 20-s exposure time, totalling 38 min of data; the dead time between each frame is 24 ms. The seeing was 1–1.5″. On 19 December, we obtained 556 r-band frames with a 20-s exposure time, totalling 3 hr 5 min of data. The dead time between each frame is again approximately 24 ms. The seeing started at 1″ but worsened to 2.5″ towards the end of the run. We subtracted a dark image and removed remaining bad/hot pixels in the vicinity of the transient by taking the median value of the eight surrounding pixels. Image subtraction was performed using a consistent method as for the other observations, using stacks formed from flare-free sections of the data taken on the same night. For the first night, which shows no flaring, we use a stack of the entire night; for the second night, we use a stack of the first 97 images (all acquired before the flare). Photometry was performed using a fixed 1.5″-radius aperture and calibrated to nearby Pan-STARRS standards.

As part of ePESSTO+ (the Public European Southern Observatory Spectroscopic Survey of Transient Objects project[165]), we observed AT2022tsd on three nights (22, 24 and 30 December 2022) in the g and r bands using the Faint Object Spectrograph and Camera (v.2; EFOSC2 (ref. 166)) mounted on the 3.58-m European Southern Observatory (ESO) New Technology Telescope (NTT) under the observing programme 1108.D-0740 (PI C. Inserra). On the first two nights, the observation sequence was 5 × 95-s exposures in g followed by 5 × 95-s exposures in r. A flare is seen at the beginning of the g-band sequence from the second epoch; otherwise, no variability was evident. On the third night, the sequence was altered such that images were obtained in alternating filters (5 × gr) and no flare was detected. The data were reduced using the standard pipeline (https://github.com/svalenti/pessto), which is based on iraf/pyraf. Image subtraction was performed using the last exposure of each sequence as a reference image; photometry was performed using a 1.0″-radius aperture in all observations.

Kitt Peak 84-inch Telescope. On 20 December 2022, we observed the position of AT2022tsd for 2 h using the Spectral Energy Distribution Machine (SEDM[167]) version 2 on the Kitt Peak 84-inch (KP84) Telescope. A total of 60 exposures of 120 s each were obtained in the clear filter. Flat-fielding was performed using a super-sky flat constructed using a median stack of all exposures taken on the field. Pan-STARRS r-band imaging was used as the reference image, which resulted in an acceptable removal of the host despite the unfiltered nature of the observations. Photometry was performed using a fixed 1.5″-radius aperture and calibrated to nearby Pan-STARRS standards. We subtracted a median flux level from all flux values.

Large Array Survey Telescope. We observed AT2022tsd using eight telescopes in the Large Array Survey Telescope (LAST[168,169]). The target was observed on 12, 13 and 15 January 2023 and also on several nights during December 2022. The 2022 observations were taken under poor conditions and are not reported here. We obtained 20-s exposures in continuous mode (that is, no dead time between images). A total of 10.9 h of observations in three nights were obtained. The observations were reduced using the LAST pipeline[168,170,171] and forced PSF photometry was conducted on the individual images in the transient position. The source position was fitted but it was forced to be within 0.5 pixels (0.62″) of the initial position. In each image, we also performed forced

Monthly Notices of the ROYAL ASTRONOMICAL SOCIETY

MNRAS **526,** 4502–4513 (2023) https://doi.org/10.1093/mnras/stad3064
Advance Access publication 2023 October 9

Extreme photometric and polarimetric variability of blazar S4 0954+65 at its maximum optical and γ-ray brightness levels

C. M. Raiteri ,[1★] M. Villata ,[1] M. I. Carnerero ,[1] S. S. Savchenko ,[2,3,4] S. O. Kurtanidze,[5] V. V. Vlasyuk,[3] A. Marchini ,[6] K. Matsumoto,[7] C. Lorey,[8] M. D. Joner ,[9] K. Gazeas ,[10] D. Carosati,[11,12] D. O. Mirzaqulov ,[13] J. A. Acosta Pulido,[14,15] I. Agudo,[16] R. Bachev,[17] E. Benítez ,[18] G. A. Borman ,[19] P. Calcidese,[20] W. P. Chen,[21] G. Damljanovic ,[22] S. A. Ehgamberdiev ,[13,23] D. Elsässer ,[8,24] M. Feige,[8] A. Frasca ,[25] H. Gaur,[26] T. S. Grishina ,[2] A. C. Gupta ,[26] D. Hiriart ,[27] M. Holland,[9] B. Horst,[8] S. Ibryamov,[28] R. Z. Ivanidze,[5] J. Jensen,[9] V. Jithesh,[29] M. D. Jovanovic ,[22] S. Kiehlmann,[30,31] G. N. Kimeridze,[5] S. Kishore,[26] E. N. Kopatskaya ,[2] O. M. Kurtanidze,[5,32] E. G. Larionova ,[2] H. C. Lin,[21] K. Mannheim,[8,33] C. Marinelli ,[34] J. Moreira Reyes,[35] D. A. Morozova ,[2] M. G. Nikolashvili,[5] D. Reinhart,[8,33] F. D. Romanov ,[36,37] E. Semkov,[17] J. Seufert,[8] E. V. Shishkina,[2] L. A. Sigua,[5] R. Skalidis,[38] O. I. Spiridonova,[3] M. Stojanovic ,[22] A. Strigachev,[17] Y. V. Troitskaya ,[2] I. S. Troitskiy ,[2] A. Tsai,[21] A. A. Vasilyev ,[2] O. Vince,[22] K. Vrontaki,[10] K. Wani,[26] D. Watts[9] and A. V. Zhovtan[19]

Affiliations are listed at the end of the paper

Accepted 2023 October 4. Received 2023 October 4; in original form 2023 August 15

ABSTRACT

In 2022 the BL Lac object S4 0954+65 underwent a major variability phase, reaching its historical maximum brightness in the optical and γ-ray bands. We present optical photometric and polarimetric data acquired by the Whole Earth Blazar Telescope (WEBT) Collaboration from 2022 April 6 to July 6. Many episodes of unprecedented fast variability were detected, implying an upper limit to the size of the emitting region as low as 10^{-4} parsec. The WEBT data show rapid variability in both the degree and angle of polarization. We analyse different models to explain the polarization behaviour in the framework of a twisting jet model, which assumes that the long-term trend of the flux is produced by variations in the emitting region viewing angle. All the models can reproduce the average trend of the polarization degree, and can account for its general anticorrelation with the flux, but the dispersion of the data requires the presence of intrinsic mechanisms, such as turbulence, shocks, or magnetic reconnection. The WEBT optical data are compared to γ-ray data from the *Fermi* satellite. These are analysed with both fixed and adaptive binning procedures. We show that the strong correlation between optical and γ-ray data without measurable delay assumes different slopes in faint and high brightness states, and this is compatible with a scenario where in faint states we mainly see the imprint of the geometrical effects, while in bright states the synchrotron self-Compton process dominates.

Key words: galaxies: active – BL Lacertae objects: general – BL Lacertae objects: individual: S4 0954+65 – galaxies: jets.

1 INTRODUCTION

With the term ‘blazar’ we indicate a jetted active galactic nucleus (AGN) with one jet directed towards us. Leptons moving at relativistic speeds along the magnetic field lines inside the jet produce low-energy synchrotron radiation and high-energy radiation through inverse-Compton scattering of soft photons. Processes involving hadrons may also be responsible for the high-energy emission (e.g. Böttcher et al. 2013). Because of the jet orientation, this radiation is relativistically Doppler beamed (e.g. Urry & Padovani 1995). Consequences of the Doppler beaming are that the flux that we observe is enhanced in comparison to what is emitted by the source, and the variability time-scales are shortened. This is why blazars often show extreme variability at all wavelengths, from the radio to the γ rays, on time-scales ranging from years to minutes (e.g. Wagner & Witzel 1995; Aharonian et al. 2007; Albert et al. 2007; Shukla & Mannheim 2020; Weaver et al. 2020). The origin of such multiscale flux changes is still debated, but it is clear that different processes must intervene to account for the variety of observed variability events. Flares suggest that particles get accelerated in the jet. The two main acceleration mechanisms that are commonly invoked are shock waves propagating in the jet (e.g. Hughes, Aller & Aller 1985; Marscher & Gear 1985), and magnetic reconnection, possibly triggered by kink instabilities (e.g. Sironi, Petropoulou & Giannios 2015; Zhang et al. 2018; Bodo, Tavecchio & Sironi 2021;

★ E-mail: claudia.raiteri@inaf.it

Table 1. Details on the optical data sets contributing to this paper.

Data set	Country	Diameter (cm)	N_{obs}	Symbol	Colour
Abastumani	Georgia	70	888	◇	dark green
ARIES	India	130	87	□	green
Athens[a]	Greece	40	177	+	grey
Belogradchik[b]	Bulgaria	60	42	+	cyan
Burke-Gaffney	Canada	61	18	◇	pink
Calar Alto[b]	Spain	220	2	∗	red
Catania (SLN)	Italy	91	3	△	blue
Connecticut	US	51	2	∗	grey
Crimean (ST-7)	Crimea	70	1	+	magenta
Crimean (ST-7; pol)[b]	Crimea	70	96	×	dark green
Hans Haffner	Germany	50	194	∘	red
Lulin (SLT)	Taiwan	40	38	∘	black
McDonald (LCO)	US	40	1	×	black
Mt. Maidanak	Uzbekistan	60	101	∘	violet
Osaka Kyoiku	Japan	51	276	□	orange
Rozhen	Bulgaria	200	6	□	red
Rozhen	Bulgaria	50/70	10	×	orange
San Pedro Martir	Mexico	84	8	□	blue
SAO RAS	Russia	100	43	∘	blue
SAO RAS	Russia	50	706	◇	red
Siena	Italy	30	438	◇	blue
Skinakas (RoboPol)[b]	Greece	130	16	×	blue
St. Petersburg[b]	Russia	40	53	+	orange
Teide (IAC80)	Spain	80	6	∗	green
Teide (LCO)	Spain	100	1	∗	black
Teide (LCO)	Spain	40	9	+	black
Tijarafe	Spain	40	130	△	green
Valle d'Aosta	Italy	80	10	+	violet
Vidojevica[c]	Serbia	140	64	□	black
Vidojevica[c]	Serbia	60	12	△	black
West Mountain	US	91	190	∘	dark green

Notes. 'LCO' refers to telescopes belonging to the Las Cumbres Observatory global telescope network
[a]University of Athens Observatory (UOAO)
[b]Also polarimetry
[c]Astronomical Station Vidojevica

4 SIZE OF THE OPTICAL EMITTING REGION

As detailed in the previous section, unprecedented intraday variability was observed in the period analysed. From causality arguments based on light traveltime, the observed minimum variability time-scale Δt_{min} can put an upper limit to the size R of the emitting region:

$$R < c\,\Delta t_{min} \times \delta/(1+z), \quad (1)$$

where c is the speed of light, δ is the Doppler factor, and z the source redshift. The value of Δt_{min} can be obtained from the well-sampled, extreme IDV episode on JD 2459737, which is shown in Fig. 4. Flux densities have been obtained from magnitudes using the calibrations by Bessell, Castelli & Plez (1998) and correcting for Galactic absorption ($A_V = 0.259$ mag from the NASA/IPAC Extragalactic Database[2]).

We modelled the flare according to Valtaoja et al. (1999):

$$\begin{aligned} F &= F_0 + A e^{(t-t_{peak})/\Delta t_1} \quad \text{if} \quad t < t_{peak} \\ F &= F_0 + A e^{(t_{peak}-t)/\Delta t_2} \quad \text{if} \quad t \geq t_{peak} \end{aligned}, \quad (2)$$

[2]https://ned.ipac.caltech.edu/

where F_0 is the base level, A the flare amplitude, t_{peak} the time of the flare peak, and Δt_1 and Δt_2 the time-scales before and after the peak, respectively.

The least-squares best-fitting model of the flare is obtained by the following parameters: $F_0 = (9.5 \pm 0.5)$ mJy, $A = (8.6 \pm 1.1)$ mJy, $t_{peak} = (2459737.459 \pm 0.003)$, $\Delta t_1 = (0.028 \pm 0.007)$ d, and $\Delta t_2 = (0.012 \pm 0.005)$ d. Setting $\Delta t_{min} \approx 17$ min, and $\delta = 13.6$ (see Section 6 and Fig. 8) we found $R < 3 \times 10^{14}$ cm, i.e. about 10^{-4} parsec. This upper limit to the emitting region size responsible for the flare is in general smaller than the typical size assumed for the blazar jets, and in particular it is more than 66 times smaller than that assumed by Raiteri et al. (1999) when applying the homogeneous model by Ghisellini et al. (1998) to the SEDs of S4 0954+65 during a faint state observed in 1994–1998. This suggests that we may be seeing flux fluctuations in a jet subregion.

We note that blazar microvariability with as short as a few minutes time-scale was also detected at γ rays, in both GeV and TeV energy domains. In the case of 3C 279 observed by the *Fermi* satellite, a very fast flare in 2018 was ascribed to magnetic reconnection in a region of about 8×10^{14} cm (Shukla & Mannheim 2020). For the microvariations observed by the High Energy Stereoscopic System (H.E.S.S.) in PKS 2155-304 (Aharonian et al. 2007), and by MAGIC in Mkn 501 (Albert et al. 2007), the inferred sizes are likely more than 10 times smaller, when typical values of $\delta \sim 10$ are assumed.

II
研究報告

YOUNG SUPERNOVA EXPERIMENT

Yen-Chen Pan
Graduate Institute of Astronomy, National Central University

1. Abstract

Transient surveys are now consistently finding transients within hours of explosion. These observations provide rare opportunities to investigate the explosion and progenitor system, and probe the circumstellar environment surrounding the SN. Interaction with a potential companion star is also visible in the first hours. We have started an international collaboration to detect extremely young explosions since 2019. Using a novel technique to combine our data with public data, we will clearly identify interesting targets as they rise, detecting transients within hours of explosion. The Lulin observatory is part of the collaboration and plays a critical role in constraining the properties of these young transients. Here I will briefly describe the program and report the current status.

2. Description of the Program

Early observations of transients place unique constraints on their progenitor systems and explosion mechanisms. To increase the number of transients detected within hours of explosion, we are starting a new survey, the Young Supernova Experiment (YSE). YSE is the collaboration between DARK (University of Copenhagen), UC Santa Cruz, University of Illinois, University of Toronto, and Northwestern University. YSE will survey $\sim 1000\,\mathrm{deg}^2$ of equatorial sky on a 3-day cadence (in $griz$) using the Pan-STARRS (PS) telescopes. We will also shadow other public transient surveys, such as ASASSN, ATLAS and ZTF, which can improve our detection and selection of SNe within hours of explosion. Because of different observatory longitudes, there will be a lag of a few hours between the public survey and PS observations. During this time, some transients will explode and rise to a point of being detectable, and more will be barely detectable in the public surveys and rise considerably in a few hours. When PS detects a new transient, we will immediately query these public surveys to determine if the transient is young. With the expected cadence of PS observations, our detected transients will be 3 days old at most, and we expect to discover $\sim$2 transients within hours of explosion per month.

We ask for Lulin ToO observations to obtain the multi-color photometry of YSE transients, and to watch the objects quickly develop. Being another few hours lag from the PS telescope, the location of Lulin observatory will be critical to constrain the extremely young transients discovered by YSE. Any young transients detected by PS telescope can be monitored by Lulin within hours, which will greatly reduce the cadence of our photometric observations. This is crucial given the light-curve evolution is expected to be dramatic within the first few days after explosion. The early Lulin observations will play an important role in catching this fast evolution and provide better constrain on the transient age.

3. Program Status and List of Publications

Currently the YSE is still active, and we have observed $\sim$150 transients for this program since 2020 with LOT. Many of these events are extremely interesting. Several papers have been published within our collaboration using the LOT data (see below for a list of publications).

1. Wang et al., "Flight of the Bumblebee: the Early Excess Flux of Type Ia Supernova 2023bee Revealed by TESS, Swift, and Young Supernova Experiment Observations", 2024, ApJ, 962, 17

2. Kilpatrick et al., “Type II-P supernova progenitor star initial masses and SN 2020jfo: direct detection, light-curve properties, nebular spectroscopy, and local environment”, 2023, ApJ, 524, 2

3. Jacobson-Galan et al., “SN 2023ixf in Messier 101: Photo-ionization of Dense, Close-in Circumstellar Material in a Nearby Type II Supernova”, 2023, ApJ, 954, 2

4. Karthik et al., “SN 2022oqm: A Bright and Multi-peaked Calcium-rich Transient”, accepted for publication in ApJ

5. Davis et al., “SN 2022ann: A type Icn supernova from a dwarf galaxy that reveals helium in its circumstellar environment”, 2023, MNRAS, 523, 2

6. Tinyanont et al., “Supernova 2020wnt: An Atypical Superluminous Supernova with a Hidden Central Engine”, 2023, ApJ, 951, 34

7. Dimitriadis et al., “A Super-Chandrasekhar Supernova Caused bythe Merger of Carbon/Oxygen White Dwarf Stars”, 2022, ApJ, 927, 78

8. Hosseinzadeh et al., “Weak Mass Loss from the Red Supergiant Progenitor of the Type II SN 2021yja”, 2022, ApJ, 935, 31

9. Jacobson-Galn et al., “Final Moments I: Precursor Emission, Envelope Inflation, and Enhanced Mass loss Preceding the Luminous Type II Supernova 2020tlf”, 2021, ApJ, 924, 15

10. Jencson et al., “AT2019qyl in NGC300: Early Outflow Collisions for a Very Fast Nova in a Symbiotic Binary”, 2021, ApJ, 920, 127

RIFT (Robotic Imager For Transients) 星瞬望遠鏡, 李君樂

RIFT is the abbreviation of Robotic Imagers For Transients, which is the first robotic astronomical observatory dedicated to the study of multi-messenger transients in Taiwan. It is also ones of the second largest research telescope in Taiwan after the Lulin One-meter Telescope (LOT). Different from LOT, RIFT is designed to be a quick-response and wide-field system. With the fully robotic control, RIFT can carry out prompt follow-up observations of transients in minutes.

Since the end of 2022, RIFT has been taking scientific data, partially for the purpose of system testing. The redback pulsar binary, PSR J1048+2339 is the primary target, which can be summarized as a r   19-20 mag variable star. Figure 3 shows the optical light curve of PSR J1048+2339. All observations were taken unfiltered with 200 seconds per frame. No magnitude calibration can be done as we did not use any filter during the observations (to optimize the limiting magnitude of the data). Nevertheless, according to the previous LOT observations (Yap et al. 2019), we know that PSR J1048+2339 is r   20 mag at the minimum phase (i.e., the grey region at phase 0.25 in Figure 3), demonstrating that RIFT can easily go down to 20 mag. Most importantly, PSR J1048+2339 exhibited many optical flares during the observations, but none of them were found in the phase interval between 0.2 and 0.3, during which the neutron star is behind the companion. We speculate that the optical flares are the result of the pulsar irradiation on the companion surface, which naturally explains the observed phenomenon. If it is true, the phase duration without flare will provide crucial information on several geometrical parameters of the binary, including the inclination, binary separation, and mass ratio of the binary, and Roche-lobe filling factor of the companion. As the binary inclinations are always important in dynamical mass measurement, our work could serve as an entirely new technique to weight neutron stars.

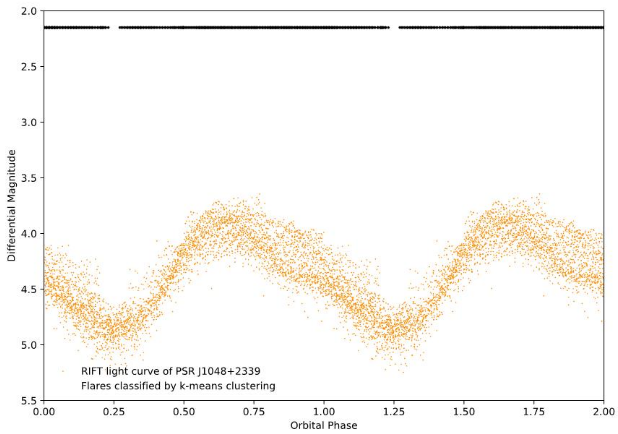

Figure 3: Light curve of PSR J1048+2339 taken by RIFT.

We will also expand the RIFT project by setting up another robotic telescope at Lulin very soon. The original plan is to have a pair of 0.5-m telescopes at Lulin. Considering the need of a wide-field telescope that will be extremely helpful in searching for the electromagnetic-wave (EM) counterparts of, e.g., gravitational-wave events, we plan to switch one of the 0.5-m telescopes to a 11-inch telescope (about 28 cm in diameter; model: RASA11 V2). Although it is a smaller telescope, the resultant field-of-view (FoV) is actually much larger than our original design (i.e., focal ratio: f/2.2. In this case, the 11-inch telescope will be an ideal tool to search for the optical emission of those systems with poorly constrained localizations, while the 0.5-m telescope can follow up the identified targets with a bigger aperture (i.e., higher signal-to-noise). We have been carrying out the feasibility study, and will purchase a new 2k $\times$ 2k scientific CMOS camera (Marana 4.2B-11) from ANDOR for the project. The camera will be ready in the summer, and we can do the telescope installation at Lulin after that.

拿鐵望遠鏡 LATTE (Lulin-ASIAA Telescope for Transients and Education)

LATTE (Lulin-ASIAA Telescope for Transients and Education) is a 50 cm reflective imaging telescope at Lulin. In its first 2 years of operation (since mid 2022), it focuses more on its education roles. It supported the training of college students in classes of observational astronomy taught by Prof. Shih-Ping Lai (NTHU, spring and fall semesters, 2023) and by Dr. Wei-Hao Wang (NTU, fall semester, 2023), public outreach for amateur astronomers and general audience on Facebook, and a collaboration project between ASIAA and TASA to study satellite monitoring. From spring of 2024, LATTE is quipped with an interface similar to LOT and SLT to become operable by Lulin staff and to join the call for science proposals for Lulin Observatories. The LATTE team in ASIAA is grateful to the Lulin staff and NCU for the continuous support. We look forward to become a more integrated member of the Lulin Observatory for both science and education.

The multiband observations of the flare activity of an M dwarf.

Chia-Lung Lin, Li-Ching Huang, Wing-Huen Ip, and Wei-Jie Hou

1. Introduction

Empirically, the temperature of M dwarf's flares was observed to be about 9,000 – 10,000 K (e.g., Kowalski et al. 2010). However, in the recent studies, people found that an M dwarf could produce flares with temperatures ranging from 5,000 K to 40,000 K (Maas et al. 2022, Howard et al, 2020). It is crucial because the temperature of flare affects not only the energy budget of flare at UV, which could further impact the habitability of surrounding terrestrial exoplanet, but also the detection of atmospheric characterization of exoplanet at NIR wavelength JWST focuses on (e.g., Howard et al. 2023).

2. Observation series

Given the fact that the behavior of flare is more complex than previously thought, we emphasize the need for detailed observation and analysis. Between 2020 and 2022, we carried out a series of the simultaneous photometric and spectroscopic observations of the flaring M dwarfs, Wolf 359 and EPIC 210651981 with SLT 40-cm telescope and LOT 1-m telescope at Lulin Observatory. Our primary goal of these observations is to enhance our understanding of flare temperature and spectral evolution in M stars.

3. Result from previous observations

From the observations of Wolf 359 on April 3 in 2021, we estimated the flare temperature of a flare to be about 7,200 K by using U-V color. This is consistent with the claim made by Lin et al. (2021). They applied the data from Howard et al. (2020) and obtained a value of 7,300 K +- 1,500 K of M dwarfs' flares on average. On December 3 in the same year, a flare from EPIC 210651981 exhibited a temperature of ~ 20,000 K estimated using the same method. It emphasizes once again the diversity of M dwarfs' flares.

On the other hand, the measurements we made for the flares from these two stars may be suffered a considerable systematic error that cannot be explicitly interpreted due to the long cadence of the V band observation. The V band data was created by convoluting the transmission of the V filter with the spectra, which was observed with a 10 min exposure each frame in order to obtain an acceptable SNR. In addition, we would like to gather data with more bands to improve the temperature measurement. Thus, in 2023, we proposed the multi-band (u, g, r, i, and z) simultaneous photometric observations of two M stars, Wolf 359 in Feb and Ross 388 in Dec, by using SLT and LOT with the instrument TRIPOL.

4. Preliminary results from the observations in 2023

On 2023 Feb 21, we observed eight flares in Wolf 359 with g, r, i, and z bands (see Panel a. in the following figure):

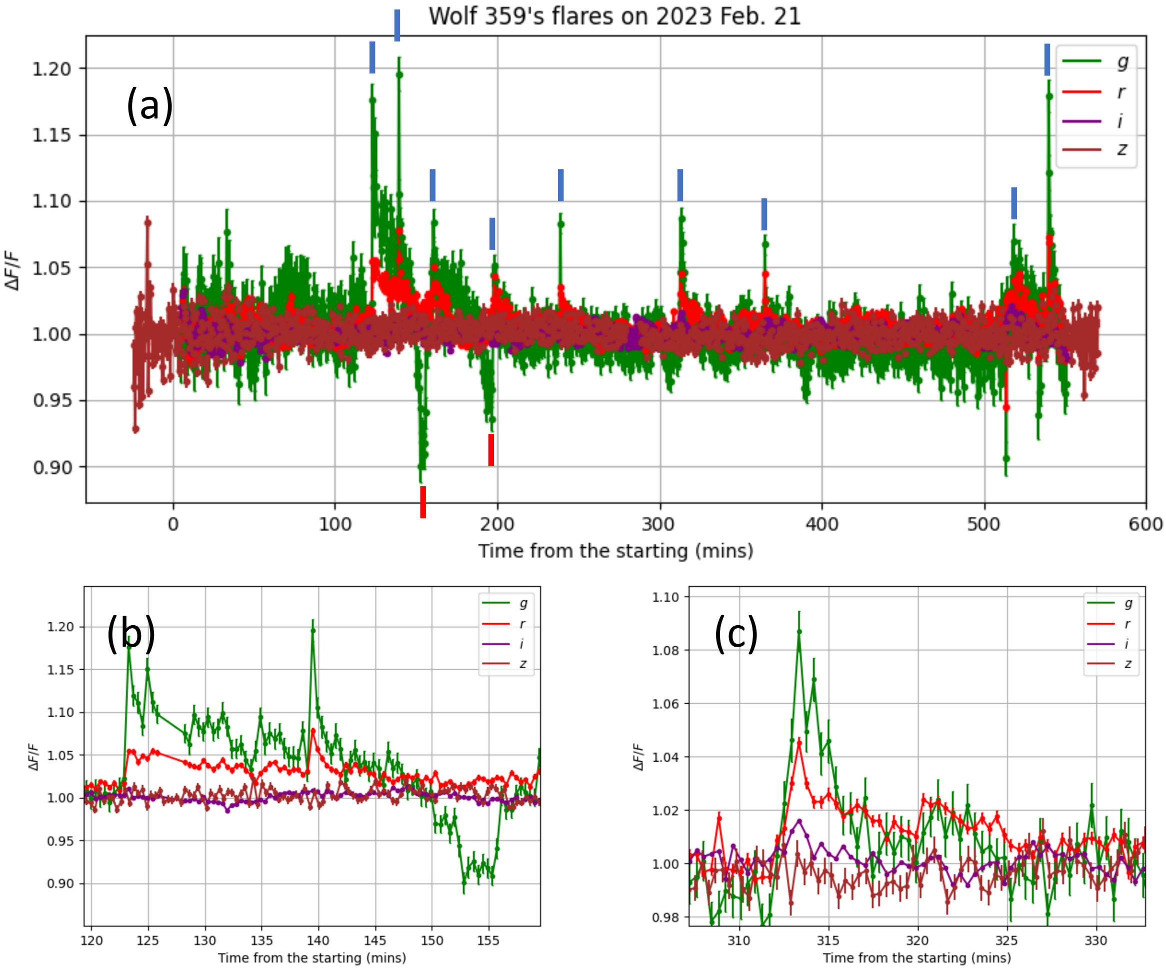

The x-axis is the time in units of minute starting from the exposure mid-time of the TRIPOL's first frame at that night. The y-axis is the normalized flux. The observed flares are marked with the blue vertical bars above them. The red vertical bars mark the flux dimming, which is only observable in the g band right after the flare. We found that the dimming is caused by one of the field stars we applied to carry out the differential photometry. Panel (b): The complex multi-flare profile starting from t=122 min. The amplitude of the flare decreases with longer wavelength and, in this case, are only apparent in g and r band. Panel (c): The only flare that shows apparent amplitude variation in g, r, and i bands. No flare can be detected in the z band light curve alone.

In the second half of 2023, we observed two potential flare events from Ross 388 on Dec. 5 and Dec. 7, respectively (see the Figure below):

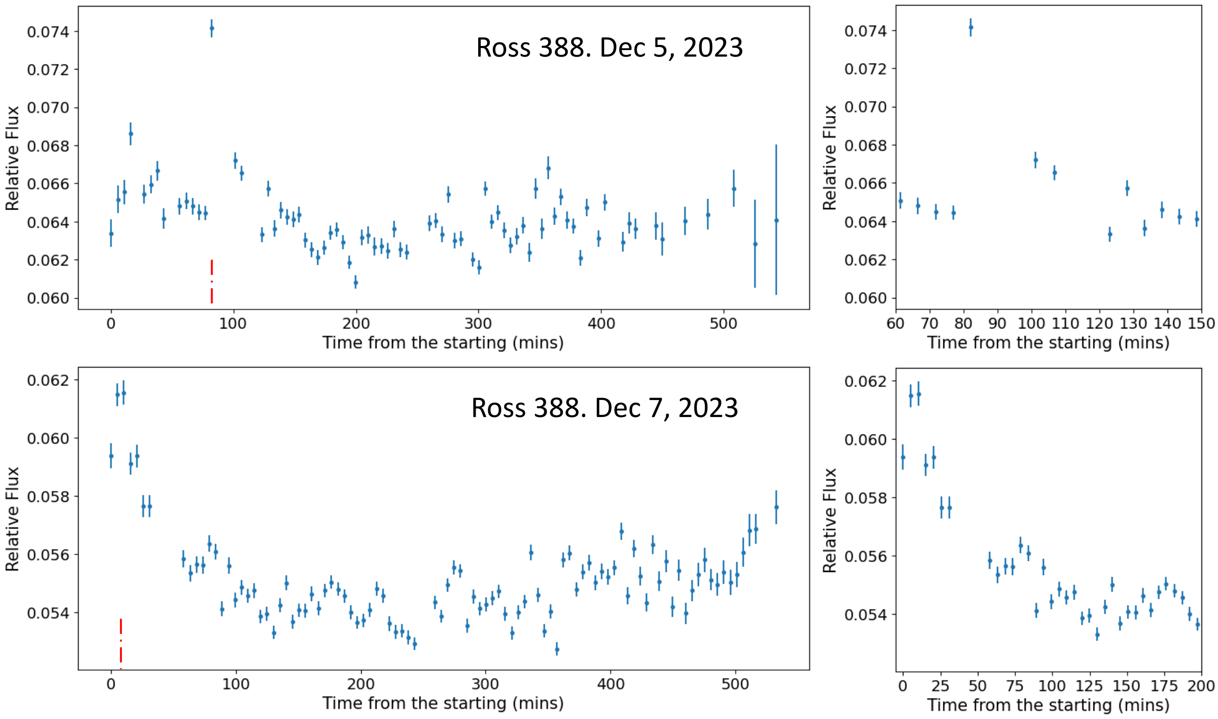

These are the light curves observed with U band by using SLT 40-cm telescope. The dashed lines represent the timing position of the peak of the potential flare events. The panels on the right highlight the profiles of these events. We will later confirm their authenticity by processing the data from TRIPOL.

5. Our Next steps

We will conclude the observations during these years and proceed data analysis to determine the flare properties of these M dwarfs. We hope to publish our findings soon.

References:

Howard, W. S., Kowalski, A.~F., Flagg, L., et al. 2023, ApJ, 959, 64

Howard, W. S., Corbett, H., Law, N.~M., et al. 2020, ApJ, 902, 115

Kowalski, A. F., Hawley, S. L., Holtzman, J. A., et al. 2010, ApJL, 714, L98

Lin, C.-L., Chen, W.-P., Ip, W.-H., et al. 2021, AJ, 162, 11

Maas, A. J., Ilin, E., Oshagh, M., et al. 2022, A&A, 668, A111

The TANGO network of lunar Impact flash observations update

Zhong-Yi Lin [1], Wing-Huen Ip[1] , Hung-Chin Lin[1] , Jim Lee[2], Xue-Hui Ma[3], Sung-Hui, Tasi[4],**Yan-Ping Chen[5]**
[1]Graduate Institute of Astronomy, NCU, Taoyuan, Taiwan, [2]Taipei Astronomical Museum, Taipei, Taiwan, [3]Ken-Ting Observatory, NMNS, TaiChung, Taiwan, [4] Kinchen Junior High School, Kinman,Taiwan, [5]Department of Physics, NCU, Taoyuan, Taiwan

Abstract

Light flashes produced by meteoroids impacting the night side of the Moon have been identified mostly during the peak activity of several major meteor showers. Routine impact monitoring has been carried out with an automatic system at NASA Marshall Space Flight Center (MSFC) since 2006. During the first five years they found a total of 240 impacts; on average one flash for every two hours of observation, with dramatically higher rates during meteor showers. In December 2017 and 2018, we participated for the first time in the monitoring campaign of lunar impact flashes by using two small telescopes at Lulin observatory during the Geminid meteor storms. Lucky, we got a few detections.

In 2022, we reconstructed the observational system at Lulin observatory and set up the Taiwan Astronomical Network of Ground-based Observations (TANGO) for lunar Impact flash observations. In this work, we will describe our monitoring system, and update TANGO network. If there is any detection of lunar impact flash, the estimation of some physical properties will be presented.

Introduction

Lunar exploration has always been at the forefront of space research and planetary science starting from the Apollo program. The Chang'e lunar program of China and NASA's Artemis project have once again cast the unmanned and manned missions to the Moon into the limelight. To prepare for permanent human habitats and in situ resource utilization on the Moon, a wide range of scientific problems and technical issues have emerged. The Solar System Exploration Research Virtual Institute (SSERVI) is an organization composed of a team of experts with different research interests in lunar science (Solar System Exploration Research Virtual Institute (nasa.gov)).Its main goal is to support the development of scientific methods and technology in connection to the Artemis mission. Besides American scientists, SSERVI has also established partnerships with space agencies and research groups from the international science community. In 2023, Prof. Wing-Huen Ip starts to organize a team, called **T**aiwan **U**niversity **L**unar **I**nvestigation **P**roject (**TULIP**), and lead the Taiwan researcher to join the SSERVI. The TULIP includes several lunar science projects: 1. Data-driven modeling (Modeling of lunar exosphere and plasma environment); 2. Observations (Observation of the lunar sodium exosphere and exo-tail); 3. Monitoring (Monitoring of the meteoroid impact events on the lunar surface); 4. Virtual lectures (Virtual lecture series on the Moon); 5. Outreach.

RoLIFE (**Ro**botic **L**ulin lunar **I**mpact **F**lashes t**E**lescopes)

One project in TULIP led by Dr. Zhong-Yi Lin is called the Lunar Impact Flash Monitoring Project. The scientific objective is to detect impact flashes produced by near-Earth meteoroids and asteroids and thereby help constrain the size-frequency distribution of near-Earth objects in the decimeter to meter range (impact flux on Earth). Furthermore, the detected events can help us to realize the physical properties of impactor and impacted area including the initial kinetic energy of the projectile, its mass, and the size of the resulting crater. Figure 1 shows that the reconstructed observational system set up using a RC12 (30-cm) telescope and a C8 (20-cm) telescope in tandem at Lulin observatory.

Figure 1. Lulin Observatory and the prototype of the lunar flash monitoring telescope system. From Lulin Observatory/NCU.

Taiwan Astronomicla Network of Ground-Based Observations (TANGO)

In association with this work, we have built an observational network with the acronym of "TANGO", namely, Taiwan Astronomy Network of Ground-base Observations. As shown in Figure 2, TANGO will be composed of several small telescopes located at different points of Taiwan including the Kenting Observatory (KTO) and the Kinchen High School (Table 1). The operation of this system is meant to mitigate the risk of unstable weather conditions over Lulin thus enhancing the chance of obtaining valuable observational data.

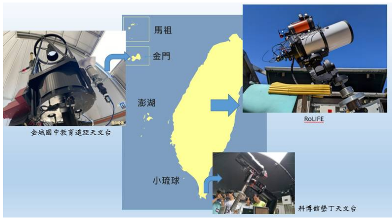

Figure 2. The TANGO project for lunar impact flash monitoring.

Table 1：List instruments of the TANGO facility

	RoLIFE (Lulin)		KTO	Kinman
Camera type	QHY174	ASI 174MM	ASI174	QHY174
Diameter	300mm	200mm	300mm	400mm
Initial focal length	2400mm	2000mm	3300mm	3430mm
Focal reducer system	1320mm (F/4.4)	0.63x (1350mm)		
Time recording system	GPS-time inserters	GPS-time inserters	NTPClock	NTPClock
FOV	29.3' x18.3'	28.9'x18.'	10'x6.3'	11.4x7.2'
Mount	CEM120		DDM60 Pro	MEII

Observations and Results

The earthshine hemisphere of the Moon is observed between 0.1 (crescent) and 0.5 (first quarter) phase and 0.5 (last quarter) to 0.1. The video field of view is oriented with the equator along the vertical axis and limb in the field of view. This maximizes the lunar surface area observed and minimizes glare from the sunlit hemisphere. Evening observations (waxing phase) cover the western or leading hemisphere while morning observations (waning phase) cover the eastern or trailing hemisphere.

Impact Observation Technique

- **Dark (not sunlit) side only**
  - Earthshine illuminates lunar features
- **Crescent and quarter phases – 0.1 to solar illumination**
  - 5 nights waxing (evening)
  - 5 nights waning (morning)
- **4-6 nights of data a month, weather dependent**

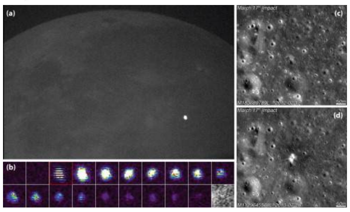

Figure 3 Image of a bright impact flash (March 17, 2013) together with a time series of the impact flash recorded by NASA/MSFC's automated Lunar and Meteor Observatory. The location of the meteoroid impact flash was subsequently identified by LRO to be the site of a new crater. From Suggs et al. (2014).

Duration of flash:	~500 ms
Estimated peak magnitude:	6.86
Peak power flux reaching detector:	$4.94 * 10^{-11}$ W/m^2
Total energy flux reaching detector:	$4.58 * 10^{-12}$ J/m^2
Detected energy generated by impact:	$3.394 * 10^7$ J
Estimated kinetic energy of impactor:	$1.6974 * 10^{10}$ J (4.06 tons of TNT)
Estimated mass of impactor:	17.5 kg
Estimated diameter of impactor:	32 cm (ρ = 1 g/cm^3)
Estimated crater diameter:	13.5 m

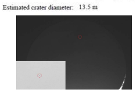

Figure 4 An lunar impact flash in 2018

RoLIFE on Feb. 27, 2023

Acknowledgements

This work was supported by grant numbers MOST 110-2112-M-008-003 and MOST 110-2112-M-008-001 from the Ministry of Science and Technology of Taiwan.

References

Cahill, J.T.S., et al., (2020) A white paper for the National Academies Planetary Science and astrobiology Decal Survey 2023-2032.
Cooke, W.J. (2006) LPSC, XXXVII, Abstract 1731.
Cooke, W.J. (2007) LPSC XXXVIII, Abstract 1986.
Ortiz, J.L., et al., (1999) MNRAS, 343, L57.
Ortiz, J.L.. et al., (2000) Nature, 405, 921.
Suggs, R. M. (2014) Icarus, 238, 23.
Yanagisawa, M. and Kisaichi, N. (2002) Icarus, 159, 31.
Yanagisawa, M., et al. (2006) Icarus, 182, 489.
Yanagisawa, M. et al. (2008) Meteorit. Planet. Sci. 2 (Suppl. 43), Abstract 5169..

中央太空所
全天影像儀

IRSL

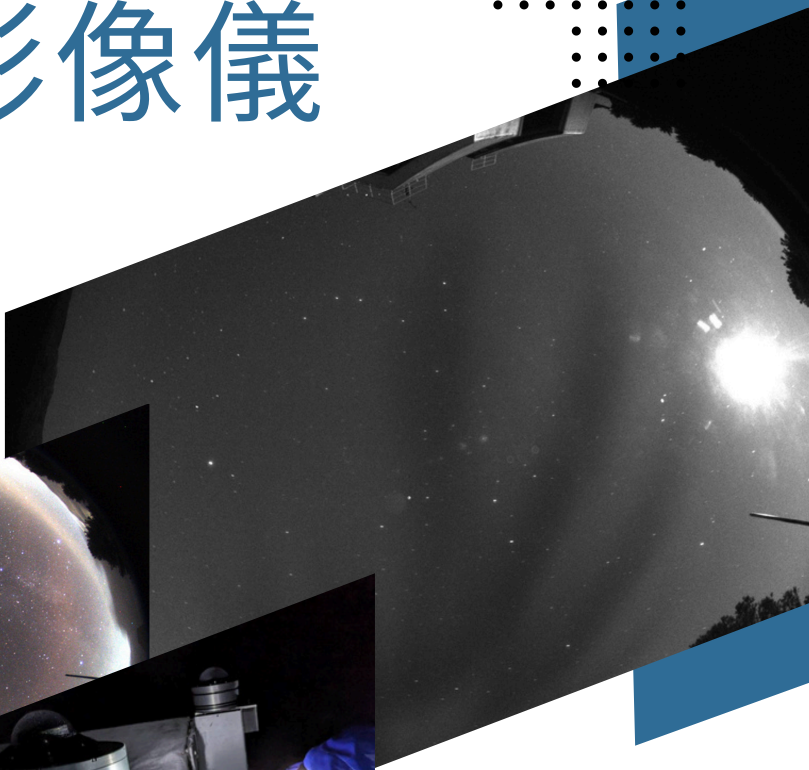

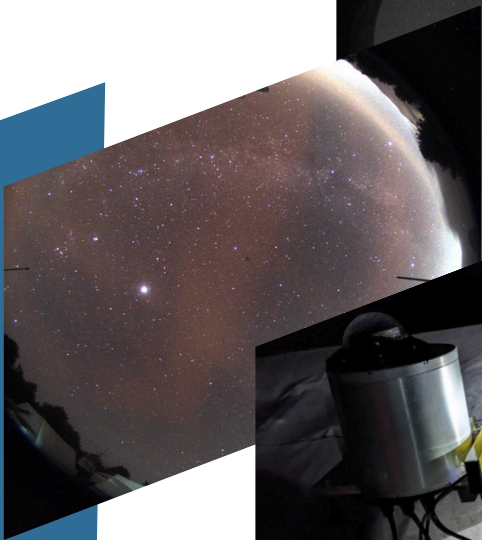

運作原理

利用感光元件加上全天影像儀長曝光時間的性質對上空微小發光的現象做觀測。

科學課題

- 白天雲量觀測
- 流星
- 電漿洞
- 大氣輝光

作者：趙政勛 / 劉正彥 博士

For More Information
https://www.lulin.ncu.edu.tw/weather/allSkyHistory/

Visit Us
https://irsl.ss.ncu.edu.tw/

全天影像儀在電離層的應用

全天影像儀(All-Sky Imager， ASI)是一種高精度的成像儀器，可用於觀測電離層夜間發光現象。自1968年首次使用以來，ASI在電離層研究方面發揮了重要作用，揭示了電離層電子含量隨大氣輝光變化的關係。在台灣，ASI自1997年起在不同天文台進行長期觀測，為電離層研究提供了寶貴的資料。

大氣輝光與電離層

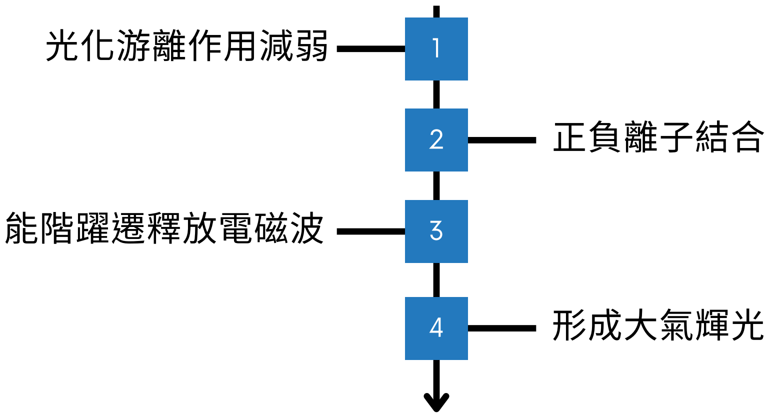

未來研究方向

於2023年11月份架設EUDA 2M黑白全天影像儀，並且於2024年採購與日本架設在夏威夷同款彩色全天影像儀繼續為臺灣提供珍貴的資料。

國 立 中 央 大 學

天 文 研 究 所

碩 士 論 文

Building a Data Processing Pipeline for Fast-turnaround Transient Follow-up in the Era of LSST

研 究 生：繆皓宇

指導教授：潘彥丞 博士

中 華 民 國 一 一 一 年 六 月

LSST 時代的資料處理——
自動化的瞬變天體數據處理流水線

摘　要

為了約束天體物理範疇中的瞬變天體在爆發早期之性質，諸如爆發機制以及前驅系統的細節，及早觀測至關重要。我們近期運用鹿林一米望遠鏡 (Lulin One-meter Telescope, LOT) 作瞬變天體之跟近觀測，並參與了數個針對瞬變天體的巡天合作項目，比如年輕超新星實驗 (Young Supernova Experiment, YSE)，以及茲威基瞬變天體設施 (Zwicky Transient Facility, ZTF)。為此，我們建構了一套自動資料處理流水線，以確保在無人介入操作的情況下，能快速並精準地處理觀測資料，達成資料管理、影像校正、測光以及數據繪圖等功能。該流水線不只能應用於處理從鹿林一米望遠鏡所取得的觀測資料，亦能處理如取自我們未來位於墨西哥的兩米望遠鏡，或其他望遠鏡之觀測資料。

National Central University

Graduate Institute of Astronomy

Master Thesis

Applying Lucky-Imaging On LOT With a Commercial CMOS Camera

Author: Yang-Peng Hsieh

Supervisors: Dr. Chow-Choong Ngeow

Jun 2023

Draft version August 31, 2023
Typeset using LATEX **twocolumn** style in AASTeX631

SN 2022oqm: A Multi-peaked Calcium-rich Transient from a White Dwarf Binary Progenitor System

S. Karthik Yadavalli,[1] V. Ashley Villar,[1] Luca Izzo,[2] Yossef Zenati,[3,*] Ryan J. Foley,[4] J. Craig Wheeler,[5] Charlotte R. Angus,[2] Dominik Bánhidi,[6] Katie Auchettl,[4,7] Barna Imre Bíró,[6,8] Attila Bódi,[9,10,11] Zsófia Bodola,[12] Thomas de Boer,[13] Kenneth C. Chambers,[13] Ryan Chornock,[14] David A. Coulter,[4] István Csányi,[6] Borbála Cseh,[9,10,15] Srujan Dandu,[4] Kyle W. Davis,[4] Connor Braden Dickinson,[4] Diego Farias,[2] Christa Gall,[2] Hua Gao,[13] Wynn V. Jacobson-Galan,[14] Nandita Khetan,[2,16] Charles D. Kilpatrick,[17] Réka Könyves-Tóth,[9,10,12,18] Levente Kriskovics,[9,10] Natalie LeBaron,[14] Kayla Loertscher,[4] X. K. Le Saux,[4] Rafaella Margutti,[14,19] Eugene A. Magnier,[13] Peter McGill,[4] Hao-Yu Miao,[20] András Pál,[9,10,21] Boróka H. Pál,[12] Yen-Chen Pan,[20] Collin A. Politsch,[22] Conor L. Ransome,[1] Enrico Ramirez-Ruiz,[4] Armin Rest,[3,23] Sofia Rest,[3,23] Olivia Robinson,[4] Huei Sears,[17,24] Jackson Scheer,[25] Ádám Sódor,[9,10,11] Jonathan Swift,[25] Péter Székely,[12,8] Róbert Szakáts,[9,10] Tamás Szalai,[12,8] Kirsty Taggart,[4] Padma Venkatraman,[14] József Vinkó,[5,9,10,12,21] Grace Yang,[25] and Henry Zhou[25]

[1]*Center for Astrophysics | Harvard & Smithsonian, 60 Garden Street, Cambridge, MA 02138-1516, USA*
[2]*DARK, Niels Bohr Institute, University of Copenhagen, Jagtvej 128, 2200 Copenhagen, Denmark*
[3]*Physics and Astronomy Department, Johns Hopkins University, Baltimore, MD 21218, USA*
[4]*Department of Astronomy and Astrophysics, University of California, Santa Cruz, CA 95064, USA*
[5]*Department of Astronomy, University of Texas at Austin, 2515 Speedway Stop C1400, Austin, TX, 78712-1205, USA*
[6]*Baja Astronomical Observatory of University of Szeged, Szegedi út Kt. 766, Baja, 6500, Hungary*
[7]*School of Physics, The University of Melbourne, VIC 3010, Australia*
[8]*ELKH-SZTE Stellar Astrophysics Research Group, Szegedi út Kt. 766, Baja, 6500, Hungary*
[9]*Konkoly Observatory, Research Centre for Astronomy and Earth Sciences, Budapest, Konkoly Thege Miklós út 15-17, 1121, Hungary*
[10]*CSFK, MTA Centre of Excellence, Budapest, Konkoly Thege Miklós út 15-17, 1121, Hungary*
[11]*MTA CSFK Lendület Near-Field Cosmology Research Group, Konkoly Thege Miklós út 15-17, Budapest, 1121, Hungary*
[12]*Department of Experimental Physics, Institute of Physics, University of Szeged, Dóm tér 9, Szeged, 6720, Hungary*
[13]*Institute for Astronomy, University of Hawaii, 2680 Woodlawn Drive, Honolulu, HI 96822, USA*
[14]*Department of Astronomy, University of California, Berkeley, CA 94720-3411, USA*
[15]*MTA CSFK Lendület "Momentum" Milky Way Research Group, Hungary*
[16]*School of Mathematics and Physics, University of Queensland, 4101, Australia*
[17]*Center for Interdisciplinary Exploration and Research in Astrophysics (CIERA), Northwestern University, Evanston, IL 60202, USA*
[18]*ELTE Eötvös Loránd University, Gothard Astrophysical Observatory, Szent Imre herceg út 112, Szombathely, 9700, Hungary*
[19]*Department of Physics, University of California, Berkeley, CA 94720, USA*
[20]*Graduate Institute of Astronomy, National Central University, 300 Zhongda Road, Zhongli, Taoyuan 32001, Taiwan*
[21]*ELTE Eötvös Loránd University, Institute of Physics and Astronomy, Pázmány Péter sétány 1/A, Budapest, 1117 Hungary*
[22]*Institute of Astronomy and Kavli Institute for Cosmology, Madingley Road, Cambridge, CB3 0HA, UK*
[23]*Space Telescope Science Institute, Baltimore, MD 21218, USA*
[24]*Department of Physics and Astronomy, Northwestern University, Evanston, IL 60208, USA*
[25]*Thacher School, 5025 Thacher Rd., Ojai, CA 93203, USA*

ABSTRACT

We present the photometric and spectroscopic evolution of SN 2022oqm, a nearby multi-peaked hydrogen- and helium-weak calcium-rich transient (CaRT). SN 2022oqm was detected 19.9 kpc from its host galaxy, the face-on spiral galaxy NGC 5875. Extensive spectroscopic coverage reveals a hot (T $\geq$ 40,000 K) continuum and carbon features observed $\sim$1 day after discovery, SN Ic-like photospheric-phase spectra, and strong forbidden calcium emission starting 38 days after discovery. SN 2022oqm has a relatively high peak luminosity ($M_B = -17$ mag) for CaRTs, making it an outlier in the population. We determine that three power sources are necessary to explain SN 2022oqm's light curve, with each power source corresponding to a distinct peak in its light curve. The first peak of the light curve is powered by an expanding blackbody with a power law luminosity, consistent with shock cooling by circumstellar material. Subsequent peaks are powered by a double radioactive decay model, consistent with two separate sources of photons diffusing through an optically thick ejecta. From the optical light curve, we derive an ejecta mass and ^{56}Ni mass of $\sim$0.89 M$_\odot$ and $\sim$0.09 M$_\odot$, respectively. Detailed

in Table 1. SN 2022oqm was found offset by 77.7″ (19.9 kpc) from the center of NGC 5875, an extended spiral galaxy at 53.5 ± 1 Mpc (Tully et al. 2013).

2.1. *Photometry*

2.1.1. *Pan-STARRS*

SN 2022oqm was observed with the Pan-STARRS telescope (PS1/2; Kaiser et al. 2002; Chambers et al. 2017) on 8 September 2022 in rz-bands through the Young Supernova Experiment (YSE) (Jones et al. 2021). Data storage/visualization and follow-up coordination was done through the YSE-PZ web broker (Coulter et al. 2022, 2023). The YSE photometric pipeline is based on `photpipe` (Rest et al. 2005), which relies on calibrations from Magnier et al. (2020) and Waters et al. (2020). Each image template was taken from stacked PS1 exposures, with most of the input data from the PS1 3π survey. All images and templates were resampled and astrometrically aligned to match a skycell in the PS1 sky tessellation. An image zero-point is determined by comparing PSF photometry of the stars to updated stellar catalogs of PS1 observations (Flewelling et al. 2020). The PS1 templates are convolved with a three-Gaussian kernel to match the PSF of the nightly images, and the convolved templates are subtracted from the nightly images with `HOTPANTS` (Becker 2015a). Finally, a flux-weighted centroid is found for the position of the SN in each image and PSF photometry is performed using "forced photometry": the centroid of the PSF is forced to be at the SN position. The nightly zero-point is applied to the photometry to determine the brightness of the SN for that epoch.

2.1.2. *Thacher, Lulin, LCO, Nickel*

We observed SN 2022oqm with the Thacher 0.7 m telescope (Swift et al. 2022), in $griz$ bands from 12 July to 9 September 2022, with the Lulin 1 m telescope in $griz$ bands from 9–30 August 2022, and with the Las Cumbres Observatory (LCO) 1 m telescopes and Sinistro imagers in $ugri$ bands from 2–10 August 2022. All images were reduced in `photpipe` (Rest et al. 2005) with bias, flat, and dark frames obtained in the same instrumental configuration as our science images. We regridded each frame to a common pixel scale and field center with `SWarp` (Bertin 2010) and performed point-spread function photometry with a custom version of `DoPhot` (Schechter et al. 1993). All photometry was calibrated using standard stars from the PS1 3π DR2 catalog (Flewelling et al. 2020) observed in the same field as SN 2022oqm. We subtracted pre-explosion $griz$ template images from PS1 using `hotpants` (Becker 2015b) and performed forced photometry at the site of SN 2022oqm in the subtracted images, which is the final photometry presented here. Part of the LCO observations are obtained from the Global Supernova Project on LCO. Imaging of SN 2022oqm was obtained in $BVri$ bands with the 1 m Nickel telescope at Lick Observatory. The images were calibrated using bias and sky flat-field frames following standard procedures and were subtracted with a reference image obtained on 12 March 2022. PSF photometry was performed, and photometry was calibrated relative to Pan-STARRS photometric standards (Flewelling et al. 2020)

2.1.3. *Konkoly, Baja Observatories*

Photometric observations of SN2022oqm were collected from Piszkesteto Station of Konkoly Observatory and from Baja Observatory of University of Szeged, Hungary. Both sites are equipped with a robotic 0.8m Ritchey-Chretien-Nasmyth telescope, manufactured by ASA AstroSysteme GmbH, Austria. Photometry was performed by applying a back-illuminated, liquid-cooled, 2048×2048 FLI ProLine PL230 CCD camera through Johnson B, V, and Sloan g', r', i' and z' bands. Image reductions were done by custom-made IRAF[1] and `fitsh`[2] scripts. Photometry of the SN was calibrated via local point sources within the CCD field-of-view using their PS1 photometry[3].

2.1.4. *Asteroid Terrestrial-impact Last Alert System (ATLAS)*

SN 2022oqm was detected in the c and o bands by ATLAS between −20 and 70 days relative to the phase of r-band peak. Using the ATClean toolkit (Rest et al. 2023), we searched for any explosion activity by running a Gaussian-weighted rolling sum on the flux/dflux of the pre-SN light curve to compare to the control lightcurves close to the SN position. The pre-SN rolling sum was within the noise of the control lightcurve sums suggesting no evidence for any pre-SN bumps in the ATLAS light curve data. We used the ATLAS forced photometry server (Tonry et al. 2018; Smith et al. 2020; Shingles et al. 2021) to recover the difference-image photometry for SN 2022oqm. To remove erroneous measurements and have significant SN flux detection at the location of SN 2022oqm, we applied several cuts on the total number of individual data points and nightly averaged data. Our first cut used the χ^2 and uncertainty values of the point-spread-function (PSF) fitting to remove discrepant data. We then obtained forced photometry

[1] https://iraf-community.github.io/

[2] https://fitsh.net/

[3] https://catalogs.mast.stsci.edu/panstarrs/

Draft version July 13, 2023
Typeset using LATEX twocolumn style in AASTeX63

A compilation of optical polarization catalogs

G. V. Panopoulou,[1] L. Markopoulioti,[2] F. Bouzelou,[2] M. A. Millar-Blanchaer,[3] S. Tinyanont,[4] D. Blinov,[2,5] V. Pelgrims,[2,5] S. Johnson,[6] R. Skalidis,[6] and A. Soam[7]

[1]Department of Space, Earth and Environment, Chalmers University of Technology, 412 93, Göteborg, Sweden
[2]Department of Physics, University of Crete, Voutes University Campus, GR-70013 Heraklion, Greece
[3]Physics Department, University of California, Santa Barbara, CA 93106, USA
[4]National Astronomical Research Institute of Thailand, 260 Moo 4, Donkaew, Maerim, Chiang Mai 50180, Thailand
[5]Institute of Astrophysics, Foundation for Research and Technology - Hellas, Vasilika Vouton, GR-70013 Heraklion, Greece
[6]Cahill Center for Astronomy and Astrophysics, California Institute of Technology, Pasadena, CA, 91125, USA
[7]Indian Institute of Astrophysics, II Block, Koramangala, Bengaluru 560034, India

Submitted to ApJS

ABSTRACT

Polarimetry of stars at optical and near-infrared wavelengths is an invaluable tool for tracing interstellar dust and magnetic fields. Recent studies have demonstrated the power of combining stellar polarimetry with distances from the *Gaia* mission, in order to gain accurate, three-dimensional information on the properties of the interstellar magnetic field and the dust distribution. However, access to optical polarization data is limited, as observations are conducted by different investigators, with different instruments and are made available in many separate publications. To enable a more widespread accessibility of optical polarimetry for studies of the interstellar medium, we compile a new catalog of stellar polarization measurements. The data are gathered from 81 separate publications spanning two decades since the previous, widely-used agglomeration of catalogs by Heiles (2000). The compilation contains a total of 55,742 measurements of stellar polarization. We combine this database with stellar distances based on the *Gaia* Early Data Release 3, thereby providing polarization and distance data for 44,568 unique stars. We provide three separate data products: an Extended Polarization Catalog (containing all polarization measurements), a Source Catalog (with distances and stellar identifications) and a Unique Source Polarization and Distance catalog (containing a subset of sources excluding duplicate measurements). We propose the use of a common tabular format for the publication of stellar polarization catalogs to facilitate accessibility and increase discoverability in the future.

Keywords: polarization — ISM — catalogs — surveys

1. INTRODUCTION

The polarization of starlight due to the interstellar medium (ISM) is a powerful probe of the interstellar magnetic field. This interstellar polarization arises as a result of dichroic absorption of the starlight by dust grains which are aligned with the ambient magnetic field (Davis & Greenstein 1951; Lazarian 2007; Andersson et al. 2015). Ever since its discovery (Hiltner 1949; Hall 1949), interstellar polarization of starlight has been invaluable for our understanding of the Galaxy's magnetic field (Ellis & Axon 1978; Heiles 1996) as well as its effects on ISM structure (Heyer et al. 2008; Clark et al. 2014) and star formation (Myers & Goodman 1991; Alves et al. 2008; Li et al. 2013; Marchwinski et al. 2012; Franco & Alves 2015; Panopoulou et al. 2016; Kandori et al. 2017). Stellar polarimetry has also played a decisive role in determining the properties of ISM dust grains (Coyne et al. 1974; Serkowski et al. 1975; Whittet & van Breda 1978; Whittet et al. 2001a; Voshchinnikov et al. 2016; Siebenmorgen et al. 2017; Andersson et al. 2022) and their interaction with the magnetic and radiation fields

Corresponding author: G. V. Panopoulou
georgia.panopoulou@chalmers.se

Polarimeter Name	Telescope	Observatory	Polarimeter Reference	RefIDs
AIMPOL	1.04 m	ARIES	Rautela et al. (2004)	24, 25, 30, 33, 34, 35, 36, 44, 49, 50, 54, 55, 56, 61, 63, 67, 68, 69, 72, 73, 78, 79, 80
IAGPOL	0.9 m	CTIO		32, 38, 43, 48
	1.5m	CTIO		10, 46
	1.6m	OPD/LNA	Magalhães et al. (1996)	29, 31, 38, 47, 48
	0.6m	IAG		15, 18, 20, 28, 29, 38, 47, 48
Turpol	2.6 m NOT	ORM	Piirola (1988)	7, 8, 9, 13, 16, 37, 70
	2.15 m	CASLEO		16
	60 cm KVA	ORM		8, 13
	0.6 m, 1.25 m	Tuorla, CAO		9
IMPOL	2m	Girawali IUCAA	Ramaprakash (1998)	36, 40, 41, 52
	1.2 m	Mount Abu		5
HIPPO	1.9 m	SAAO	Potter et al. (2010)	27
HIPPI	3.9 m AAT	Siding Spring	Bailey et al. (2015)	51, 58, 68
RoboPol	1.3 m	Skinakas	Ramaprakash et al. (2019)	39, 45, 53, 57, 62, 65, 66
DiPol	60 cm KVA	ORM	Piirola et al. (2005)	16, 42
DiPol-2	NOT	ORM	Piirola et al. (2014)	74
	60 cm KVA	ORM		42
	4.2 m WHT	ORM		74
	2.2 m UH88	Maunakea		74
	60 cm (T60)	Haleakla		74
	1.27 m (H127)	University of Tasmania		74
HPOL	0.9 m	Pine Bluff	Wolff et al. (1996),	22, 23
	3.5 m WIYN	Kitt Peak	Nordsieck & Harris (1996)	22
FORS 1, 2	VLT	Paranal	Patat & Romaniello (2006)	11, 19, 59, 64
PlanetPol	4.2 m WHT	ORM	Hough et al. (2006)	26
VMI	0.5 m	VMI	Topasna et al. (2013)	60, 71, 75, 77
TRIPOL	1m	Lulin	Sato et al. (2019)	54
EMPOL	1.2 m	Mount Abu	Ganesh et al. (2020)	76
ALFOSC	2.6 m NOT	ORM	(1)	37
UCTP	1.9m	SAAO	Cropper (1985)	21
Beauty & the Beast	1.6m	OMM	Manset & Bastien (1995)	17
CASPROF	2.1 m	CASLEO	Gil-Hutton et al. (2008)	14
no name	0.9 m	McDonald	Breger (1979)	12
no name	1.6 m	OMM	Angel & Landstreet (1970)	3
Hatpol	3.8 m UKIRT	Maunakea	Hough et al. (1991)	6
Vatican Polarimeter	1.8 m	Lowell	Magalhães et al. (1984)	2
Minipol	1, 1.5, 2.2 m	Univ. of Arizona	Frecker & Serkowski (1976)	1
Hall	1.06 m	Lowell	McMillan (1976)	1
no name	2.1, 4 m	Kitt Peak	Kinman & Mahaffey (1974)	0

Table 3. Instrument/Telescope information. (1): www.not.iac.es/instruments/alfosc/polarimetry/. Abbreviations: AIMPOL - ARIES IMaging POLarimeter; ARIES - Aryabhatta Research Institute of Observational Sciences; CTIO - Cerro Tololo InterAmerican Observatory; IAG - Instituto de Astronomía, Geofísica e Ciências Atmosféricas; OPD/LNA - Pico dos Dias Observatory, Laboratório Nacional de Astrofísica; HIPPO - HIgh speed Photo-POlarimeter; SAAO - South African Astronomical Observatory; AAT - Anglo-Australian Telescope, HIPPI - HIgh Precision Polarimetric Instrument; NOT - Nordic Optical Telescope; ORM - Roque de los Muchachos; WHT - William Herschel Telescope, WIYN - Winsconsin-Indiana-Yale-NOAO; FORS - FOcal Reducer and low dispersion Spectrograph; VMI - Virginia Military Institute; UCTP - University of Cape Town polarimeter; OMM - Observatoire du Mont Mégantic, CASLEO - Complejo Astronómico El Leoncito; CAO - Crimean Astrophysical Observatory; KVA - Kungliga Vetenskapsakademien telescope; UKIRT - United Kingdom Infrared Telescope.

Long-term monitoring of comet 29P/Schwassmann–Wachmann from the Lulin Observatory Z. -Y. Lin[1]

[1] *Graduate Institute of Astronomy, National Central University, Taoyuan, Taiwan 32001 (zylin@astro.ncu.edu.tw)*

Introduction: Comets are some of the most easily observable astronomical phenomena, but we understand little about them, especially some comet outbursts. Many comets have out- bursts, but 29P/Schwassmann–Wachmann 1, hereafter P/SW 1, is unique because it averages 7.3 outbursts a year. This comet is unusual in that, while normally hovering at around the 16–17th magnitude, it can suddenly undergo an outburst, and the blow-up can propel the comet from obscurity to as bright as the 10th magnitude. So far, the detected outbursts have no clear sign of periodicity. In this work, we present preliminary results, including morphological analysis and investigation of the color($B-V$, $V-R$, and $R-I$)and brightness slopes of the dust coma and dust production ($Af\rho$, $\dot{M}$, total ejected masses) of comet P/SW 1 during the quiet and active periods, especially during the quadruple outbursts that occurred in late September of 2021. Additionally, we investigate the color change during the outbursts of comet P/SW 1.

Observations and reduction: All images of comet P/SW 1 were obtained using a Johnson– Cousins *R* filter with an effective central wavelength of 700 nm and an FWHM of 100 nm. These observations were all made by the 0.4 m telescope equipped with the U42 CCD at the Lulin Observatory. All photometric calibration was performed using the field star magnitudes provided by the PanSTARRS (PS1) data release 1 (DR1) catalog converted to Johnson–Cousins filter set equivalents using the transformation equations derived by Tonry et al. 2012

Lightcurve: In total, we observed at least 12 outbursts during which the brightness increased to greater than 1.5 mag listed in Table 1. These detected out- bursts are comparable with the results of the Centaur Comet Observing Campaign by MISSION 29P.

Table 1. List of the relatively large outbursts from 2018 to 2021.*

No.	Duration	Δ (au)	r_H (au)	α (°)	Maximum date (mag)
1	2018 Aug 2–12	4.977–4.886	5.776–5.775	6.7–5.3	Aug 3 (14.30)
2	2018 Sept 24–Oct 15	4.804–4.958	5.772–5.771	2.9–6.2	Sept 25 (12.07)
3	2018 Nov 22–Dec 7	5.466–5.625	5.769	9.6–9.8	Nov 24 (13.24)
4	2019 May 10–May 12	6.522–6.502	5.768	6.3–6.5	May 10 (14.42)
5	2019 June 28–30	5.896–5.865	5.769	9.9–10.0	June 28 (15.04)
6	2019 July 28–Aug 6	5.437–5.306	5.771	9.8–9.3	Aug 5 (14.48)
7	2020 Feb 3–15	6.180–6.343	5.788–6.789	8.7–7.7	Feb 3 (13.22)
8	2020 July 31–Aug 25	5.887–5.508	5.815–5.820	9.9–9.7	July 31 (12.82)
9	2020 Nov 19–26 [6]	4.890–4.927	5.838–5.839	3.0–4.0	Nov 20 (13.07)
10	2021 Jan 14–20 [7]	5.507–5.602	5.850–5.851	9.3–9.5	Jan 14 (14.67)
11	2021 Aug 25–30	6.047–5.972	5.907–5.909	9.6–9.7	Aug 25 (14.14)
12	2021 Sept 25–Oct 21	5.575–5.227	5.916–5.923	9.4–7.3	Sept 29 (11.18)

*The orbital properties [Δ, r_H, and α (phase angle)] are taken from the NASA JPL Horizons ephemeris service.

We compared the maximum magnitude time of the relatively large outbursts, about three magnitudes brighter than the quiescent level (~17.0). We found that their time interval (See table 1, Nos. 2–3, Nos. 7–8, and Nos. 8–9) was coincidentally a multiple of 60. However, if we compare the two tumultuous outbursts (Nos. 2 and 12), the time interval is roughly 1100 d and this duration does not seem to be a multiplicative number of the estimated time. interval (~60 d) or the period of the cryovolcano eruptions (~57.7 d).

September's quadruple outburst: This was the first time that comet P/SW 1 had ever been detected in a state of near-constant activity, continuously throwing gas and dust into space. The brightness of comet P/SW 1 rose steadily until September 29, appearing as a super-compact object or a most concentrated coma (figure 1) with a maximum brightness of the 11th magnitude. In other words, the comet's brightness was at least 100 times brighter than before it started becoming active. Figure 1 shows the development of September's quadruple outburst from the quiescent level (September 21–24, top panels) to the outburst state (September 25–28, bottom panels).

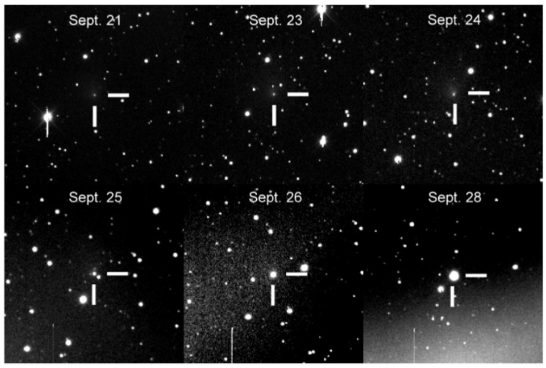

Fig. 1 Development of the 2021 September outburst of comet P/SW 1. from night to night. North is up, east to the left, and the field of view is After the first outburst on September 25, the coma is readily seen to expand from night to night. North is up, east to the left, and the field of view is 2.63 across.

Acknowledgments: This work was based on observations obtained at Taiwan's Lulin Observatory. We thank the staff members for their assistance with the observations. This work was supported by grant numbers NSC 101-2119-M-008-007-MY3 and NSC 102-2112-M- 008-003-MY3, and by grant numbers MOST 110-2112-M-008-003 and MOST 110-2112-M-008-001 from the Ministry of Science and Technology of Taiwan.

References: [1] Z.-Y. Lin 2023 *Publ. Astron. Soc. Japan* (2023) 00 (0), 1–14; [2] Miles, R. 2016, Icarus, 272, 387 [3]Tonry, J. L., et al. 2012, ApJ, 750, 99

The Astronomer's Telegram

1. Recurrent Nova M31N 2008-12a: pre-discovery observations with LATTE at Lulin Observatory, Zhang M., Zhao J., Wang W., et al., The Astronomer's Telegram, No. 16365

GRB Coordinates Network

1. ZTF23aabmzlp/AT2023azs: Lulin 1m LOT optical observations, Yang S., Chen T.-W., Hsiao H.-Y., et al., GRB Coordinates Network, Circular Service, No. 33255 (2023)

2. GRB 230414B: Lulin 40cm-SLT optical limit, Chen T.-W., Yang S., Lin C.-S., et al., GRB Coordinates Network, Circular Service, No. 33631

3. AT2023lcr (ATLAS23msn/ZTF23aaoohpy): Kinder observations with Lulin observatory and a probable plateau in the g-band light curve, Chen T.-W., Yang S., Tsai A.-L., et al., GRB Coordinates Network, Circular Service, No. 34043

4. GRB 231115A: Kinder observations with Lulin observatory, Chen T.-W., Lin C.-S., Levan A. J., et al., GRB Coordinates Network, Circular Service, No. 35052

5. GRB 231117A: afterglow candidate detection from Kinder observations with Lulin observatory, Yang S., Chen T.-W., Lin C.-S., et al., GRB Coordinates Network, Circular Service, No. 35083

6. GRB 231117A: Kinder observations with Lulin observatory for AT 2023yba without fading in r band, Chen T.-W., Yang S., Lin C.-S., et al., GRB Coordinates Network, Circular Service, No. 35105

Transient Name Server AstroNote

1. ATLAS23ddk (AT2023cqt): discovery of a transient object in Messier 064 (6 Mpc), Smith K. W., Chen T. W., Hsiao H. Y., et al., Transient Name Server AstroNote 2023-53

2. Kinder follow-up observations of AT 2023zaw - a rapid chromatic decline, Lee M. H., Zeng K. J., Chen T. W., et al., Transient Name Server AstroNote 2023-338

III
工作報告

營運報告

鹿林天文台一米望遠鏡 (LOT) 觀測時數統計 (2003-2023)

侯偉傑、林宏欽、蕭翔耀、林啟生

鹿林天文台自 2002 年 9 月開始有人員常駐，2003 年鹿林一米望遠鏡 (LOT) 上線後，開始有正式觀測時數紀錄，可供瞭解鹿林長期的夜間觀測狀況。表 2 為 2003-2023 共 21 年的統計結果，鹿林天文台年平均觀測時數為 1458.96 小時。

由圖 4(a) 為 LOT 歷年觀測總時數，2023 年的觀測總時數約為 1492 小時，與歷年平均觀測時數 (1459 小時) 相差不大。圖 4(b) 為月觀測時數長條圖，參考 2003 至 2023 年的平均月觀測時數可將一年可分為四個觀測季:

- 最佳觀測季：10-12 月，天氣晴朗穩定且晝短夜長。
- 次佳觀測季：1-3 月，天氣晴朗穩定，但夜間時間較最佳觀測季短。
- 最差觀測季：4-6 月。4 月開始進入雨季，5-6 月受梅雨影響，天氣最差。
- 次差觀測季：7-9 月。主要受颱風影響，天氣變化大。此外夏季晝長夜短，每晚可觀測時間比冬季短得多。

不過 2023 年的觀測時數分布與歷年平均有些差異，最佳觀測季為 2-4 月，次佳則為 1 月與 11、12 月。也許是 2023 年冬季為暖冬的影響，不過是否會維持這樣的趨勢還需要再觀察。

Table 2: 鹿林天文台 LOT 觀測時數統計表 (2003-2023)

	月份												
	1	2	3	4	5	6	7	8	9	10	11	12	Total
2003	78.75	142.5	147.5	126.5	129.75	24	222.5	137.75	142	149.25	166.5	271.5	1738.5
2004	125	145.98	163	110.5	106.25	133	48	142	116	219.75	214.5	232.45	1756.43
2005	163.25	94.75	143	144.75	136.25	45	167.75	76	129.25	210.25	216.25	129	1655.5
2006	129	149	126.05	86.8	59.5	39.3	91.57	111.65	60.05	150.6	71.75	132	1207.27
2007	127.32	128.55	116.4	53.75	106.6	54	128.88	56.6	69.55	172.63	160.55	261.09	1435.92
2008	179	118.25	138.5	85.25	98.25	37	88.4	118.95	59.8	191.38	152.55	211.17	1478.5
2009	234.52	165.7	146.75	71.8	167.4	81.75	76.6	6.8[1]	0[1]	175.6	175.8	169.8	1472.52
2010	206.9	100.6	181.3	75.8	86.05	26.5	99.85	98.3	109.95	139.8	163.65	169.65	1458.35
2011	90.8	123.8	75.9	151.45	56.6	61.5	81.75	97.9	90.1	136.95	87.2	115.25	1169.2
2012	113.42	64.88	168.23	32.75	74.3	35.15	106.4	35.7	117.35	214.51	93.81	132.21	1188.71
2013	153.58	183.63	134.26	55.83	41.02	80.14	88.05	72.2	107.84	200.57	136.1	86	1339.22
2014	269.62	109.8	78.7	135.95	32.4	33.7	114.65	110.9	134.39	232.33	166.15	137.3	1555.89
2015	188.55	131.65	111.1	124	64.2	146.9	87.45	45.1	93.25	145.4	197.05	161.2	1495.85
2016	75.4	60.25	72.8	82.9	86.05	114.05	123.95	61	42.85	142.2	171.85	193.27	1226.57
2017	160.85	105.3	96.4	86.9	84.55	76.1	105.25	139.9	128.2	187.8	134.55	156.7	1462.5
2018	110.4	66.7	173.7	125.7	190.7	70.35	80.65	50.35	93.45	142.05	148.15	170.05	1422.25
2019	196.3	136.35	124	124.35	39.1	56.55	77.35	58.2	137.45	193.75	200.29	180.2	1523.89
2020	234.4	191.1	121.35	98.75	88.35	137.9	102.5	78.3	82.28	163.82	185.65	125.44	1609.84
2021	227.78	197.37	167.98	125.74	87.16	13.8[2]	90.4	71.08	116.42	132.21	129.6	202.8	1562.34
2022	144.95	120.92	126.97	126.11	26.08	44.65	146.67	94.92	61.55	144.77	171.92	184.73	1394.24
2023	134.26	194.71	203.63	138.47	72.45	64.64	101.27	53.78	86.39	76.21	210.45	156.06	1492.32
Average*	157.84	130.22	133.74	104.20	85.06	63.96	103.13	82.56	96.64	169.12	161.39	169.49	1458.96

* Average 為扣除最高及最低值後取平均
[1] 2009 年因受莫拉克颱風八八風災影響，自八月八日起至十月初約 2 個月期間道路中斷並停電，無法觀測。所以 2009 年八、九月觀測時數很少，甚至為 0。
[2] 2021 年 6 月雷擊造成圓頂故障，約有 20 日無法觀測。

(a) LOT 歷年觀測時數統計圖 (2003-2023)

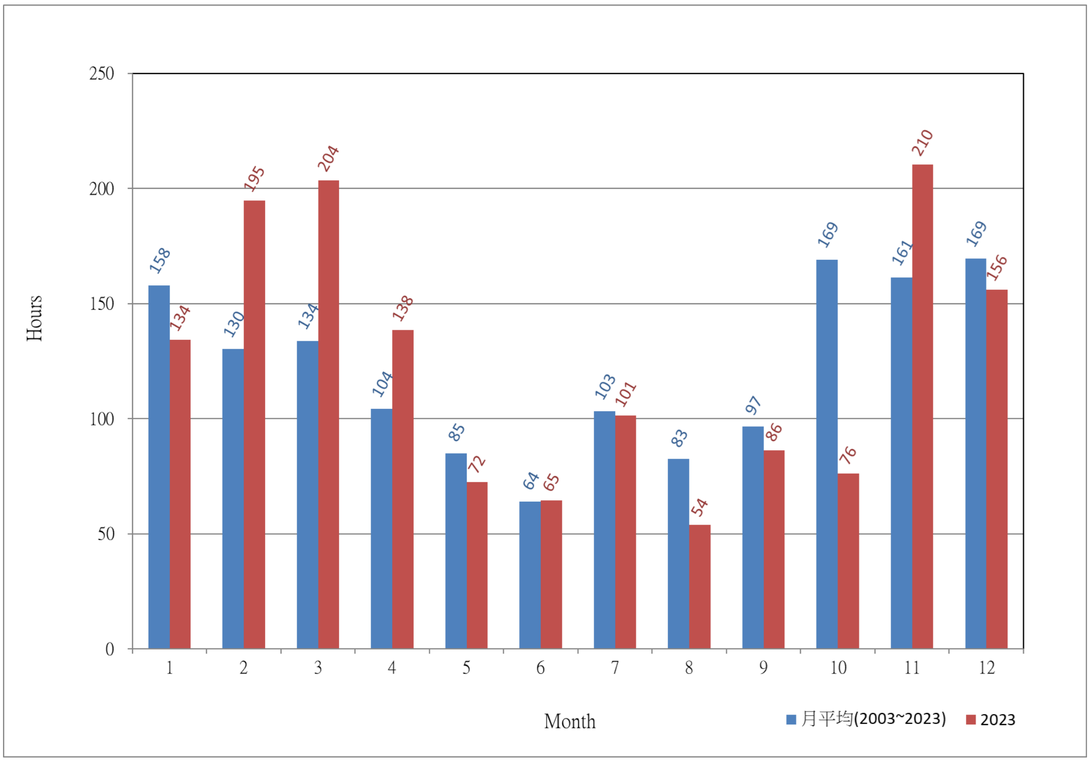

(b) LOT 月平均觀測時數統計圖 (2003-2023)

Figure 4: 鹿林天文台 LOT 觀測時數統計圖 (2003-2023)

LOT 觀測研究計畫統計 (2023)

侯偉傑

鹿林天文台一米望遠鏡 (LOT) 觀測研究計畫時間安排以 4 個月為一個觀測期，一年分為三期（A = 1-4 月、B = 5-8 月、C = 9-12 月），其中字母開頭：E 為天文教學觀測、R 為國內研究計畫、*R 為國際合作計畫，大型計畫 EDEN 亦為國際合作計畫。

2023 年的觀測計畫如圖 5 所示，教學觀測有 15 個，佔 30%。國內研究計畫有 20 個，佔 40%。國際合作計畫有 15 個，佔 30%。

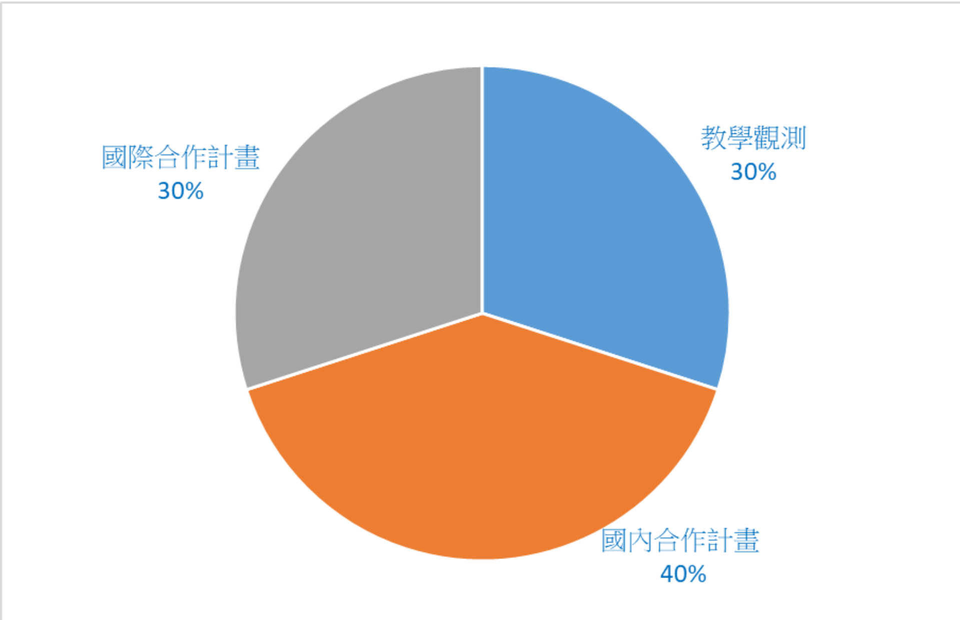

Figure 5: LOT 計畫比例圓餅圖 (2023)

LOT Semester 2023A
(01 January - 30 April, 2023)

Education Program:

E01 - Student Training for NTHU's "Fundamentals of Observational Astronomy" Course
PI: Shih-Ping Lai (slai@phys.nthu.edu.tw)

E02 - Education Training of the NCKU Astronomy Club
PI: Chen Bing-Chih (alfred@ncku.edu.tw)

E03 - Training for Who Joined in Pan-STARRs Asteroid Campaign of Students from High Schools in NCHU
PI: Lin Shih-Chao (shichao.lin@gmail.com)

E04 - Introduction to the Stellar Spectroscopy
PI: Wang Chia-Hui (hayata1204@gmail.com)

E05 - Winter educational training of NTHU Astronomy Club members
PI: Pu Sy-Yun (psyn@gapp.nthu.edu.tw)

Large Program:

EDEN - Exo-earth Discovery and Exploration Network
PI: Wen-Ping Chen (wchen@astro.ncu.edu.tw)

Research Program:
(Programs which have international CoIs are marked with *)

*R01 - Lulin Supernova Program
PI: Yen-Chen Pan (ycpan@astro.ncu.edu.tw)

R02 - The multi–band observations of the flare activity of an M dwarf
PI: Lin Chia-Lung (m1059006@gm.astro.ncu.edu.tw)

R03 - The study of the dust to gas ratio and rotation in comet C/2022 E3
PI: Zhong-Yi Lin (zylin@astro.ncu.edu.tw)

R04 - LOT follow-up of transient events and new discovery objects from ZTF
PI: Zhong-Yi Lin (zylin@astro.ncu.edu.tw)

*R05 - Monitoring Accretion onto a Low-mass Brown Dwarf
PI: Ya-Lin Wu (yalinwu@ntnu.edu.tw)

R06 - Characterizing the Physical Properties of Oort-Cloud Asteroids
PI: Yu-Chi Cheng (ycc312@g.ncu.edu.tw)

R07 - Taxonomical Confirmation of Outer Main-Belt Asteroids Recorded in SDSS-MOC4

PI: Yu-Chi Cheng (ycc312@g.ncu.edu.tw)

LOT Semester 2023B
(01 May - 31 August, 2023)

Education Program:

E01 - Hands-on Class of "Introduction to Astrophysics"
PI: Chin-Ping Hu (cphu0821@gm.ncue.edu.tw)

E02 - Observation Training for CYCU Astronomy Club
PI: Hung-Chin Lin (hclin@astro.ncu.edu.tw)

E03 - Education Training of the NCKU Astronomy Club
PI: Bing-Chih Chen (alfred@ncku.edu.tw)

E04 - Training Observation for the Course "Advanced Astronomical Observations"
PI: Daisuke Kinoshita (kinoshita@astro.ncu.edu.tw)

E05 - Introduction to the Stellar Spectroscopy II
PI: Chia-Hui Wang (hayata1204@gmail.com)

Large Program:

EDEN - Exo-earth Discovery and Exploration Network
PI: Wen-Ping Chen (wchen@astro.ncu.edu.tw)

Research Program:
(Programs which have international CoIs are marked with *)

*R01 - Lulin Supernova Program
PI: Yen-Chen Pan (ycpan@astro.ncu.edu.tw)

R02 - Establishing Mira's Period-Luminosity Relation in zy-Band with LOT
PI: Chow-Choong Ngeow (cngeow@astro.ncu.edu.tw)

R03 - ToO Observations of Cosmic Transient Events
PI: Albert Kong (akong@phys.nthu.edu.tw)

*R04 - Multicolor observations of Near-Earth Asteroids II
PI: Zhong-Yi Lin (zylin@astro.ncu.edu.tw)

R05 - The study of the dust to gas ratio and rotation in long- and short-period comets
PI: Zhong-Yi Lin (zylin@astro.ncu.edu.tw)

R06 - Chemical Abundance of Recent Bright Comet by LISA
PI: Yu-Chi Cheng (yuchi.cheng@gapps.ntnu.edu.tw)

*R07 - Monitoring Accretion onto a Low-mass Brown Dwarf
PI: Ya-Lin Wu (yalinwu@ntnu.edu.tw)

*R08 - Gold factories in the Universe: discovering and understanding the nature of kilonovae
PI: Ting-Wan Chen (janet.chen@tum.de)

R09 - Chromospheric Activity of Flaring G and K Type Eclipsing Binaries
PI: Li-Ching Huang (lchuang@ntnu.edu.tw)

LOT Semester 2023C
(01 September - 31 December, 2023)

Education Program:

E01 - Training Program for NCHU Students
PI: Yu-Yen Chang (yuyenchang@phys.nchu.edu.tw)

E02 - LISA Spectroscopy of the Starburst Galaxy NGC 253
PI: Wei-Hao Wang (whwang@asiaa.sinica.edu.tw)

E03 - Practical Class of ”Observational Astronomy”
PI: Albert Kong (akong@phys.nthu.edu.tw)

E04 - Colour-magnitude diagrams of star clusters: determining their relative ages
PI: Ting-Wan Chen (twchen@astro.ncu.edu.tw)

E05 - Student Training for NTHU's "Fundamentals of Observational Astronomy" Course
PI: Shih-Ping Lai (slai@phys.nthu.edu.tw)

Research Program:
(Programs which have international CoIs are marked with *)

*R01 - Lulin Supernova Program
PI: Yen-Chen Pan (ycpan@astro.ncu.edu.tw)

R02 - Completing the y-Band Light Curves for RR Lyrae in the SDSS Stripe 82 Region
PI: Chow-Choong Ngeow (cngeow@astro.ncu.edu.tw)

R03 - The study of the dust to gas ratio and rotation in long- and short-period comets
PI: Zhong-Yi Lin (zylin@astro.ncu.edu.tw)

*R04 - LOT follow-up of transient events and new discovery objects from ZTF (ToO)
PI: Zhong-Yi Lin (zylin@astro.ncu.edu.tw)

R05 - ToO Observations of Cosmic Transient Events (ToO)
PI: Albert Kong (akong@phys.nthu.edu.tw)

R06 - The multi–band observations of the flare activity of an M dwarf (plus SLT)
PI: Chia–Lung Lin (m1059006@gm.astro.ncu.edu.tw)

*R07 - The Astrometric Performance Test of LOT
PI: Zhong-jie Zheng (azhengzj@gdou.edu.cn)

R08 - Spectral and Temporal Polarization Variation of Herbig Ae/Be and T Tauri Stars
PI: Wen-Ping Chen (wchen@astro.ncu.edu.tw)

*R09 - Investigation of the physical properties of MBC P/2018 P3 (PANSTARRS)
PI: Zhong-Yi Lin (zylin@astro.ncu.edu.tw)

R10 - Characterizing Mercury's Sodium Exosphere
PI: Chen-Yen Hsu (pandaangela915@gmail.com)

*R11 - Gold factories in the Universe: discovering and understanding the nature of kilonovae (ToO)
PI: Ting-Wan Chen (twchen@astro.ncu.edu.tw)

*R12 - Extending the photometric monitoring of superluminous supernovae to very late phases
PI: Ting-Wan Chen (twchen@astro.ncu.edu.tw)

R13 - Accretion variability of Herbig Ae/Be stars
PI: Jyun-Heng Lin (41141905S@gapps.ntnu.edu.tw)

*R14 - Monitoring Accretion onto Brown Dwarfs in Taurus
PI: Ya-Lin Wu (yalinwu@ntnu.edu.tw)

R15 - Spectroscopic Survey on Themis Asteroids
PI: Yu-Chi Cheng (yuchi.cheng@gapps.ntnu.edu.tw)

R16 - Chemical Abundance of Recent Bright Comet by LISA
PI: Yu-Chi Cheng (yuchi.cheng@gapps.ntnu.edu.tw)

R17 - Characterizing UVEX: The New Spectrograph at Lulin Observatory
PI: Wei-Jie Hou (weij@astro.ncu.edu.tw)

R18 - Chromospheric Activity of Flaring M Type Eclipsing Binaries
PI: Li-Ching Huang (lchuang@ntnu.edu.tw)

鹿林天文台合作計畫

台灣位處太平洋西側，在廣大的太平洋上（橫跨 6 個時區）只有夏威夷有天文台，對於觀測隨時間變化的天文現象或是全球不同經度的天文台（包括太空望遠鏡）針對特定天體的聯合觀測，鹿林天文台扮演舉足輕重的角色。多年來鹿林天文台積極參與國際合作計畫，與各國天文台建立良好合作模式，並取得優良成果。

鹿林天文台地處高山，遠離都市光害，且海拔高度在逆溫層之上，晴天率較高，是國內天文觀測條件最好的地點之一。原 TAOS 計畫結束留下的平頂天文台，近年則提供給國內天文教研單位設置望遠鏡進行遠端觀測，充分發揮研究及教學功能。

國際合作計畫

1. 全球蠍虎 BL 類星體聯合觀測計畫（The Whole Earth Blazar Telescope - GLAST-AGILE Support Program, WEBT-GASP）：監測活躍星系核，藉此研究黑洞與噴流的性質。

2. 史維基瞬變探測器計畫（Zwicky Transient Facility, ZTF）：將天文研究推進到時間加上空間的 4D 階段，可望對可見光時域天文學作出重大的科學貢獻。中央大學與清華大學以 TANGO 的名義參與的 ZTF 計劃已在 2023 年 9 月結束。在參與的 6 年其間，臺灣的團隊參與了超過 40 篇的 ZTF 論文（包含共同作者）。而由中央大學團隊所主導的論文有 12 篇。

3. 伊甸園觀測網（Exoearth Discovery and Exploration Network, EDEN）：搜尋鄰近太陽之 M 型恆星可能位於適居區內的系外行星。於 2023 年 4 月結束。

4. 年輕超新星巡天計畫（Young Supernova Experiment）：使用 Pan-STARRS telescopes 在 ZTF 天區進行巡天，藉由兩者之間經度的差距來探測瞬變天體早期的演化。

5. 千級新星發現計畫（Kinder: kilonova finder）：使用 40cm-SLT 對 ATLAS 巡天所發現的鄰近（<100 Mpc）天體進行即時觀測，找出亮度快速下降的天體為千級新星候選者，再藉由 ePESSTO+ 以及 ENGRAVE 計畫的望遠鏡拍攝光譜確認。以期獨立於重力波觀測外發現千級新星。

國內合作計畫

1. 台灣流星觀測網 TMDS (Taiwan Meter Detection System)：聯合全台五個地點共 14 個流星觀測站，調查流星基本物理特性、找尋未知流星群與流星群的非預期爆發現象。

2. 星瞬望遠鏡 RIFT (Robotic Imager For Transients)：接收重力波、微中子和高能電磁波觀測中發現的緻密星瞬變事件，並全自動進行此類事件的後續觀測。

3. 拿鐵望遠鏡 LATTE (Lulin-ASIAA Telescope for Transients and Education)：五十公分望遠鏡，搭配七片濾鏡與 CCD 相機，除研究、遠端教學觀測外，部分時間供大眾提出目標申請。

4. 月閃觀測望遠鏡 RoLIFE (Robotic Lunar Impact Flashes tElescope)：通過監測流星體撞擊月球表面所產生的閃光來加以分析與統計，補足流星體大小天體的數量估算的分布資訊。

團體參觀及教學觀測 (2023)

如表 3 所示，2023 年參觀團體共 42 團，總人次為 772 人。其中以藍字標示的團體為 LOT 教學觀測，占 193 人次。其他則為自行申請的團體參觀，占 523 人次。

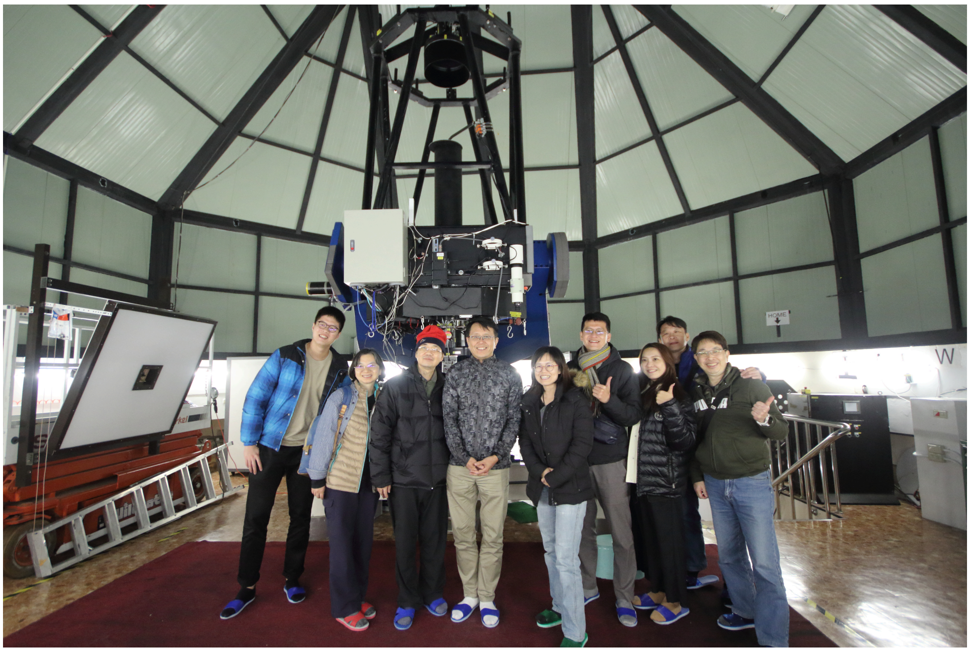

Figure 6: 南投地方法院

Figure 7: 台南口埤實驗國小

Table 3: 2023 年參觀團體

日期	單位	人數
1 月 9 日	成大物理系	6
1 月 17 日	台大 +清大天文社	72
2 月 2 日	彰興國中	34
2 月 4 日	成功大學天文社	8
2 月 8 日	師大地科所	8
2 月 11 日	瑞祥高中	23
2 月 25 日	暨大附中	14
3 月 3 日	新加坡南洋理工大學暨中正大學通識中心	19
3 月 4 日	丹鳳高中	9
3 月 10 日	清大天文所	20
4 月 28 日	台南復興國小	28
4 月 29 日	中央天文社	29
5 月 5 日	蘭潭國小	11
5 月 25 日	台南市口埤實驗小學	22
5 月 26 日	南投分局副局長一行	8
5 月 27 日	彰化師大物理系	11
6 月 8 日	台中黎明國中	12
6 月 11 日	淡水社大	21
6 月 19 日	師大台語天文學	9
6 月 27 日	中大天文所進階天文觀測	3
7 月 15 日	花蓮縣天文協會	20
7 月 21 日	鳳山高中	10
7 月 22 日	中大 EMBA	12
8 月 12 日	竹塹社大	27
8 月 27 日	中原大學天文社	17
8 月 28 日	蘇貞昌前院長一行	11
9 月 8 日	德國教授和學生	18
10 月 7 日	玉管處	30
10 月 13 日	天文所碩一	14
10 月 15 日	玉管處	30
10 月 20 日	清華大學天文	17
10 月 27 日	中央大學職工會	26
10 月 28 日	中興大學觀測天文	12
11 月 10 日	清大天文所	15

11 月 17 日	中央大學職工會	16
11 月 18 日	台大天文 (1)	16
11 月 19 日	台大天文 (2)	16
11 月 23 日	南投地方法院	11
11 月 25 日	台南口埤實小	18
12 月 2 日	中大天文所校友親屬團	19
12 月 9 日	竹塹社大	33
12 月 30 日	美國華僑	17

團體參觀及教學觀測人數統計 (2010-2023)

鹿林天文台做為國內唯一的研究型天文台，負有天文教學及科普推廣的責任。從開台起便受理各單位及團體參觀，由天文台人員協助導覽解說，並於 2010 年開始統計參觀人數。如圖 8 所示，從 2010 年開始參觀人次逐年上升，2018 年參觀人數達 908 人。但因 2019 年底 Covid-19 疫情影響，2020 至 2022 年間天文台暫停參觀人數大幅下滑。而 2023 年疫情解封後，參觀恢復正常，因此可以看到 2023 年參觀人數明顯上升。

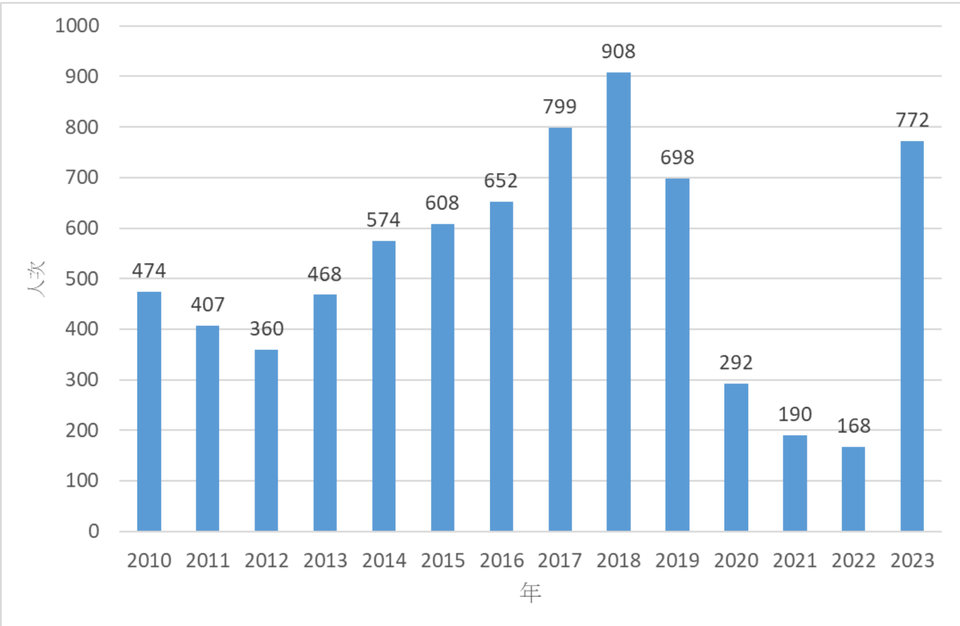

Figure 8: 鹿林天文台歷年參觀人次統計 (2010-2023)

更新與維修

LOT

LOT 和 SLT 圓頂環形電軌之集電架更新

侯偉傑、林宏欽、石皓偉

1. LOT 與 SLT 圓頂天窗馬達的電源是由環形電軌與集電架供電，自啟用以來已運作 20 多年，集電架的碳刷頭因長期磨損開始出現電火花，圓頂轉到某些角度時供電常斷斷續續，造成圓頂天窗控制系統異常。

2. 即使圓頂天窗控制系統加裝了 UPS 不斷電系統，有時還是會出現天窗狀態錯誤，造成觀測程式突然停止、天窗失去與望遠鏡同步甚至是無法正常開關天窗等問題。

3. 2023 年 2 月 14 日更新 LOT 整組集電架連同電刷頭。更換完後操作圓頂旋轉，就沒有聽見接觸不良產生電火花的聲音，也沒有發生圓頂控制箱斷又復電的問題。次日，更換 SLT 集電架及電刷頭測試後亦正常。

4. LOT 圓頂更新集電架後起初運作正常，但後來 ACE SmartDome 圓頂控制系統逐漸開始出現「Ajar (天窗半開)」的錯誤訊息。2023 年 4 月 2 日檢查發現有些集電架脫軌，研判是集電架裝設時角度沒有調整好。調整集電架的角度，讓施力朝向電軌方向，操作圓頂測試結果良好，之後便沒有再出現脫軌現象。

(a) (b)

Figure 9: (a)SLT 更換集電架 (b)LOT 集電架脫軌

AutoSlew PC 更新

侯偉傑、林宏欽

Autoslew-PC 的作業系統 Windows7 已經停止更新，若繼續使用可能會有安全性隱患，因此將電腦的作業系統更新成 Windows10。LOT 的控制系統 Autoslew 為德國 ASA 客製化程式，因此需特別訂製更新版本，將作業系統與 Autoslew 版本同時升級。

在電腦更新至 Windows10 後由 ASA 德國工程師 Philipp Keller 遠端連線進行新版 Autoslew 安裝。在操作上新版的 Autoslew 與舊版有兩個不同：

1. LOT-PC 與 Autoslew-PC 的連線方式需要改成 ASCOM Alpaca。

Alpaca 為 ASCOM 所開發之跨平台連接系統，可讓在不同平台安裝的儀器電腦互相連線，且使用內網連線，不須再使用實體線路連接。Autoslew 安裝時 Philipp 已經架設好 Alpaca Server，而 LOT 需要使用 Alpaca Cilent，而要使用 Alpaca Client 需要先安裝 ASCOM Platform 6.6 版 (或更新的版本)。安裝完後連線望遠鏡或對焦器時選擇 ASCOM，出現 Chooser 視窗後點選上方 Alpaca，然後選 Enable Discovery。然後在選單中找到 Autoslew Telescope 或是 Autoslew Focuser 即可。須注意若更換新電腦或是重灌可能需要開通防火牆 prot。

2. 不使用 GPS 來校時，而是改用 NTP Server。

Philipp 建議使用 NTP Server 來做校時，而不是原本 Autoslew 的 GPS 校時功能。但發現 NTP 校時有時會出問題，導致無法正常追蹤。後來將 Autoslew 的校時功能都關掉，並在 Autoslew-PC 上安裝 SiTech TimeServer 來做校時。

LOT、SLT 的 ACP 與 FocusMax 更新

侯偉傑

ACP Observatory 已發布 9.0 版，修正了一些內在 bugs，因此考慮將我們電腦中的版本也更改成 ACP 9.0。不過 ACP 9.0 僅支援與 FocusMax V5 連線，因此採購新版 Focux Max 後將電腦中的兩套軟體一同更新。ACP 9 與 FocusMax V5 的安裝與設定請見與附錄 A.1。

LOT-PC 換新

侯偉傑

112 年採購新電腦主機，將原本 LOT 電腦更換，並且將 OS 更新成 Windows 11 系統。更換電腦加上更新系統無法使用移植的方式將原本的軟體移至新電腦，所以需要全部重裝。在安裝時也將步驟記下做成報告備忘，詳見附錄 A.2。

鹿林天文台 LOT 圓頂接地施作報告

張永欣 2024/03/22

2021/06/12 16:43 鹿林天文台遭到直接雷擊，造成圓頂內多項週邊設備損壞。

經現場勘查，研判雷電首先擊中 LOT 圓頂上端的氣象儀全毀，風速、風向計爆開，然後電流侵入到圓頂門軌道上，開門位置感應的極限開關，開關供電為 AC-220V 的 R 相，然後高壓電沿著電纜之 R 相紅色線，一路進入掛在圓頂上跟著旋轉的圓頂天窗開關門控制箱。

Figure 10: 圓頂上方風速風向計與開關箱內火燒情形

強大的高壓致使三相電源中的 R 相、S 相之間放電，黃色線與路徑上均有明顯火燒痕跡，除了燒毀變頻器及主斷路器外，樓下與電腦連接的圓頂旋轉控制器也受到嚴重破壞。

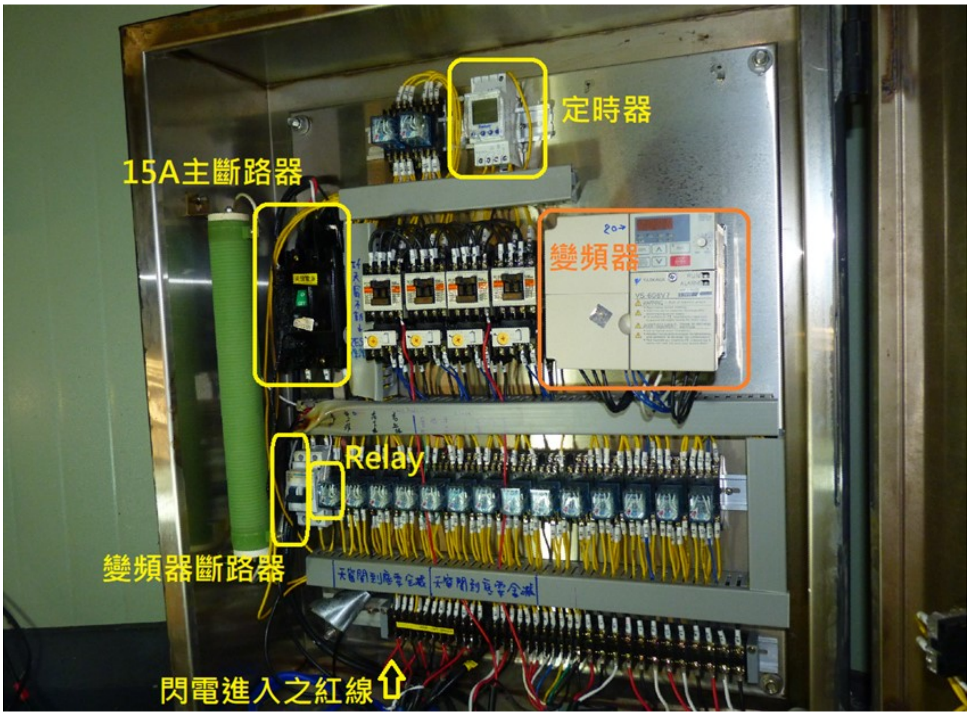

Figure 11: 天窗開關箱內結構與破壞情形

雷電擊中全金屬的 LOT 外殼時，圓頂軌道雖為金屬，但是支撐輪與驅動輪均為絕緣材質，能量無除發散，所以改侵入最靠近開關門的電源電路，造成破壞，還好 2005 年施做之避雷吸收器，有效隔離了電源突波，避免災情擴散到其他區域。

Figure 12: 圓頂軌道與支撐輪間結構

Figure 13: 2005 年 2 月增設之避雷突波吸收器

所以除了避雷突波吸收器隔離措施，必須將圓頂外殼也接地，以進一步有效防止直接雷擊遭受的破壞。

LOT 圓頂可以同一方向旋轉超過數圈以上，結構上沒有固定點可以施做金屬接地，旋轉時軌道還會些微內外偏移及上下浮動，圓頂開關門所使用的電源採用軌道電刷供電，圓頂旋轉方向為雙向，所以集電靴臂若是採用拖曳臂方式，必須成對的一正一反安裝，如下（圖五）所示，但是此一類現成的集電靴接觸面積太小，可承受瞬間高壓的阻抗過大，所以自行設計一接觸面積大，又可達成雙向拖曳臂浮動接觸的集電靴機構嘗試安裝。

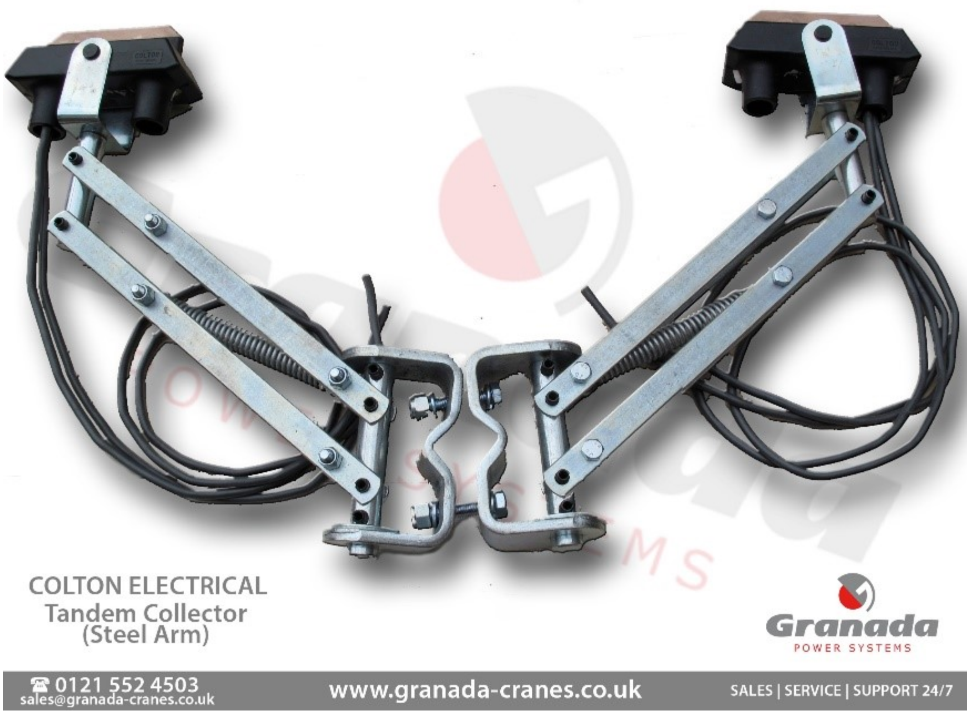

Figure 14: 雙向軌道電刷（集電靴）

如上圖市售集電靴反向安裝，簡化平行結構後，類似我們常見於汽車的剪式千斤頂，拆掉中間的螺桿、螺母，改成彈簧，上方加上純銅片，底座依現場安裝空間，配合適當壓力的行程高度，浮動保持平貼接觸面。

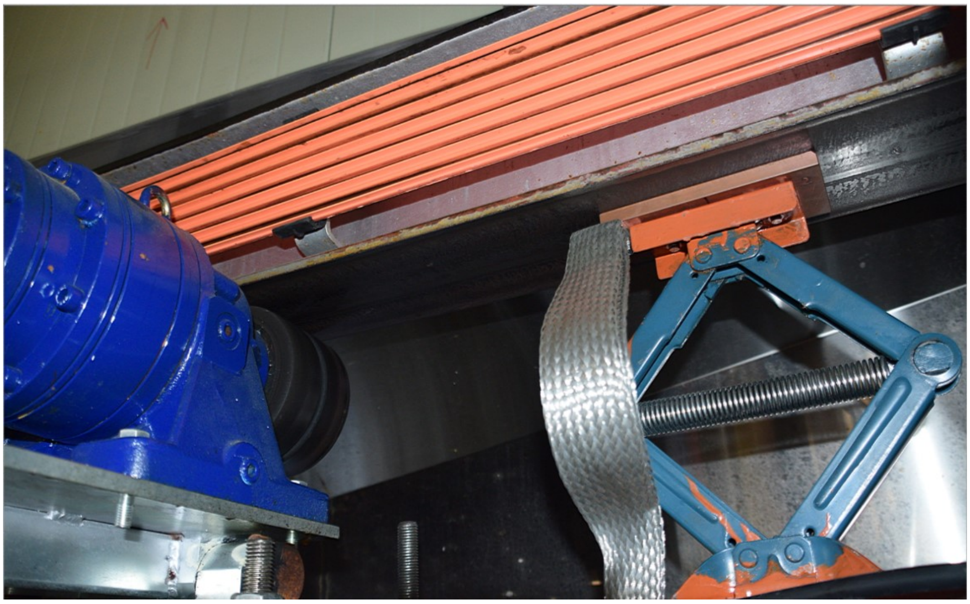

Figure 15: 集電靴浮動平貼軌道表面

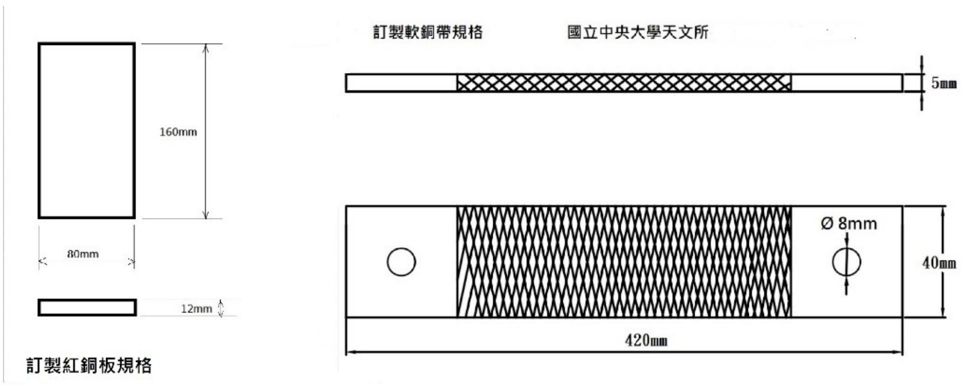

Figure 16: 集電靴純銅板與軟銅導電帶規格

由於所有設計參數均是沒得參考的預設值，集電靴製作完成後，於 2022 年 4 月即安裝在 LOT 圓頂軌道下方，進行運轉測試，經過一年數次的檢查都沒有異常的磨耗及故障，磨耗面均勻，所以於 2023 年 5 月進行接地的連接。

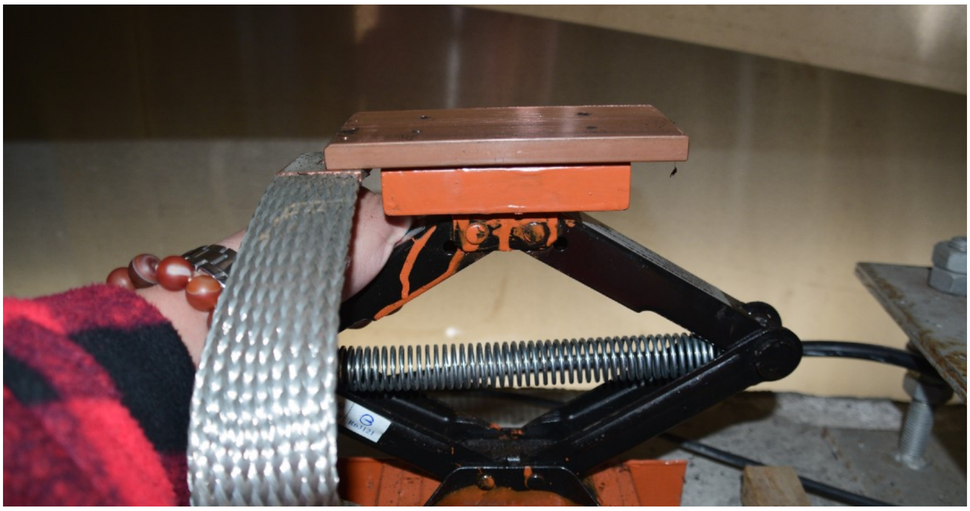

Figure 17: 自製集電靴經過一年磨耗情形

因為集電靴與軌道間是動態的狀況，為避免接觸異常失去保護作用，所以圓頂軌道上共設置 2 個集電靴，位於天文台離地高度最凸出的北側，2 個之間相隔軌道圓周 120 度角，避雷電路沿線週邊 1 公尺之內不可以有電器設備，以避免發生意外的放電迴路，所以走線天文台的西北方角落，垂下後進入到人員不易接觸且地面較為潮濕的天文台西側空地，設計如圖18。

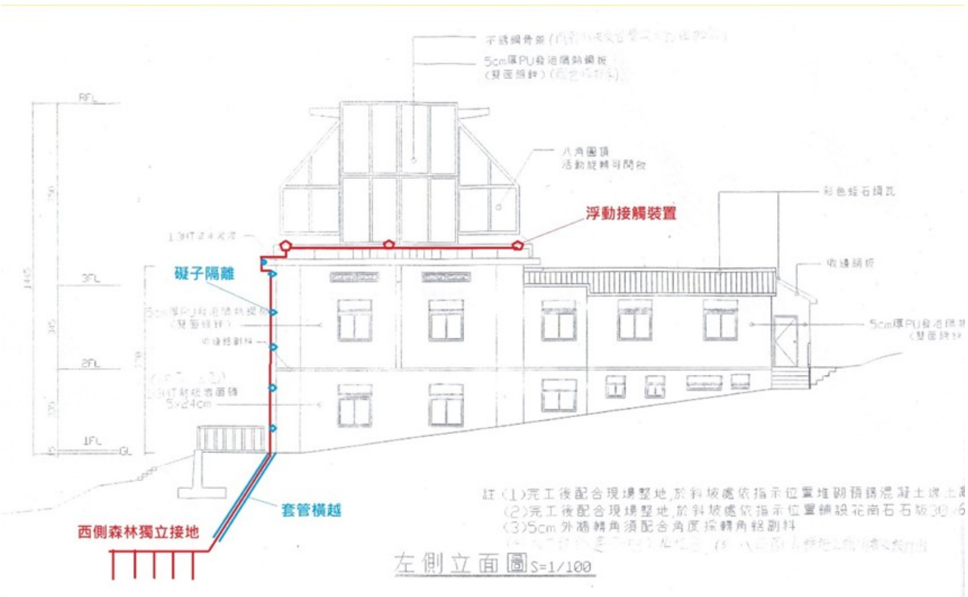

Figure 18: LOT 防雷接地示意圖

接地線為單層覆皮之 $50mm^2$ 純銅粗絞線，電路沿線轉彎處以礙子隔離固定，避免風吹晃動破壞絞線，翻越水平台面牆角向下處有加裝一礙子架如圖九，用以固定礙子並避免水泥平台表面崩落。

Figure 19: 礙子架

接地線抵達地面前約 1 公尺高度處，設置接地電阻測試點，方便未來每年檢查用。

Figure 20: E-P-C 三點接地電阻測試點

鹿林天文台位於山頂上，地底下以破碎的頁岩為主，地表的砂土質層很薄，保水性非常差，在不做大規模地質改良的狀況下，很難達到低電阻的要求，所以必須將接地的面積盡量做大，以達到低電阻的要求，我預計打入地面下 8 支～10 支的接地棒，破碎頁岩雖然有不少空隙，但是很硬且很大塊，在打入接地棒前必須先用一長鑽頭鑽開導孔通路，才能讓接地棒順利打入，因此受限於鑽頭長度限制，無法打到如平地要求的 1.8 公尺深度，僅能達到 1 公尺深度左右。

起初我們以為大樹的樹根附近，可以比較好鑽孔，結果我們錯了，水泥鑽頭完全鑽不過軟質的樹根，所以只能沿著預計走線不斷的試鑽，最後主放電電路共打入 9 支接地棒，其中 3 支與原本舊有的避雷針系統並線，以擴大放電效果，走線總長約 30 公尺，另外三點接地電阻測試點的 P、C 兩支，也依照規範設置在正確的點位上。

Figure 21: 與避雷針系統並線

為確保接線品質及耐用度，線路與接地棒均採用鋁熱劑火藥熔接方式施做。

Figure 22: 鋁熱劑火藥熔接

避雷接地的電阻要求以不超過 10 歐姆為標準，依 E-P-C 三點接地電阻測試 PC 兩點位於天文台東側方向，E 點 - C2 點直線距離 20 公尺，我們第一次就取得 8.68 歐姆的地阻值，接地完成達標。

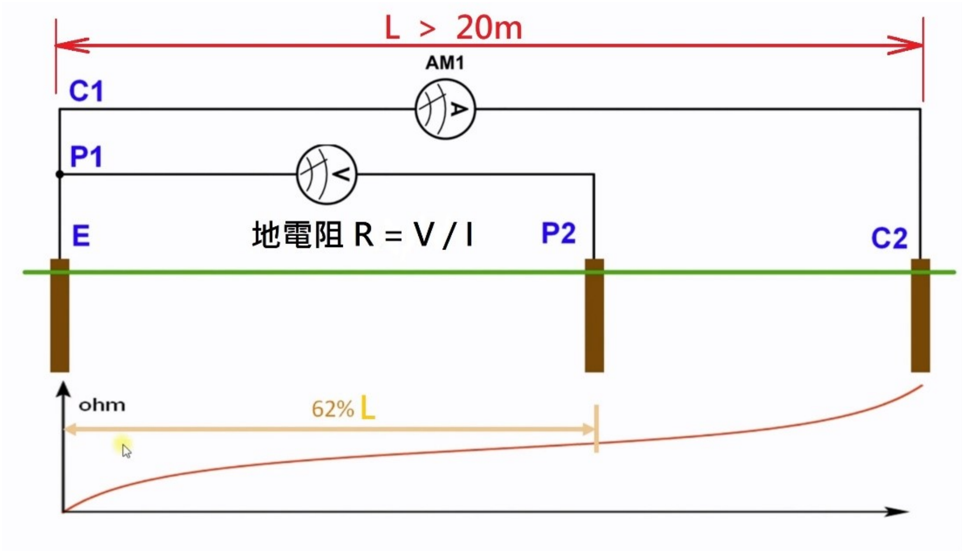

Figure 23: E-P-C 三點接地電阻測試

Figure 24: 實測地阻值 8.68 歐姆

LOT Pointing Model

侯偉傑

2023 年 4 月開始覺得 LOT Pointing Model 有問題，有使用 Pointing Model 比沒有使用還差，目標可能會移出視野外。因此決定重作，重作步驟可參考附錄 A.3。6/5 第一次重作，添加了 100 個位置，測試低仰角的位置偏移不超過 1/4 個 FOV。至 9/30 又添加位置到 144 個位置，測試後 Pointing 在天頂位置非常準，低仰角位置雖然偏移中心但不遠，且追蹤有得到改善。

SOPHIA 2048BX CCD 相機維修紀要

林宏欽

1. 2022 年 3 月 LOT 主力 SOPHIA 2048BX 相機工作溫度突然無法降到-80 C，且工作溫度逐漸升高無法保持，研判是 CCD 腔體破真空所致，向廠商反應。
2. 2022 年 4 月 SOPHIA 2048BX 相機狀況迅速惡化，影像中央出現一個黑色圓形區塊，乃是感光晶片中央結霜所致，相機內部水氣嚴重的話會損壞電子元件，切勿繼續使用，儘快聯絡廠商送修。
3. SOPHIA 2048BX 相機交由臺灣代理商轉送美國 PI 原廠維修，相機上標籤序號資料如下：
   Model# SOP
   System ID: 142977-2-1
   Model ID: SOP2048BX-U-SH-FM-Q-F-MG-W
   S/N: 04396017

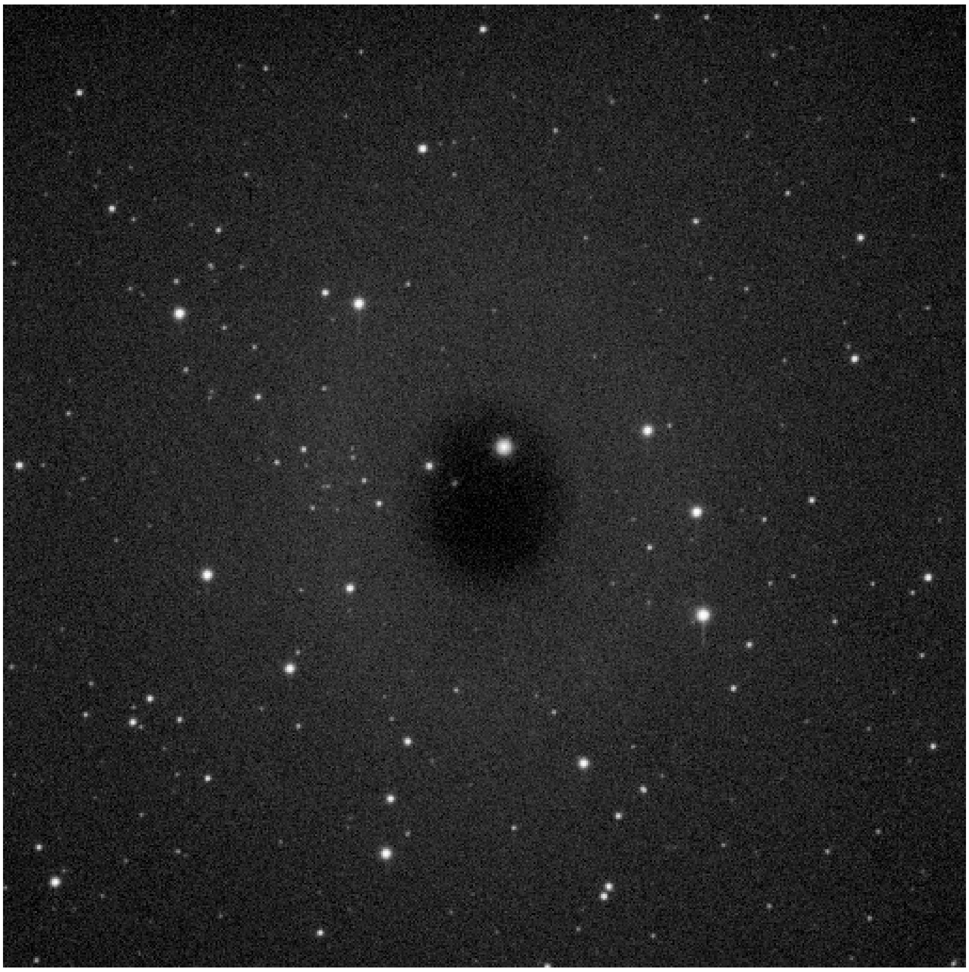

4. SOPHIA 2048BX 相機使用多年已過一般保固，但尚有永久真空保固 (XP Vacuum Chamber Limited Lifetime Warranty)，經向原廠爭取後，最終保固成立，只需支付來回運費。
5. SOPHIA 2048BX 相機維修進度因 COVID-19 疫情影響，電子元件缺料及工程等問題一直推遲，歷時 1 年多，2023 年 6 月相機終於修復回來。在所上先做初步測試，經連續幾天開機拍攝 BIAS 燒機測試，工作溫度可穩定在-80 C，BIAS 平均值穩定在 ~600。

6. 2023 年 8 月將 SOPHIA 2048BX 相機送上山，進行連線測試正常，準備下一 LOT 觀測季上線。

7. 2023 年 9 月 SOPHIA 2048BX 相機在 MaxIm DL V5/V6 軟體控制皆出現影像無法下載問題，故取消上線，LOT 用原先的 Andor 936 CCD 相機進行觀測。

8. 經交叉測試發現 SOPHIA 2048BX 相機在舊 LOT-PC (英文 Win10) 可正常使用，但在新 LOT-PC (中文 Win11 改英文) 有問題，最後用其他英文 Win11 PC 測試也還是不行！確認影像無法下載問題與 Windows 11 有關，在原廠提供新版 LightField 軟體 (V6.17.7.2311) 後解決，準備下一 LOT 觀測季上線。

9. LOT-WIN11-PC+PI ASCOM V0.0.0.4 測試，MaxIm DL 拍完暫停，再拍會出現”Error starting exposure. Could not invoke ’StartExposure’ Reason: Exception occurred.”！

10. LOT-WIN11-PC+ PI ASCOM Driver 更新為 V1.7.0.2008 測試 OK，但拍攝時會顯示”No cooler control”，且 FITS 檔頭內沒有寫入 CCD 工作溫度！停止拍攝時會恢復顯示，原廠表示工作溫度除非有重設不然還是會保持原設定。因尚未有新版 PI ASCOM Driver 暫時就用 V1.7.0.2008，觀測過程中需注意一下溫度是否-80 C！並請知會各觀測計畫人員。

SLT

Andor 934 CCD 相機

林宏欽

1. 天文相機性能對觀測影響甚巨，現有的備用相機都是超過 10 年的老舊機種，觀測資料品質較差，因此決定採購一台較好的備用相機，在經費及性能的考量下，決定採購 Andor iKon-M 934 DU934P-BEX2-DD 天文科研用冷卻 CCD 相機 (https://andor.oxinst.com/products/ikon-xl-and-ikon-large-ccd-series/ikon-m-934)，規格如下:
   - 背照式深耗盡 CCD 科學級晶片, 晶片等級 1, 含抑制近紅外紋影效應功能
   - 1024 x 1024 畫素, 13umx13um 像元, 成像區 13.3*13.3 mm
   - 峰值量子效率: 95% , 近紫外至近紅外波段 (400nm-900nm) QE>80%
   - CCD 腔體真空密封、永久真空保證
   - 熱電致冷可到-80°C，水冷可到-100°C
   - C-mount 與內建機械快門
   - 讀出速率：5, 3, 1, 0.05 MHz
   - 16 bits 類比數位轉換 (16 bits ADC)
   - USB 2.0 資料傳輸介面
   - 支援 MaxIm DL 軟體：相機控制、影像顯示、資料分析
   - 軟體開發工具 software development kits (SDKs) for Windows 10 and Linux
   - 出廠測試報告，包括：Gain, Linearity, Dark current, Read noise for 3, 1, 0.05 MHz readout speeds @ -80°C
   - 1 個備用機械快門
2. 快門是消耗品，國外採購費時，需隨時保有一個備用快門避免因故障中斷觀測。
3. 拆掉 Andor 934 相機前面黃銅 C-mount 增大光路開口並避免反光。
4. 因 Andor 934 相機和先前用的 Andor 936 相機機械尺寸、焦深 (Back Focus Distance) 等規格不一樣，必須製作新的 Andor 934 -to- FLI CFW adapter (for SLT)。
5. Andor 934 相機是 BEX2-DD 晶片，QE 性能優於 Andor 936 的 BV 晶片，尤其對紅藍端的影像可達到更深星等！SLT 搭配 Andor 934 在 SDSS u' 濾鏡 300 秒曝光可以到 19 星等! Andor 934 晶片只有 Andor 936 的 1/4，即視野只有 Andor 936 的 1/4，但是對大部分觀測來說還是很足夠。經討論後決議：SLT 繼續用新的相機 Andor 934 BEX2-DD 相機。
6. 新相機可能會有問題，應在保固期內儘量使用、發現並解決問題，確保其性能及穩定性。

Andor 934 相機參數測量

林宏欽

1. 測量 Andor 934 BEX2-DD 相機參數 gain, readout noise，參考以下網頁，
   - QSI 532ws CCD Camera Performance: Conversion Factor and Readout Noise http://www.stargazing.net/david/qsi/ccdperfcfrn.html

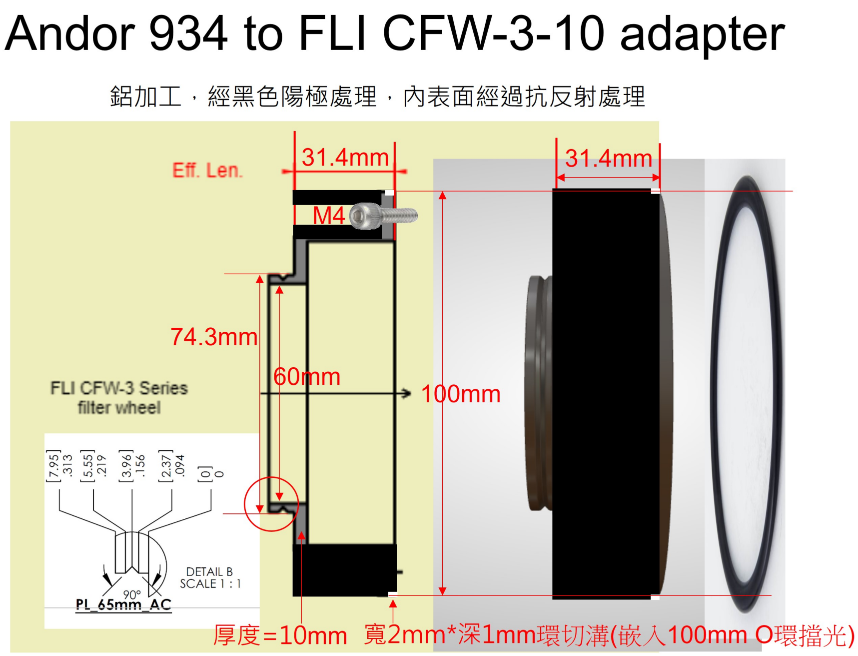

- The Handbook of Astronomical Image Processing 2nd Edition (by Richard Berry and James Burnel) 的 Chapter 8
  https://www.amazon.com/Handbook-Astronomical-Image-Processing/dp/0943396824

2. 拍攝所需的 BIAS, DARK, FLAT 檔案 (10 組)：

   - FLAT 需用穩定光源，LED 燈打開後預熱 30 分鐘，採間接照明拍 DOME FLAT
   - BIAS, DARK, FLAT 需使用相同設定拍攝 (-80C, readout rate, preamp gain....)

3. 註冊並下載 AIP4WIN 軟體，解壓縮後，執行 AIPv2.4.10.NonReg.exe，進行測量
   https://groups.io/g/AIP4Win

4. 測量 Andor 934P 相機參數

   AIP4WIN > Characterize CCD camera > Basic CCD Test

5. 測試結果：

   Andor DU934P-BEX2-DD
   型號 =DU934P-BXDD
   S/N=CCD-26868
   晶片 =E2V CCD47-10

相機模式設定：
A/D Channe=16-bit
HS Speed=1MHz
VS Speed=2.25us
Pre-Amp Gain=4x
Baseline Clamp=ON
工作溫度 =-80°C

10 組影像統計測量後平均值如下：
Conversion Factor (electrons/ADU)=1.088
Readout Noise (electrons RMS)=8.831

SLT 圓頂閉合不全

侯偉傑、石俊雄

2023 年 6 月林啟生發現 SLT 圓頂無法完全關閉，即圓頂天窗在程式顯示 Closed 時卻還有縫隙 (圖26 (a) and (b))。因進入午後雷陣雨季節，所以暫時先在結束觀測時將望遠鏡與電腦用帆布蓋上。

6/21 與駐站助理石俊雄至現場勘查測試，有時能正常閉合，但有時會閉合不全，且在關閉時會出現巨大聲響。最後發現兩片天窗接近閉合時彎折處卡住導致 (圖 25)，可能是長久的熱漲冷縮導致材料變形。

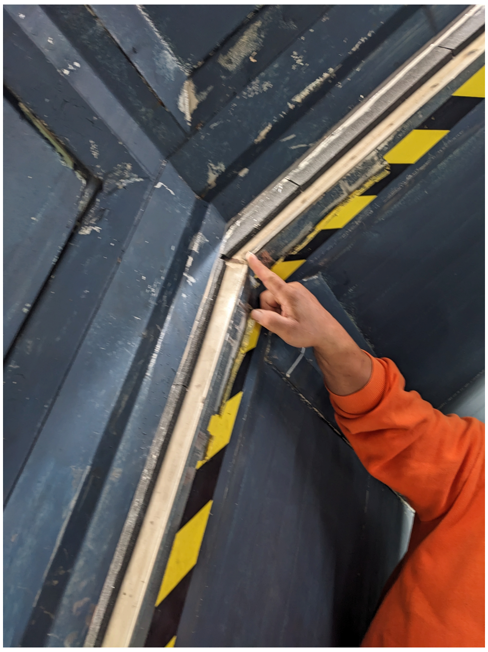

Figure 25: SLT 天窗卡住的位置

利用板手等工具將左邊天窗會卡住的位置向內扳，讓左右天窗在不會卡住即可順利關上，不會留細縫。經過幾次測試都可以正常關閉 (圖 26 (c) and (d))。

(a) (b) (c) (d)

Figure 26: (a)(b) 圓頂閉合不全，全關的狀態還留有縫隙。(c)(d) 整修後可以正常關閉，且未留有縫隙。

SLT Pointing Model

侯偉傑

11 ~ 12 月觀測時發現 slew 的位置不太準確，且某些天區 Sidereal Tracking 不準確，約 3 分鐘的影像就會看到明顯脫線。前者還可以使用 ACP Observatory 的 Auto Centering 功能來解決，但後者對拍攝影像的影響甚大。本來以為是望遠鏡平衡問題，但調整完後問題並沒有解決，所以後來認為是極軸不準或是 pointing model 的問題。

在依照 Ascension 200HR German Equatorial Mount Instruction Manual 的步驟做完第一次 pointing model，並參考 Polor Axis Alignment Err 數值調整極軸，原本極軸誤差 1x1 角分，調整後重做 Pointing model 測量極軸誤差 1x0.5 角分，測試無導星追蹤 300sec 星點成點狀！重作 Pointing Model 的步驟請參考附錄 B.4。

LWT

LWT ME 赤道儀故障修復報告

林宏欽

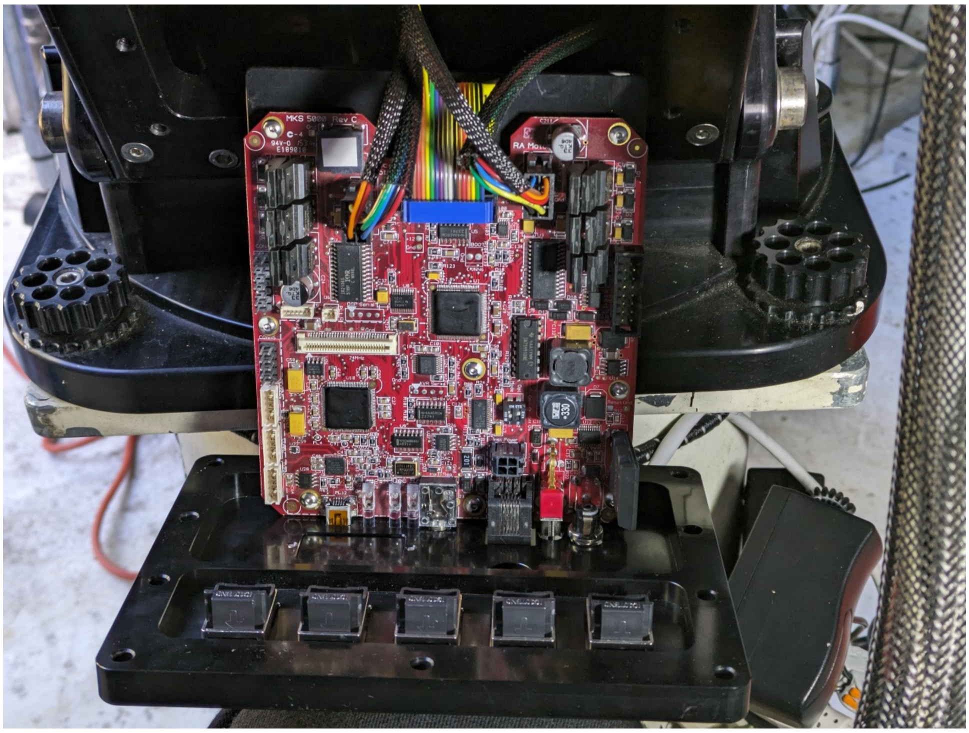

1. LWT 的 Paramount ME 赤道儀 MKS-5000 控制機板因不明原因受損！經查網路上資訊顯示：MKS-5000 對靜電、接地環路、電壓尖峰或其他條件等外部影響非常敏感！這與我們 LWT 和 NCUO24 的 MKS-5000 控制機板多次損壞經驗相符。可嘗試加裝 USB 隔離器看是否可解決此問題。USB 隔離器的缺點是傳輸速度相當慢，因赤道儀控制不需高速傳輸故不影響。

2. 因 COVID-19 疫情影響電子元件嚴重缺料，MKS-5000 控制機板長期缺貨進而停產，而新一代的 MKS-6000 控制機板則遲遲沒有正式發售。聯繫許久最終廠商提供了一片 MKS-5000 機板，更換後終於恢復運作！

3. 此次 ME 赤道儀故障，總共停工了約半年，建議須有備品 (MKS 6000 Upgrade Kit for the Paramount ME Classic GEM 升級套件)。因國外儀器設備的關鍵零組件取得相當費時 (3-6 個月)，有備品方能馬上替換恢復觀測作業，避免萬一故障觀測停擺。

LWT Pointing Model

侯偉傑

在 LWT 整修復原後，雖有沿用舊的 pointing model，但實際上的 slew 狀況並不好。參考 https://www.youtube.com/watch?v=6cy9pKSLwXk&ab_channel=SoftwareBisque 影片重建 TPoint。重建後的 RMS 為 15.1 arcsec, 而 LWT 的視野為 1.38deg^2，所以目標基本上都會在畫面中心。

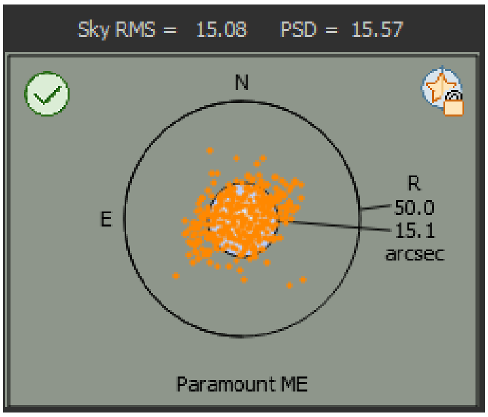

其他軟硬體設施

NAS 故障與修復

2023/3/8 停電復電後將儀器重新開機，但發現 NAS 第三顆硬碟亮紅燈，更換硬碟後卻無法正常重建 RAID。早上上傳觀測資料時也沒辦法上傳。在經過幾次嘗試修復後無果，最後送回中大請鎮魁重置處理。在送下山這段時間，將原本饒老師的 LWT Nas 拿來代替故障的 NAS。最後 JK 成功修復 NAS，並在 4/1 送回山上當作備援。

鹿林問題回報系統

侯偉傑

天文台人員以輪值方式作業，平常利用口頭或是信件交接。口頭交接雖清楚但容易忘記，信件有時不會詳細描述。在 2021 年發生 LOT 赤道儀異常，因為沒有將問題

以文字與照片等形式記錄下來，所以與天文所器材室職員描述問題時經常溝通不良。

2022 年初助理們討論，希望有個方式可以記錄問題與處理過程，以便報告製作與未來發生時的查閱。當時是以 google sheet 來製作，以簡單的表格形式來記錄，若有照片等附件需先上傳至 google drive 並在表格欄位填上連結網址 (如圖 27)。

B1 fx 發生日期

	B	C	D	E	F	G	H
1	發生日期	狀況分類	狀況敘述(簡單填寫即可)	解決方式(簡單填寫即	狀況子分類	回報者	檔案位置1
29	2022/04/13	流星	流星E1B軟體當掉兩次	重開	軟體		
30	2022/04/14	LOT	RA軸卡住一次，控制箱內出現紅	緊急停止開關壓下後鬆	赤道儀		
31	2022/04/14	LWT	觀測時，MaxIm DL卡在filter movin	MaxIm DL關掉重開	軟體		
32	2022/04/20	LOT	autoflat 不知如何使用 readout m	修改"C:\Users\Public\	ACP autoflat		
33	2022/04/22	網路	網速降至幾百kbps，幾乎無法上	後來發現是中華電信訊號強度太弱，將4G路由器放到影印機旁的窗邊就			
34	2022/04/26	SLT	圓頂開關時 error 老問題，但新	必須到現場手動開啟	圓頂		
35	2022/04/26	SLT	次鏡對焦座迫緊螺絲鬆掉	將望遠鏡調製準焦位	次鏡對焦座		https://drive.google.
36	2022/5/1	SLT	五月初對焦系統ROBOFOCUS	解決方案： 1. RS232 Hub 換孔。 2. 連線方式改成：focus max > ascom			
37	2022/5/5	LWT	ACP連不上天窗停掉，以為是鐵	重開SWITH ON之後解決 .			
38	2022/5/5	SLT	對焦系統ROBOFOCUS觀測時	1. RS232 Hub 換孔。 2. 連線方式改成：focus max > ascom device hu			
39	2022/05/05	LWT	LWT 傳檔案到 nas 有跳出傳輸	重開電腦			
40	2022/05/06	SLT	次鏡對焦座迫緊螺絲再次	鎖緊螺絲，注意大螺	次鏡對焦座		
41	2022/05/06	網路	網速降至幾百kbps，幾乎無法上	路由器放在LWT卻依舊無網路，投訴中華電信後，將路由器重開後即有			
42	2022/05/28	LOT	赤道儀RA無法驅動	重新插拔赤道儀RA馬	赤道儀		https://drive.google.
43	2022/06/23	LWT	無法使用 acp autoflat	未解決，先使用maxir	acp autoflat		
44	2022/7/24	LOT	7月24日近4點多，LOT跑SCRIP	經重開AUTOSLEW視窗之後正常		林啟生	
45	2022/08/12	LOT	ASI 174 與 PHD2 可以連線，但	可能是 Dome 的 com	ACE Smart[	WJ	

Figure 27: 舊版狀態回報紀錄 (Google Sheet)

但製作 2022 年報時，發現整理起來相當不易，因為同一個主題有好幾條狀態更新的回報，並散落在整個表格之中，需要人工判斷。且整理完後如同 2022 年報中的流水帳，閱讀也不容易。因此決定製作類似 Stack Overflow 的形式的回報系統，可以創建主題並回覆以便閱讀與整理。2023 年利用在天文台區域網路架設的測試網站來製作這個系統。

利用 Django 架設網站、使用 CKeditor 富文本 (Rich Text Format) 編輯器使內容能夠加入圖片、影片等。利用 Django Tags 與 Filter 套件讓使用者可以尋找、過濾想找的主題 (圖 28)。

名稱 標籤1 lot 標籤2 --------- 已解決? ------- 查詢

Created	Last Update	Title
23-09-15	24-01-08	✕ LOT 使用光譜儀時會有 RA 方向跳動 mount autoslew lot uvex lisa
23-09-14	23-12-27	✕ LOT 更新 win11 後遇到一些問題 lot dome thesky6
23-11-29	23-11-29	✓ LOT指向錯亂之處理方式 autoslew lot sync
23-09-01	23-09-01	✓ SOPHIA2048B溫度顯示異常 lot
23-05-10	23-05-10	✓ LOT 圓頂 ACE smartdome 無法打開天窗，也無法運動 lot dome
23-04-22	23-04-22	✓ LOT Thesky6/ACP slew 時出現 err thesky lot

« 1 »

Figure 28: 新版問題回報系統

不過目前助理還沒有每次發生狀況都到系統來更新，可能還要繼續熟悉使用方式與建立遇到問題就回報的習慣。未來系統也可以依助理們的習慣來改善。

在 2023 年創建或更新狀態的回報共有 27 則，全部列於附錄V(以主題創建時間順序排列)，其中還有 5 則尚未解決。附錄 C.27為回報系統的使用方式。因為利用 pyppeteer 套件將網頁轉成 PDF，所以影片檔案無法正常顯示。

鹿林全天相機壓克力半球遮罩內部結露與處理

林宏欽

1. Lulin 全天相機型號為 ALCOR ALPHEA 6CW All Sky Camera (S/N#127423)，採用 ASI 178MC 相機及 1/2”1.55mm IR MP 魚眼鏡頭，自 2019 年 5 月啟用以來一直穩定運作，2023 年 12 月相機壓克力半球遮罩內部出現結露現象，詢問原廠表示需要更新密封 O-ring 及乾燥劑，約每 3 年一次。

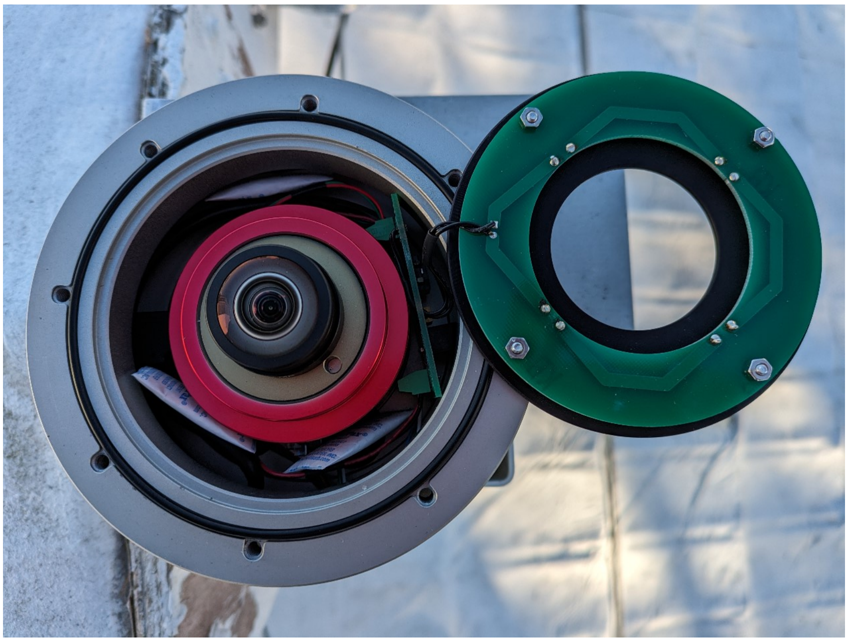

2. 打開相機遮罩內有 3 小包 MiniPax 分子篩乾燥劑，因沒有備用 MiniPax 乾燥劑包，所以嘗試將 MiniPax 包裝袋剪開後，更新裡面的分子篩，封口折好用釘書針固定後裝回。

3. 更換 O-ring 並清潔壓克力遮罩及鏡頭。

4. 最後開機實測，沒有再出現結露現象。

5. 考慮採購一些 MiniPax 乾燥劑備用。

太空所 IRSL 全天影像儀 EUDA-2M 安裝

林宏欽

1. 中大太空所安裝新的 IRSL 全天影像儀 Alcor System EUDA-2M All Sky Camera，主要規格為：ASI 294MM Pro 相機搭配 4.5mm F/2.8 全周魚眼鏡頭，相機工作溫度為-10C，降低熱噪訊
2. 相機有 5 個濾鏡如下，
   Filter position 1 -> focus position 500 ADU, Filter name OI 630-10
   Filter position 2 -> focus position 500 ADU, Filter name OI 557-10
   Filter position 3 -> focus position 250 ADU, Filter name OI 777-10
   Filter position 4 -> focus position 250 ADU, Filter name Na 589-10
   Filter position 5 -> focus position 1500 ADU, Filter name L3=NoFilter
   其中 OI 濾鏡對大氣暉光等特定現象觀測可提高訊噪比
3. 使用 BK7 玻璃球罩，玻璃透光性與折射率等光學性質較佳、成像較好、強度較高、耐候性和耐溫性較佳
4. 設計用一 L 型支撐座固定在 LOT 大門上方斜屋頂
5. 2023 年 12 月 20 日安裝啟用後，運作穩定，效果良好。
6. 白天設定在 Na 濾鏡、光圈開到最小 F16，避免感光晶片直接日曬。
7. 考慮拍攝目標為大氣暉光，每張曝光 2 分鐘以得到較高訊噪比。
8. ASI 294MM Pro 拍攝應使用 Bin 2x2 模式，4144 x 2822 解析度，4.63 um 像素，14 位元。建議增益設定為 Gain=121 (High Gain Mode 充分利用讀取雜訊和動態範圍) ，偏移 OFFSET= 30 (或驅動程式預設提供的值)。
9. ASI294 相機的讀取雜訊很特殊。當 120 或更高時，HCG（高轉換增益）模式會自動啟用，該模式可在較高增益下將讀取雜訊降低到更低水平，而不會損失動態範圍。讀取雜訊將降至 2e- 以下，而動態範圍將保持在 13 級。根據您的目標，您可以設定較低的增益以獲得更高的動態範圍（較長的曝光）或設定較高的增益以獲得較低的雜訊（例如短曝光或幸運成像）。1
10. 因 USB-to-RS232 連線一直不穩@@@ => 改用 PC 的內接 COM1=>OK

其他

缺水問題因應措施討論

蕭翔耀

近20年臺灣乾旱事件！

肇始時間	延續時間	解旱原因
2001.11.	2002.7.	雷馬遜颱風
2003.1.	2004.7.	敏督利颱風
2006.1.	2006.5.	梅雨鋒面
2009.2.	2009.9.	莫拉克颱風
2011.1.	2011.5.	梅雨鋒面
2014.9.	2015.5.	梅雨鋒面
2017.10.	2018.6.	梅雨鋒面
2020.2.	2021.5.	梅雨鋒面

臺灣大學氣候天氣災害研究中心

根據最近二十年統計，約每兩年到三年便會發生一次乾旱。需事先規畫因應措施。2023 年初中南部缺水嚴重，三月初玉山國家公園管理處也表示山區水源不足，因離梅雨鋒面至少還有兩個月，因此需要提早準備。

根據鹿林天文台水電紀錄及住宿人次統計，平均一人一天使用約 100 公升，而山上水塔滿水將有 24 公噸。基於山上水塔 20 噸儲水供 3-4 人使用，草擬方案如下：

1. 若玉管處大水塔停止供水給天文台，請所有訪客下山，並停止訪客上山。
2. 若玉管處大水塔停止供水給天文台，只維持駐站人員 1 人、觀測助理 1 人、其他必要人員 1-2 人。

因為 3 月為環工所經常性長期採樣期，與環工所溝通後決定以方案一並放寬條件，讓除天文台人員外可提供兩位人員，以便執行任務。於三月 19 日起進行管制，並通告各單位。直至 5 月中旬開始充沛降雨，研判水源充足並解除人數管制。

鹿林天文台設置 AED「自動體外心臟電擊去顫器」

林宏欽

鹿林天文台所在的鹿林前山曾發生數次健行遊客因身體不適昏倒，送醫搶救不治的不幸事件！因車輛無法到達天文台，最近的救護人員到達現場至少需時一小時，為了在第一時間搶救生命，在中大學術基金會的贊助及中大衛生保健組的協助下，2023 年 8 月 12 日於鹿林天文台設置 AED「自動體外心臟電擊去顫器」，希望在高山缺氧的環境強化急救防護體系，確保天文台人員和登山者的生命安全。(詳見中大新聞網 https://ncusec.ncu.edu.tw/news/headlines_content.php?H_ID=4144)

鹿林天文台生活注意事項英文版

Precautions of living in Lulin Observatory

戴辰宇

Information

For the first time visitors, please watch the video.
大愛電視～發現節目【高山之眼－鹿林天文台】
The weather forecast website for Lulin
鹿林天文台 - 觀星｜交通部中央氣象署 (cwa.gov.tw)

Genenral

1. The observatory is located in Yushan National Park. Please follow the regulations of the national park.
2. Please be aware of the altitude (2862 m) of the observatory. If you have any syndromes or discomfort, please inform the on-site staffs first, and prepare your own personal medication.
3. Cherish resources. (eg: water, electricity)
4. Smoking or open fire are prohibited

Food

1. Observatory accommodation includes three meals. However, you will have to DIY the breakfast. The restaurant provides items such as powdered milk, cereal, toast, jam, etc.
2. No need to bring your own dishes.
3. Vegetarians or those with dietary restrictions, please make sure to prepare some food for yourselves.
4. Avoid using disposable utensils

Clothing

1. In summer, nighttime temperatures range from 10 to 20 degrees Celsius, while in winter, nighttime temperatures drop to 0-5 degrees Celsius. Please prepare warm clothing.

Housing

1. Please bring your own towels and toothbrush with toothpaste. Observatory will provide body wash, shampoo, etc.
2. Please keep the accommodation area quiet.
3. Please use electrical appliances with caution and avoid electrical wire fires.

4. On nights available for observation, it is strictly prohibited to have outdoor lighting and outdoor activities. After nightfall, please close the curtains and blinds to shield indoor lighting in order to avoid interfering with the observation.

Outdoor activity

1. The hiking trails in Yushan National Park are restricted areas, and unauthorized access is not allowed.
2. The area near the observatory is within the Yushan National Park recreational zone. If you plan to hike on nearby trails/forest roads, please go in groups, bring communication devices and rain gear, and inform the on-site staff or your group leader for safety precautions. Please also be aware of the evening hours when returning.
3. If it is necessary for any observatory station to turn on lights during nighttime observations, please close the dome. If you need to open the dome for work, please inform other observatory personnel and use minimal or red lighting while avoiding light directed toward the sky.

IV
新聞報導

歷年媒體新聞統計 (1998-2023)

1998 年至 2023 年中大天文所與鹿林天文台的相關新聞媒體報導統計如下:

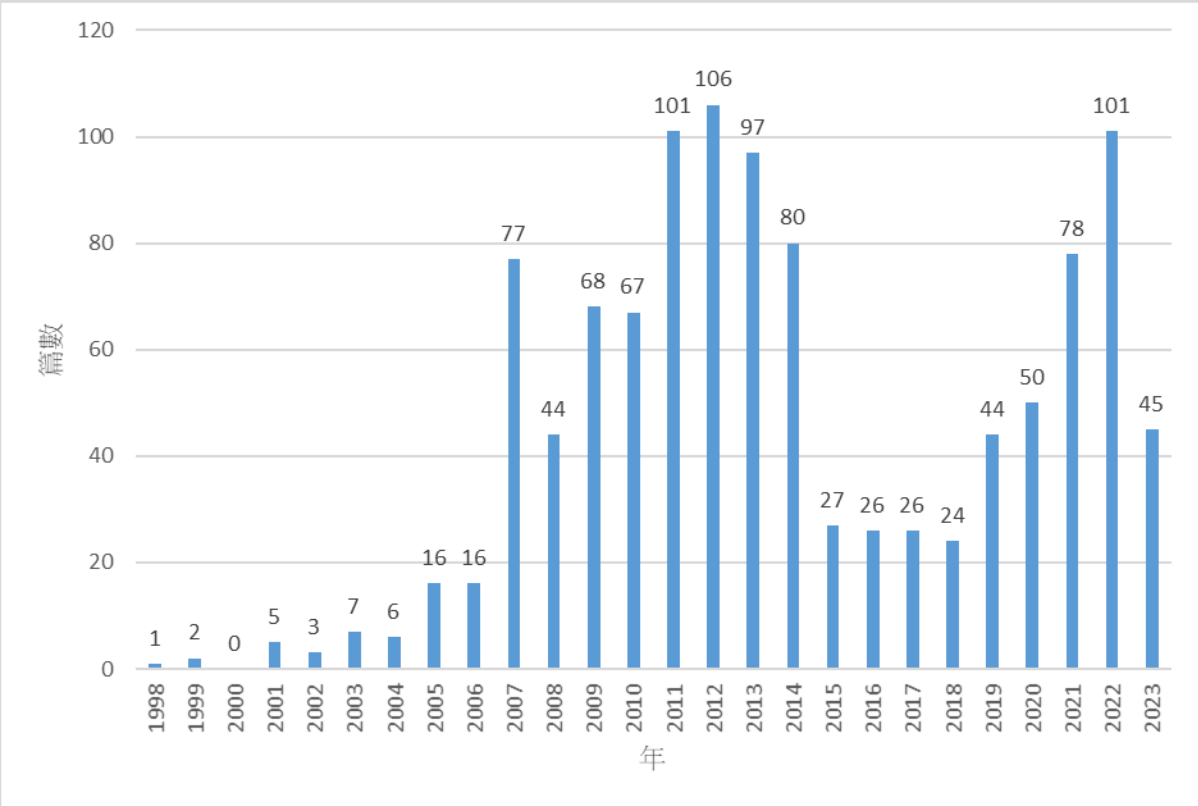

Figure 29: 中央天文所與鹿林天文台相關新聞報導統計 (1998-2023)

媒體新聞

一代報人　百年青史　中央大學頒贈「余紀忠」小行星以為感念

2023/11/02 蕃薯藤
《中國時報》創辦人余紀忠先生。余先生的一生，以言論報國，為台灣當代民主自由的實踐，留下相當重要的遺產。中央大學感念其奉獻及精神，將編號 603200 余紀忠小行星頒贈余紀忠文教基金會董事長余範英，期許余紀忠先生的信念能夠繼續守護台灣，讓世人不忘民主自由的可貴。

中國時報創辦人余紀忠先生(1910-2002)為國立中央大學傑出校友，非常關心且支持母校的發展。中央大學在 1999 年頒授名譽文學博士學位，以表彰其對社會、文化和國家的貢獻，並於 2008 年與余紀忠文教基金會共同成立「余紀忠講座」，邀請各領域學者擔任主講人，一同帶領師生探討學術議題。

余紀忠小行星，編號 603200，2006 年 7 月 5 日由中央大學鹿林天文台林宏欽及美國馬里蘭大學的葉泉志博士共同發現，大小約在 1 公里之間。余紀忠小行星繞行太陽一圈 3.47 年（軌道週期），離太陽最近時（近日點）為 3.05 億公里，最遠時（遠日點）為 3.83 億公里。

余紀忠文教基金會董事長余範英表示，他的父親余紀忠先生，一生以「政治民主、民族認同、穩定大局」為重要信念，前半生投筆從戎，報效國家，後半生創辦報紙，與時代相互書寫。感謝影響父親至深的中央大學頒贈小行星以為感念，抬頭仰望星空時，得以和父親對話，內心很感動！

中央大學從 2006 年開始的鹿林巡天計畫，不但曾發現台灣史上的第一顆彗星，同時也發現了 800 多顆小行星，使台灣成為亞洲發現小行星最活躍的地方之一。卓越的天文研究成果，充份展現台灣人以小搏大、努力不懈的精神，期許透過小行星的命名與頒贈，看見台灣更多可貴的價值。

原文轉載自【2023-10-31/蕃薯藤】

緬懷余紀忠言論報國　中大贈小行星

2023/11/02 中時新聞網
余紀忠文教基金會自 2008 年以來與國立中央大學合辦講座，活動 10 月 31 日盛大舉行，除邀中央研究院院士吳玉山，以烏俄戰爭為主題擔任主講人外，校方為緬懷《中國時報》創辦人余紀忠以言論報國的精神，將編號 603200 余紀忠小行星致贈給基金會董事長余範英，期許其信念能繼續守護台灣，讓世人不忘民主自由的可貴。

中央大學校長周景揚說，每年舉辦余紀忠講座，展現人文關懷與對各領域的學識重視，余紀忠是中大傑出校友之一，辦理講座之際，將小行星頒贈給余紀忠文教基金會，期許其信念繼續守護台灣，精神永遠高掛星空。

余範英則說，父親一生以「政治民主、民族認同、穩定大局」為重要信念，前半生投筆從戎報效國家，後半生創辦報紙，與時代相互書寫，他有自己的民主思想與理想抱負，其一生也就是《中國時報》的故事，感謝影響父親至深的中央大學舉辦頒贈儀式，如今抬起頭來，就可以跟爸爸的小行星說說話。

余紀忠小行星編號 603200，於 2006 年 7 月 5 日由中央大學鹿林天文台林宏欽及美國馬里蘭大學的葉泉志博士共同發現，大小約 1 公里。命名緣由感念其秉持自由、民主、愛國家、開明、理性、求進步的信念，以政治民主、民族認同的言論方針，在歷史變局中力主穩定大局，為台灣當代民主自由實踐留下重要遺產。

今年講座主講人吳玉山，研究專長為社會主義國家政治與經濟轉型、兩岸關係與國際關係理論等，演講題目「烏俄戰爭對台灣的啟示：比較、互動與示範」，探討「台灣會不會是下一個烏克蘭？」他從安全與族群面向比較台灣與烏克蘭的不同，也探討烏俄戰爭對於海峽兩岸與世界各國所帶來的示範作用。

他提到，台灣與烏克蘭皆有 2 個相同難解的困境，包含因地緣位置延伸出的國家安全考量，及民族認同問題，期盼大眾共同關注此議題，善盡台灣為世界公民之一的社會責任。

原文轉載自【2023-11-01/中時新聞網】

紀念一代報人余紀忠　中大頒贈小行星

2023/11/01 人間福報
中央大學於今日余紀忠講座，舉行余紀忠小行星（Yuchichung）頒贈儀式，緬懷《中國時報》創辦人余紀忠先生，中央大學感念其奉獻及精神，將編號 603200 余紀忠小行星頒贈余紀忠文教基金會董事長余範英，期許余紀忠先生的信念能夠繼續守護台灣，讓世人不忘民主自由的可貴。

中時創辦人余紀忠先生(1910-2002)為國立中央大學傑出校友，非常關心且支持母校的發展。中央大學在 1999 年頒授名譽文學博士學位，以表彰其對社會、文化和國家的貢獻，並於 2008 年與余紀忠文教基金會共同成立「余紀忠講座」，邀請各領域學者擔任主講人，一同帶領師生探討學術議題。

余紀忠小行星，編號 603200，2006 年 7 月 5 日由中央大學鹿林天文台林宏欽及美國馬里蘭大學的葉泉志博士共同發現，大小約在 1 公里之間。余紀忠小行星繞行太陽一圈 3.47 年（軌道週期)，離太陽最近時（近日點）為 3.05 億公里，最遠時（遠日點）為 3.83 億公里。

余紀忠文教基金會董事長余範英表示，他的父親余紀忠先生，一生以「政治民主、民族認同、穩定大局」為重要信念，前半生投筆從戎，報效國家，後半生創辦報紙，與時代相互書寫。感謝影響父親至深的中央大學頒贈小行星以為感念，抬頭仰望星空時，得以和父親對話，內心很感動！

中央大學從 2006 年開始的鹿林巡天計畫，不但曾發現台灣史上的第一顆彗星，同時也發現了 800 多顆小行星，使台灣成為亞洲發現小行星最活躍的地方之一。卓越的天文研究成果，充份展現台灣人以小搏大、努力不懈的精神，期許透過小行星的命名與頒贈，看見台灣更多可貴的價值。

原文轉載自【2023-10-31/人間福報】

台中央大學辦余紀忠講座　緬懷一代報人精神

2023/11/01 中國評論通訊社
中評社桃園 10 月 31 日電（記者　盧誠輝）台灣中央大學與余紀忠文教基金會 30 日共同舉辦“余紀忠講座暨余紀忠小行星頒贈儀式”，除邀請“中央研究院”院士吳玉山演講外，也特別頒贈由該校鹿林天文台所發現的小行星，並以余紀忠命名，緬懷余紀忠一代報人永垂不朽的精神，由余紀忠的女兒、余紀忠文教基金會董事長余範英代表接受。

已故的《中國時報》創辦人余紀忠是大陸時期中央大學的傑出校友，非常關心且支持母校的發展，該校在 1999 年頒授名譽文學博士學位給余紀忠，表彰他對社會、文化和國家的貢獻，並於 2008 年與余紀忠文教基金會共同成立“余紀忠講座”，邀請各領域學者擔任主講人，一同帶領師生探討學術議題。

中央大學校長周景揚表示，學校從 2008 年開始舉辦“余紀忠講座”，每年都會邀請各領域學術地位崇高的學者擔任主講人，除展現該校對人文社會的關懷、理工科學與大學教育的重視，並彰顯余紀忠一生對國家社會關懷的理念，今年特別舉辦余紀忠小行星頒贈儀式，除余紀忠是學校最傑出的校友之外，也希望能藉此緬懷余紀忠一代報人永垂不朽的精神。

余紀忠小行星，編號 603200，2006 年 7 月 5 日由台灣中央大學鹿林天文台林宏欽及美國馬里蘭大學的葉泉志博士共同發現，大小約在 1 公里之間。余紀忠小行星繞行太陽一圈 3.47 年（軌道週期），離太陽最近時（近日點）為 3.05 億公里，最遠時（遠日點）為 3.83 億公里。

原文轉載自【2023-10-31/中國評論通訊社】

感念奉獻精神　中央大學小行星命名余紀忠

2023/11/01 國立教育廣播電台
中央大學於 10 月 31 日舉行余紀忠小行星（Yuchichung）頒贈儀式，緬懷《中國時報》創辦人余紀忠先生。

余紀忠小行星，編號 603200，2006 年 7 月 5 日由中央大學鹿林天文台林宏欽及美國馬里蘭大學的葉泉志博士共同發現，大小約在 1 公里之間。余紀忠小行星繞行太陽一圈 3.47 年（軌道週期），離太陽最近時（近日點）為 3.05 億公里，最遠時（遠日點）為 3.83 億公里。

中央大學指出，感念其奉獻及精神，將編號 603200 余紀忠小行星頒贈余紀忠文教基金會董事長余範英，期許余紀忠先生的信念能夠繼續守護台灣，讓世人不忘民主自由的可貴。

中央大學從 2006 年開始的鹿林巡天計畫，不但曾發現台灣史上的第一顆彗星，同時也發現了 800 多顆小行星，使台灣成為亞洲發現小行星最活躍的地方之一。

原文轉載自【2023-10-31/國立教育光播電台】

中央大學感念余紀忠頒贈「小行星」緬懷

2023/11/01 中央通訊社
中央大學感念中國時報已故創辦人余紀忠對社會的貢獻，今天將編號 603200 的「余紀忠小行星」頒贈給余紀忠文教基金會董事長余範英，期許余紀忠的信念能繼續守護台灣。

中央大學今天發布新聞稿指出，中國時報已故創辦人余紀忠為中央大學傑出校友，非常關心且支持母校發展；中央大學在 1999 年頒授名譽文學博士學位給余紀忠，表彰其對社會、文化和國家的貢獻，並於 2008 年與余紀忠文教基金會共同成立「余紀忠講座」，邀請各領域學者擔任主講人。

中央大學今天在余紀忠講座中，舉行余紀忠小行星（Yuchichung）頒贈儀式，緬懷其一生以言論報國，為台灣當代民主自由的實踐，留下重要遺產。

余紀忠文教基金會董事長余範英表示，父親余紀忠一生以「政治民主、民族認同、穩定大局」為重要信念，前半生投筆從戎，報效國家，後半生創辦報紙，與時代相互書寫，感謝中央大學頒贈小行星以為感念，自己抬頭仰望星空時，得以和父親對話，內心很感動。

中央大學表示，從 2006 年開始的鹿林巡天計畫，除發現台灣史上第 1 顆彗星，還發現 800 多顆小行星，期許透過小行星的命名與頒贈，看見台灣更多可貴的價值；編號 603200 的余紀忠小行星，是在 2006 年 7 月 5 日由中央大學鹿林天文台台長林宏欽及美國馬里蘭大學的博士葉泉志共同發現，大小約 1 公里之間。

原文轉載自【2023-10-31/中央通訊社】

籌建中大鹿林天文台！葉永烜獲總統科學獎

2023/10/30 非凡新聞

浩瀚神秘的太空，讓人充滿好奇心想一探究竟！中研院院士葉永烜不僅是 NASA 卡西尼土星任務的發起者之一，也參與了台灣第一顆科學衛星任務，奠定我國太空科技發展的基礎，同時他也非常重視人才培養，希望能延攬國內外優秀年輕學者，為台灣天文教育更進一步，多項卓越貢獻，讓葉永烜榮獲 2023 總統科學獎的殊榮。

無人探測器「卡西尼號」，在 1997 年成功發射翱翔在土星上空，拍攝出大大小小的碎石顆粒，緊緊環繞在土星外圍，形成了一圈美麗又壯觀的碎石環，NASA 的卡西尼土星任務，由 3 位創議者進行研究，而其中一位就是來自台灣的中研院院士葉永烜。

中研院院士 葉永烜：「人類的社會是要用天象來解釋的，所以天文跟人文是有點像很緊密的。」

葉永烜院士是國際行星科學研究領導者，對於彗星物理學、行星動力學和衛星磁層相互作用等領域有開創性的貢獻，像是卡西尼土星任務，就提出了土星環大氣層及游離層的大氣模型和帶電粒子電磁層動力學作用的開創理論，並在土星環構造進行研究 。

中研院院士 葉永烜：「做科學家，你要做研究工作是很長很長的路，你看我就做了 50 年，中間一定有很多很多困難存在，一定要靠著硬性來克服的。」

葉永烜從美國返台定居後，成立臺灣太空科學聯盟，橋接產官學資訊交流合作，整合我國太空科技能力。

中研院院士 劉兆漢：「他在中央大學理學院院長任內，把台灣本土的天文真正提供好幾個檔次，未來我們人類去探測外層的太陽系的行星，比方說海王星、冥王星為的這個打的基礎。」

不只在學術界有成果，也無私的為社會貢獻，葉永烜籌建中央大學鹿林天文台，不僅成為國家級設施，也成功推動時域天文學，成為產出重大科學價值及太陽系研究的重要平台，同時，也向業界募款，設立「年輕 天文學者 講座」，希望能延攬過內外優秀年輕學者，一同推動台灣的天文教育。

中央大學天文所技士 張光祥：「我對葉老師最感動的就是說，他在推動台灣的一些基礎科學的建設不辭辛勞，他有想到就說，要怎麼給年輕人機會，還要怎麼建造台灣在高山上，最適合的地點建天文台，他都是領頭的帶著我們來做。」

葉永烜認為，人才培育非常重要，因此，他也投入 K-12 科教發掘特殊人才，希望能提升台灣的科學教育。

中研院院士 葉永烜：「我會覺得一個合理的教育應該是，每一個小孩子不管他的家境的條件，應該都在一個同樣的出發點，就是他能夠看到有給他機會，去看到一樣遠的地方去，不管你是大城市還是在鄉下地方。」

葉永烜院士為臺灣太空科學界持續貢獻心力，提升我國在天文領域的能見度及影響力，今年榮獲總統科學獎實至名歸，未來將持續培養更多頂尖人才，傳承這份榮譽。

本文轉載自【2023-10-27/非凡新聞】

2023 總統科學獎　中央大學葉永烜院士與傑出校友李文雄院士同台輝映

2023/10/27　ＴＵＮ大學網

中央大學天文研究所葉永烜院士與傑出校友李文雄院士今年雙雙榮獲「2023 總統科學獎」之肯定，10 月 24 日在總統府由總統蔡英文親自頒授表揚，肯定他

們的卓越貢獻。葉永烜院士以跨國界的高度，表達他的感念、隱憂和未來期許；李文雄院士則以跨領域的廣度，分享他學術生涯上三個關鍵性決定。

總統蔡英文表示，李文雄院士多年來跨領域探索生物演化的難題，並且提出前瞻的見解，為分子演化和生物遺傳學，持續開創新的研究方向。葉永烜院士則致力於太空科技及行星科學研究，除了多次參與國際合作的太空任務，更投入產官學的資訊交流合作及人才培育，提升臺灣的太空科技能力。

李文雄院士致詞時，分享學術生涯上三個關鍵性決定。他大學唸的是土木系，碩士班唸地球物理所，博士班攻讀應用數學。他在博士論文時決定將數學應用到生物學上，這是學術界少有人走的路，也是關鍵性的決定。其次，1979 年在 DNA 資料累積的年代，他全力以赴，所發表的論文被引用超過 4000 次，其中一篇 DNA 序列比較論文更推翻當代的主流觀點。他於 1989 年在中研院創立分子生物學研究室，將理論與實驗結合，進而發現人類與黑猩猩基因體的核苷酸序列只有相差 1.24%，引起很大的震撼。

李文雄院士 2003 年獲遺傳暨演化界最高榮譽「巴仁獎」，是亞裔第一人，也是第一位當選美國國家科學院士的華人演化學者，2006 年獲頒中央大學傑出校友。從一位農家子弟，到一位卓越的科學家，他說，「一個人的能力，比想像中多許多！」

葉永烜院士對於得獎充滿了感念之意。他感謝臺灣這塊土地，1948 年收容父母這一代，在戰亂之中得到重生機會。也感謝中央大學讓他在臺灣學術研究得以從新開始。25 年來，感謝國科會的支持，進行太陽系探索的基礎研究。實驗室的研究生已在準備 25 年後對天王星和海王星的探測，年輕一代，希望無窮！

面對科學教育的未來，他也提出隱憂。除小行星撞地球之外，人類社會在未來可能面臨四大危機，分別是大流行病、人工智慧的誤用、氣候變遷和世界大戰。他引用美國前總统羅斯福夫人 Eleanor Roosevelt 的話，「只說和平是不夠的，必須要相信和平；只相信和平是不夠的；必需要努力爭取和平。」台灣才能安居樂業，世界才能永續發展。

他最後呼籲，優秀人才是國家的棟樑，爭取國際頂尖人才，要有更宏觀的思維，其中也包括人道精神、公平正義和和平共處等國際公約。有些國家為了強大而拋棄這些價值，希望臺灣因為這些價值而強大！

中大葉永烜與傑出校友李文雄　總統科學獎同台輝映

2023/10/26 經濟日報

中央大學天文研究所葉永烜院士與傑出校友李文雄院士今年雙雙榮獲「2023 總統科學獎」肯定，昨(24)日在總統府由總統蔡英文頒授表揚，肯定他們的卓越貢獻。葉永烜以跨國界的高度，表達他的感念、隱憂和未來期許；李文雄則以跨領域的廣度，分享他學術生涯上三個關鍵性決定。

蔡總統表示，李文雄院士多年來跨領域探索生物演化的難題，並且提出前瞻的見解，為分子演化和生物遺傳學，持續開創新的研究方向。葉永烜院士則致力於太空科技及行星科學研究，除了多次參與國際合作的太空任務，更投入產官學的資訊交流合作及人才培育，提升臺灣的太空科技能力。

李文雄致詞時，分享學術生涯上三個關鍵性決定。他大學唸的是土木系，碩士班唸地球物理所，博士班攻讀應用數學。他在博士論文時決定將數學應用到生物學上，這是學術界少有人走的路，也是關鍵性的決定。其次，1979 年在 DNA 資料累積的年代，他全力以赴，所發表的論文被引用超過 4000 次，其中一篇 DNA 序列比較論文更推翻當代的主流觀點。他於 1989 年在中研院創立分子生物學研究室，將理論與實驗結合，進而發現人類與黑猩猩基因體的核苷酸序列只有相差 1.24%，引起很大的震撼。

李文雄 2003 年獲遺傳暨演化界最高榮譽「巴仁獎」，是亞裔第一人，也是第一位當選美國國家科學院士的華人演化學者，2006 年獲頒中央大學傑出校友。從一位農家子弟，到一位卓越的科學家，他說，「一個人的能力，比想像中多許多！」

葉永烜對於得獎充滿了感念之意。他感謝臺灣這塊土地，1948 年收容父母這一代，在戰亂之中得到重生機會。也感謝中央大學讓他在臺灣學術研究得以從新開始。25 年來，感謝國科會的支持，進行太陽系探索的基礎研究。實驗室的研究生已在準備 25 年後對天王星和海王星的探測，年輕一代，希望無窮！

面對科學教育的未來，他也提出隱憂。除小行星撞地球之外，人類社會在未來可能面臨四大危機，分別是大流行病、人工智慧的誤用、氣候變遷和世界大戰。他引用美國前總统羅斯福夫人 Eleanor Roosevelt 的話，「只說和平是不夠的，必須要相信和平；只相信和平是不夠的；必需要努力爭取和平。」台灣才能安居樂業，世界才能永續發展。

他最後呼籲，優秀人才是國家的棟樑，爭取國際頂尖人才，要有更宏觀的思維，其中也包括人道精神、公平正義和和平共處等國際公約。有些國家為了強大而拋棄這些價值，希望臺灣因為這些價值而強大！

原文轉載自【2023-10-25/經濟日報】

總統科學獎頒獎　表彰獲獎者傑出貢獻

2023/10/26 工商時報

李文雄院士專注於分子演化的研究，運用數學和統計分析專業，為許多演化生物學的難題提出前瞻見解。李院士針對分子演化的過程與機制，以及演化史與物種間的親緣關係開發創新計算工具，獲得學術界廣泛使用，加速相關研究的進展。他的研究率先發現分子時鐘速度取決於世代的長短，並開發出相應的統計方法，推翻當時主流觀點，打破過往認為 DNA 序列變化以恆速進行的觀念。

李院士及其團隊的研究成果，為分子演化和生物遺傳學領域帶來深遠的影響；不僅推動「分子時鐘理論」的應用，在遺傳性別差異、人類演化及病毒演化等領域持續不懈創新研究方向，更是首位榮獲遺傳與演化學最高榮譽—「巴仁獎」的亞裔學者。

胡正明院士：發明鰭式電晶體 克服半導體物理極限

胡正明院士的科學研究成果極為傑出豐碩，他領導研究團隊於 1999 年成功開發「鰭式電晶體」（FinFET），改善晶片過熱與微型化問題，將半導體製程帶入新境界，獲國際電機電子工程學會（IEEE）譽為「微電子領航者」。

胡院士於加州大學柏克萊分校任教長達四十餘年，出版過五本半導體教科書，發表研究論文超過 1,000 篇，獲得 150 項美國專利，其在學術教育上的傑出成就與貢獻，獲得 IEEE 教育獎、SRC 亞里士多德獎、柏克萊傑出教學獎的肯定。2001 年他回臺擔任台積電首任技術長，領導研發團隊持續發表領先全球的 FinFET 原型，並及早部署 FinFET 技術與專利，奠定臺灣半導體產業在國際上的領先地位。

葉永烜院士：領導多項國際太空任務 推動臺灣行星科學研究

葉永烜院士為彗星物理學、行星動力學、衛星與磁層之間相互作用等領域的知名科學家，他發表的研究論文超過 500 篇，其中有 60 餘篇刊登於《自然》和《科學》等國際頂尖期刊上，為人類瞭解太陽系和行星起源提供珍貴資料。

葉院士是歐洲太空總署(ESA)和美國國家航空暨太空總署(NASA)合作「卡西尼-惠更斯號計畫」的主要創議者之一。於 1998 年回臺定居並任教於中央大學，推動臺灣行星科學研究發展，帶領研究團隊在土衛二的噴氣中發現含有大量的水氣，讓人類得以進一步認識土星系統，探索外星宜居環境的可能性及生命起源，為臺灣的太空科技發展奠定堅實基礎。

科學研究的先驅及標竿 嘉惠臺灣社會及全球產業

本屆三位獲獎者在專業領域投注畢生心血締造豐碩成果，不只嘉惠學術界，更在社會與全球產業帶來龐大貢獻。三位獲獎者培育許多專業科研人才，將科學研究成果涓滴無私地傳遞給年輕研究者，讓臺灣的科技實力持續在國際間發光發熱，獲獎實至名歸。

原文轉載自【2023-10-25/工商時報】

2023 總統科學獎　中央大學葉永烜院士與傑出校友李文雄院士同台輝映

2023/10/26 蕃薯藤
中央大學天文研究所葉永烜院士與傑出校友李文雄院士今年雙雙榮獲「2023 總統科學獎」之肯定，10 月 24 日在總統府由總統蔡英文親自頒授表揚，肯定他們的卓越貢獻。葉永烜院士以跨國界的高度，表達他的感念、隱憂和未來期許；李文雄院士則以跨領域的廣度，分享他學術生涯上三個關鍵性決定。

總統蔡英文表示，李文雄院士多年來跨領域探索生物演化的難題，並且提出前瞻的見解，為分子演化和生物遺傳學，持續開創新的研究方向。葉永烜院士則致力於太空科技及行星科學研究，除了多次參與國際合作的太空任務，更投入產官學的資訊交流合作及人才培育，提升臺灣的太空科技能力。

李文雄院士致詞時，分享學術生涯上三個關鍵性決定。他大學唸的是土木系，碩士班唸地球物理所，博士班攻讀應用數學。他在博士論文時決定將數學應用到生物學上，這是學術界少有人走的路，也是關鍵性的決定。其次，1979 年在 DNA 資料累積的年代，他全力以赴，所發表的論文被引用超過 4000 次，其中一篇 DNA 序列比較論文更推翻當代的主流觀點。他於 1989 年在中研院創立分子生物學研究室，將理論與實驗結合，進而發現人類與黑猩猩基因體的核苷酸序列只有相差 1.24%，引起很大的震撼。

李文雄院士 2003 年獲遺傳暨演化界最高榮譽「巴仁獎」，是亞裔第一人，也是第一位當選美國國家科學院士的華人演化學者，2006 年獲頒中央大學傑出校友。從一位農家子弟，到一位卓越的科學家，他說，「一個人的能力，比想像中多許多！」

葉永烜院士對於得獎充滿了感念之意。他感謝臺灣這塊土地，1948 年收容父母這一代，在戰亂之中得到重生機會。也感謝中央大學讓他在臺灣學術研究得以從新開始。25 年來，感謝國科會的支持，進行太陽系探索的基礎研究。實驗室的研究生已在準備 25 年後對天王星和海王星的探測，年輕一代，希望無窮！

面對科學教育的未來，他也提出隱憂。除小行星撞地球之外，人類社會在未來可能面臨四大危機，分別是大流行病、人工智慧的誤用、氣候變遷和世界大戰。他引用美國前總統羅斯福夫人 Eleanor Roosevelt 的話，「只說和平是不夠的，必須要相信和平；只相信和平是不夠的；必需要努力爭取和平。」台灣才能安居樂業，世界才能永續發展。

他最後呼籲，優秀人才是國家的棟樑，爭取國際頂尖人才，要有更宏觀的思維，其中也包括人道精神、公平正義和和平共處等國際公約。有些國家為了強大而拋棄這些價值，希望臺灣因為這些價值而強大！

原文轉載自【2023-10-25/蕃薯藤】

獲 2023 總統科學獎　中央大學葉永烜憂人類將面臨四大危機

2023/10/26 今日新聞
中央大學天文研究所葉永烜院士與傑出校友李文雄院士今年雙雙榮獲「2023 總統科學獎」肯定，昨（24）日在總統府由總統蔡英文親自頒授表揚，肯定他們的卓越貢獻。葉永烜以跨國界的高度，表達他的感念、隱憂和未來期許，他提出除小行星撞地球之外，人類社會在未來可能面臨四大危機，分別是大流行病、人工智慧的誤用、氣候變遷和世界大戰；李文雄院士則以跨領域的廣度，分享他學術生涯上三個關鍵性決定。

蔡英文表示，李文雄院士多年來跨領域探索生物演化的難題，並且提出前瞻的見解，為分子演化和生物遺傳學，持續開創新的研究方向。葉永烜院士則致力於太空科技及行星科學研究，除了多次參與國際合作的太空任務，更投入產官學的資訊交流合作及人才培育，提升臺灣的太空科技能力。

李文雄院士致詞時，分享學術生涯上三個關鍵性決定。他大學唸的是土木系，碩士班唸地球物理所，博士班攻讀應用數學。他在博士論文時決定將數學應用到生物學上，這是學術界少有人走的路，也是關鍵性的決定。其次，1979 年在 DNA 資料累積的年代，他全力以赴，所發表的論文被引用超過 4000 次，其中一篇 DNA 序列比較論文更推翻當代的主流觀點。他於 1989 年在中研院創立分子生物學研究室，將理論與實驗結合，進而發現人類與黑猩猩基因體的核苷酸序列只有相差 1.24%，引起很大的震撼。

李文雄院士 2003 年獲遺傳暨演化界最高榮譽「巴仁獎」，是亞裔第一人，也是第一位當選美國國家科學院士的華人演化學者，2006 年獲頒中央大學傑出校

友。從一位農家子弟，到一位卓越的科學家，他說，「一個人的能力，比想像中多許多！」

葉永烜對於得獎充滿了感念之意，他感謝臺灣這塊土地，1948 年收容父母這一代，在戰亂之中得到重生機會。也感謝中央大學讓他在臺灣學術研究得以從新開始。25 年來，感謝國科會的支持，進行太陽系探索的基礎研究。實驗室的研究生已在準備 25 年後對天王星和海王星的探測，年輕一代，希望無窮！

面對科學教育的未來，葉永烜也提出隱憂。除小行星撞地球之外，人類社會在未來可能面臨四大危機，分別是大流行病、人工智慧的誤用、氣候變遷和世界大戰。他引用美國前總統羅斯福夫人 Eleanor Roosevelt 的話，「只說和平是不夠的，必須要相信和平；只相信和平是不夠的；必需要努力爭取和平。」台灣才能安居樂業，世界才能永續發展。

他最後呼籲，優秀人才是國家的棟樑，爭取國際頂尖人才，要有更宏觀的思維，其中也包括人道精神、公平正義和和平共處等國際公約。有些國家為了強大而拋棄這些價值，希望臺灣因為這些價值而強大！

原文轉載自【2023-10-25/今日新聞】

雙喜臨門！中大教授葉永烜與傑出校友李文雄榮獲「總統科學獎」

2023/09/19 工商時報

中央大學今天表示，天文研究所暨太空科學與工程學系教授葉永烜、傑出校友李文雄分別是今年總統科學獎「數理科學組」、「生命科學組」得主。今年總統科學獎共選出 3 位得獎人，預定於 10 月 24 日舉行頒獎典禮，將由總統親自頒獎。

葉永烜是國際行星科學研究領導者，對於彗星物理學、行星動力學和衛星-磁層相互作用等領域，有開創性的貢獻。他推動亞洲大洋洲地球科學發展，成立亞洲大洋洲地球科學學會 (AOGS) 並擔任第一屆會長，促成國際合作，同時開啟台灣行星科學研究先河及時域天文學發展，對小行星觀測新發現有重大貢獻。

葉永烜籌建中央大學鹿林天文台，推動時域天文學，成為產出重大科學價值國際合作及太陽系研究亮點的重要平台。他對人才培育更是不遺餘力，推動中央大學與台達電子文教基金會共同設立「年輕天文學者講座」，延攬國外優秀年輕

學者推動台灣天文教育推廣。

李文雄是中央大學第二屆傑出校友，在分子演化的學術研究有卓越的貢獻並享有國際名望。尤其在 RNA 病毒演化的研究上有重要的貢獻，他的研究有助於了解病毒如何演化成為更有傳播性的病媒，解釋人類大流行病為何大多由 RNA 病毒所引起。

另外李文雄的團隊也發現，靈長類祖先的 ACE2 與新冠病毒的 S-protein 結合力很弱，但 ACE2 在人類與舊世界猴子的共同祖先發生了一個突變，大幅增加 ACE2 與 S-protein 的結合力，致使人類容易被新冠病毒感染。

李文雄指導過超過 120 名的博士後和博士生，其中有多位在學術界上扮演要角。他所領導中央研究院生物多樣性研究，建立學程招募國際研究生，厚實國內研究動能，拓展台灣在相關領域的國際知名度。除培育優秀人才之外，並網羅國際人才，引進微生物多樣性、生物資訊與基因體等領域研究。

本文轉載自【2023-09-19/工商時報】

雙喜臨門！中大教授葉永烜與傑出校友李文雄榮獲「總統科學獎」

2023/09/19 中時新聞網

中央大學今天表示，天文研究所暨太空科學與工程學系教授葉永烜、傑出校友李文雄分別是今年總統科學獎「數理科學組」、「生命科學組」得主。今年總統科學獎共選出 3 位得獎人，預定於 10 月 24 日舉行頒獎典禮，將由總統親自頒獎。

葉永烜是國際行星科學研究領導者，對於彗星物理學、行星動力學和衛星-磁層相互作用等領域，有開創性的貢獻。他推動亞洲大洋洲地球科學發展，成立亞洲大洋洲地球科學學會 (AOGS) 並擔任第一屆會長，促成國際合作，同時開啟台灣行星科學研究先河及時域天文學發展，對小行星觀測新發現有重大貢獻。

葉永烜籌建中央大學鹿林天文台，推動時域天文學，成為產出重大科學價值國際合作及太陽系研究亮點的重要平台。他對人才培育更是不遺餘力，推動中央大學與台達電子文教基金會共同設立「年輕天文學者講座」，延攬國外優秀年輕學者推動台灣天文教育推廣。

李文雄是中央大學第二屆傑出校友，在分子演化的學術研究有卓越的貢獻並享

有國際名望。尤其在 RNA 病毒演化的研究上有重要的貢獻，他的研究有助於了解病毒如何演化成為更有傳播性的病媒，解釋人類大流行病為何大多由 RNA 病毒所引起。

另外李文雄的團隊也發現，靈長類祖先的 ACE2 與新冠病毒的 S-protein 結合力很弱，但 ACE2 在人類與舊世界猴子的共同祖先發生了一個突變，大幅增加 ACE2 與 S-protein 的結合力，致使人類容易被新冠病毒感染。

李文雄指導過超過 120 名的博士後和博士生，其中有多位在學術界上扮演要角。他所領導中央研究院生物多樣性研究，建立學程招募國際研究生，厚實國內研究動能，拓展台灣在相關領域的國際知名度。除培育優秀人才之外，並網羅國際人才，引進微生物多樣性、生物資訊與基因體等領域研究。

本文轉載自【2023-09-19/中時新聞網】

雙喜臨門！中大院士、傑出校友榮獲總統科學獎

2023/09/19 中華新聞雲
「總統科學獎」之設立，以提升臺灣在國際學術界之地位為宗旨，尤以對臺灣社會有重大貢獻之基礎學術研究人才。中央大學(十八)日表示，中央大學天文研究所暨太空科學與工程學系葉永烜院士榮膺「數理科學組」得主，傑出校友李文雄院士則為「生命科學組」得主。本次共遴選出三位得獎人，將由總統親自頒獎，以表彰其傑出榮譽。

中央大學葉永烜院士是國際行星科學研究領導者，他推動亞洲大洋洲地球科學發展，並籌建中央大學鹿林天文台，推動時域天文學，成為產出重大科學價值國際合作及太陽系研究亮點的重要平台。推動中央大學與台達電子文教基金會共同設立「年輕天文學者講座」，延攬國外優秀年輕學者推動臺灣天文教育推廣。

李文雄院士是中央大學第二屆傑出校友，在分子演化的學術研究有卓越的貢獻並享有國際名望。尤其在ＲＮＡ病毒演化的研究上有重要的貢獻。另外他們團隊也發現，靈長類祖先的ＡＣＥ２與新冠病毒的 S-protein 結合力很弱，但ＡＣＥ２在人類與舊世界猴子的共同祖先發生了一個突變，大幅增加ＡＣＥ２與 S-protein 的結合力，致使人類容易被新冠病毒感染。

李院士已指導過超過一百二十名的博士後和博士生，除培育優秀人才之外，並網羅國際人才，引進微生物多樣性、生物資訊與基因體等領域研究。他亦創建

基因體高通量定序核心設施，並對外提供服務，促進我國基因體及生物科技研究。

本文轉載自【2023-09-19/中華新聞雲】

三院士獲總統科學獎兩人出自中央大學

2023/09/19 人間福報

【記者曾博群綜合報導】2022-2023 年總統科學獎共有 3 人獲殊榮，中央大學天文研究所暨太空科學與工程學系葉永烜院士獲得「數理科學組」得主，傑出校友李文雄院士為「生命科學組」得主，中大表示，兩人不僅研究傑出卓越，對提升我國學術聲譽，有深遠的影響。

葉永烜是國際行星科學研究領導者，對於彗星物理學、行星動力學和衛星-磁層相互作用等領域，有開創性的貢獻。中大表示，他推動亞洲大洋洲地球科學發展，促成國際合作，大幅提高亞太地區研究能見度。同時開啟台灣行星科學研究先河及時域天文學發展，對小行星觀測新發現有重大貢獻。

此外，葉永烜籌建中央大學鹿林天文台，推動時域天文學，成為產出重大科學價值國際合作及太陽系研究亮點的重要平台。中大表示，他對人才培育不遺餘力，推動中央大學與台達電子文教基金會共同設立「年輕天文學者講座」，延攬國外優秀年輕學者推動台灣天文教育推廣，並投入 K-12 科教發掘特殊人才。

李文雄在分子演化的學術研究有卓越的貢獻並享有國際名望，尤其在 RNA 病毒演化的研究上有重要貢獻，有助於了解病毒如何演化成為更有傳播性的病媒，解釋人類大流行病為何大多由 RNA 病毒所引起。另外，團隊也發現，人類與舊世界猴子的共同祖先發生突變，致使人類容易被新冠病毒感染。

李文雄指導超過 120 名博士後和博士生，所領導的中央研究院生物多樣性研究，建立學程招募國際研究生，厚實國內研究動能，並網羅國際人才，引進微生物多樣性、生物資訊與基因體等領域研究，亦創建基因體高通量定序核心設施，促進我國基因體及生物科技研究。

本文轉載自【2023-09-19/人間福報】

中央大學葉永烜院士與傑出校友李文雄院士榮獲「總統科學獎」

2023/09/19 Yahoo!新聞

象徵我國最高科學榮譽的「總統科學獎」揭曉，中央大學天文研究所暨太空科學與工程學系葉永烜院士榮膺「數理科學組」得主，傑出校友李文雄院士則為「生命科學組」得主。中央大學表示，他們不僅研究傑出卓越，對提升臺灣學術聲譽及國際競爭力，以及增進人類生活福祉更有深遠的影響。

中央大學葉永烜院士是國際行星科學研究領導者，對於彗星物理學、行星動力學和衛星-磁層相互作用等領域，有開創性的貢獻。他推動亞洲大洋洲地球科學發展，成立亞洲大洋洲地球科學學會 (AOGS) 並擔任第一屆會長，促成國際合作，大幅提高亞太地區研究能見度。同時開啟臺灣行星科學研究先河及時域天文學發展，對小行星觀測新發現有重大貢獻。

葉院士推動多項跨國研究計畫，提升臺灣國際能見度及影響力。並籌建中央大學鹿林天文台，推動時域天文學，成為產出重大科學價值國際合作及太陽系研究亮點的重要平台。他對人才培育更是不遺餘力，推動中央大學與台達電子文教基金會共同設立「年輕天文學者講座」，延攬國外優秀年輕學者推動臺灣天文教育推廣。作育英才，桃李滿門，並投入 K-12 科教發掘特殊人才。

李文雄院士是中央大學第二屆傑出校友，在分子演化的學術研究有卓越的貢獻並享有國際名望。尤其在 RNA 病毒演化的研究上有重要的貢獻，他的研究有助於了解病毒如何演化成為更有傳播性的病媒，解釋人類大流行病為何大多由 RNA 病毒所引起。另外他們團隊也發現，靈長類祖先的 ACE2 與新冠病毒的 S-protein 結合力很弱，但 ACE2 在人類與舊世界猴子的共同祖先發生了一個突變，大幅增加 ACE2 與 S-protein 的結合力，致使人類容易被新冠病毒感染。

李院士已指導過超過 120 名的博士後和博士生，其中有多位在學術界上扮演要角。他所領導中央研究院生物多樣性研究，建立學程招募國際研究生，厚實國內研究動能，拓展臺灣在相關領域的國際知名度。除培育優秀人才之外，並網羅國際人才，引進微生物多樣性、生物資訊與基因體等領域研究。他亦創建基因體高通量定序核心設施，並對外提供服務，促進我國基因體及生物科技研究。

「總統科學獎」的設立，以提升臺灣在國際學術界之地位為宗旨，尤以對臺灣社會有重大貢獻的基礎學術研究人才。本次共遴選出 3 位得獎人，預定於 10 月 24 號舉行頒獎典禮，將由總統親自頒獎，表彰傑出榮譽。

本文轉載自【2023-09-19/Yahoo!新聞】

葉永烜、李文雄、胡正明 3 院士獲總統科學獎

2023/09/19 自由時報

〔記者蘇永耀／台北報導〕總統科學獎委員會今（15）日公布「2022-2023 年總統科學獎」得獎名單，共 3 位得獎人獲得此殊榮，分別為「數理科學組」葉永烜院士、「生命科學組」李文雄院士及「應用科學組」胡正明院士。

總統府指出，今年膺選的總統科學獎得獎人葉永烜院士、李文雄院士及胡正明院士，分別長期深耕數理科學、生命科學、應用科學等專業領域，並不斷進行科學創新突破，成果豐碩，成就非凡。每位得獎人的科學成就及重要貢獻，不僅提升台灣學術聲譽及國際競爭力，對於增進人類生活福祉更有深遠的影響，實為台灣學術界的最高典範。

中央大學天文所及太空科學所-國鼎講座教授葉永烜，在學術貢獻上是國際行星科學研究領導者，對於彗星物理學、行星動力學和衛星-磁層相互作用等領域，有開創性的貢獻，在社會貢獻上則成功建立、推動及參與多項跨國研究計畫，提升台灣國際能見度及影響力。

中研院生物多樣性研究中心特聘研究員李文雄，在學術貢獻上對分子演化的學術研究有卓越的貢獻並享有國際名望，並在 RNA 病毒演化的研究，於此次新冠肺炎疫情扮演重要角色，社會貢獻上則領導中研院生物多樣性研究，厚實國內研究動能，拓展台灣在相關領域的國際知名度。

國立陽明交通大學終身講座教授胡正明，在學術貢獻上為 1990 年代末發明了 FinFET 電晶體。FinFET 的設計解決了傳統平面晶體管的許多限制，這發明在電晶體設計上取得了重大突破，為未來半導體技術的進一步發展奠定了基礎。社會貢獻上則透過這項發明而對全球積體電路技術產生影響，且帶領台灣半導體產業維持領先優勢。

總統科學獎的設立，是以提升台灣在國際學術界之地位為宗旨，並獎勵數理科學、生命科學、社會科學及應用科學領域在國際學術研究上具創新性且貢獻卓著之學者，尤以對台灣社會有重大貢獻之基礎學術研究人才為優先獎勵對象。

依照《總統科學獎遴選要點》規定，總統科學獎委員會由中央研究院院長擔任召集人，國家科學及技術委員會主任委員擔任副召集人，共由 15 位委員組成。本獎項自民國 90 年開始舉辦，每兩年頒發一屆，是我國最高榮譽之科學研究獎項。

總統科學獎委員會表示，本屆總統科學獎共計收到 20 件提名案，經各遴選小組進行審查，以及總統科學獎委員會聯席會議討論票選後，計遴選出 3 位得獎人

提報總統府核定表揚。

為表彰得獎人之貢獻，預定於 10 月 24 日舉行頒獎典禮，將由總統親自頒發獎狀 1 幀、獎座 1 座及獎金新台幣 200 萬元。

本文轉載自【2023-09-19/自由時報】

好壯觀！8/13 英仙座流星雨　觀測條件極佳每小時近 100 顆

2023/08/11　中廣新聞網
8 月 13 日是英仙座流星雨極大期、高峰期，中央大學天文所博士後研究員林忠義表示，喜愛天文的天文迷可以找一處遠離城市、燈光黑暗，場域較為開闊的安全區域，以躺、臥方式觀看。每小時可達近 100 顆流星，千萬不要錯過觀賞機會。(李明朝報導)

北半球三大流星雨之一的英仙座流星，從 7 月中旬到 8 月底，都是屬於英仙座流星雨的活躍期。中大天文所博士後研究員林忠義表示，英仙座流星的高峰期，預計在 8 月 13 日，就在新月前 3 天，觀測條件極佳，估計每小時天頂流星數（ZHR）可達 100 顆左右，想看滿天流星劃過天際的朋友千萬別錯過。

外界好奇英仙座流星雨從哪裡來？，林忠義表示，流星雨是由流星體以極高的速度進入地球大氣層引起的。由於透視的影響，流星幾乎是從天空中的同一點（稱輻射點）出來的，但實際上它們以平行的軌跡運動。每個流星雨幾乎都有一個母體，對於英仙座流星雨來說，其母體視來自一顆編號 109 號周期彗星－史威伕-塔托彗星(109P/Swift-Tuttle)。

這次要如何觀賞英仙座流星雨？林忠義表示，英仙座流星雨的輻射點位於英仙座，但要看到流星不需要找到輻射點，因為流星會在整個天空中以許多不同的方向飛行。因此近日或者當天，可以找一個遠離城市燈光黑暗、場域開闊的安全區域，以躺、臥方式觀看。英仙座流星雨以明亮等聞名，縱使處在光害的城市區域也有機會看到流星。

原文轉載自【2023-08-10/中廣新聞網】

天上的「台灣」現蹤　台北天文館捕捉到與礁湖星雲同框

2023/07/10　自由時報

台灣是在地球上小而美的國家，但民眾不知道的是，在天上也有著一顆與台灣同名的小行星，台北市立天文科學教育館表示，近期館方在「台灣」小行星最

接近地球時捕捉到其蹤跡，且恰巧與夏季夜空中相當美麗而知名的「礁湖星雲」同框，提醒民眾兩者將在 9 月下旬再次相遇，要是錯過就要再等 14 年。

台北市立天文館介紹，編號 2169 的「台灣」，位於火星與木星間的小行星帶中，以約 4.7 年的週期環繞台灣運行，其直徑僅約 14 至 19 公里，目前亮度接近 17 等，比肉眼可見極限還暗約 1 萬 6000 倍，黯淡到只有大望遠鏡才能看見，即使 6 月底至 7 月初「台灣」最接近地球，但兩者仍有 2.86 億公里的距離。

天文館表示，由於地球軌道位在「台灣」內側，所以會如「彎道超車」般超前小行星，使小行星出現看似後退的「逆行」現象，而「台灣」目前正在與地球最接近的位置附近，並將以「逆行」方式穿越人馬座中美麗的「礁湖星雲」，6 日凌晨，館方設置在中央大學天文所鹿林天文台的遙控望遠鏡，即捕捉到兩者同框的難得美景。

天文館介紹，「礁湖星雲」在光害稀少的環境中用雙筒望遠鏡即可輕易看見，也是天文攝影中最常拍攝的目標之一，「台灣」今年將兩度穿越「礁湖星雲」，一次在 7 月上旬以逆行穿越，另一次則在 9 月下旬以順行通過，要是錯過，「台灣」下次再與礁湖星雲相遇，要等到 14 年後的 2037 年 9 月。

本文轉載自【2023-07-08/自由時報】

「台灣小行星」同框礁湖星雲　錯過再等 14 年

2023/07/10 中時新聞網

大家知道天上有顆以「台灣」為名的小行星嗎？這顆編號 2169 的小行星現正位於最接近地球的位置，並將「逆行」穿越人馬座中美麗的礁湖星雲。北市天文館表示，7 月 6 日凌晨以設置於中央大學天文所鹿林天文臺的遙控望遠鏡，捕捉兩者同框的難得美景，與民眾分享在地球外的另個台灣。

天文館表示，台灣小行星位於火星與木星間的主小行星帶中，以約 4.7 年的週期環繞太陽運行，直徑僅約 14 至 19 公里，目前的亮度接近 17 等，比肉眼可見極限還暗約 1.6 萬倍，即使在 6 月底至 7 月初最接近地球的這段時間，也有 2.86 億公里之遙。

天文館也說，由於地球軌道位在台灣小行星內側，所以會如彎道超車般超前小

行星，使小行星出現看似後退的逆行現象。特別的是，台灣小行星今年將兩度穿越夏季夜空中知名的礁湖星雲，一次在 7 月上旬以逆行穿越，另一次則在 9 月下旬以順行通過，而台灣小行星下次再與礁湖星雲相遇，要等到 14 年後的 2037 年 9 月了。

天文館補充，礁湖星雲是夏季夜空中相當美麗而知名的天體，在光害稀少的環境中用雙筒望遠鏡即可輕易看見，也是天文攝影中最常拍攝的目標之一，不過台灣小行星則黯淡到只有大望遠鏡才能得見了。

本文轉載自【2023-07-08/中時新聞網】

地球以外的「台灣小行星」　7 月同框夏季礁湖星雲

2023/07/10 聯合新聞網

星空中，有一顆以「台灣」為名、編號 2169 的小行星，7 月正處於地球最接近的位置附近，更將「逆行」穿越人馬座中美麗的礁湖星雲。台北天文館說，設置在中央大學天文所鹿林天文台的遙控望遠鏡，7 月 6 日凌晨捕捉到兩者同框的難得美景，今年 9 月還能再見到此景，錯過就得再等 14 年。

天文館表示，台灣小行星位在火星與木星間的主小行星帶中，以約 4.7 年的周期環繞太陽運行，直徑僅約 14 至 19 公里，目前的亮度接近 17 等，比肉眼可見極限還暗約 1 萬 6 千倍，即使最接近地球的 6 月底至 7 月初期間，仍有 2.86 億公里之遙。

館方指出，地球軌道位在台灣小行星內側，所以會如「彎道超車」般超前小行星，使小行星出現看似後退的「逆行」現象。

特別的是，台灣小行星今年將 2 度穿越夏季夜空中知名的「礁湖星雲」，分別於 7 月上旬逆行穿越、9 月下旬順行通過，至於台灣小行星與礁湖星雲下次相遇，得等到 14 年後的 2037 年 9 月。

天文館分享，礁湖星雲是夏季夜空中相當美麗且知名的天體，在光害稀少的環境中，民眾用雙筒望遠鏡即可輕易看見，也是天文攝影中最常拍攝的目標之一。不過，台灣小行星則黯淡到只有大望遠鏡才能看見。

本文轉載自【2023-07-08/聯合新聞網】

位在地球外的台灣　北市天文館拍到台灣小行星與礁湖星雲浪漫邂逅

2023/07/10 Yahoo!新聞

全台天文愛好者有福了！這個夏天，將有機會欣賞到一場天上的浪漫邂逅，那就是以「台灣」為名的小行星與美麗的礁湖星雲的相會。台北天文館已經在七月六日凌晨，利用中央大學天文所鹿林天文台的遙控望遠鏡，拍攝到這兩個天體同框的難得畫面，並且公開分享給大家。

北市天文館指出，台灣小行星是一顆位於火星與木星間的主小行星帶中的小行星，編號二一六九，直徑約十四至十九公里，以約四點七年的週期環繞太陽運行。由於地球軌道位在台灣小行星內側，所以每當地球超越小行星時，小行星就會出現看似後退的「逆行」現象。

今年七月上旬和九月下旬，台灣小行星將分別以逆行和順行的方式穿越人馬座中的礁湖星雲，而下次要再見到台灣小行星再與礁湖星雲相遇的景象，則是要等到十四年後的二０三七年九月了。

天文館表示，礁湖星雲是一個由數千顆恆星組成的開放星團，也是夏季夜空中最美麗而知名的天體之一，在光害較少的地方，用雙筒望遠鏡就可以看見它的輝煌。不過，要看見台灣小行星，就需要大型望遠鏡和相機了，因為它現在的亮度只有一七等，比肉眼可見極限還暗約一萬六千倍。即使如此，它仍然是我們在地球以外的另一個台灣，值得全台關注和驕傲。

本文轉載自【2023-07-07/Yahoo!新聞】

2023 桃園天文嘉年華活動開跑　七天活動精彩不斷

2023/07/04 台灣民眾電子報

為鼓勵民眾積極參與天文科學教育，臺灣科學特殊人才提升計畫於 7 月 1 日至 7 月 7 日，在中央大學舉辦為期七天的「2023 桃園天文嘉年華」。以中央大學天文台為基地，由教育部及桃園市政府教育局指導，協同臺北市立天文科學教育館等單位共同舉辦。期望桃園能引領風騷，成為台灣天文教育的先鋒。

天文是對 3 歲的幼兒到 80 歲以上的長者，啟發科學興趣的最佳工具，因此臺灣科學特殊人才提升計畫規劃全民天文教育「AE4ALL」（Astronomy Education for All），透過中大天文所的設備和教學資源，結合全國各個天文教育團隊的力

量，舉辦「桃園天文嘉年華」增強臺灣的天文科學教育。

「2023 桃園天文嘉年華」7 月 1 日舉行開幕式，由葉永烜院士主講的科普講座「威廉的天空」開啟序幕，「天文故事館」則是藉由生動的故事引導兒童深入探索天文的奧秘。「摺紙天文學」的活動更引起了廣大的關注。這項特別活動獲得了日本摺紙大師西川誠司的授權，並由台灣摺紙協會的李政憲老師和連崇馨老師帶領學員一起親手摺製天文望遠鏡。進行活動的過程中，充滿了歡笑和探索的樂趣。活動不僅讓學員對天文有了更深入的理解，而且還巧妙地將科學與藝術結合在一起，為參與者帶來了全新的學習體驗。

活動連續七天不間斷，每日都有來自國內天文科學領域的專家進行不同主題的科普演講，還有「行動天文館」、「系外行星展」兩大展覽供一般民眾參觀；或是以兒童為對象的「天文故事館」，開放學齡前與小學生投稿的「天文繪畫比賽」；另外還有從實踐與觀測中學習的寶貴機會，例如透過摺紙理解科學原理的「摺紙天文學」、模擬彗星組成與撞擊的「科學實驗」，或是讓學生實際操作天文望遠鏡的「大學生夜間天文觀測」以及「太陽及太空天氣觀測」，帶給民眾豐富天文知識。

臺灣科學特殊人才提升計畫所籌畫的全民天文教育致力以不同的方式向大眾表現天文之美，期望透過多樣的活動，啟發學生對天文領域的興趣與認識。詳細活動介紹可至相關網站查詢，歡迎民眾到現場一同參與，在中大探索天文的奧妙！

本文轉載自【2023-07-03/台灣民眾電子報】

桃市暑期辦天文嘉年華

2023/07/04 國語日報

桃園市教育局規畫於今年暑假，在國立中央大學辦理「桃園天文嘉年華」，提供高中、國中及國小各十校，每校三十個名額參加，從活動中了解天文知識，體驗宇宙的奧祕。

桃園市教育局國小教育科候用校長孫俊國說，活動安排在七月十一日至十五日，提供三十所中小學、九百名學生參加；另外，也舉辦相關的教師研習活動。

本文轉載自【2023-07-03/國語日報】

探索天文別錯過　2023 桃園天文嘉年華等你來

2023/07/04 中國廣播公司

到底有沒有外星人、行星中有無生命跡象？為了讓民眾瞭解太空、天文，中央大學推動臺灣科學特殊人才提升計畫，舉辦「2023 桃園天文嘉年華」活動，除了科普演講、「行動天文館」、「系外行星展」展覽、還有以兒童為對象的「天文故事館」、及「大學生夜間天文觀測」啟發學生對天文領域的興趣與認識。（李明朝報導）

暑假來臨，中央大學正在舉辦一場「2023 桃園天文嘉年華」，中大天文所表示，嘉年華活動，是由臺灣科學特殊人才提升計畫所籌畫的全民天文教育，以中央大學天文研究所為基地，由教育部及桃園市政府教育局指導，協同臺北市立天文科學教育館、台灣儀器科技研究中心、嘉義市天文協會、及中華民國天文學會合作。

2023 桃園天文嘉年華活動內容多元、豐富。中研院院士、中央大學天文研究所教授葉永烜說，今年天文嘉年華，有個很特別的地方就是跟大家介紹系外行星，就是在太陽系外，發現很多很多行星，科學家、天文學家想探索這些系外行星裏，有沒有適合生命存在的星體，拿來跟太陽系、地球做比較。

活動除了安排主題科普演講，還有「行動天文館」、「系外行星展」供一般民眾參觀，或是以兒童為對象的「天文故事館」，以及開放學齡前與小學生投稿的「天文繪畫比賽」；另外還有從實踐與觀測中學習的寶貴機會，例如透過摺紙理解科學原理的「摺紙天文學」、模擬彗星組成與撞擊的「科學實驗」，或是讓學生實際操作天文望遠鏡的「大學生夜間天文觀測」以及「太陽及太空天氣觀測」，啟發學生對天文領域的興趣與認識。

本文轉載自【2023-07-03/中國廣播公司】

桃園天文嘉年華活動開跑　七天活動精彩不斷

2023/07/04 理財周刊

為鼓勵民眾積極參與天文科學教育，臺灣科學特殊人才提升計畫於 7 月 1 日至 7 月 7 日，在中央大學舉辦為期七天的「2023 桃園天文嘉年華」。以中央大學天文台為基地，由教育部及桃園市政府教育局指導，協同臺北市立天文科學教育館等單位共同舉辦。期望桃園能引領風騷，成為台灣天文教育的先鋒。

天文是對 3 歲的幼兒到 80 歲以上的長者，啟發科學興趣的最佳工具，因此臺灣科學特殊人才提升計畫規劃全民天文教育「AE4ALL」（Astronomy Education for All），透過中大天文所的設備和教學資源，結合全國各個天文教育團隊的力量，舉辦「桃園天文嘉年華」增強臺灣的天文科學教育。

「2023 桃園天文嘉年華」7 月 1 日舉行開幕式，由葉永烜院士主講的科普講座「威廉的天空」開啟序幕，「天文故事館」則是藉由生動的故事引導兒童深入探索天文的奧秘。「摺紙天文學」的活動更引起了廣大的關注。這項特別活動獲得了日本摺紙大師西川誠司的授權，並由台灣摺紙協會的李政憲老師和連崇馨老師帶領學員一起親手摺製天文望遠鏡。進行活動的過程中，充滿了歡笑和探索的樂趣。活動不僅讓學員對天文有了更深入的理解，而且還巧妙地將科學與藝術結合在一起，為參與者帶來了全新的學習體驗。

活動連續七天不間斷，每日都有來自國內天文科學領域的專家進行不同主題的科普演講，還有「行動天文館」、「系外行星展」兩大展覽供一般民眾參觀；或是以兒童為對象的「天文故事館」，開放學齡前與小學生投稿的「天文繪畫比賽」；另外還有從實踐與觀測中學習的寶貴機會，例如透過摺紙理解科學原理的「摺紙天文學」、模擬彗星組成與撞擊的「科學實驗」，或是讓學生實際操作天文望遠鏡的「大學生夜間天文觀測」以及「太陽及太空天氣觀測」，帶給民眾豐富天文知識。

臺灣科學特殊人才提升計畫所籌畫的全民天文教育致力以不同的方式向大眾表現天文之美，期望透過多樣的活動，啟發學生對天文領域的興趣與認識。詳細活動介紹可至相關網站查詢，歡迎民眾到現場一同參與，在中大探索天文的奧妙！

本文轉載自【2023-07-03/理財周刊】

桃園天文嘉年華活動開跑　七天活動精彩不斷

2023/07/04 台灣好新聞

為鼓勵民眾積極參與天文科學教育，臺灣科學特殊人才提升計畫於 7 月 1 日至 7 月 7 日，在中央大學舉辦為期七天的「2023 桃園天文嘉年華」。以中央大學天文台為基地，由教育部及桃園市政府教育局指導，協同臺北市立天文科學教育館等單位共同舉辦。期望桃園能引領風騷，成為台灣天文教育的先鋒。

天文是對 3 歲的幼兒到 80 歲以上的長者，啟發科學興趣的最佳工具，因此臺灣科學特殊人才提升計畫規劃全民天文教育「AE4ALL」（Astronomy Education for

All），透過中大天文所的設備和教學資源，結合全國各個天文教育團隊的力量，舉辦「桃園天文嘉年華」增強臺灣的天文科學教育。

「2023 桃園天文嘉年華」7 月 1 日舉行開幕式，由葉永烜院士主講的科普講座「威廉的天空」開啟序幕，「天文故事館」則是藉由生動的故事引導兒童深入探索天文的奧秘。「摺紙天文學」的活動更引起了廣大的關注。這項特別活動獲得了日本摺紙大師西川誠司的授權，並由台灣摺紙協會的李政憲老師和連崇馨老師帶領學員一起親手摺製天文望遠鏡。進行活動的過程中，充滿了歡笑和探索的樂趣。活動不僅讓學員對天文有了更深入的理解，而且還巧妙地將科學與藝術結合在一起，為參與者帶來了全新的學習體驗。

活動連續七天不間斷，每日都有來自國內天文科學領域的專家進行不同主題的科普演講，還有「行動天文館」、「系外行星展」兩大展覽供一般民眾參觀；或是以兒童為對象的「天文故事館」，開放學齡前與小學生投稿的「天文繪畫比賽」；另外還有從實踐與觀測中學習的寶貴機會，例如透過摺紙理解科學原理的「摺紙天文學」、模擬彗星組成與撞擊的「科學實驗」，或是讓學生實際操作天文望遠鏡的「大學生夜間天文觀測」以及「太陽及太空天氣觀測」，帶給民眾豐富天文知識。

臺灣科學特殊人才提升計畫所籌畫的全民天文教育致力以不同的方式向大眾表現天文之美，期望透過多樣的活動，啟發學生對天文領域的興趣與認識。詳細活動介紹可至相關網站查詢，歡迎民眾到現場一同參與，在中大探索天文的奧妙！

本文轉載自【2023-07-03/台灣好新聞】

桃園天文嘉年華中央大學開跑　啟發全民科學興趣

2023/07/04 ettoday 新聞網
「2023 桃園天文嘉年華」1 日起迄 7 日、在中央大學展開，由葉永烜院士主講的科普講座「威廉的天空」開啟序幕。中央大學 3 日表示，天文是對 3 歲的幼兒到 80 歲以上的長者，啟發科學興趣的最佳工具。

因此臺灣科學特殊人才提升計畫規劃全民天文教育「AE4ALL」（Astronomy Education for All），舉辦「桃園天文嘉年華」增強臺灣的天文科學教育，並以中央大學天文台為基地，由教育部及桃園市政府教育局指導，協同臺北市立天文科學教育館等單位共同舉辦。期望桃園能引領風騷，成為台灣天文教育的先鋒。

為期 7 天的「2023 桃園天文嘉年華」活動，每天都有來自國內天文科學領域的專家進行不同主題的科普演講，還有「行動天文館」、「系外行星展」兩大展覽供一般民眾參觀；或是以兒童為對象的「天文故事館」，開放學齡前與小學生投稿的「天文繪畫比賽」；另外還有從實踐與觀測中學習的寶貴機會，例如透過摺紙理解科學原理的「摺紙天文學」、模擬彗星組成與撞擊的「科學實驗」，或是讓學生實際操作天文望遠鏡的「大學生夜間天文觀測」以及「太陽及太空天氣觀測」，帶給民眾豐富天文知識。

本文轉載自【2023-07-03/ettoday 新聞網】

桃園天文嘉年華活動開跑　七天活動精彩不斷

2023/07/04 Yahoo!新聞

為鼓勵民眾積極參與天文科學教育，臺灣科學特殊人才提升計畫於 7 月 1 日至 7 月 7 日，在中央大學舉辦為期七天的「2023 桃園天文嘉年華」。以中央大學天文台為基地，由教育部及桃園市政府教育局指導，協同臺北市立天文科學教育館等單位共同舉辦。期望桃園能引領風騷，成為台灣天文教育的先鋒。

天文是對 3 歲的幼兒到 80 歲以上的長者，啟發科學興趣的最佳工具，因此臺灣科學特殊人才提升計畫規劃全民天文教育「AE4ALL」（Astronomy Education for All），透過中大天文所的設備和教學資源，結合全國各個天文教育團隊的力量，舉辦「桃園天文嘉年華」增強臺灣的天文科學教育。

「2023 桃園天文嘉年華」7 月 1 日舉行開幕式，由葉永烜院士主講的科普講座「威廉的天空」開啟序幕，「天文故事館」則是藉由生動的故事引導兒童深入探索天文的奧秘。「摺紙天文學」的活動更引起了廣大的關注。這項特別活動獲得了日本摺紙大師西川誠司的授權，並由台灣摺紙協會的李政憲老師和連崇馨老師帶領學員一起親手摺製天文望遠鏡。進行活動的過程中，充滿了歡笑和探索的樂趣。活動不僅讓學員對天文有了更深入的理解，而且還巧妙地將科學與藝術結合在一起，為參與者帶來了全新的學習體驗。

活動連續七天不間斷，每日都有來自國內天文科學領域的專家進行不同主題的科普演講，還有「行動天文館」、「系外行星展」兩大展覽供一般民眾參觀；或是以兒童為對象的「天文故事館」，開放學齡前與小學生投稿的「天文繪畫比賽」；另外還有從實踐與觀測中學習的寶貴機會，例如透過摺紙理解科學原理的「摺紙天文學」、模擬彗星組成與撞擊的「科學實驗」，或是讓學生實際操作天文望遠鏡的「大學生夜間天文觀測」以及「太陽及太空天氣觀測」，帶給民眾豐

富天文知識。

臺灣科學特殊人才提升計畫所籌畫的全民天文教育致力以不同的方式向大眾表現天文之美，期望透過多樣的活動，啟發學生對天文領域的興趣與認識。詳細活動介紹可至相關網站查詢，歡迎民眾到現場一同參與，在中大探索天文的奧妙！

本文轉載自【2023-07-03/Yahoo!新聞】

提倡森林永續　中央大學命名臺大實驗林小行星「Ntuef」

2023/07/03 蕃薯藤

國立中央大學於 112 年 6 月 30 日國立臺灣大學生物資源暨農學院實驗林管理處（簡稱臺大實驗林）74 週年處慶，舉行臺大實驗林（Ntuef）小行星頒贈儀式，將中央大學鹿林天文臺發現的編號 528489 臺大實驗林小行星致贈給臺大實驗林管理處處長蔡明哲，彰顯臺大實驗林對於臺灣森林生態保育的貢獻。

臺大實驗林成立於 1902 年，位於臺灣中部，範圍橫跨南投鹿谷、信義、水里三個鄉鎮，地形從海拔 220 米上升到玉山主峰海拔 3,952 米，佔地 32,764 公頃，約佔臺灣全島的 1%，高溫多雨、海拔差距大等因素，造就多樣的生物棲息環境。

森林乃國家命脈，林地攸關社稷安危，臺大實驗林以森林永續經營為最高目標。中大今年更開設超過 700 門 SDGS 永續相關課程，培養學生議題分析、創意思考、跨域整合以及社會實踐能力。臺灣大學與中央大學對於永續發展方向一致，十年樹木百年樹人，在長期永續發展實踐上皆會持續匯聚永續量能，引領風潮。

臺大實驗林小行星，2008 年 10 月 20 日由中央大學天文所鹿林天文臺蕭翔耀及美國馬里蘭大學的葉泉志博士共同發現，大小約 1 公里。臺大實驗林小行星繞行太陽一圈 3.37 年（軌道週期），離太陽最近時（近日點）為 2.81 億公里，最遠時（遠日點）為 3.93 億公里，目前運行到獅子座。

中央大學副校長許秉瑜表示臺灣的森林幾乎涵蓋北半球所有的森林種類，其珍稀性需要人們的愛護及重視，而臺大實驗林在生態保育及學術研究皆不遺餘力，長年致力於永續發展實踐並維護森林生態的貢獻。近年來更造林撫育超過 450 公頃，期許此次頒贈小行星能讓這理念高掛天空，讓臺灣森林保育的信念

傳承下去。

中央大學鹿林天文臺地處臺大實驗林轄區，擁有得天獨厚的自然環境。2006 年開始的鹿林巡天計畫，不但曾發現臺灣史上的第一顆彗星，同時也發現了 800 多顆小行星，使臺灣成為亞洲發現小行星最活躍的地方之一。卓越的天文研究成果，充份展現臺灣人以小搏大、努力不懈的精神，期許透過小行星的命名與頒贈，讓臺灣更能展露獨特價值。

本文轉載自【2023-06-30/蕃薯藤】

提倡森林永續　中央大學命名臺大實驗林小行星"Ntuef"

2023/07/03 新網新聞網

國立中央大學於 112 年 6 月 30 日國立臺灣大學生物資源暨農學院實驗林管理處（簡稱臺大實驗林）74 週年處慶，舉行臺大實驗林(Ntuef)小行星頒贈儀式，將中央大學鹿林天文臺發現的編號 528489 臺大實驗林小行星致贈給臺大實驗林管理處處長蔡明哲，彰顯臺大實驗林對於臺灣森林生態保育的貢獻。

提倡森林永續重要性，由中央大學副校長許秉瑜將臺大實驗林小行星銘版頒贈給臺灣大學生物資源暨農學院實驗林管理處處長蔡明哲。(國立中央大學提供)

臺大實驗林成立於 1902 年，位於臺灣中部，範圍橫跨南投鹿谷、信義、水里 3 個鄉鎮，地形從海拔 220 米上升到玉山主峰海拔 3,952 米，佔地 32,764 公頃，約佔臺灣全島的 1%，高溫多雨、海拔差距大等因素，造就多樣的生物棲息環境。

森林乃國家命脈，林地攸關社稷安危，臺大實驗林以森林永續經營為最高目標。中大今年更開設超過 700 門 SDGS 永續相關課程，培養學生議題分析、創意思考、跨域整合以及社會實踐能力。臺灣大學與中央大學對於永續發展方向一致，十年樹木百年樹人，在長期永續發展實踐上皆會持續匯聚永續量能，引領風潮。

臺大實驗林小行星，2008 年 10 月 20 日由中央大學天文所鹿林天文臺蕭翔耀及美國馬里蘭大學的葉泉志博士共同發現，大小約 1 公里。臺大實驗林小行星繞行太陽一圈 3.37 年（軌道週期），離太陽最近時（近日點）為 2.81 億公里，最遠時（遠日點）為 3.93 億公里，目前運行到獅子座。

中央大學副校長許秉瑜表示，臺灣的森林幾乎涵蓋北半球所有的森林種類，其珍稀性需要人們的愛護及重視，而臺大實驗林在生態保育及學術研究皆不遺餘力，長年致力於永續發展實踐並維護森林生態的貢獻。近年來更造林撫育超過 450 公頃，期許此次頒贈小行星能讓這理念高掛天空，讓臺灣森林保育的信念傳承下去。

中央大學鹿林天文臺地處臺大實驗林轄區，擁有得天獨厚的自然環境。2006 年開始的鹿林巡天計畫，不但曾發現臺灣史上的第一顆彗星，同時也發現了 800 多顆小行星，使臺灣成為亞洲發現小行星最活躍的地方之一。卓越的天文研究成果，充份展現臺灣人以小搏大、努力不懈的精神，期許透過小行星的命名與頒贈，讓臺灣更能展露獨特價值。

本文轉載自【2023-06-30/新網新聞網】

提倡森林永續　中央大學命名台大實驗林小行星「Ntuef」

2023/07/03 工商時報

為表彰 2008 年 10 月 20 日由中央大學天文所鹿林天文台觀測員蕭翔耀及美國馬里蘭大學博士葉泉志共同發現「台大實驗林小行星」，中央大學今（30）日在台大生物資源暨農學院實驗林管理處 74 周年處慶上，舉行「台大實驗林小行星」頒贈儀式，將編號 528489 的「台大實驗林小行星」致贈給台大實驗林管理處處長蔡明哲，彰顯台大實驗林對於本土森林生態保育的貢獻。

「台大實驗林小行星」大小約 1 公里，繞行太陽一圈的軌道週期為 3.37 年，離太陽最近時的近日點為 2.81 億公里，最遠時的遠日點為 3.93 億公里，目前運行到獅子座。

而台大實驗林成立於 1902 年，位於台灣中部，範圍橫跨南投鹿谷、信義、水里 3 個鄉鎮，地形從海拔 220 米上升到玉山主峰海拔 3952 米，佔地 3 萬 2764 公頃，約占台灣全島的 1%，地理環境高溫多雨、海拔差距大等因素，造就多樣的生物棲息環境。

森林乃國家命脈，林地攸關社稷安危，台大實驗林以森林永續經營為最高目標。中央大學今年更開設超過 700 門 SDGS 永續相關課程，培養學生議題分析、創意思考、跨域整合以及社會實踐能力。兩校對於永續發展方向一致，致力長期在永續發展實踐上，持續匯聚量能。

中央大學副校長許秉瑜表示，台灣的森林幾乎涵蓋北半球所有的森林種類，其珍稀性需要人們的愛護及重視，而台大實驗林在生態保育及學術研究皆不遺餘力，長年致力於永續發展實踐並維護森林生態的貢獻。近年來更造林撫育超過450 公頃，期許此次頒贈小行星能讓這理念高掛天空，讓台灣森林保育的信念傳承下去。

中央大學提到，鹿林天文台地處台大實驗林轄區，擁有得天獨厚的自然環境。2006 年啟動的「鹿林巡天計畫」，不但曾發現台灣史上的第一顆彗星，同時也發現了 800 多顆小行星，使台灣成為亞洲發現小行星最活躍的地方之一。期許透過小行星的命名與頒贈，讓台灣更能展露獨特價值。

本文轉載自【2023-06-30/工商時報】

提倡森林永續　中央大學命名台大實驗林小行星

2023/07/03 人間福報

國立中央大學於 30 日國立台灣大學生物資源暨農學院實驗林管理處（簡稱台大實驗林）74 周年處慶，舉行台大實驗林（Ntuef）小行星頒贈儀式，將中央大學鹿林天文台發現的編號 528489 台大實驗林小行星致贈給台大實驗林管理處處長蔡明哲，彰顯其對於台灣森林生態保育的貢獻。

森林乃國家命脈，林地攸關社稷安危，台大實驗林成立於 1902 年，位於台灣中部，範圍橫跨南投鹿谷、信義、水里三個鄉鎮，地形從海拔 220 米上升到玉山主峰海拔 3952 米，佔地 32764 公頃，約佔台灣全島的 1%，高溫多雨、海拔差距大等因素，造就多樣的生物棲息環境。

台大實驗林小行星，2008 年 10 月 20 日由中央大學天文所鹿林天文台蕭翔耀及美國馬里蘭大學的葉泉志博士共同發現，大小約 1 公里。台大實驗林小行星繞行太陽一圈 3.37 年（軌道週期），離太陽最近時（近日點）為 2.81 億公里，最遠時（遠日點）為 3.93 億公里，目前運行到獅子座。

中央大學副校長許秉瑜表示，台灣森林幾乎涵蓋北半球所有的森林種類，其珍稀性需要人們的愛護及重視，而台大實驗林在生態保育及學術研究皆不遺餘力，長年致力於永續發展實踐並維護森林生態的貢獻，近年來更造林撫育超過450 公頃，期許此次頒贈小行星能讓這理念高掛天空，讓台灣森林保育的信念傳承下去。

中央大學鹿林天文台地處台大實驗林轄區，2006 年開始的鹿林巡天計畫，不但曾發現台灣史上的第一顆彗星，同時也發現了 800 多顆小行星，使台灣成為亞洲發現小行星最活躍的地方之一。卓越的天文研究成果，充份展現台灣人以小搏大、努力不懈的精神，期許透過小行星的命名與頒贈，讓台灣更能展露獨特價值。

本文轉載自【2023-06-30/人間福報】

日出位置非固定　全年軌跡呈現 8 字形

2023/06/09　中廣新聞網
太陽從東方升起，每天同時間的位置不是固定而是呈現 8 字形，不少天文迷歷經 1 年時間拍攝驗證，中央大學鹿林天文台也完成太陽軌跡合成圖再次證明。鹿林天文台助理蕭翔耀表示，太陽軌跡呈現８字圖，因地球自轉軸傾斜 23.5 度，且繞太陽軌道不是正圓形；同時觀測軌跡最左側跟最右側，就是太陽最北跟最南位置，這個時候是接近夏至跟冬至的時刻。(李明朝報導)

不少國人喜歡觀看日出，國內也有熱門景點，不過，太陽雖然從東方緩緩升起，但不是固定軌跡，有天文迷在固定地點、時間拍攝 1 年時間，太陽是呈現 8 字軌跡。

中央大學鹿林天文台同樣也歷經 1 年，間隔 1 至 2 星期，拍攝時間為白天 7 點 20 分，完成太陽軌跡，再把太陽位置合成，呈現 8 字型。天文台助理蕭翔耀說，太陽是從東邊出來，其實並不是每天都同時從正東方出來，經過超過一年的時間，每次間隔一個多禮拜，採固定同樣的時間拍攝，太陽位置變化逐一合成，呈現 8 字圖。之所以會呈現 8 字圖，是因為地球自轉軸傾斜 23.5 度，且繞太陽軌道不是正圓形。

另外，蕭翔耀表示，合成圖最左側跟最右側軌跡，代表太陽位置最北跟最南，這兩點地點就是接近夏至跟冬至的時刻。

蕭翔耀表示，天文工作主要是夜間，為了捕捉日出，有時還需要犧牲睡眠，然而結果出來，還是非常值得。

原文轉載自【2023-06-08/中廣新聞網】

10 年來距地球最近、最亮超新星　小望遠鏡就可觀測

2023/06/08　中時新聞網

1 顆位於風車星系的超新星上月被發現，是 10 年來距離地球最近、也最亮的超新星。天文館表示，該顆超新星亮度處於高原期，用小望遠鏡有機會看見，數周後其亮度將逐漸下降，要藉大型望遠鏡才能看見。

日本業餘天文學家板垣公上月在俗稱風車星系 M101 星系中發現 1 顆超新星，通報國際天文學聯合會後，命名為 SN 2023ixf。天文館表示，當時得知超新星被發現後，當天晚間即透過中央大學鹿林天文台遠距望遠鏡，拍攝到超新星清晰影像，並進行各波段亮度分析，隨後上傳到國際變星觀測協會，為天文研究提供重要資料。

天文館介紹，SN 2023ixf 屬於Ⅱ型超新星，是大質量恆星生命終結時，核心塌縮導致劇烈爆炸的結果，其亮度可遽增至太陽 10 億倍，能被遙遠的觀測者觀察到，是研究恆星演化的重要線索。

天文館表示，天文學家每年平均發現數百顆超新星，大多因距離非常遙遠而亮度很低，SN 2023ixf 位置相對較近，成為繼 2014 年出現的 SN 2014J 之後，10 年來距離最近、也最亮的超新星。

天文館表示，SN 2023ixf 亮度目前處於高原期，比肉眼可見極限星等僅暗約 60 倍，在良好觀測條件下以小望遠鏡有機會看見，數周後其亮度將逐漸下降，要藉大型望遠鏡才能看見。
原文轉載自【2023-06-07/中時新聞網】

投縣府召開天文意見領袖座談　徵詢暗空公園活動及管理想法

2023/06/08 台灣新生報

為徵詢天文意見?袖對於合歡山暗空公園地區發展的看法，南投縣府六日於清境國民賓館舉辦「天文意見領袖座談」由觀光處長陳志賢親自主持，透過簡報與意見交流，收集意見將持續精進各項管理措施。

許縣長上任後積極打造南投為宜居城市，並推動低碳及永續的觀光發展。「暗空公園」推動理念，從光害防制著手，並扎根至天文教育，讓觀光產業能更深度永續，觀光處將落實施政理念持續深化推動。

座談會包括合歡山暗空公園總規劃主持人國立暨南國際大學曾永平教授、清境

永續發展協會李從秀理事長、清境觀光協會張宏毅理事長、台北市天文協會劉志安理事長、台中市天文協會呂其潤理事長、嘉義市天文協會邱榮輝理事長(線上參加)、台南市天文協會莊建庭理事長(線上參加)、台灣親子觀星會阮驛琇理事長、全國大學天文社聯盟曾美茵理事長、國立中央大學天文所鹿林天文台林宏欽台長(線上參加)、中研院天文所王為豪副所長(線上參加)及包括退輔會清境農場、台大梅峰農場、南投林區管理處等單位均派代表出席。

由暨大、觀光處及風景區管理所等單位，分別簡報仁愛鄉地方創生、203 南投星空季規劃、鳶峰委外經營以及自治條例進度，總規劃並簡報說明 4 月初 IDA 親自前台灣視察情形，並討去年決議事項執行進度。與會各單位及代表均踴躍發言，縣府也一一紀錄，將作為今年各項管理措施及活動規劃參考。

觀光處表示，今年疫情解除管制，預期將有大量觀光客前來合歡山暗空公園，前已積極進行各項整備工作鳶峰遠端天文觀測系統已測試完成，正進行委外經營正式開幕前準備，二 0 二三南投星空季將於七月一日於清境國小展開，七月二日鳶峰將正式對外營運。縣府持續行銷,並同時注意落實各項光害防制及管制事宜，在推動觀光發展下同時兼顧環境保育以及永續發展。二 0 二三南投星空季相關活動訊息，可查詢樂旅南投臉書粉絲頁或南投旅遊網。
原文轉載自【2023-06-07/台灣新生報】

10 年來最亮超新星現身風車星系　小望遠鏡可拍攝

2023/06/08 中央通訊社
台北市立天文館表示，一顆位在風車星系中、由大質量恆星死亡時產生的超新星近期被發現，是 10 年來距離地球最近也最亮的超新星，用小型望遠鏡即可拍攝，值得觀測。

台北市立天文科學教育館今天發布新聞稿表示，5 月 20 日凌晨，日本業餘天文學家板垣公一在俗稱風車星系的 M101 中發現一顆亮度約 14.9 等的超新星，隨即通報國際天文學聯合會，並依超新星命名規則，將其命名為 SN 2023ixf。

天文館指出，得知訊息後，當晚即透過設置於中央大學鹿林天文台的 5 公分小望遠鏡，以重複曝光 2 分鐘的方式清楚拍攝到這顆超新星，並進行各波段亮度分析，隨後將資料上傳至美國變星觀測者學會等天文組織，與國際共享觀測成果。

天文館說明，SN2023ixf 屬於「核塌縮超新星」，是大質量恆星在生命終結時核心塌縮，導致劇烈爆炸的結果，亮度會在爆發後短暫上升再下降，甚至可以遽增到太陽的 10 億倍，所以能被遙遠的觀測者觀察到，是研究恆星演化的重要線

索。

天文館介紹，SN2023ixf 所在的風車星系距離地球約 2100 萬光年，是繼 2014 年出現的 SN2014J 後，最近也最亮的超新星，且風車星系所在的大熊座仰角高、易觀察，一直以來都是天文愛好者喜歡拍攝的目標。

若想觀測 SN2023ixf，天文館表示，它的亮度目前仍處於高原期，約 11 等左右，比肉眼可見極限星等暗約 60 倍，所以在良好觀測條件下，用小望遠鏡曝光就可以拍攝到，世界各地已有相當多觀測者分享在自家樓頂拍攝的結果。

不過，天文館強調，能否拍攝出清晰的 SN2023ixf，取決於觀測者本身對攝影及器材的熟悉程度，目前 SN2023ixf 已經比風車星系的核心還要亮，所以曾拍過風車星系的人，一定拍得到 SN2023ixf；但沒有深空天體拍攝經驗或想直接用肉眼欣賞會比較困難，「的確是有可能，但就是一個挑戰」。

天文館表示，要成為「核塌縮超新星」的恆星，質量至少會是太陽的 8 倍以上，雖然平均每年會有數百顆被發現，但像此次這樣以 5 公分望遠鏡就能拍攝的機會實屬難得，值得同好們一同投入觀測行列。

原文轉載自【2023-06-07/中央通訊社】

台東「最美星空」音樂會　縣府以「6 最」邀大家看星星

2023/05/25 聯合新聞網
2023 年「台東最美星空」音樂系列活動 6 月 22 日登場，今年 8 場次音樂會分布各鄉鎮舉行，特別的是今年邁入第 6 年，縣府以「6 最」為主軸，邀大家來台東看星星、聽音樂。

縣長饒慶鈴說，這 6 最包括最長、最強、最高、最多、最跳及最美等，以最高為例就是活動拉到海拔 1 千多公尺的利稻村，最遠則是到蘭嶼舉行，給大家感受不同的星空之美。

台東因無光害是全台、世界觀星最美的地方之一，為行銷台東的星空，6 年前縣府推出最美星空音樂系列活動，廣受好評，吸引累積逾 3 萬人次到訪台東參與活動觀星聽音樂。

2018 年甚至與國立中央大學合作，將鹿林天文台所發現的第 281561 號小行星，命名為台東「Taitung」星，編號第 278986 號小行星則命名為陳樹菊「Chenshuchu」星。

今年 8 場次最美星空音樂會，分別於 6 月 22 日海端利稻分校、 7 月 15 日關山紅石溪畔、7 月 22 日東河金樽陸連島、8 月 12 日大武尚武海濱公園、8 月 13 日池上天堂路、8 月 19 日長濱八仙洞、9 月 9 日蘭嶼椰油國小及 9 月 16 日綠島人權紀念館。

縣府表示，今年音樂會卡司陣容堅強有宇宙人、洪佩瑜、旺福、老王樂隊、麋先生、好樂團、法蘭 Fran、慢慢說樂團、柏霖 PoLin、琳誼 Ring、魏嘉瑩、邱軍、Cicada、Fann 芳怡等多組人氣歌手及樂團。

另還有三金大提琴演奏家范宗沛、豎琴獵人李哲音、愛樂 Taiwan JustMusic 藝術總監歐聰陽聯袂演出，以及 16 組在地樂團好聲音。

原文轉載自【2023-05-24/聯合新聞網】

雙北竹桃、沖繩、鹿兒島都拍到！　週三「火球」劃天

2023/05/12 TVBS 新聞網
10 日晚上七點半，在雙北以及桃竹地區，都有民眾目睹一個像流星的飛行物，但是飛行速度又很慢。甚至在日本沖繩以及鹿兒島，也有民眾拍下形容像「火球」。專家分析，以它飛行速度以及軌道判斷，應該是「人造天體」，其實不算少見，但剛好軌道很低又在晚上，才能幸運被民眾看見。

10 日晚上七點半，民眾在台北車站附近抬頭一看，一個光點平飛過去，七點 32 分也有人在迴龍捷運站看到，甚至往南走。

在新竹也有人目睹，一道白色光束劃過天空，所有人一開始都以為是飛機或是空拍機，但看到後面的長長火光，覺得像流星，只是飛行速度又比流星慢很多。

中央大學的科學館：「也在晚上七點 32 分拍攝到，這光束以拋物線的軌跡飛行。」

國立中央大學天文研究所助理張永欣：「它的飛行速度非常的慢，軌道非常的低，這兩點就可以判定它是人造的天體，至於是不是太空垃圾這個很難講，因為人造衛星墜落也是這樣。」

不只在台灣被不少民眾目睹，就連日本九州鹿兒島以及沖繩，都有民眾大約也在台灣時間七點半左右，拍到像火球般的東西。

專家分析，以觀測時間來比對，不是傳聞的大陸發射火箭，應該是人造天體，其中有可能是太空垃圾，或是發射失敗的太空船、人造衛星，以及火箭殘骸等等，而這情形不算少見。

國立中央大學天文研究所助理張永欣：「它的位置軌道很低然後比較北邊，如果它發生在我們頭頂上的話，大概注意到的人很少，因為沒有人會抬頭仰望頭頂。」

至於這個，台日都有人目睹的人造天體，最後墜落在哪裡，專家表示，因為沒有針對這天體，做「三點定位」的觀察，無法得知軌跡。

這回人造天體墜落，剛好飛行軌跡低又在晚上，天時地利人合，民眾才能幸運目睹。

原文轉載自【2023-05-11/TVBS 新聞網】

增加觀星、賞螢等旅遊商機！天文學者提倡降光污染

2023/04/26 聯合新聞網
學者表示，台灣因為地狹人稠，因此就算高山也可能會有光污染的問題；呼籲政府能主導、加上民間配合，才能有效降低光污染，除了達到保育生態的效果，另外也能增加觀星、賞螢等旅遊商機。

中央大學鹿林天文台台長林宏欽告訴中央社記者，最初「光害」是天文觀測時所提出，因為研究時感受到都市燈光的影響愈來愈嚴重；後來慢慢發現不只是天文的問題，隨著都市發展，光的範圍愈來愈大，對人的作息、動植物也都會有影響。

林宏欽指出，光污染主要影響可能包含失眠，或是過亮、閃爍等對夜行性的動物會干擾其生活型態，甚至影響繁衍；開車時可能會因照明或球場、運動場的投射燈，在某些角度會有眩光導致安全性問題。

林宏欽進一步說明，因為台灣不大，各地或多或少會受到光的影響，甚至高山上還是可能感受到平地的光。他舉例，在玉山的鹿林天文台，約仰角 20 至 30 度、平地沒有雲的時候，可以看得到嘉南平原的燈火；甚至阿里山上也能看見澎湖花火節的煙火。

此外，林宏欽提到，現在大部分燈具都改用 LED 燈，在照明上效果高，雖有節能減碳的效果，但反而在亮度上比之前更嚴重。他建議可以改變光的方向，如路燈的照明，可以只照地面，避免影響行車、住宅；或是減少不必要的燈光、降低亮度，如廣告會使用的雷射光等，更進一步節約能源。

林宏欽認為，適度的減光其實是有助於地方經濟發展。如日本美星町有一座對外開放的天文台，當地民眾達成共識，晚間會拉上窗簾、減少光源等，地方政府也有立法，讓觀星變成一種晚間的觀光資源。

他再舉例，其實台灣也有類似的作法。季節性如菁桐老街一帶，近期開始有觀賞螢火蟲的活動，當地晚間就會用暗色玻璃紙將燈具包覆，然後配合交通管制，避免車燈直射，降低光害來保護自然生態，也帶來商機。

另外，林宏欽說，合歡山國際暗空公園就有清境民宿業者一同配合，「白天能在清境旅遊，夜晚則在減光的情況下能觀賞星空、銀河」。

根據合歡山國際暗空公園官網，清境民宿集中區域雖然不在合歡山暗空公園範圍內，但改善所有室外照明是為合歡山暗空公園被接受採認的重要承諾；民宿會員將室外照明加裝定時裝置，且設定為晚上 9 時準時關閉照明，調整照明角度、加裝燈罩來有效減低光的溢散。

林宏欽提到，在台灣這樣的案例畢竟是少數，還是需要政府單位主導，不論是訂定規範，或是增加限制燈光的保護區；單純只依靠民間的力量，有時很難達到理想的效果。

原文轉載自【2023-04-25/聯合新聞網】

用台語教天文　蔡安理獲傑出貢獻獎

2023/02/23 自由時報
昨天是二二一世界母語日，中央大學天文研究所博士後研究員蔡安理運用天文專業為台語盡一份心力，每日將美國國家航空暨太空總署（NASA）的天文文章翻譯成台語，迄今累積七百篇，並在台灣師範大學開設「台語天文學」課程，昨獲教育部「推展本土語言傑出貢獻獎」肯定。

每日翻譯 NASA 文章 累計 700 篇
教育部長潘文忠以台語表示，十一位得獎者有學者、天文學家、出版社頭家等，他們長久打拚、用盡心力推展和保存母語。特別是終身奉獻獎得主台師大英語系退休教授黃美金，以非原住民族身分，一生研究原住民語言，對泰雅語

著力最深，還組織相關學者完成三套台灣南島語言叢書，涵蓋全部的台灣原住民族語言，從語法的角度作體系的分析，貢獻卓著。

黃美金畢生致力研究原民語
黃美金指出，原住民族語言已是國家語言，使用族語的環境卻未因此顯著增加，講族語的長者不斷凋零。台灣是南島語言的根，有學者預言族語恐在五十年內斷絕，如此將找不到台灣的根，只要她還有能力，就會繼續致力於保存南島語言。

蔡安理從小在家講台語，她表示，父親教誨「台灣人要會說台灣話」，讓她萌生母語意識，二o二o年十二月起開始從事 NASA 科普網站文章的台文翻譯工作，且正式向 NASA 申請獲准設立官方網站「逐工一幅天文圖」，每日將一篇英文的天文文章翻譯為台語，建立台語科學學術詞彙庫，製作不同類型的台語天文節目。

蔡安理說，清華大學有一位香港教授用廣東話教天文學，有一位中學老師用台語教地球科學，都讓她更堅定地想用台語教天文，感謝中央大學天文所教授陳文屏支持，她在台師大開設台語天文學選修課，學生要用台語作期末報告，期許讓母語正常化。

昨天同時榮獲傑出貢獻獎的還有：中正大學教授何德華、前衛出版社社長林文欽、客家電視台新聞部顧問徐兆泉、苗栗縣三義鄉育英國小龍騰分校教師徐煥昇、屏東大學教授劉明宗、屏東大學講師謝秀珠、阮劇團、苗栗縣南庄鄉東河國小、台灣基督教長老教會雙連教會。

原文轉載自【2023-02-22/自由時報】

黃美金獲本土語言終身奉獻獎蔡安理用台語講天文學

2023/02/22 聯合新聞網
教育部今天頒發「推展本土語言傑出貢獻獎」，台師大退休教授黃美金致力族語研究 30 餘年，獲得「終身奉獻獎」殊榮；中央大學天文所博士後研究員蔡安理在台師大開設「台語天文學」課程，獲頒個人獎。

黃美金並非原住民，本來研究重點放在華語及英語教學，但在美國取得語言學博士學位後，指導教授建議她，回台後不用再研究華語，因為華語不會死，應好好研究正在消失中的原住民族語言。

黃美金返台任教於台師大，先是深入苗栗縣泰安鄉進行田野調查，從此愛上族

語，全心投入族語復振之路；她認為要延續本土語的生命，不能只在教室中學習，更要在家裡、路上說出口，讓語言存活在日常生活之中。

黃美金發表得獎感言，認為這個獎項屬於所有一同研究族語結構、撰寫 3 套族語叢書，以及協助保存語料和音檔的語言學家們；她並說，雖然族語復振已慢慢步入軌道，但尚未完全落實，族語雖成為國家語言，但使用的環境並未顯著增加，部落長者卻不斷凋零，許多珍貴的語言與文化資產正逐漸消失。

中央大學天文所博士後研究員蔡安理今天獲頒個人獎項，她從 2020 年 12 月開始，每天用台語翻譯一篇美國國家航空暨太空總署（NASA）的科普文章，推出「逐工一幅天文圖」，至今已翻譯了 700 多篇；她也製作不同類型的台語天文節目，並於台灣師範大學開設「台語天文學」課程。

蔡安理指出，翻譯最困難的是描述、解釋天文學現象，必須建立台語科學學術詞彙，許多事情都須「開疆闢土」，但她認為，生活、藝術、文學、音樂都可以用母語表達，唯獨碰到科學專業就不行，這不是一種正常的語言現象。

蔡安理發表得獎感言謙虛表示，爸媽從小和她講台語，前輩們努力整合台語書寫系統，加上許多學者的協助，她才有辦法用台語翻譯天文學，進而開課訓練學生用台語講科學；她說，今天得到的應是一個團體獎，因個人只占了小小一部份。

教育部長潘文忠致詞指出，所有得獎者都經過長久打拚，為母語保存用盡心力；他並說，國家語言發展法的立法是一項重要里程碑，政府也持續投入經費，並將本土語言列入中小學課程，希望「說我們的話」成為台灣的主流價值。
原文轉載自【2023-02-21/聯合新聞網】

5 萬年一遇　綠尾彗星掠過地球　今明最接近　雙筒望遠鏡就能發現蹤跡

2023/02/02 世界日報
一顆罕見的綠色彗星上個月掠過太陽之後，正朝地球飛奔而來。將於 1、2 日兩天到達最接近地球的位置，距離大約 2600 萬哩，或 0.28 個天文單位(Astronomical Unit，AU)，遠超過地球與月球之間距離 100 倍以上，所以不會有相撞的風險。

這顆被命名為 C/2022 E3 (ZTF)的彗星，是由天文學家波林(Bryce Bolin)和馬西(Frank Masci)利用史維基瞬變探測器(Zwicky Transient Facility，ZTF)的廣域探測照相機在去年 3 月 2 日發現的，其軌道圍繞著太陽系的最外圍，路途遙遠，時間

漫長。

天文學家推算，這是 C/2022 E3 (ZTF)5 萬年來首次行經地球；換句話說，它上次飛越地球的時候，人類還處於石器時代。

C/2022 E3 (ZTF)於 1 月 12 日抵達近日點，距離大約 1 億哩，或 1.11AU。當這顆彗星接近地球的時候，民眾可以在北極星附近發現它頂著迷濛的綠色彗髮(coma)，拖著淡黃色的塵埃尾與微弱的離子尾。彗髮是環繞在彗星核心周圍的雲狀物，彗星接近太陽時，太陽的熱力會使彗核物質熔解並昇華為氣體，就形成了彗髮，使得彗星的外觀在望遠鏡觀測下呈現模糊的樣貌。彗星的顏色會由於所在軌道位置的不同，以及化學成分的變化而改變。

北半球比南半球更適合觀察 C/2022 E3 (ZTF)，在足夠黑暗的夜空下，用肉眼即可模糊看見它微弱模糊的漫射污跡，但大多數民眾仍需要至少雙筒望遠鏡才能清楚辨識。

離開地球之後，C/2022 E3 (ZTF)將繼續朝火星前進，預計在 10 日抵達最接近位置。

ZTF 是一個大型國際合作天文研究計畫，其一半經費由美國自然科學基金會所提供，另一半則由加州理工學院所領導的國際團隊分擔，台灣清華大學和中央大學組成的探高計畫也參與其中。

原文轉載自【2023-02-０1/世界日報】

玉山國家公園推全新天文環境教育課程　帶領民眾一窺塔塔加高海拔清靜星空

2023/01/13 台灣好新聞
玉山國家公園管理處自 101 年通過環境教育設施場所認證以來，已推出有關高山生態、臺灣獼猴、臺灣黑熊、貓頭鷹、登山安全、布農文化等環境教育課程，近年更攜手玉山國家公園解說志工，組成環境教育志工小組，在志工們的腦力激盪與巧手打造下，自即日起強勢推出「塔塔加暗空悄悄話」環境教育課程，帶領民眾一窺塔塔加高海拔清靜的星空。

宇宙中無時無刻有碰撞、大爆炸、新生和衰退在進行著，但因為接近真空的關係，使我們只得見宇宙中的顏色和形貌，卻不聞其聲，宇宙中安安靜靜，但卻有許多訊息在交流，就像在對我們訴說悄悄話，用心聽，才聽得見。

對星空充滿好奇的我們，可以從認識塔塔加的星空開始，玉山國家公園塔塔加遊憩區位於海拔 2,610 公尺之高山，除了有豐富的自然生態環境外，因光害、塵害、污染很少，是觀星的極佳地點，全臺最高的天文臺-國立中央大學「鹿林天文臺」即設置於此區內。

本課程適合國小 5 年級以上學童，課程將帶領學員認識塔塔加的星空，並搭配國小高年級天文先備知識，引發學員們探究自然、夜空之興趣，學習戶外觀星必備常識與禮儀、親自參與當季星空解說與明瞭四季星空變化之關係。課程中亦會 DIY 製作一個「黑盒子」【我的星座觀察盒】，就算是大白天也可以看見自己的星座在夜空中閃耀的樣子!這個「黑盒子」蘊藏神秘的力量，可以讓人安靜下來，想像置身宇宙的世界!

在臺灣，通常要到高海拔山區才較能感受暗黑的夜空，當我們遠離都市喧囂，想要置身在群星璀璨的天球底下，玉山國家公園塔塔加是我們最好的選擇!而日常生活中我們該如何盡一己之力來維護美好的夜空、如何降低光害對環境及人體的影響?各種我們沒想到、沒想過的生活習慣，都可以在「塔塔加暗空悄悄話」這個課程中細細思考，下一次仰望星空，我們會發現，宇宙浩瀚無垠，而我們與其息息相關，當我們開始關心天上的一顆亮星，就開始了我們的觀星之路!

記者吳素珍／南投報導
2023 年 1 月 12 日 週四 下午 4:48
玉山國家公園解說志工「環境教育志工小組」研發天文課程，用心將玉山的美好帶給大眾 。
玉山國家公園解說志工「環境教育志工小組」研發天文課程，用心將玉山的美好帶給大眾 。

玉山國家公園管理處自 101 年通過環境教育設施場所認證以來，已推出有關高山生態、臺灣獼猴、臺灣黑熊、貓頭鷹、登山安全、布農文化等環境教育課程，近年更攜手玉山國家公園解說志工，組成環境教育志工小組，在志工們的腦力激盪與巧手打造下，自即日起強勢推出「塔塔加暗空悄悄話」環境教育課程，帶領民眾一窺塔塔加高海拔清靜的星空。

宇宙中無時無刻有碰撞、大爆炸、新生和衰退在進行著，但因為接近真空的關係，使我們只得見宇宙中的顏色和形貌，卻不聞其聲，宇宙中安安靜靜，但卻有許多訊息在交流，就像在對我們訴說悄悄話，用心聽，才聽得見。

玉山國家公園前往集集國中進行天文課程推廣。
玉山國家公園前往集集國中進行天文課程推廣。
對星空充滿好奇的我們，可以從認識塔塔加的星空開始，玉山國家公園塔塔加遊憩區位於海拔 2,610 公尺之高山，除了有豐富的自然生態環境外，因光害、塵害、污染很少，是觀星的極佳地點，全臺最高的天文臺-國立中央大學「鹿林天文臺」即設置於此區內。

學生將太陽系家族捧在手中感受行星間的距離比例遠近。
學生將太陽系家族捧在手中感受行星間的距離比例遠近。
本課程適合國小 5 年級以上學童，課程將帶領學員認識塔塔加的星空，並搭配國小高年級天文先備知識，引發學員們探究自然、夜空之興趣，學習戶外觀星必備常識與禮儀、親自參與當季星空解說與明瞭四季星空變化之關係。課程中亦會 DIY 製作一個「黑盒子」【我的星座觀察盒】，就算是大白天也可以看見自己的星座在夜空中閃耀的樣子!這個「黑盒子」蘊藏神秘的力量，可以讓人安靜下來，想像置身宇宙的世界!

在臺灣，通常要到高海拔山區才較能感受暗黑的夜空，當我們遠離都市喧囂，想要置身在群星璀璨的天球底下，玉山國家公園塔塔加是我們最好的選擇!而日常生活中我們該如何盡一己之力來維護美好的夜空、如何降低光害對環境及人體的影響?各種我們沒想到、沒想過的生活習慣，都可以在「塔塔加暗空悄悄話」這個課程中細細思考，下一次仰望星空，我們會發現，宇宙浩瀚無垠，而我們與其息息相關，當我們開始關心天上的一顆亮星，就開始了我們的觀星之路!

學生專注於星座觀察盒中的世界。
學生專注於星座觀察盒中的世界。
玉山國家公園為擁有繽紛多樣資源的環境教育設施場所，全年度受理預約報名「塔塔加暗空悄悄話 」、「猴你在一起」、「塔塔加的詠嘆調 」、「熊愛玉山」、「做貓頭鷹的朋友」、「登山教育」、「認識布農文化 」等 7 套環境教育課程，歡迎大小朋友揪團上山走走，樂活學習!課程詳細內容請至玉山國家公園官網 環境教育專區查詢

文轉載自【2023-01-12/台灣好新聞】

中大新聞網

夏威夷大學系統總校長訪問中央大學　探討未來跨校科學合作

焦點新聞

2023.11.30 文/地球科學前瞻應用研究中心

夏威夷大學系統總校長 Prof. David Lassner 蒞臨中央大學，探討未來雙方跨校科學合作。照片地球科學前瞻應用研究中心提供

夏威夷大學系統總校長 Prof. David Lassner 與教育部國際司秘書歐季曦女士（Ms. Tina Ou）11 月 23 日一同蒞臨中央大學進行合作訪問，本次除討論兩校合作的相關事項，中央大學也藉此機會表彰感謝夏威夷大學兩位教授對於台灣海氣象監測實力與大氣科學研究的貢獻。

夏威夷大學(University of Hawai'i System)是一所全球頂尖的研究型大學，成立於 1907 年，擁有 10 個校區、19 個學院，其中天文學、地球科學、海洋科學等領域均以卓越的研究成果而聞名於世。

中央大學首先感謝夏威夷大學海洋科學系教授 Pierre Jacques Flament 在與本校長期合作期間致力於建立更加完善的海洋與大氣災害預警系統。台灣作為一個四面環海的海島型國家，海氣象的監測至關重要，與台灣海岸相關的產業及遊憩活動密不可分。Dr. Flament 向中央大學及台灣的海洋研究人員傳授他的專業知識、技術和豐富經驗，提升台灣在海氣象監測方面的實力，也進一步確保大眾在海岸環境中更加安全。

此外，訪問中也對夏威夷大學海洋地球科學技術學院陳宇能教授表示感謝。陳宇能教授不僅協助中大深入了解影響臺灣劇烈天氣的特性與相關機制，更在中央大學擔任講座教授，推動了兩校在大氣科學領域的合作。

在研究合作討論中，由天文所周翊所長、地科系郭力維副主任、葉一慶副教授分別介紹中央大學在天文、地科及海洋領域的研究成果及目標，討論兩校未來研究合作的可行性。另外，由大氣系主任楊舒芝主持，計畫先行推動大氣系與夏威夷大學展開雙聯學位的合作。中央研究院葉永烜院士更表示，期待未來看見兩校在天文研究領域上的合作。

此次訪問不僅肯定了雙方長期合作的共識，也為未來的學術交流和共同研究奠定了基礎，期待兩校的合作帶來更優異的研究成果同時提供學生更豐富多元的學習資源。

中央大學周景揚校長表彰夏威夷大學海洋科學系教授 Pierre Jacques Flament 對台灣海氣象監測的貢獻。照片地球科學前瞻應用研究中心提供

中央大學周景揚校長表彰夏威夷大學海洋地球科學技術學院陳宇能教授對大氣科學的研究貢獻。照片地球科學前瞻應用研究中心提供

一代報人 百年青史　中央大學頒贈「余紀忠」小行星以為感念

焦點新聞

2023.10.31 文／天文所、秘書室

中央大學校長周景揚（左）頒贈余紀忠小行星銘版給余紀忠文教基金會董事長余範英（右），感念余紀忠先生守護台灣的信念。黃鈞蔚攝

中央大學於 10 月 31 日余紀忠講座，舉行余紀忠小行星（Yuchichung）頒贈儀式，緬懷《中國時報》創辦人余紀忠先生。余先生的一生，以言論報國，為台灣當代民主自由的實踐，留下相當重要的遺產。中央大學感念其奉獻及精神，將編號 603200 余紀忠小行星致贈余紀忠文教基金會董事長余範英，期許余紀忠先生的信念能夠繼續守護台灣，讓世人不忘民主自由的可貴。

中國時報創辦人余紀忠先生(1910-2002)為國立中央大學傑出校友，非常關心且支持母校的發展。中央大學在 1999 年頒授名譽文學博士學位，以表彰其對社會、文化和國家的貢獻，並於 2008 年與余紀忠文教基金會共同成立「余紀忠講座」，邀請各領域學者擔任主講人，一同帶領師生探討學術議題。

余紀忠小行星，編號 603200，2006 年 7 月 5 日由中央大學鹿林天文台林宏欽及美國馬里蘭大學的葉泉志博士共同發現，大小約在 1 公里之間。余紀忠小行星繞行太陽一圈 3.47 年（軌道週期），離太陽最近時（近日點）為 3.05 億公里，最遠時（遠日點）為 3.83 億公里。

余紀忠文教基金會董事長余範英表示，他的父親余紀忠先生，一生以「政治民主、民族認同、穩定大局」為重要信念，前半生投筆從戎，報效國家，後半生創辦報紙，與時代相互書寫。感謝影響父親至深的中央大學頒贈小行星以為感念，抬頭仰望星空時，得以和父親對話，內心很感動！

中央大學從 2006 年開始的鹿林巡天計畫，不但曾發現台灣史上的第一顆彗星，同時也發現了 800 多顆小行星，使台灣成為亞洲發現小行星最活躍的地方之一。卓越的天文研究成果，充份展現台灣人以小搏大、努力不懈的精神，期許透過小行星的命名與頒贈，看見台灣更多可貴的價值。

中央大學天文所葉永烜院士介紹余紀忠小行星的發現經過。黃鈞蔚攝

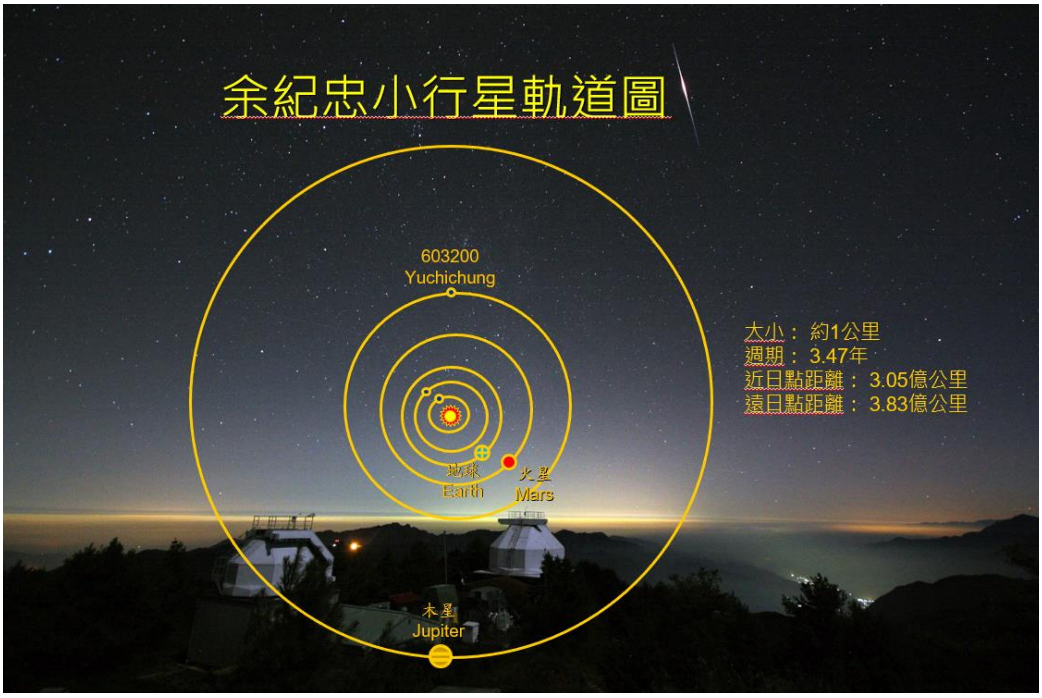

余紀忠小行星經國際天文聯合會（IAU）命名通過，編號為 603200，運行太陽一週約 3.47 年。
照片中央大學天文所提供

2023 總統科學獎　中央大學葉永烜院士與傑出校友李文雄院士同台輝映

焦點新聞

2023.10.25 文／秘書室

中央大學天文研究所葉永烜院士(左)與傑出校友李文雄院士(中)今年雙雙榮獲「2023 總統科學獎」之肯定，中央大學校長周景揚（右）出席表達恭賀之意。陳如枝攝

中央大學天文研究所葉永烜院士與傑出校友李文雄院士今年雙雙榮獲「2023 總統科學獎」之肯定，10 月 24 日在總統府由總統蔡英文親自頒授表揚，肯定他們的卓越貢獻。葉永烜院士以跨國界的高度，表達他的感念、隱憂和未來期許；李文雄院士則以跨領域的廣度，分享他學術生涯上三個關鍵性決定。

總統蔡英文表示，李文雄院士多年來跨領域探索生物演化的難題，並且提出前瞻的見解，為分子演化和生物遺傳學，持續開創新的研究方向。葉永烜院士則致力於太空科技及行星科學研究，除了多次參與國際合作的太空任務，更投入產官學的資訊交流合作及人才培育，提升臺灣的太空科技能力。

李文雄院士致詞時，分享學術生涯上三個關鍵性決定。他大學唸的是土木系，碩士班唸地球物理所，博士班攻讀應用數學。他在博士論文時決定將數學應用到生物學上，這是學術界少有人走的路，也是關鍵性的決定。其次，1979 年在 DNA 資料累積的年代，他全力以赴，所發表的論文被引用超過 4000 次，其中一篇 DNA 序列比較論文更推翻當代的主流觀點。他於 1989 年在中研院創立分

子生物學研究室，將理論與實驗結合，進而發現人類與黑猩猩基因體的核苷酸序列只有相差 1.24%，引起很大的震撼。

李文雄院士 2003 年獲遺傳暨演化界最高榮譽「巴仁獎」，是亞裔第一人，也是第一位當選美國國家科學院士的華人演化學者，2006 年獲頒中央大學傑出校友。從一位農家子弟，到一位卓越的科學家，他說，「一個人的能力，比想像中多許多！」

葉永烜院士對於得獎充滿了感念之意。他感謝臺灣這塊土地，1948 年收容父母這一代，在戰亂之中得到重生機會。也感謝中央大學讓他在臺灣學術研究得以從新開始。25 年來，感謝國科會的支持，進行太陽系探索的基礎研究。實驗室的研究生已在準備 25 年後對天王星和海王星的探測，年輕一代，希望無窮！

面對科學教育的未來，他也提出隱憂。除小行星撞地球之外，人類社會在未來可能面臨四大危機，分別是大流行病、人工智慧的誤用、氣候變遷和世界大戰。他引用美國前總统羅斯福夫人 Eleanor Roosevelt 的話，「只說和平是不夠的，必須要相信和平；只相信和平是不夠的；必需要努力爭取和平。」台灣才能安居樂業，世界才能永續發展。

他最後呼籲，優秀人才是國家的棟樑，爭取國際頂尖人才，要有更宏觀的思維，其中也包括人道精神、公平正義和和平共處等國際公約。有些國家為了強大而拋棄這些價值，希望臺灣因為這些價值而強大！

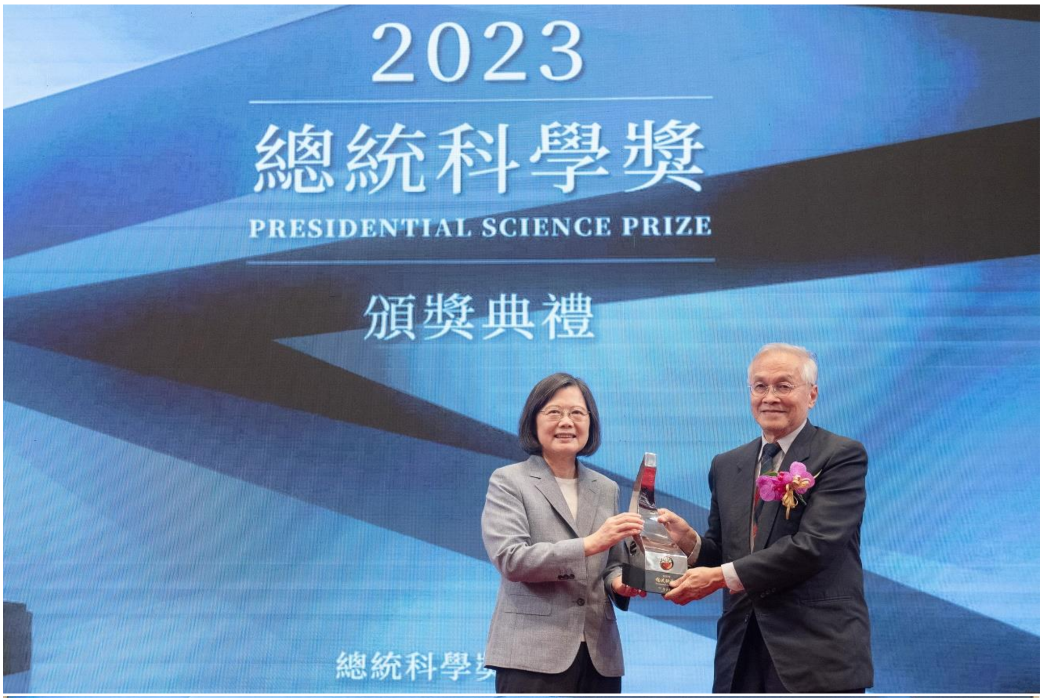

總統頒發 2023 年總統科學獎予獲獎人葉永烜院士。照片國科會提供 中央大學師長與總統和得獎者合影，留下珍貴的鏡頭。照片國科會提供

雙喜臨門！中央大學葉永烜院士與傑出校友李文雄院士榮獲「總統科學獎」

焦點新聞

2023.09.18 文／秘書室

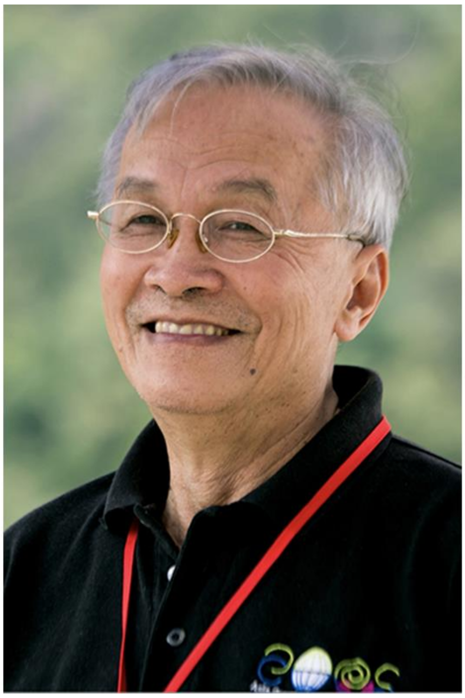

「2022-2023 總統科學獎」揭曉，中央大學葉永烜院士榮膺「數理科學組」得主（左），傑出校友李文雄院士則為「生命科學組」得主（右）。照片天文所與中研院提供

象徵我國最高科學榮譽之「總統科學獎」揭曉，中央大學天文研究所暨太空科學與工程學系葉永烜院士榮膺「數理科學組」得主，傑出校友李文雄院士則為「生命科學組」得主。他們不僅研究傑出卓越，對提升臺灣學術聲譽及國際競爭力，以及增進人類生活福祉更有深遠的影響。

中央大學葉永烜院士是國際行星科學研究領導者，對於彗星物理學、行星動力學和衛星-磁層相互作用等領域，有開創性的貢獻。他推動亞洲大洋洲地球科學發展，成立亞洲大洋洲地球科學學會 (AOGS) 並擔任第一屆會長，促成國際合作，大幅提高亞太地區研究能見度。同時開啟臺灣行星科學研究先河及時域天文學發展，對小行星觀測新發現有重大貢獻。

葉院士推動多項跨國研究計畫，提升臺灣國際能見度及影響力。並籌建中央大學鹿林天文台，推動時域天文學，成為產出重大科學價值國際合作及太陽系研究亮點的重要平台。他對人才培育更是不遺餘力，推動中央大學與台達電子文教基金會共同設立「年輕天文學者講座」，延攬國外優秀年輕學者推動臺灣天

文教育推廣。作育英才，桃李滿門，並投入 K-12 科教發掘特殊人才。

李文雄院士是中央大學第二屆傑出校友，在分子演化的學術研究有卓越的貢獻並享有國際名望。尤其在 RNA 病毒演化的研究上有重要的貢獻，他的研究有助於了解病毒如何演化成為更有傳播性的病媒，解釋人類大流行病為何大多由 RNA 病毒所引起。另外他們團隊也發現，靈長類祖先的 ACE2 與新冠病毒的 S-protein 結合力很弱，但 ACE2 在人類與舊世界猴子的共同祖先發生了一個突變，大幅增加 ACE2 與 S-protein 的結合力，致使人類容易被新冠病毒感染。

李院士已指導過超過 120 名的博士後和博士生，其中有多位在學術界上扮演要角。他所領導中央研究院生物多樣性研究，建立學程招募國際研究生，厚實國內研究動能，拓展臺灣在相關領域的國際知名度。除培育優秀人才之外，並網羅國際人才，引進微生物多樣性、生物資訊與基因體等領域研究。他亦創建基因體高通量定序核心設施，並對外提供服務，促進我國基因體及生物科技研究。

「總統科學獎」之設立，以提升臺灣在國際學術界之地位為宗旨，尤以對臺灣社會有重大貢獻之基礎學術研究人才。本次共遴選出 3 位得獎人，預定於 10 月 24 日舉行頒獎典禮，將由總統親自頒獎，以表彰其傑出榮譽。

推動天文科普　中大引領亞太地區 K-12 天文研討會

焦點新聞

2023.08.14 文／天文所

K-12 國際天文教育研討會開幕式合影。天文所提供

中央大學天文所於 8 月 14 日至 17 日舉辦為期四天的亞太地區 K-12 國際天文教育研討會。此次盛會為 2023 年國際天文聯合會亞太地區會議（APRIM 2023）之正式衛星會議，吸引來自臺灣、中國、日本、韓國、泰國、伊朗、澳洲、美國等國家的參與，深入探討宇宙相關知識的科普及教學經驗分享。

K-12 國際天文教育研討會（International Conference on K-12 Astronomy Education）旨在匯聚來自亞太地區的教育工作者，共同分享 K-12 天文學課堂及戶外活動的實踐經驗。內容囊括學前班、小學、初中和高中等各個教育階段，深入探討宇宙相關知識的傳遞與教學過程。不僅有助於各國學者瞭解周邊地區的天文教育現況，也能讓本國教師能夠在國際平臺上分享他們的心得和見解，藉此機會與優秀的教育者交流互動，協力探討提升天文教育策略與方法的新途徑。

研討會開幕由國家科學及技術委員會自然處羅夢凡處長、桃園市政府青年事務所涂淳惠副局長及桃園市政府教育局王昭人股長等人出席，表達對於天文教育交流與普及的重要性。與會學者將共同回顧並探討學生在學校和社會中所獲得的宇宙知識，其中包括天體的歷史、位置、多樣化的宇宙現象等。透過國際學

者和教師的深入對話，檢視對學生期望的適切性，以及探究各學科領域（如物理、化學、歷史、地理、地球科學等）中是否足夠涵蓋宇宙相關內容。

中大天文所期望藉由本次研討會引領天文教育的新潮流，促進知識分享、跨文化對話，並在更寬廣的天文學領域中激發更多的探索與創新，成為臺灣天文教育歷程中的重要里程碑。未來希望讓臺灣的天文科學教育與國際接軌，進一步建立系統性且高效的天文教育指南，讓臺灣在天文科學領域發光發熱。

活動發起人葉永烜院士為研討會拉開序幕。天文所提供

活動主辦人陳文屏教授提倡科普天文教育的重要性。天文所提供

中央大學鹿林天文台新設高山 AED　提升安全健康防護體系

焦點新聞

2023.08.13 文／學務處衛保組

中央大學鹿林天文台今年 8 月新增設自動體外去顫器（AED），並強化人員的急救安全教育訓練，建構健康安全體系。照片天文所提供

中央大學在海拔 2862 的鹿林前山設置全國最高的鹿林天文台，為確保科學家、觀測員、參訪人員和登山者的生命安全，今年 8 月在鹿林天文台新增自動體外去顫器（AED），並強化人員急救安全教育訓練，希望在高山容易缺氧的環境，建構健康安全環境，以強化急救防護體系。

推動這項工作的中央大學衛保組表示，在高山上使用 AED 是非常重要的，因為高山氧氣含量較低，遇到心臟驟停的患者，情況將更為緊急。尤其在高山救援隊伍可能需要花更長的時間才能到達事故現場，因此及早施行急救措施尤為重要，設置 AED 希望提高救援的成功率。

中央大學不僅於校園廣設 AED，同時加強校園急救安全教育訓練，以確保每位成員皆能夠掌握基本的急救知識與技能。校園每年至少舉辦 30 場急救教育訓練，致力於讓每個人都能熟練掌握心肺復甦術和自動體外去顫器的使用技巧，使校園成為守護生命的安全堡壘。

鹿林天文台設置 AED，是中大推動安全與健康的另一重要里程。首先要確保在寒冷環境中使用 AED，電池能夠正常運作；若情況緊急，要懂得心肺復甦術，以保持血液循環。並在第一時間與當地的救援隊伍保持聯繫，告知正確位置和情況，希望善盡大學之社會責任。

自動體外去顫器（AED）設置在中央大學鹿林天文台的控制中心。照片天文所提供

自動體外去顫器（AED）在中大天文台入口處設置明顯標示，以確保登山客的安全。照片天文所提供

2023 桃園天文嘉年華活動開跑　七天活動精彩不斷

焦點新聞

2023.07.03 文／天文所

開幕式長官合影，由左至右為國立中央大學林沛練學務長，臺灣科學特殊人才提升計畫主持人葉永烜院士、桃園市教育局林威志副局長、中央大學楊鎮華研發長。照片天文所提供

為鼓勵民眾積極參與天文科學教育，臺灣科學特殊人才提升計畫於 7 月 1 日至 7 月 7 日，在中央大學舉辦為期七天的「2023 桃園天文嘉年華」。以中央大學天文台為基地，由教育部及桃園市政府教育局指導，協同臺北市立天文科學教育館等單位共同舉辦。期望桃園能引領風騷，成為台灣天文教育的先鋒。

天文是對 3 歲的幼兒到 80 歲以上的長者，啟發科學興趣的最佳工具，因此臺灣科學特殊人才提升計畫規劃全民天文教育「AE4ALL」（Astronomy Education for All），透過中大天文所的設備和教學資源，結合全國各個天文教育團隊的力量，舉辦「桃園天文嘉年華」增強臺灣的天文科學教育。

2023 桃園天文嘉年華」7 月 1 日舉行開幕式，由葉永烜院士主講的科普講座「威廉的天空」開啟序幕，「天文故事館」則是藉由生動的故事引導兒童深入探索天文的奧秘。「摺紙天文學」的活動更引起了廣大的關注。這項特別活動獲得了日本摺紙大師西川誠司的授權，並由台灣摺紙協會的李政憲老師和連崇馨老師帶領學員一起親手摺製天文望遠鏡。進行活動的過程中，充滿了歡笑和

探索的樂趣。活動不僅讓學員對天文有了更深入的理解，而且還巧妙地將科學與藝術結合在一起，為參與者帶來了全新的學習體驗。

活動連續七天不間斷，每日都有來自國內天文科學領域的專家進行不同主題的科普演講，還有「行動天文館」、「系外行星展」兩大展覽供一般民眾參觀；或是以兒童為對象的「天文故事館」，開放學齡前與小學生投稿的「天文繪畫比賽」；另外還有從實踐與觀測中學習的寶貴機會，例如透過摺紙理解科學原理的「摺紙天文學」、模擬彗星組成與撞擊的「科學實驗」，或是讓學生實際操作天文望遠鏡的「大學生夜間天文觀測」以及「太陽及太空天氣觀測」，帶給民眾豐富天文知識。

臺灣科學特殊人才提升計畫所籌畫的全民天文教育致力以不同的方式向大眾表現天文之美，期望透過多樣的活動，啟發學生對天文領域的興趣與認識。詳細活動介紹可至相關網站查詢，歡迎民眾到現場一同參與，在中大探索天文的奧妙！

活動首場科普講座由葉永烜院士主講「威廉的天空」。照片 天文所提供


父母帶著孩子一同參與「摺紙天文學」活動。照片天文所提供

提倡森林永續　中央大學命名臺大實驗林小行星「Ntuef」

焦點新聞

2023.06.30 文／天文所

提倡森林永續重要性，由中央大學副校長許秉瑜將臺大實驗林小行星銘版頒贈給臺灣大學生物資源暨農學院實驗林管理處處長蔡明哲。蔡沛倫攝

國立中央大學於 112 年 6 月 30 日國立臺灣大學生物資源暨農學院實驗林管理處（簡稱臺大實驗林）74 週年處慶，舉行臺大實驗林（Ntuef）小行星頒贈儀式，將中央大學鹿林天文臺發現的編號 528489 臺大實驗林小行星致贈給臺大實驗林管理處處長蔡明哲，彰顯臺大實驗林對於臺灣森林生態保育的貢獻。

臺大實驗林成立於 1902 年，位於臺灣中部，範圍橫跨南投鹿谷、信義、水里三個鄉鎮，地形從海拔 220 米上升到玉山主峰海拔 3,952 米，佔地 32,764 公頃，約佔臺灣全島的 1%，高溫多雨、海拔差距大等因素，造就多樣的生物棲息環境。

森林乃國家命脈，林地攸關社稷安危，臺大實驗林以森林永續經營為最高目標。中大今年更開設超過 700 門 SDGS 永續相關課程，培養學生議題分析、創意思考、跨域整合以及社會實踐能力。臺灣大學與中央大學對於永續發展方向一致，十年樹木百年樹人，在長期永續發展實踐上皆會持續匯聚永續量能，引領風潮。

臺大實驗林小行星，2008 年 10 月 20 日由中央大學天文所鹿林天文臺蕭翔耀及美國馬里蘭大學的葉泉志博士共同發現，大小約 1 公里。臺大實驗林小行星繞行太陽一圈 3.37 年（軌道週期），離太陽最近時（近日點）為 2.81 億公里，最遠時（遠日點）為 3.93 億公里，目前運行到獅子座。

中央大學副校長許秉瑜表示臺灣的森林幾乎涵蓋北半球所有的森林種類，其珍稀性需要人們的愛護及重視，而臺大實驗林在生態保育及學術研究皆不遺餘力，長年致力於永續發展實踐並維護森林生態的貢獻。近年來更造林撫育超過 450 公頃，期許此次頒贈小行星能讓這理念高掛天空，讓臺灣森林保育的信念傳承下去。

中央大學鹿林天文臺地處臺大實驗林轄區，擁有得天獨厚的自然環境。2006 年開始的鹿林巡天計畫，不但曾發現臺灣史上的第一顆彗星，同時也發現了 800 多顆小行星，使臺灣成為亞洲發現小行星最活躍的地方之一。卓越的天文研究成果，充份展現臺灣人以小搏大、努力不懈的精神，期許透過小行星的命名與頒贈，讓臺灣更能展露獨特價值。

中央大學副校長許秉瑜致詞。蔡沛倫攝

臺大實驗林長期維護台灣森林保育，特以小行星銘版感謝其付出。蔡沛倫攝

V
附錄

A.1 FocuxMax V5 設定

侯偉傑

安裝

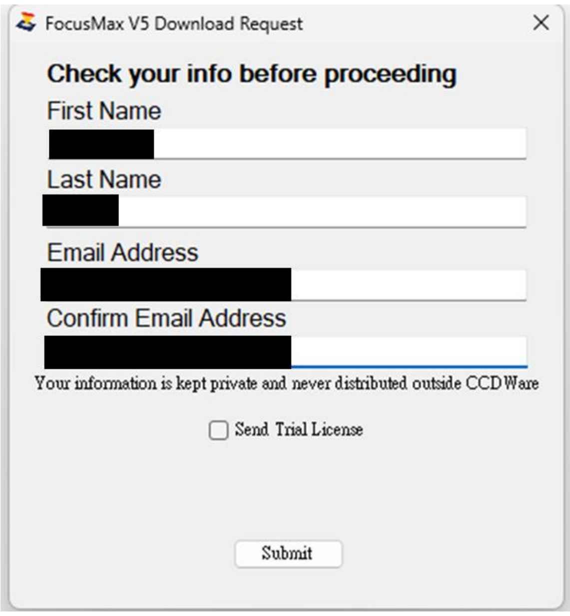

輸入資料與 License file 請問明新

安裝完後要將 license 檔案複製到 FocusMax V5 安裝的資料夾中

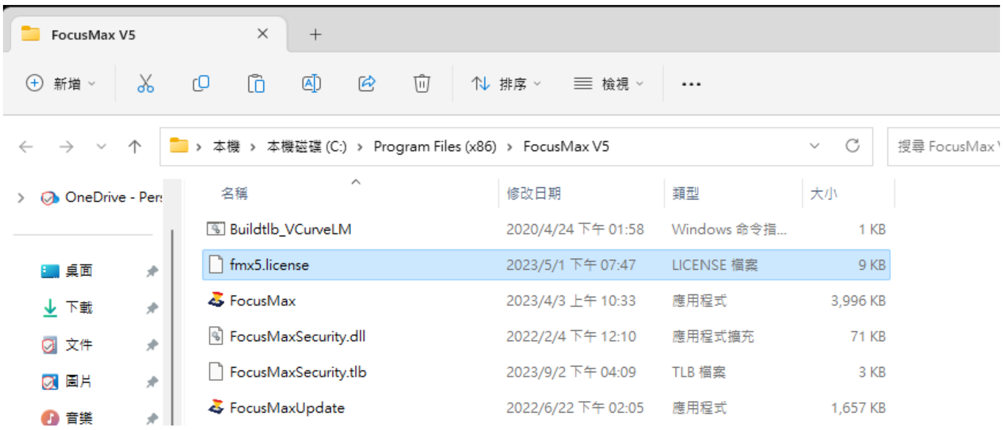

設定 Configuration

第一次打開要先選 ini 檔：system 1 > ... > 選 Hardware1

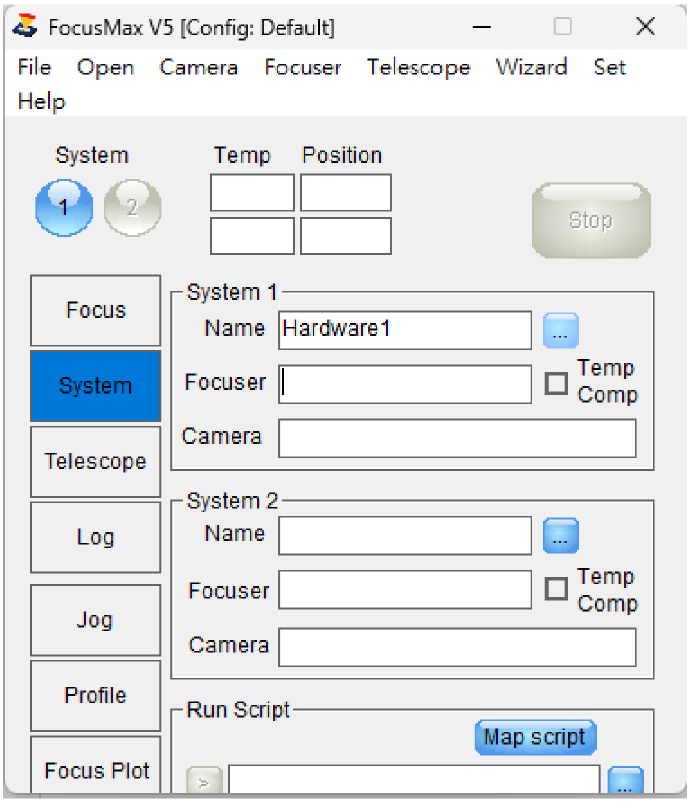

然後打開上面 Tabs 中的 Open > Preferences 準備設定 Focuser, Camera

Camera & Focuser Connection

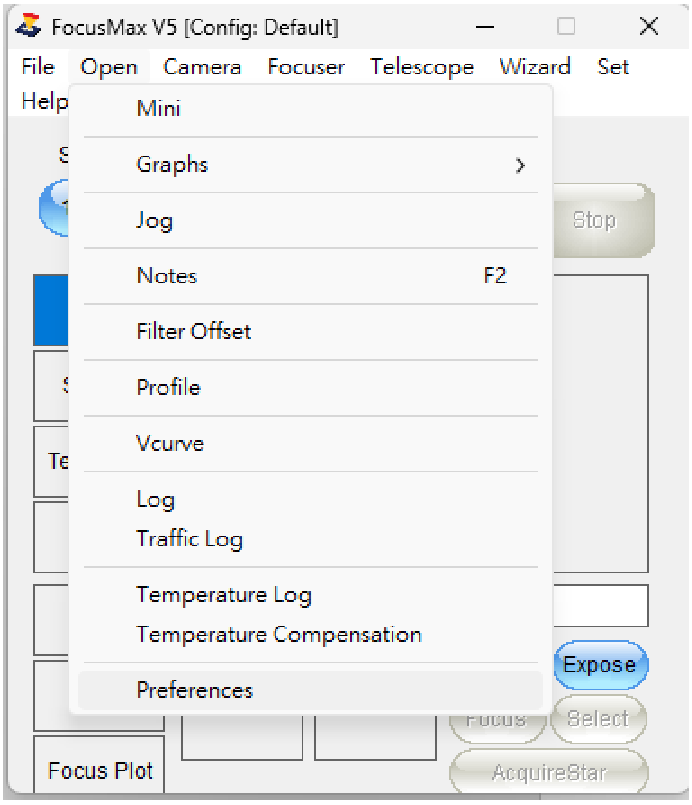

Preferences 視窗 > System1 區塊

- Camera control 選 MaxIm DL
- Number 選 1 (代表 MaxIm DL 中的 Camera 1)
- Filter wheel 不用選，連上後會自己出現
- 然後可以按上方藍色 Camera 按鈕連連看

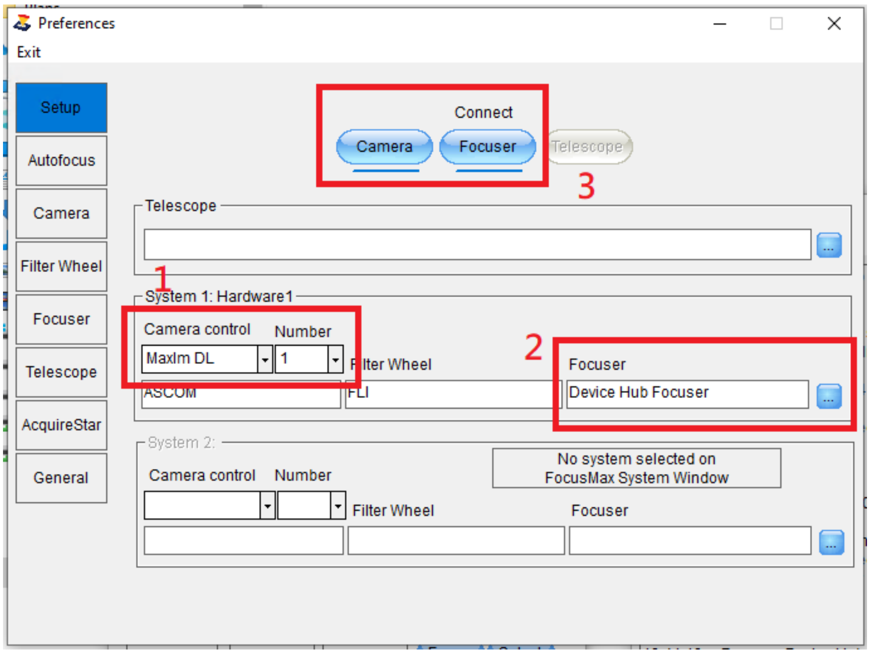

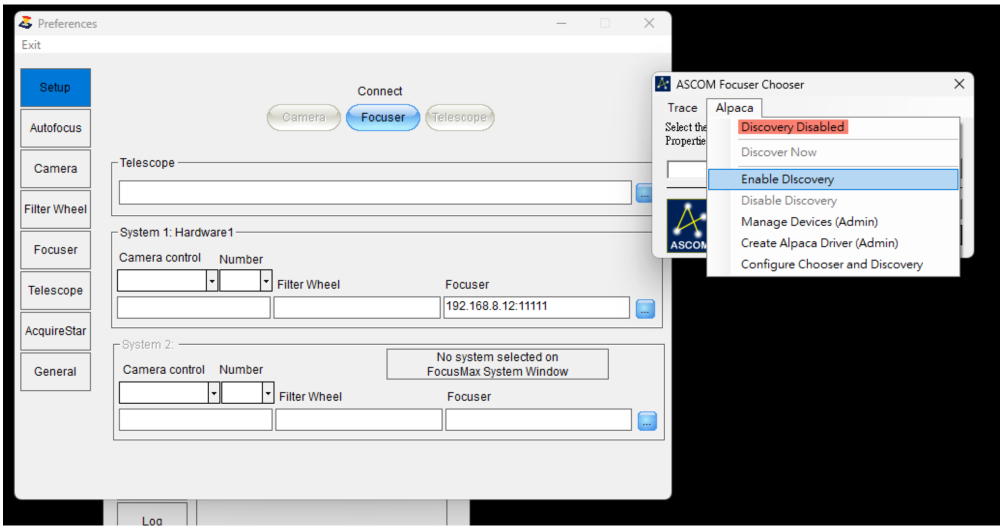

Preferences 視窗 > System1 區塊

- Focuser 旁邊的 ... 按鈕 > ASCOM Focuser Chooser 視窗 > Alpaca > Enable Discovery (請看注 1)
- 然後選單會出現 New ALPACA DEVICE ... ，選它
- 然後按上方藍色 Focuser 按鈕連連看

注：

LOT 連線 Autoslew 需要使用 ASCOM Remote Client，需要 ASCOM Platform 6.5 以上才有內建。

安裝後第一次開啟才需要設定這些，之後只要按首頁的「藍色 1 按鈕」即可自動連線。

First Light

安裝後第一次開啟還需要執行 First Light

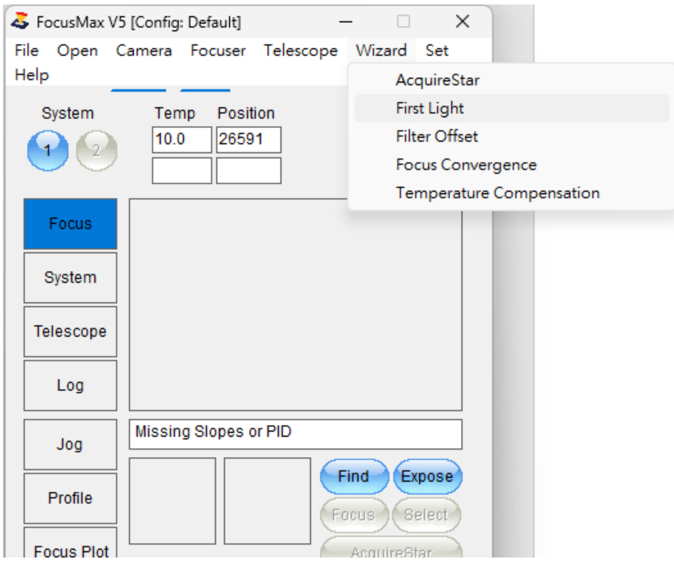

點選 First Light 後會出現提示視窗，遵照提示視窗指示直到出現 Vcruve 視窗。

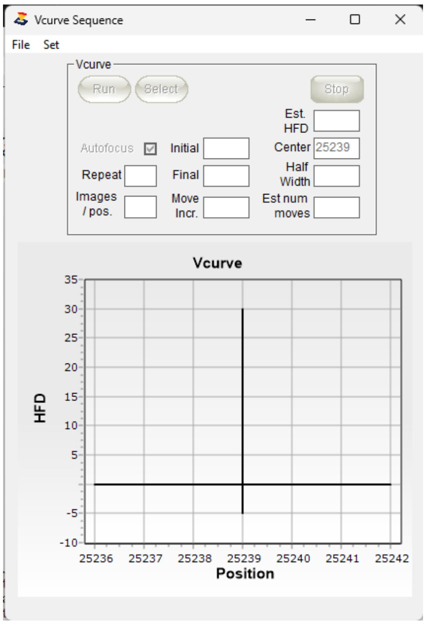

做完 Vcuver 就可以使用了。點選 Focus 就會開始對焦。

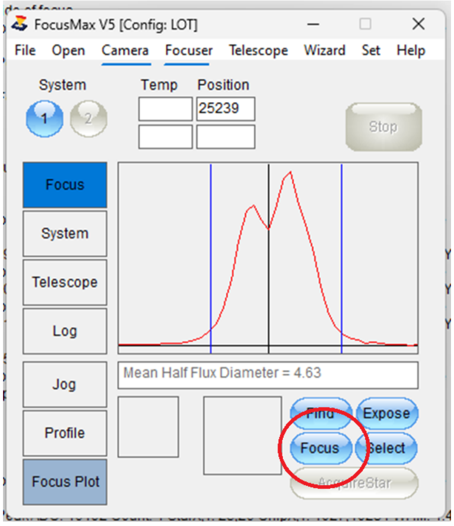

可以看 Log 查看狀態，若對焦完成會顯示 AutoFocus Completed。

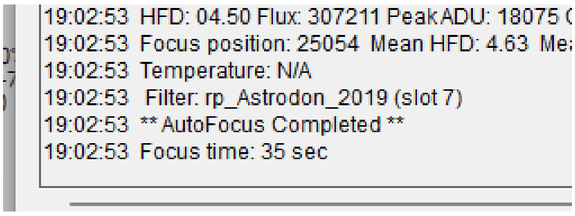

其他

剛設定好的 FocusMax 對焦在每個選定的焦位置都會拍攝約 10 張照片來測量 HFD，若選擇的星點較暗則會花較久的時間(約 5 分鐘)。

若希望在較短時間內對好焦，可以調整 Preferences > Autofocus 中的 Near Focus Sample 設定，將數字調小即可。

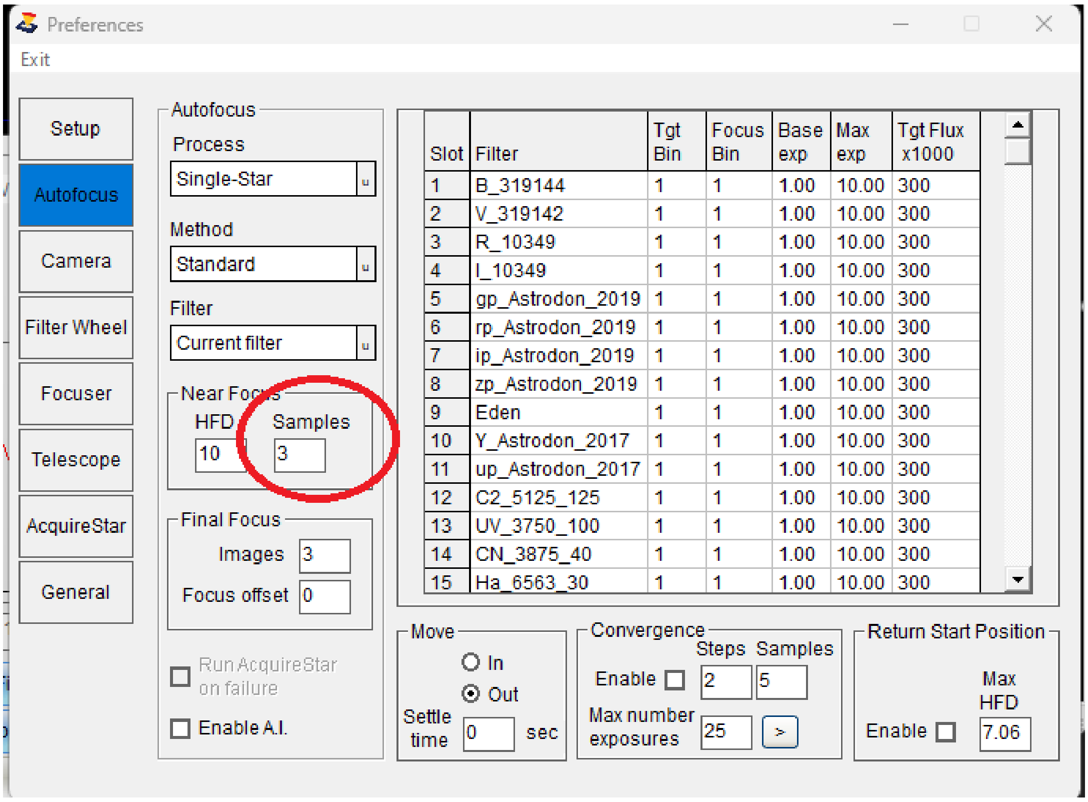

A.2 LOT PC 設定集

侯偉傑

ACE SmartDome

第一次使用需要以管理員身分執行，第二次開始就直接打開就好

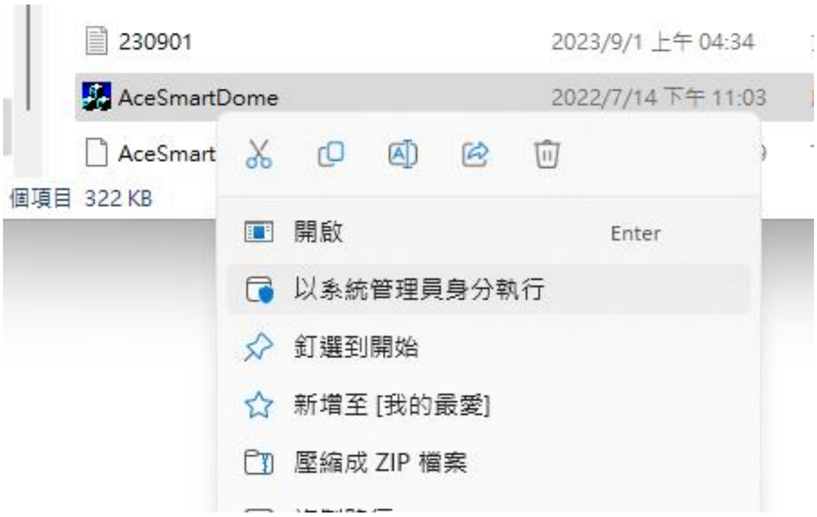

打開後連線用 TCP/IP 連線，按 connect 會要求輸入 IP，IP 為 192.168.8.51

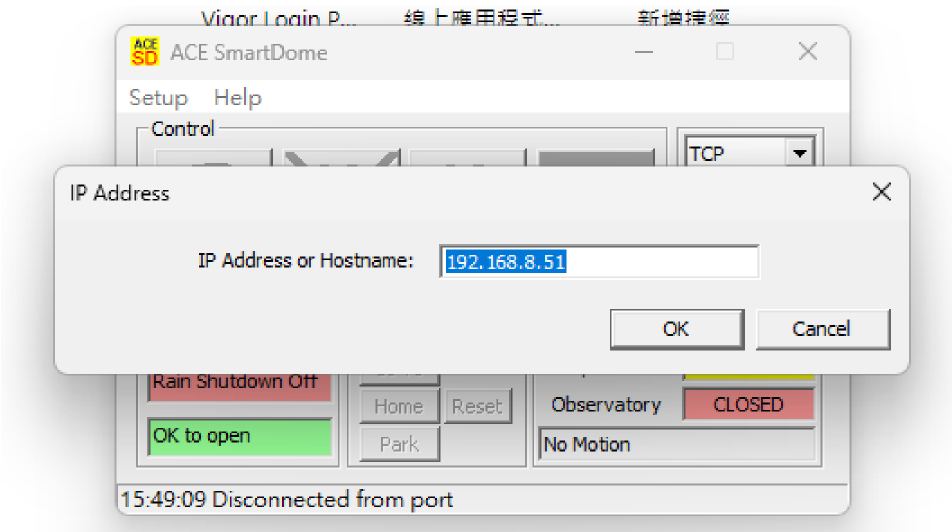

連線後設定 park 位置為 5 degree，這樣 park 時圓頂看起來與建築物是正的。

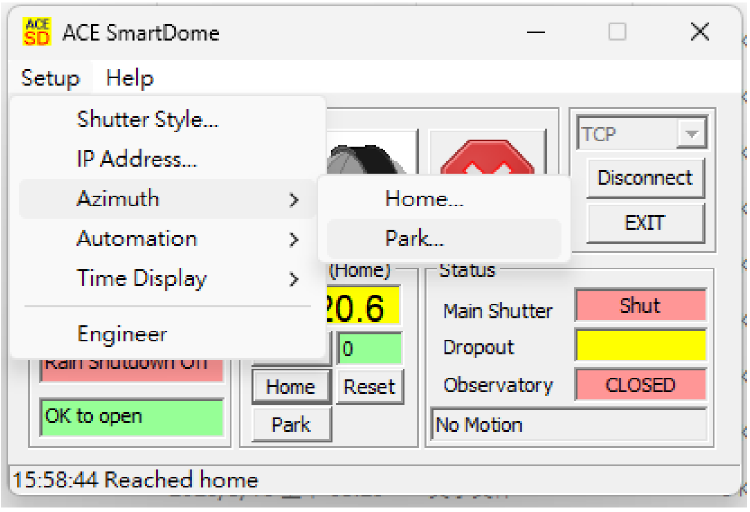
ACE SmartDome
Setup
Help
Shutter Style...
IP Address...
Azimuth
Automation
Time Display
Engineer
Home...
Park...
TCP
Disconnect
EXIT
(Home)
20.6
0
Home
Reset
Park
Status
Main Shutter
Shut
Dropout
Observatory
CLOSED
No Motion
OK to open
15:58:44 Reached home

MaxIm DL 5/6

Camera : Andor iKon-L 936

安裝完 AndorAscomSDK2 驅動之後可以直接在 ASCOM 中找到 Andor 選項

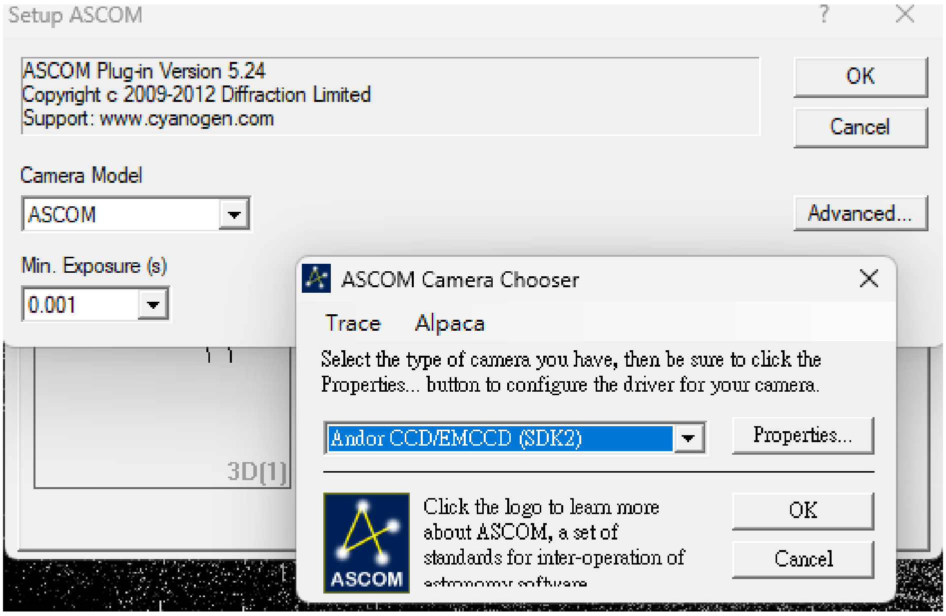

第一次連線需要改：

- Readout Mode : 1 MHz
- Pre-Amp Gain : 4x

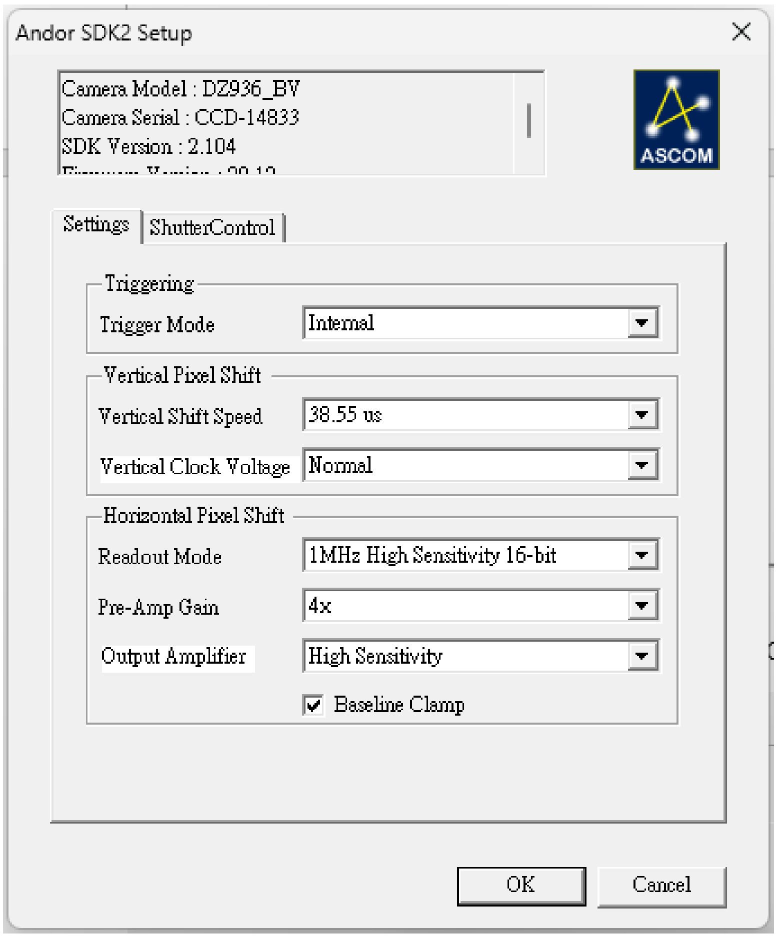

Filter Wheel

https://www.dropbox.com/s/oz9jmy51ureij3m/ACESmartFilterASCOM.exe?dl=0
需要使用此版驅動才能正常運作

選擇 ASCOM

1. 依濾鏡順序輸入濾鏡名

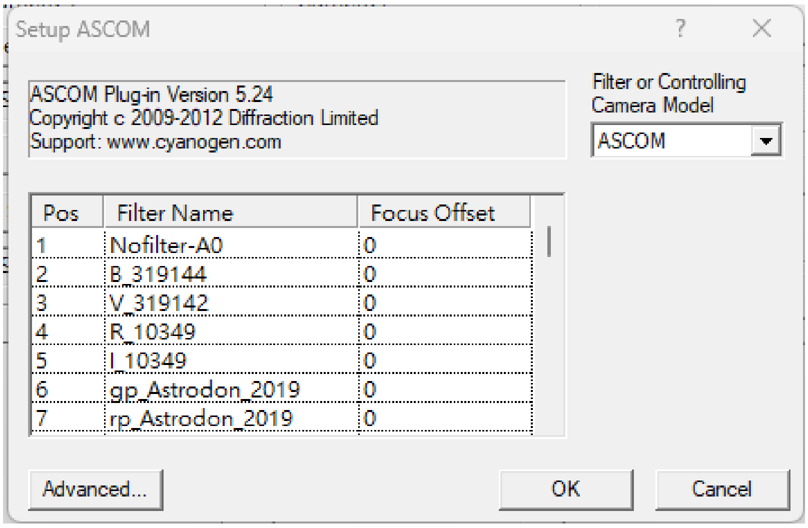

2. Advanced... > ACE SmartFilter > Properties...
   選擇 Com Port
   新 LOT SmartFilter 有上下兩盤，各有十格位置，可以裝 18 片濾鏡(上下盤各一格空濾鏡)，所以 Filter name 從 Filter0 到 Filter19
   Filter0 到 Filter19 的 Focus offset 的 0 也要十個

然後都按 OK 即可連線

ACP Observatory

設定座標

第一次開啟需要設定座標。

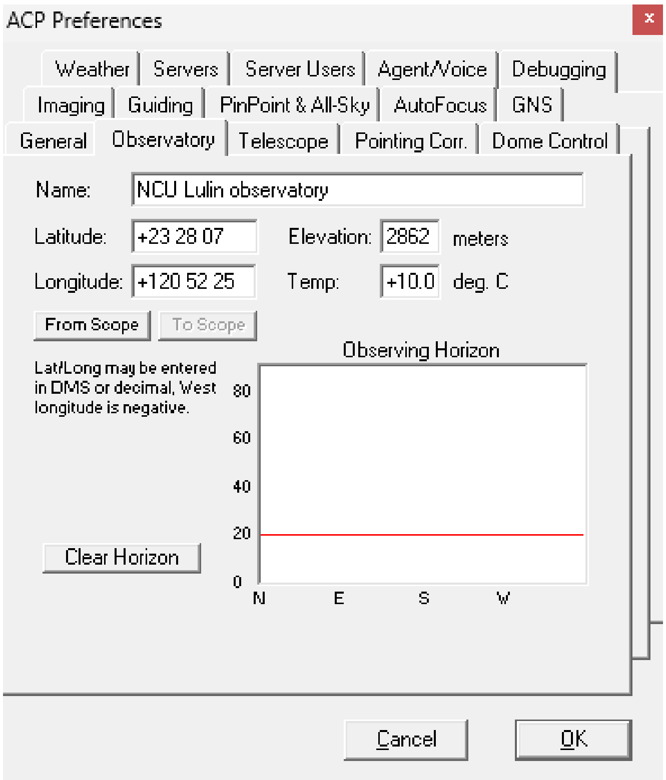

設定望遠鏡

Telescope > Setup

Alpaca > Enable Discovery > 選 NEW ALPACA DEVICE > 都按 OK

選項最後自己會變成 Autoslew Telescope (Alpaca)

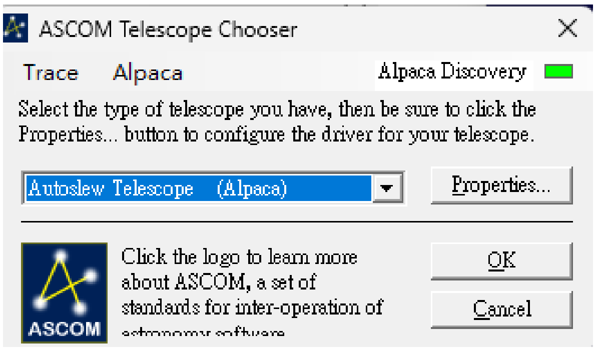

連線後再到 ACP Preferences > Telescope 設定參數

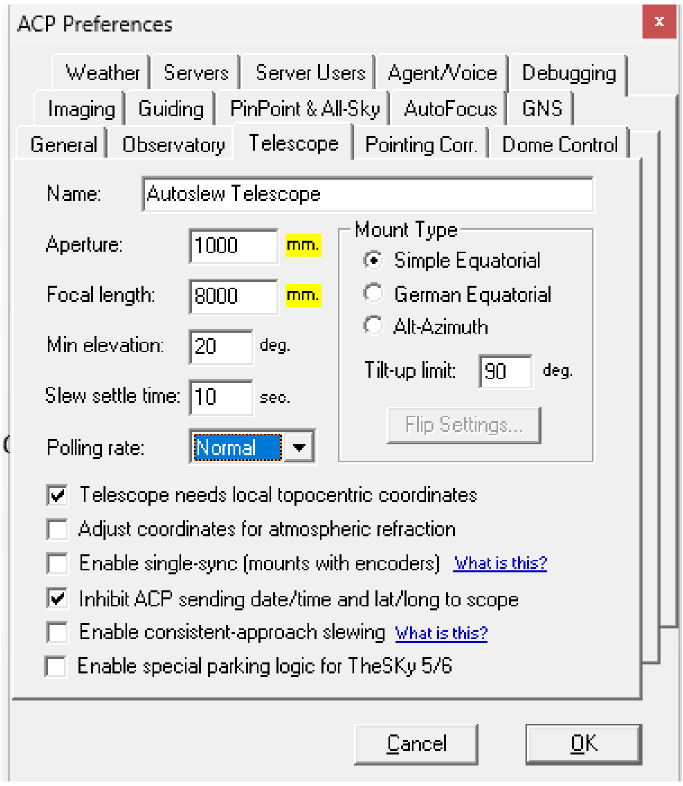

Dome Control

ACP Preferences > Dome Control > Select Dome > 選 ACE Smart Dome

然後設定參數如下

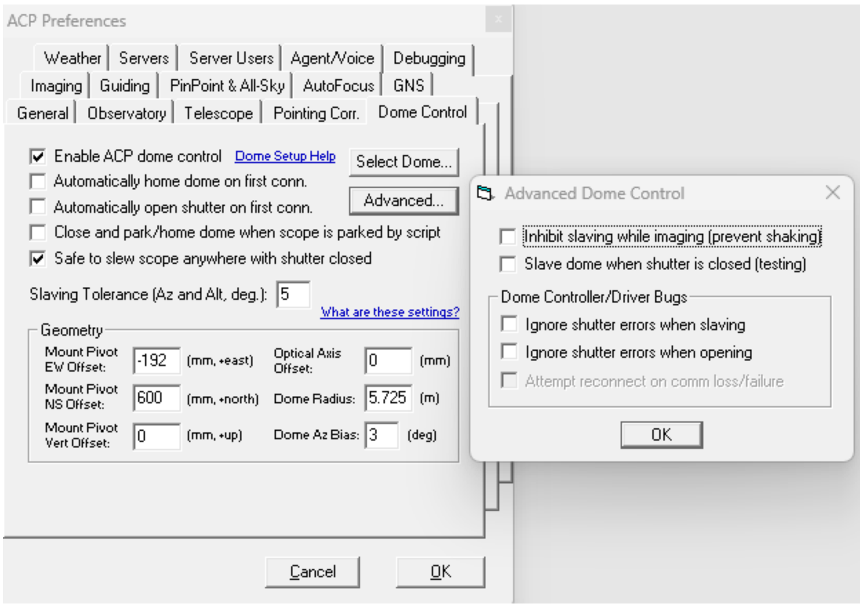

PinPoint

設定如下

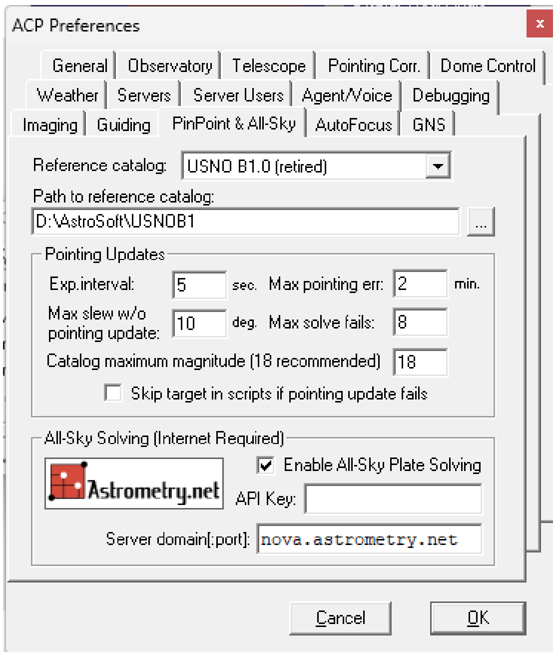

AquireImages.js

為了讓 script 中的 $DATETIME 參數可以使用，需要從其他望遠鏡中複製 “C:\Program Files (x86)\ACP Obs Control\Scripts\AquireImages.js” 這個檔案到新電腦的此路徑。
注意：目前這個檔案是基於 ACP9 修改的，若不是 ACP 9 用此檔可能會出問題。所以需要另外修改

ACP Config

可以將舊電腦的 “C:\Users\Public\Documents\ACP Config” 複製到新電腦。
或是修改

PHD2

導星相機為 ZWO ASI 174，要連線需要先安裝驅動
https://www.zwoastro.com/downloads
到網址下載這兩個驅動並安裝

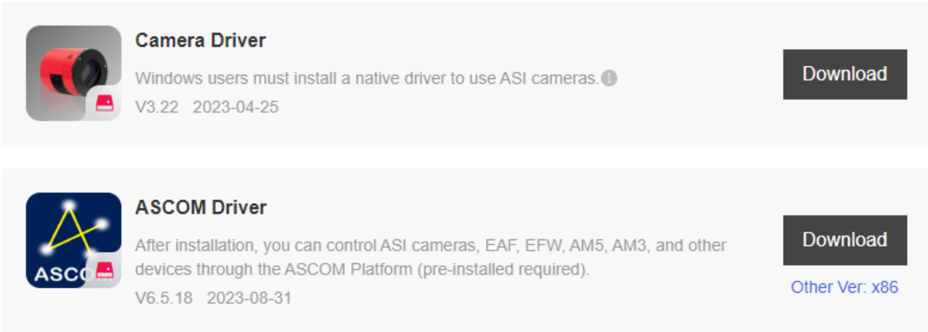

到進階設定中，導星頁面找到校準區塊的「焦長」改成 8000 mm

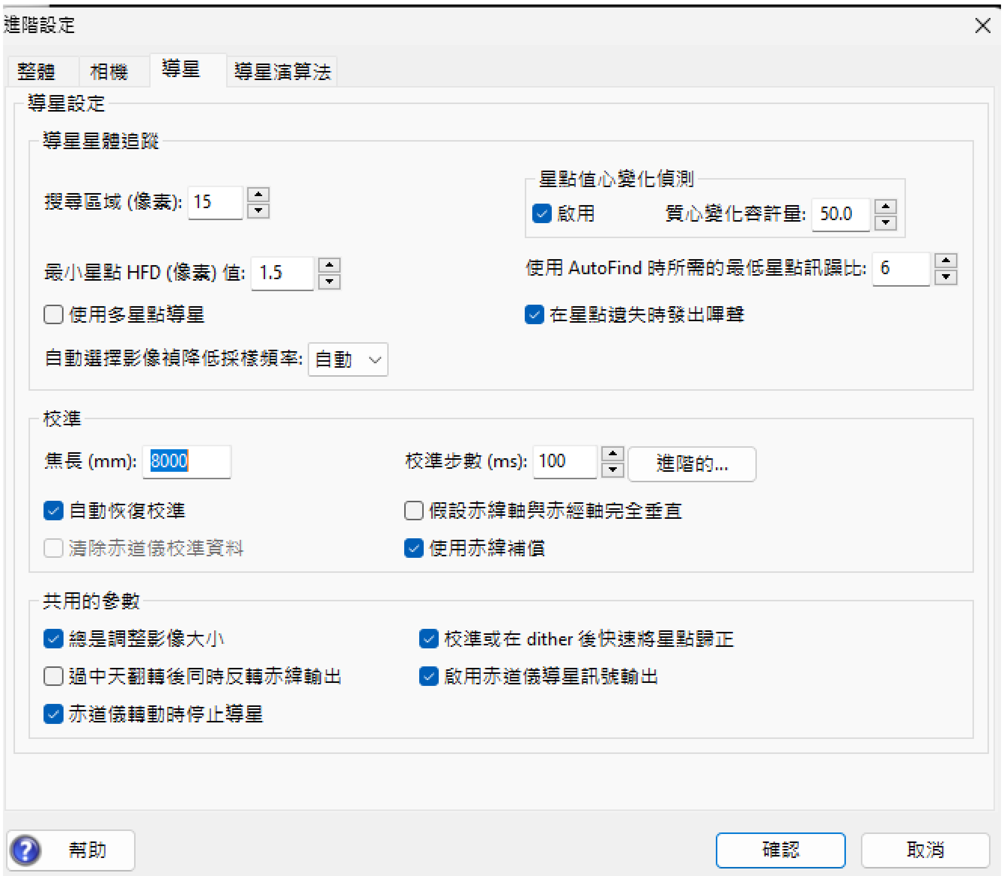

相機頁面將「相機特有屬性」的「影像合併」改成 2 (較不受雜訊影響)

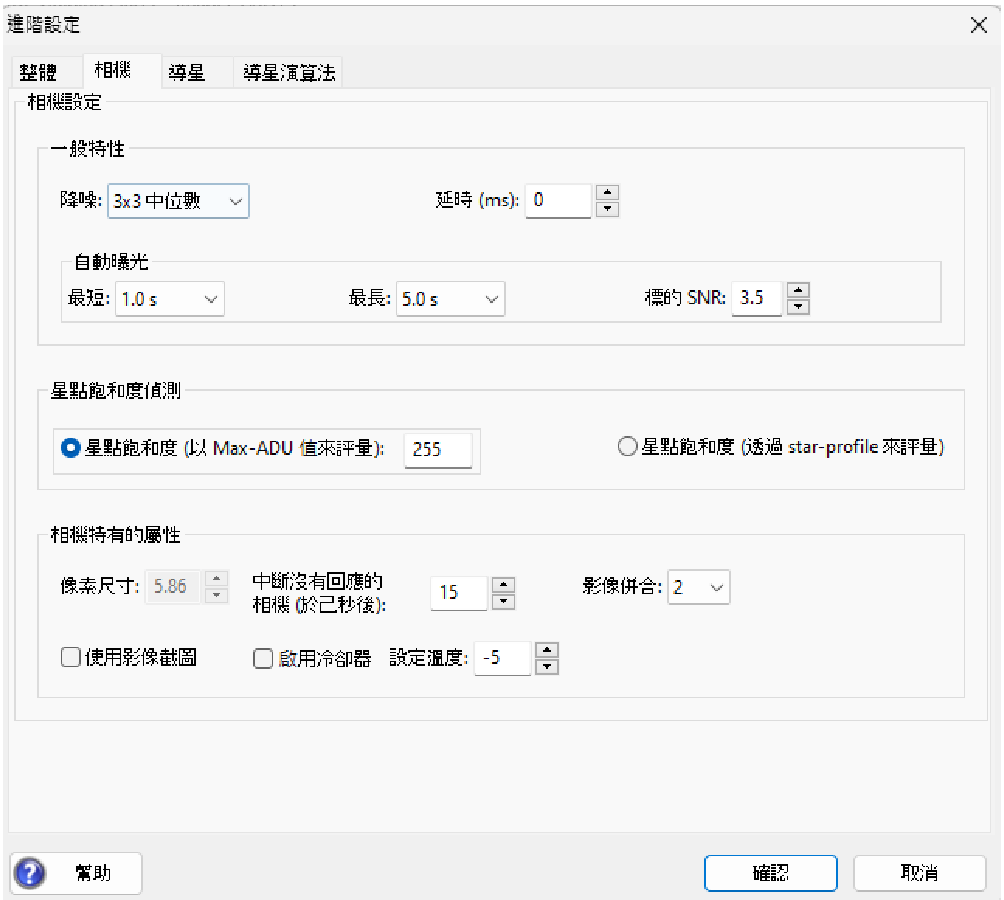

第一次執行或換儀器需要強制校準 (選星之後 Shift-Click)

TheSky 6

連線望遠鏡需要使用 Telescope API
需要到 ASCOM 官網下載 plug-in
https://ascom-standards.org/Downloads/Plugins.htm

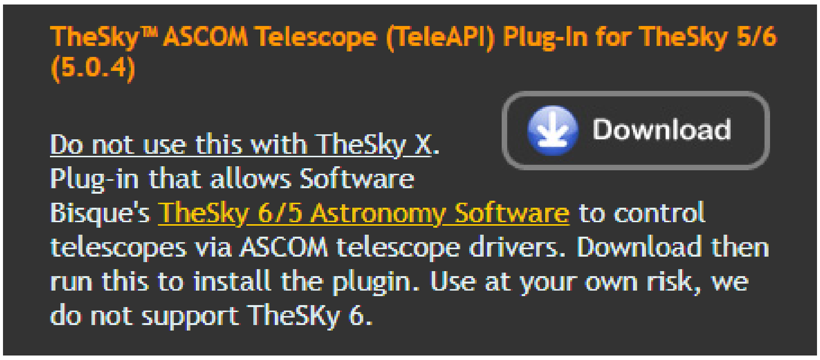

須注意 TheSky6 版本必須為 6.0.0.65 (Help > About TheSky6 可以檢查)

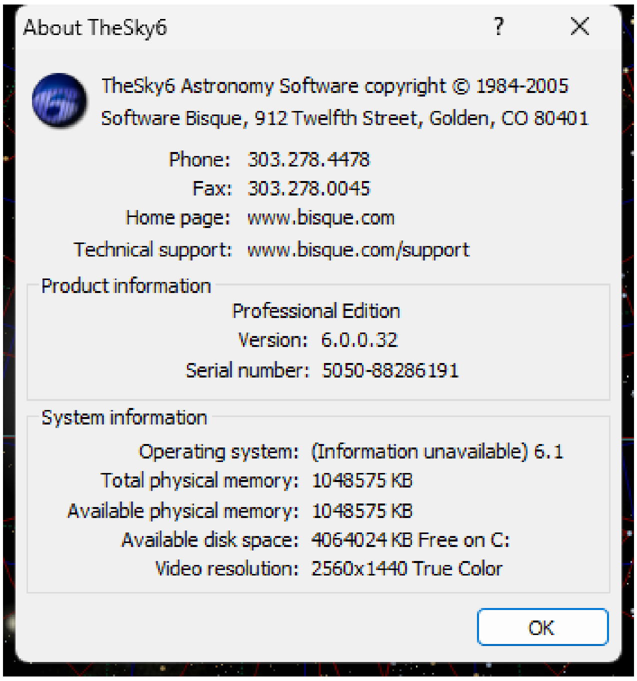

若是 6.0.0.32，會造成 Move To 功能無法正常 slew 到 J2000 座標位置。
到 AstroSoft\TheSky6pro 中找到並執行 TheSkyV6.0.0.65Update.exe 之後即可
更新後版本會升至 6.0.0.65，此時再使用 Move To 功能 J2000 就有效了。

SiTech TimeServer

到 AstroSoft 中找到 SiTechTimeServerInterface1_1.exe，或是到 http://siderealtechnology.com/SiTechTimeServerInterface1_1.exe 下載。之後安裝 TimeServer。

安裝好後要利用”Adminstrator”開啟，之後到 Software Config 頁面設定 ip。
前兩個都設定 192.168.8.10 ，填好後按下按鈕測試連線。
有時需要多按幾次才能成功連線，都連線成功後按下左下方 Save Configuration 按鈕。

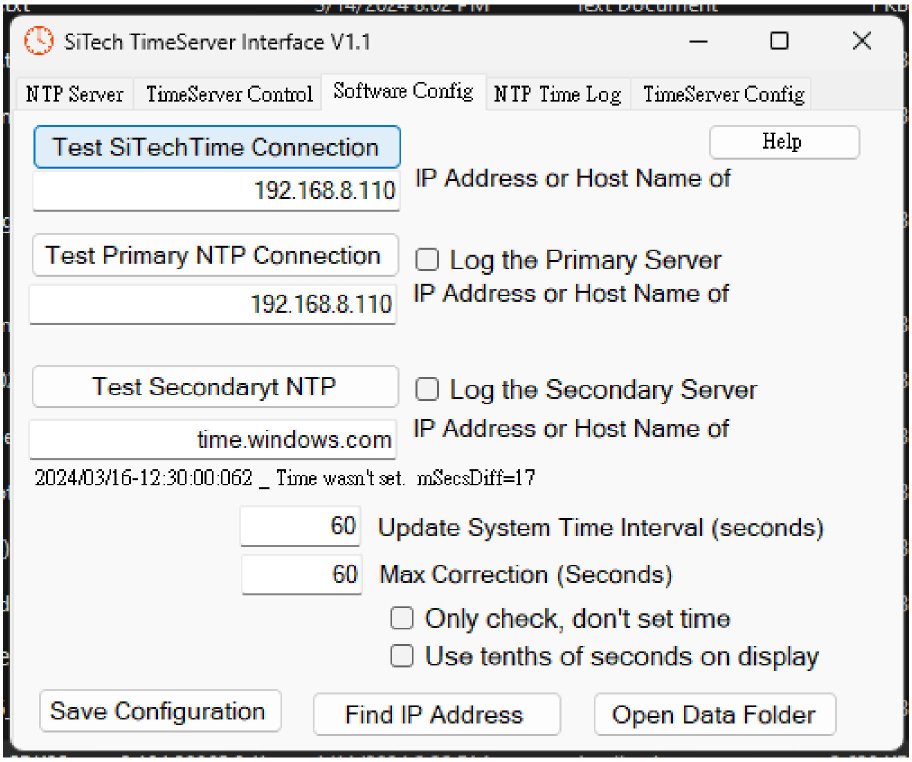

Spectroscope

LISA

SPOX

https://www.shelyak.com/produit/module-spox/?lang=en&attribute_modele-de-spectroscope=LISA&attribute_longueur-du-cable=Without+cable
到此網頁的 Softwares and drivers 找 The WINDOWS application to control the SPOX module from your pc (file to unzip) 下載

選 COM 連線

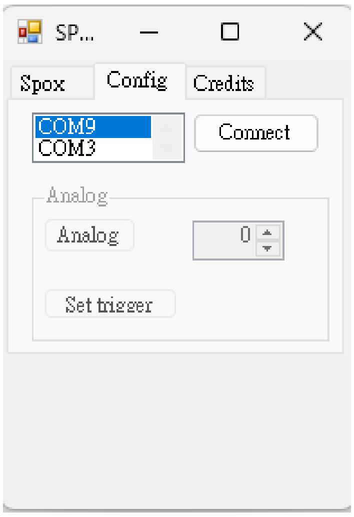

UVEX

Detrema

https://www.shelyak.com/produit/uvex-motorized/?lang=en
Softwore 找 Demetra UVEX Version 下載

A.3 LOT Pointing Model 重作步驟

侯偉傑

本篇按照 ASA Autoslew Manual 的作法來作 Pointing Model，因操作時沒有全部截圖，所以有些圖來自 Manual 中。

調整 Pointing 需要一直拍影像確認星點位置，所以可以將相機換成行星相機搭配 Live View 來操作會較方便。

若已經有 Pointing Model 且認為這個是不準確的，那要先將舊的 Pointing mdel 清除。

點選 Clear and reset Configuration

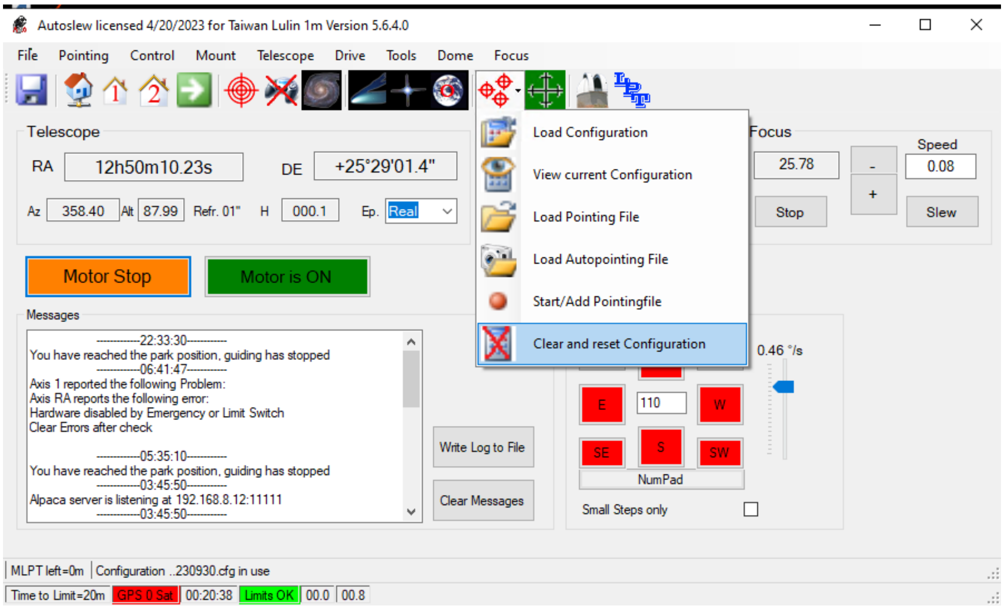

先將望遠鏡移到某顆星，並確認它在 FOV 的中央。然後 Sync。(可以用 Thesky 操作)

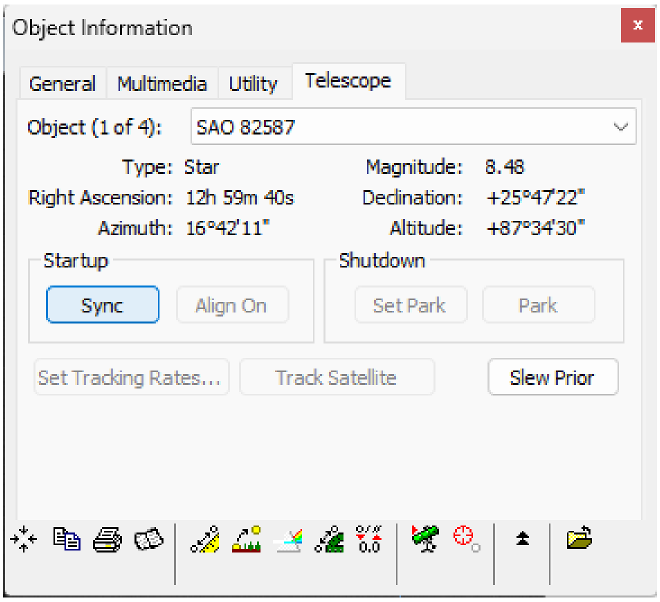

點選 Start/Add Pointingfile，跳出的視窗按 OK

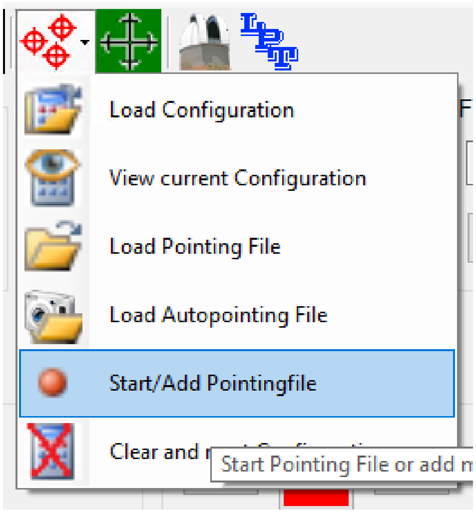

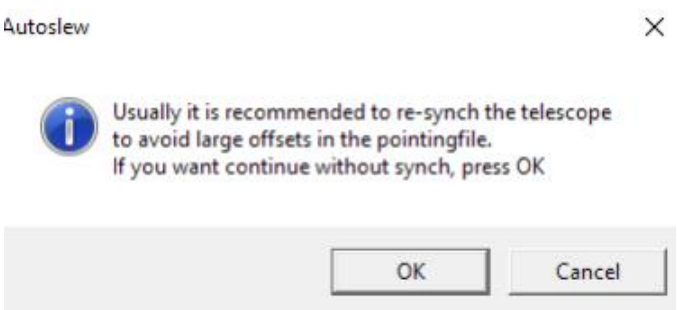

選擇儲存的位置與設定檔案名稱

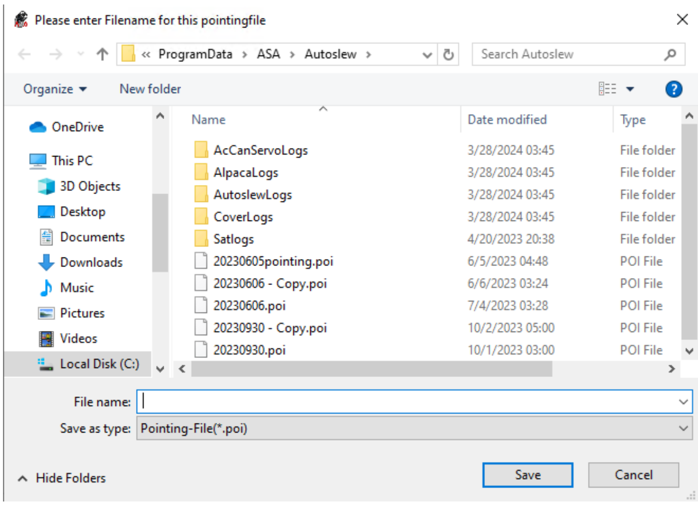

左下角會顯示 Please slew to star 1 now

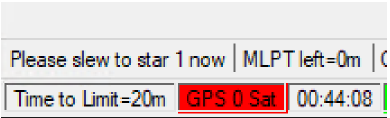

目前的望遠鏡位置應該還在剛剛作 sync 的星上，再選一次這顆星然後 slew。此時這顆星應該在 FOV 中央，按下 autoslew 的 Confirm。

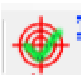

Confirm 之後左下角會顯示 Please slew to star 2 now
Thesky 選星 slew，等 slew 結束後檢查星點是否在 FOV 中央，若不在中央就用 autoslew control panel 控制使之移到中央。
然後再按下 Confirm。

重複這個動作直到認為點數夠多了。盡量讓目標位置遍佈在全天空中。

按下 Stop Pointingfile、然後按 Calculate Configuration

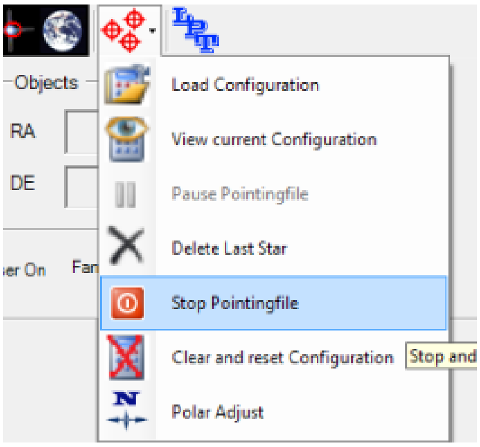

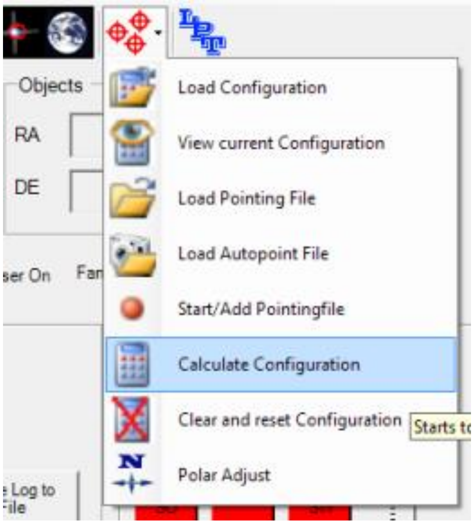

選 normal Optimization 然後 start

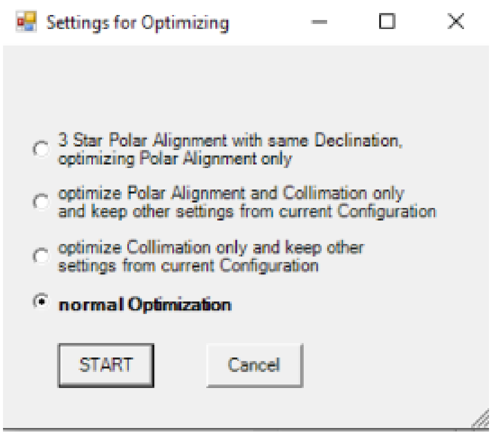

選 Use now

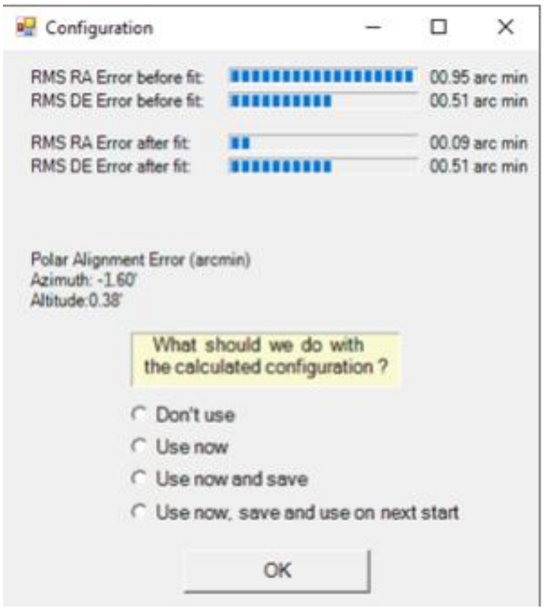
Configuration
RMS RA Error before fit: 00.95 arc min
RMS DE Error before fit: 00.51 arc min
RMS RA Error after fit: 00.09 arc min
RMS DE Error after fit: 00.51 arc min
Polar Alignment Error (arcmin)
Azimuth: -1.60'
Altitude:0.38'
What should we do with the calculated configuration ?
Don't use
Use now
Use now and save
Use now, save and use on next start
OK

B.4 SLT Pointing Model 重作步驟

侯偉傑

本篇參考自 PlaneWave Ascension 200HR German Equatorial Mount Instruction Manual。

先檢查設定

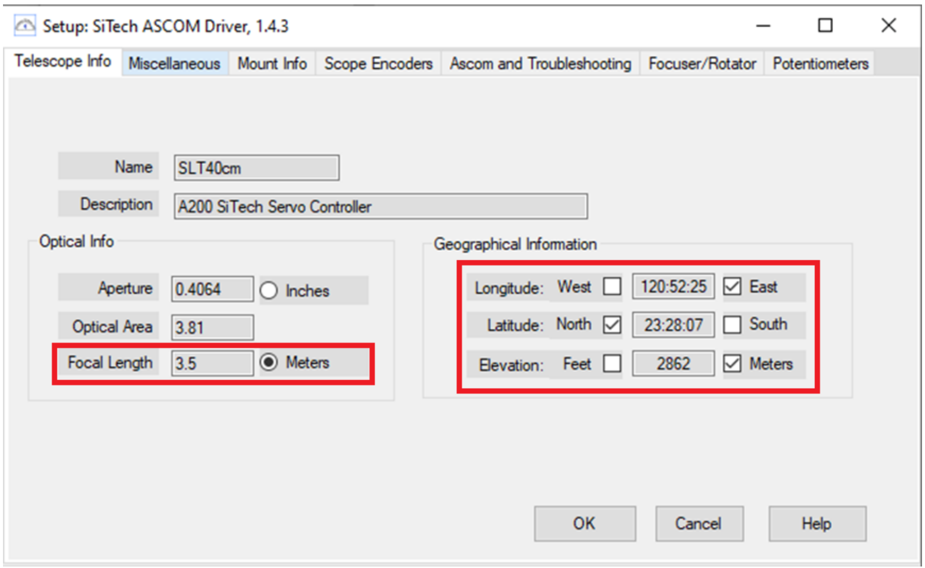

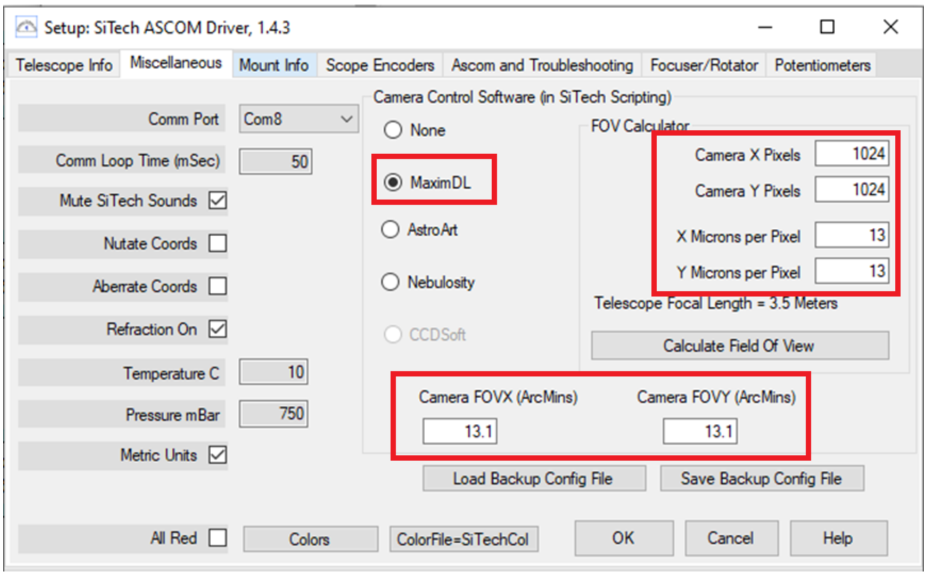

先將望遠鏡 Home。

打開 Sky Chart 與 PointXP

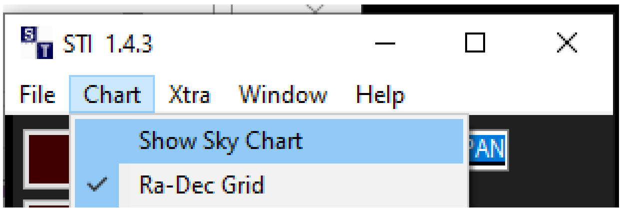

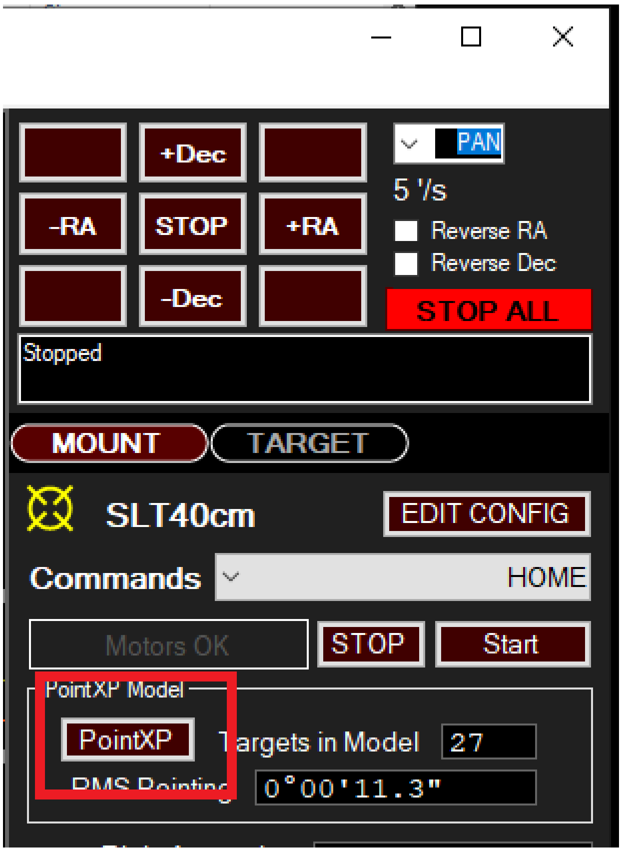

如果之前有做過 Pointing model(Targets in Model 不是 0)要按”Clear Terms And Cal Stars”

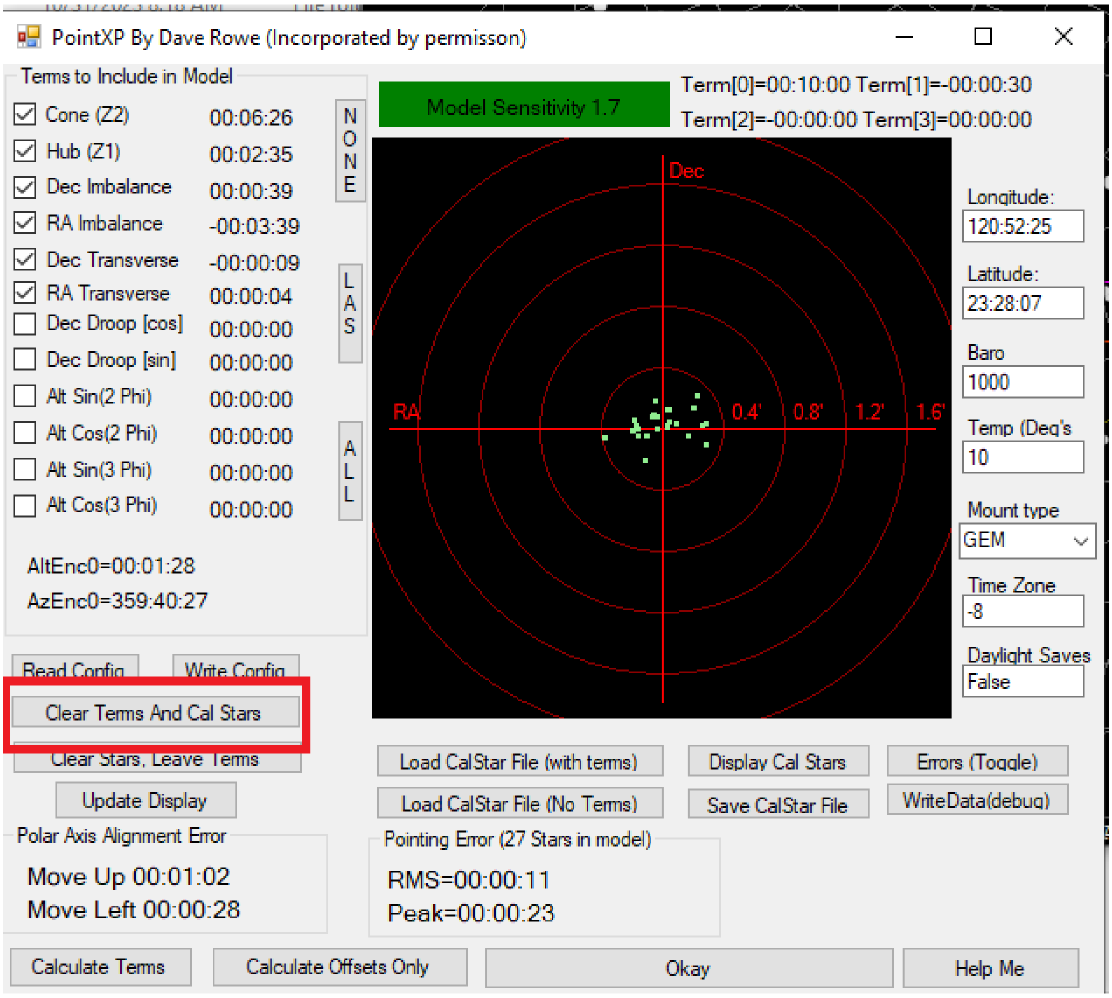

在 Commands 選”RUN SCRIPT”，調整 Number of cal points，可能設個 20~40 個點就可以了，不過要做多一點也是可以。將 Pause after each slew 勾選，因為這個 STI 僅能控制赤道儀，無法控制圓頂，所以 slew 到定位之後要等圓頂到再手動繼續。

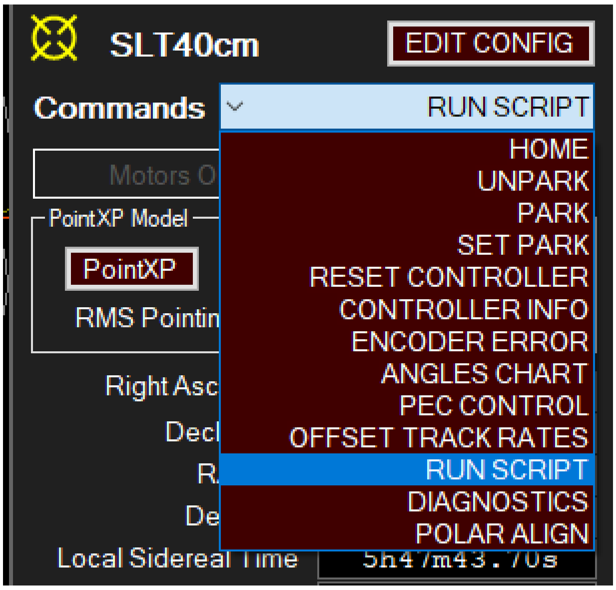

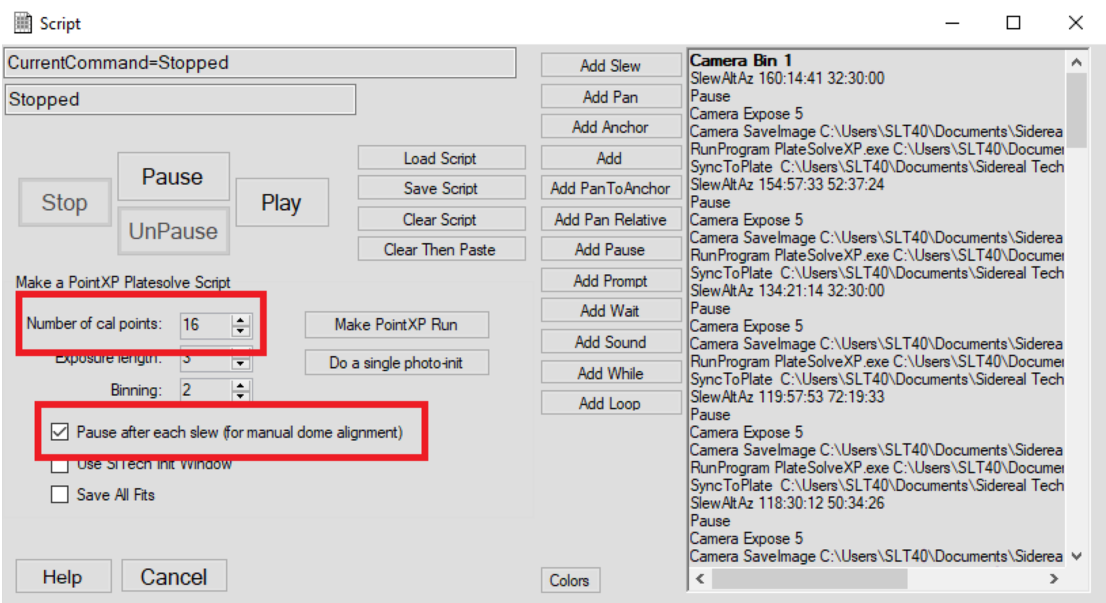

設定好後按” Make PointXP Run”。會出現 CalPointsXP 視窗，按 SE 或框中其他方位，再按 Make Points，這樣點的順序就不用讓圓頂每次都大幅移動。然後關掉這個視窗。

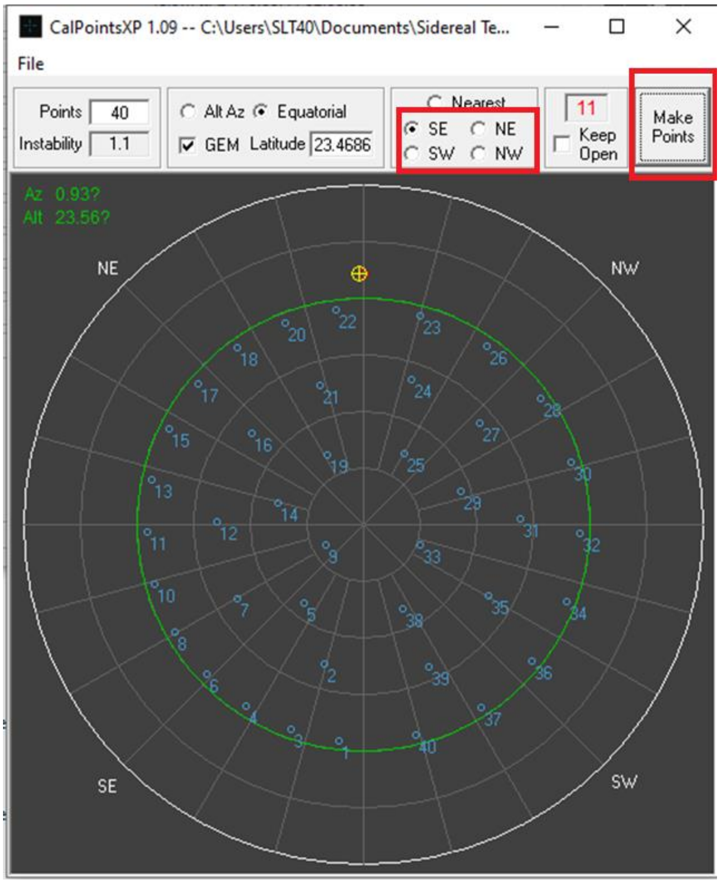

回到 Script 視窗按 Play，程式開始會移動望遠鏡到各個點，然後拍照解星場位置。在每次 slew 結束後就檢查攝影機看 point 是否與 slit 方向一致，等一致就按 play。程式會自動拍影像解星場，如果這個時候出現 error “path not found”，可能表示沒有安裝 APM Star Catalog，請到 PlaneWave 網站>Software and updates>SiTech Interface(STI)下載 AMP Star Catalog Installer 並安裝。

所有的點都做完之後，可以檢查 Polar Axis Alignment Error 與 Pointing Error，看看是否有需要再做調整或重作。

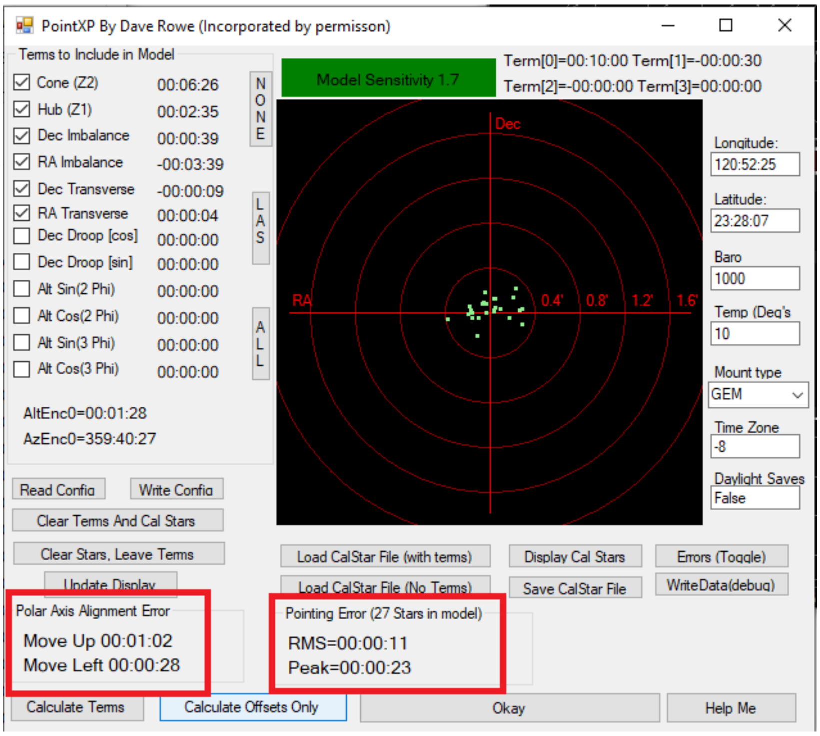

最後再到 Home 的視窗，Primary 與 Secondary Axis 都有一個 Find Transition Angle 的按鈕。先按 Secondary Axis，等望遠鏡移到定位之後，Transition Angle 數值會大概在 90。然後再按 Primary，一樣到定位後數值會大約再 270。然後就按 OK，程式會儲存 C:\Users\SLT40\Documents\Sidereal Technology\STI\HomePointXP.PXP，可以將這個檔案複製一個並標註日期，以便未來使用。

注意一定要按 OK，不可以按 Cancel 或是把視窗關掉，不然前面步驟都要重做。

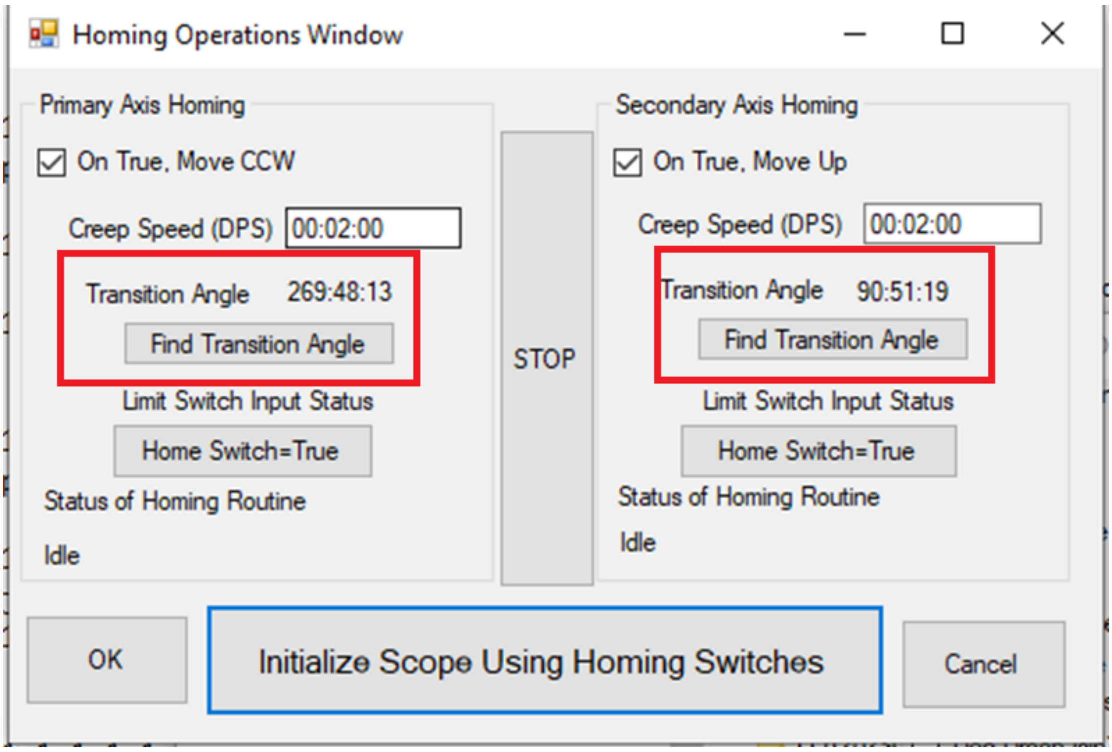

C.5 SLT 影像在 RA 方向跳動 (尚未解決)

SLT影像在RA方向跳動

Tags: slt

Problem:

Ra方向跳動問題，12號有一張，

Solution:

14號開始觀測前依偉傑建議把電腦時間改為非自動，由校時軟體校正，14號未發生跳動，請再觀察。

admin reported at 2023-03-16

Problem:

17跟18日沒有，19日一次，20日1次，21日沒有，22日5次，都是janet，23日6次都是janet，24日忠義4次，janet 4次 .

Solution:

尚不知道原因

admin reported at 2023-03-24

Problem:

將 SiTech 校時改成 NTP 校時，再觀察看看是否會出現此問題。

admin reported at 2023-04-23

Problem:

觀察 SiTech 校時軟體的 Log 與晃動的影像時間戳，發現兩者並沒有相關，基本可以排除是校時軟體產生的問題。

但還是無法確定是什麼問題。

weij reported at 2023-06-19

Problem:

與翔耀將 SLT RA/Dec 的渦輪渦桿重新上油，並檢查赤道儀平衡。

要再觀察看看是否還會出現。

weij reported at 2023-06-20

Problem:

整理了以往的跳動資料，發現有一些點發生在東邊天空接近子午線附近
猜測是翻身前停止追蹤

但遠離子午線的位置也有發生，以東邊天空發生次數較多，不太確定是什麼原因

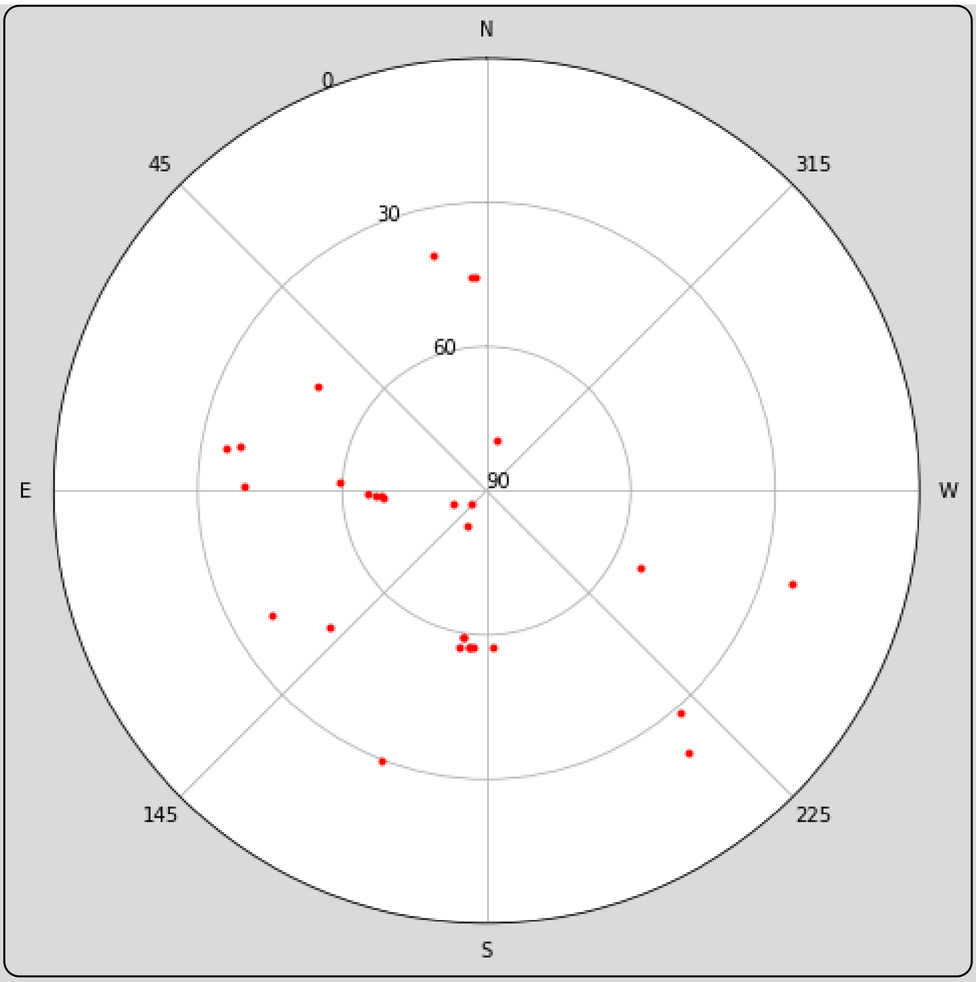

Solution:

在 SiTech Config 中找到 GEM Auto Flip Track 選項勾選。
也許可以避免子午線附近的停追問題？

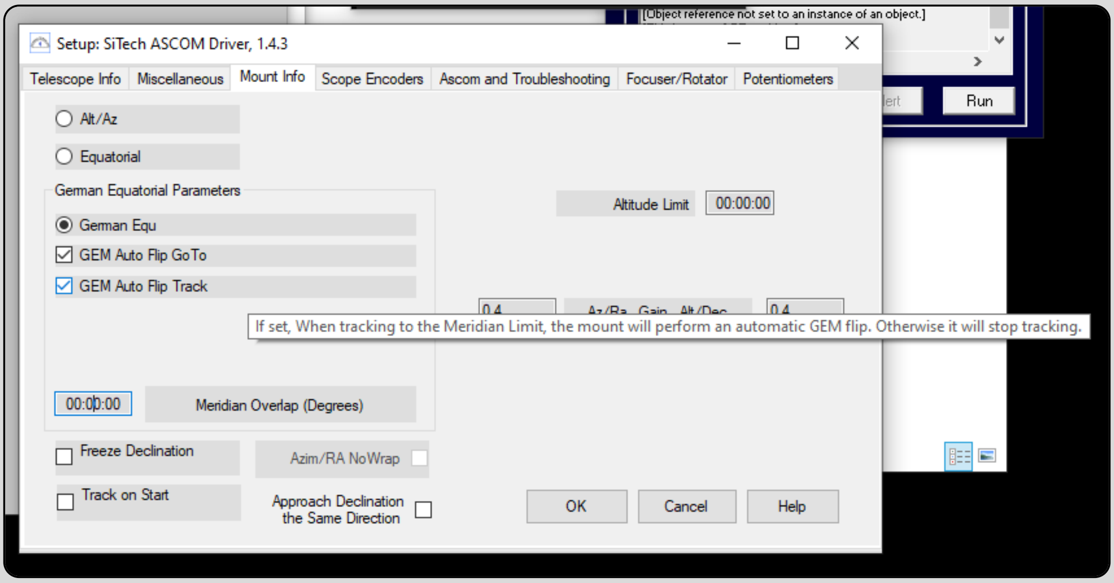

另外之前有發現追蹤時 Dec 有緩慢移動的問題，所以將 Freeze Declination 勾選，使追蹤時不移動 Dec 軸。

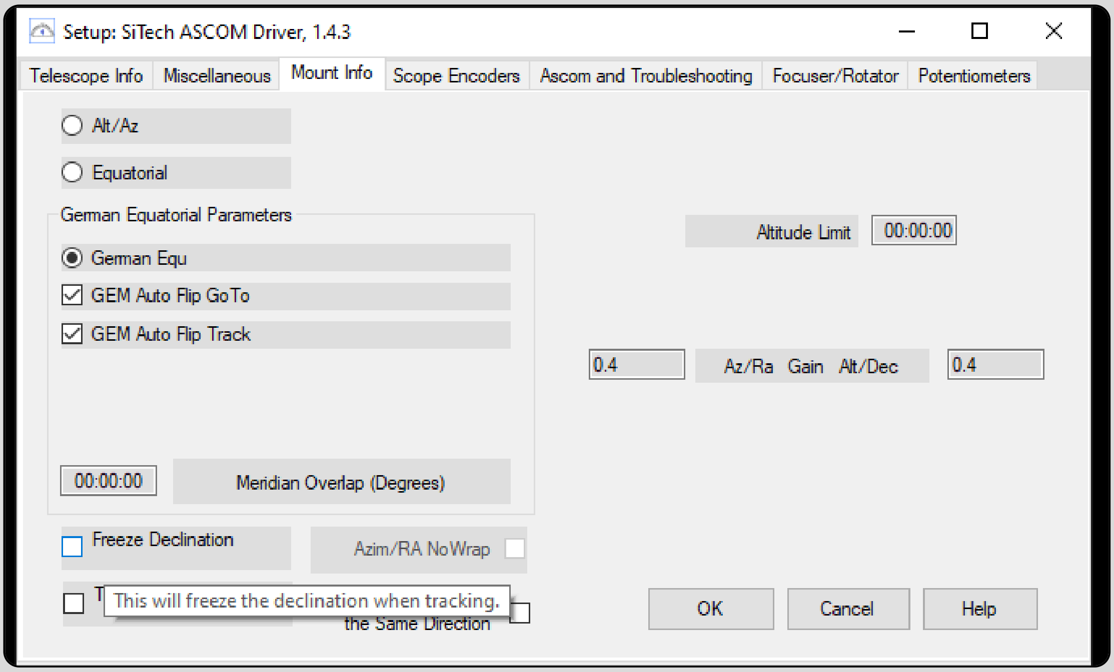

weij reported at 2023-12-25

C.6 新版 autoslew 需更改連線方式

Autoslew 電腦更新 win10，新版 autoslew 需要更改連線方式

Tags: autoslew

Problem:

Autoslew 電腦更新 win10，新版 autoslew 無法使用傳統rs232連線，需要更改連線方式

Solution:

Autoslew-PC 與 LOT-PC 都需要打開 11111 port。

打開 port 後，LOT 要使用 Alpaca 來找
Alpaca > Enable Discovery

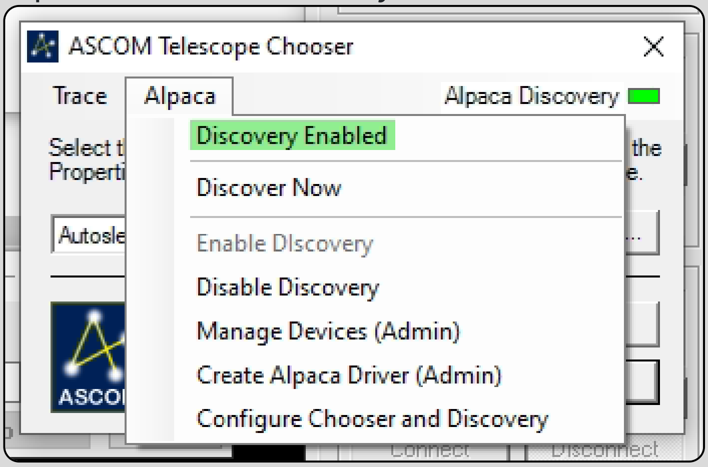

如果找到 Alpaca Discovery 旁邊的圖示會變綠色

然後選單會出現 "Autoslew Telescope (Alpaca)"，選擇然後連線即可

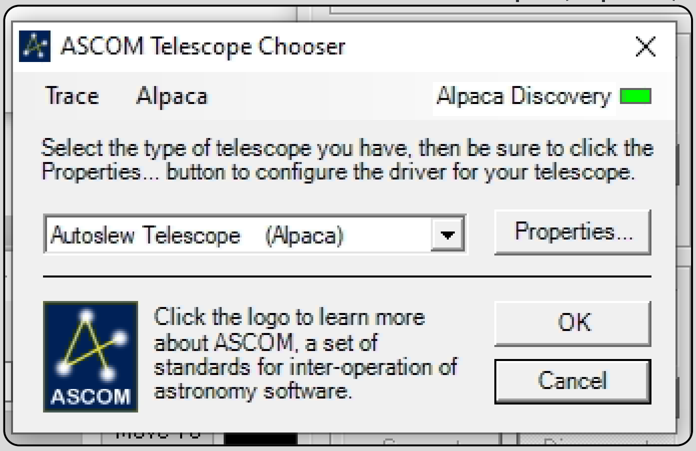

Focuser 也是同樣的操作方式

admin reported at 2023-04-21

C.7 LOT Thesky6/ACP slew 時出現 err

LOT Thesky6/ACP slew 時出現 err

Tags: thesky lot

Problem:

LOT TheSky 或 ACP 在 slew 時會出現 Telescope is not ready, please clear Error

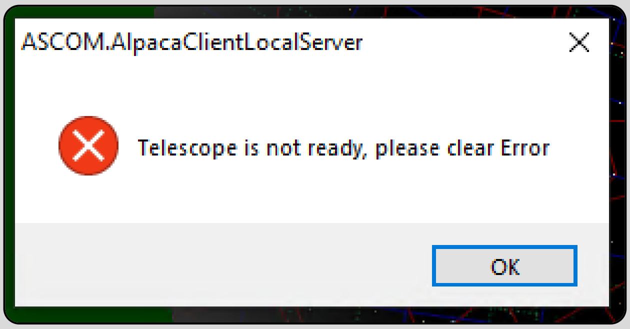

Solution:

1. 檢查 LOT 緊急開關是否有開
2. 檢查是否有 Clear Servoerror 按鈕。若有，按下去即可。

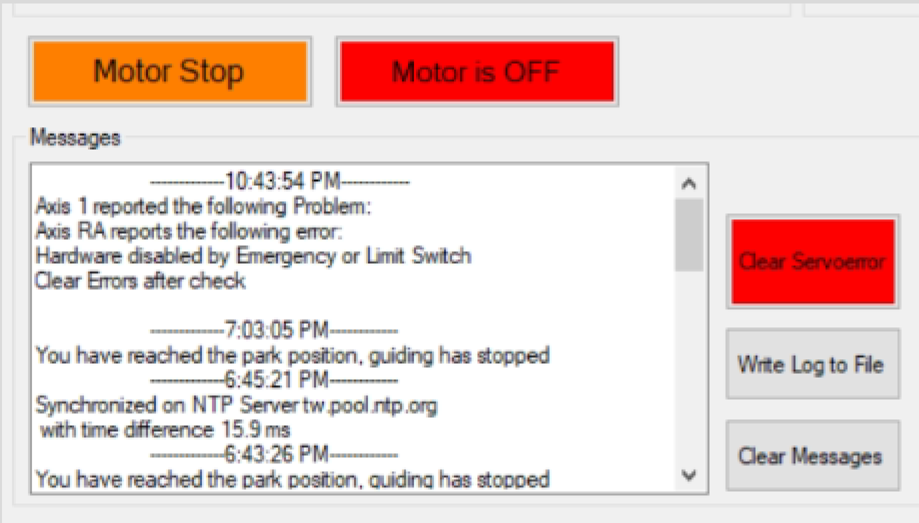

admin reported at 2023-04-22

C.8 若無預警停電，電一斷網路就全斷

若無預警停電，電一斷網路就全斷，也無法去遠端控制LWT&SLT關機

Tags: internet

Problem:

幾次無預警停電，電一斷網路就全斷，也無法去遠端控制LWT&SLT關機

admin reported at 2023-03-19

Solution:

4G Route現在是放在TAOS-D，因離基地台最近訊號最好，TAOS-D是有UPS，但撐不了太久（5-10分鐘！？）。

LWT, SLT, TAOS-C&D一停電網路就全斷應該是因為SLT機櫃Switch HUB沒電所致，需要找個UPS過去給機櫃內Switch HUB用。

admin reported at 2023-03-20

Solution:

將台長將 LOT ACE SmartDome接延長線拉到觀測是隔壁的UPS上。
原本的 UPS 已經拿到 SLT 網路機櫃上。

weij reported at 2023-05-02

C.9 LWT FocusMax 無法連線

LWT 使用備份硬碟開機，ATCLibServer.exe會跳出一串錯誤，然後FocusMax無法連線

Tags: lwt focus

Problem:

使用克隆的硬碟開機，但ATCLibServer.exe會掉出一串錯誤，然後 FocusMax無法連線

Solution:

將原硬碟與 clone的硬碟都裝上電腦，去原硬碟找

"(原硬碟代號):\Users\User\AppData\Local\ATCLibServer\ATCLibServer.exe_Url_fyo5pzs3ve0cz242s21usncb1zapx4az\1.0.3.0\use
這個檔案複製並取代
"C:\Users\User\AppData\Local\ATCLibServer\ATCLibServer.exe_Url_fyo5pzs3ve0cz242s21usncb1zapx4az\1.0.3.0\user
這個檔案然後再開啟 ATCLibServer 就OK

admin reported at 2022-04-08

Problem:

在測試備份硬碟時又出現一次此情況

Solution:

依照上面方法實施後解決。

因為檔案可能很常用到，所以後來放在 "\\192.168.8.2\lulinstaff\autoftp\ATCLibServer" 這個資料夾中

admin reported at 2023-04-23

Problem:

依照 2023-04-23 回報的方法有可能無效。

Solution:

後來發現這個應該是電腦沒有偵測到對焦器導致的，試著重插對焦器的USB應該就能解決。

weij reported at 2023-05-15

C.10 AUTOSLEW 的 RA 重開機後依舊無法驅動

AUTOSLEW的RA重開機後依舊無法驅動

Tags: autoslew

Problem:

更新成W10後，重開機一樣Ra需重新load CME進去才能驅動

Solution:

更新成W10後，重開機一樣Ra需重新load CME進去才能驅動

admin reported at 2023-04-28

Solution:

將藍盒子 Accelnet (標籤 : RA2) 換成標籤 : RA
目前斷電重開不用再做CME2 Reload

weij reported at 2023-05-22

C.11 流星 W1B 無訊號，顯示藍色畫面

流星W1B無訊號，顯示藍色畫面

Tags: 流星

Problem:

W1B在流星的新電腦上又出現藍色無訊息畫面(程式有當掉)

Solution:

把擷取卡換到ALLSKY電腦可以正常運作，暫時又換到ALLSKY電腦上

admin reported at 2023-04-27

Solution:

把圖中的設定改到1去，就有影像了

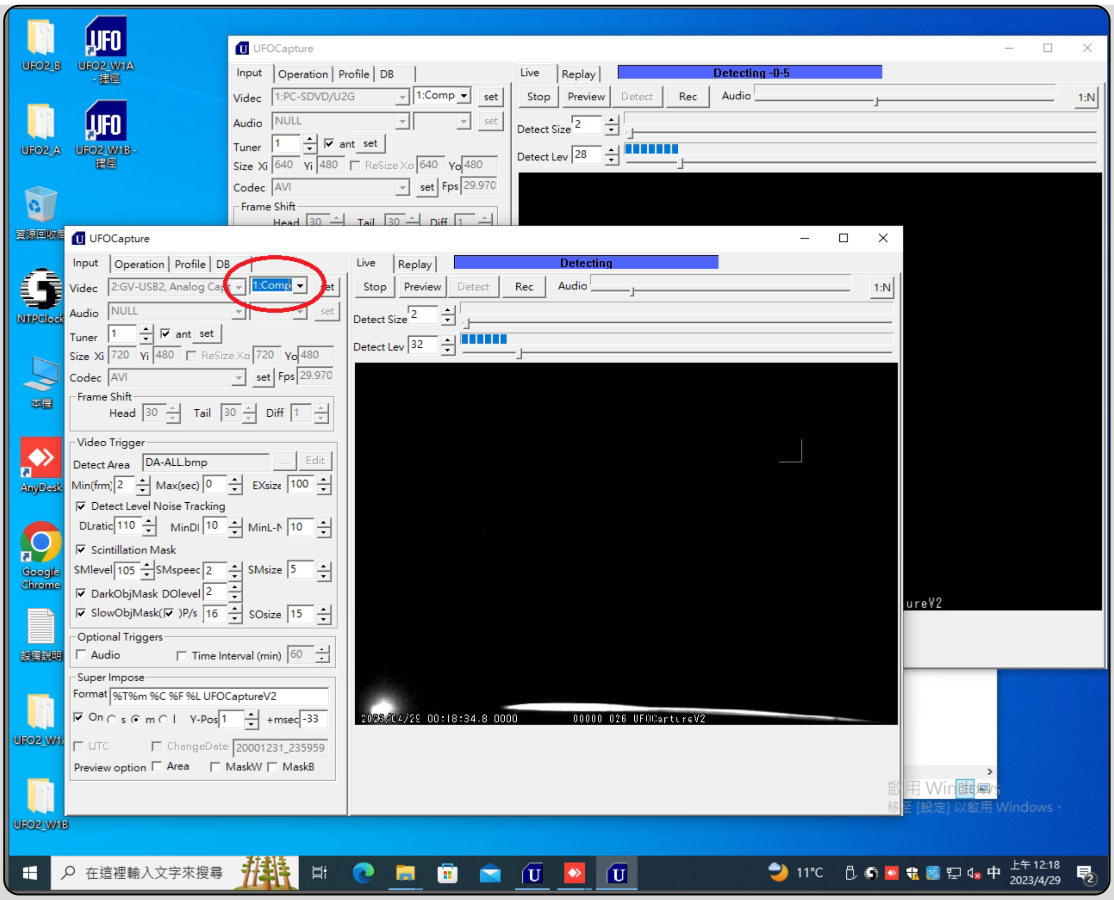

admin reported at 2023-04-28

C.12 SLT 圓頂叫不動無錯誤訊息

SLT圓頂叫不動無錯誤訊息

Tags: slt

Problem:

HOMEFind叫不動，手動按旋轉按鈕也不動

Solution:

電箱內變頻器error，電源重開解決

admin reported at 2023-04-28

C.13 LWT 圓頂無法連線

LWT圓頂無法連線

Tags: lwt dome

Problem:

無法連線或連了立刻斷(老問題)

斷電斷comport都沒用，ASCOM有時可以連，但無法轉動

可能接觸不良?

Solution:

現場手動控制左右轉一下就解決

admin reported at 2023-04-29

C.14 SLT 影像內有時會沒有 WCS

SLT 影像內有時會沒有WCS

Tags: slt wcs

Problem:

婷琬&安理反應，所拍的影像內有時會沒有WCS

婷琬的狀況會發生在同一個目標內，有的濾鏡會沒有寫入，但又不是因為星點太少辨識不出

admin reported at 2023-04-30

Problem:

學姊上山有與她討論：

1. target 不在 FOV 的問題大量發生在 2019~2020，當時確實有 pointing 的問題，不過現在基本上已經解決。
2. 若當天僅有一兩個目標缺少 wcs 可能是ACP plate-solve 無法解出，但這種問題不大。
   不過在 202212 有發生大約一個禮拜全部資料都沒有WCS，也許是我在調整ACP參數時不小心動到 Always Plate-Solve 參數選項導致的。

還請各位多多幫忙，時不時檢查參數是否有勾。

weij reported at 2023-06-21

C.15 LOT 圓頂 ACE smartdome 無法打開天窗，也無法連動

LOT 圓頂 ACE smartdome 無法打開天窗，也無法連動

Tags: lot dome

Problem:

5/10天窗無法由軟體打開，用按鈕可以

也無法連動，上去用按的圓頂會動

軟體重開無效，無任何錯誤訊息

樓上控制盒也沒有錯誤訊息

Solution:

圓頂內控制盒重開解決

durian reported at 2023-05-10

C.16 TheSky 無法 sync

TheSky 無法 sync

Tags: thesky sync

Problem:

在使用TheSky Sync coordinate to target 時，
試了很多次都沒反應，重開也無效。

Solution:

將 TheSky 的 Telescope 連線改成 ASCOM Autoslew Telescope 就可以了

admin reported at 2023-06-06

C.17 LWT 天窗無法開啟

LWT天窗無法開啟

Tags: lwt dome

Problem:

6/23下午巡視望遠鏡，無法開啟天窗

Solution:

用電腦連線，但一時也無法開啟，試了好幾次僅會回到Home的位置而無開啟，後來試著先close，再open才行

durian reported at 2023-06-23

C.18 LWT 電腦 USB 無法讀取

LWT電腦USB無法讀取

Tags: lwt pc

Problem:

7/10老大發現所有COM port都不見，是過許多都不行

Solution:

更換電腦

durian reported at 2023-07-11

C.19 SOPHIA2048B 溫度顯示異常

SOPHIA2048B溫度顯示異常

Tags: lot

Problem:

SOPHIA2048B測試溫度顯示異常，有時一百張僅五六張有溫度資訊

Solution:

28-30有再重新測試，並檢視各軟體驅動狀況，發現PIASCOM灌回舊版0.4可以正常顯示

durian reported at 2023-09-01

C.20 Flat 拍不完

Flat 拍不完

Tags: slt autoflat

Problem:

SLT的SKYFLAT老是拍不完，大約都只能拍4個濾鏡，已經找到兇手，27日傍晚拍攝時有注意到了但來不及截圖下來.

譬如當天亮拍攝時，每個濾鏡會先試拍，如所附圖檔，SUBFRAME中會看到有白色跟黑色部分，ACP會去看數值，然後決定要不要用這個濾鏡拍和拍幾秒 !!!

結果ACP是以白色區域看數值，以此為例，白色部分數值已經滿了，黑色才20K 左右，因此就跳過不拍此濾鏡，而之後的濾鏡也是碰到此情況，AUTOFLAT就此停了 !!!! 導致只能拍3或4個濾鏡而已.

推測可能是相機參數設定問題 !!! 導致試拍時有黑跟白的區域 !!!! 以前ANDOR936沒有這個情況 !!!

PS：因為濾鏡拍不完，我有將LOT跟SLT的AUTOFLAT拍攝秒數調整___ 後來才發現SLT有以上情況

cslin reported at 2023-09-06

Problem:

不確定舊的 Andor 驅動程式是否會有這個問題。

現在的 Andor 相機會有過曝時數值回到300的問題。
當ACP所拍的測試影像已經過曝，數值卻是300。ACP就會以為不夠亮而增長曝光時間。

然後就會一直等15秒，再拍張最長秒數的影像，以此循環。
最後就是後面的濾鏡都沒拍到。

Solution:

將ACP AutoFlatConfig 內參數修改成：

TargetBackgroundADU 27000 ; Target flatfield mean in ADU
TargetADUTolerance 20000 ; Tolerance on the above
MinExposure 5 ; Minimum exposure (as short as possible)
MaxExposure 5 ; Maximum exposure (until you see too many stars)

...

StarDriftSeconds 1 ; Scope stops for this long between flats

此設定讓ACP儲存 ADU 為 7000 ~ 47000 的 Flat，曝光只會是 5s。
曝光範圍若更大，ACP 會設定秒數試圖拍到 ADU 接近 TargetBackgroundADU ，也就是 27000。
這樣有點浪費時間，背景 ADU 不同可以用歸一化處理。

StarDriftSeconds 設定為 1 讓同filter每張flat之間只等 1 秒，因為 reading、downloading 的時間已經足夠。

需要看看是否還有問題

weij reported at 2023-09-06

Problem:

2023-09-06 回報的方法無法解決這個問題

目前看來是 backgroundADU test 使用 subframe 太小，很容易偵測到 65000 然後以為背景太亮

Solution:

新增了一個參數

TestImageSize 1024 ; Size of test image in pixels

讓 ACP 在測量 backgroundADU 時使用 full frame，也許就不會有這個問題

要在觀察看看是否拍不完

weij reported at 2023-09-14

Solution:

最後還是將 ACP "平均 ADU" 可接受的範圍調整到 5000~51000 才能全拍完

weij reported at 2023-09-20

C.21 LOT 更新 win11 後遇到一些問題 (尚未解決)

LOT 更新 win11 後遇到一些問題

Tags: lot dome thesky6

Problem:

LOT 更新 win11 後目前遇到兩個問題

1. ACESmartDome 在某個角度 (145?) 時會自動關閉天窗
2. thesky6 使用 "move to" 功能時，既使選擇 J2000，一樣會 slew 到 current 去。

weij reported at 2023-09-14

Problem:

3、MaxIm DL 5 Load先前W10的設定檔Load進來濾鏡設定全沒，但MaxIm DL 6 沒問題

4、FocusMax無法透過MaxIm DL 6 找到CCD，只能回去用MaxIm DL 5

durian reported at 2023-09-28

Problem:

thesky6 使用 "move to" 功能時，既使選擇 J2000，一樣會 slew 到 current 去。

Solution:

此問題是 TheSky6 版本太就造成，造成此問題的版本為 6.0.0.32

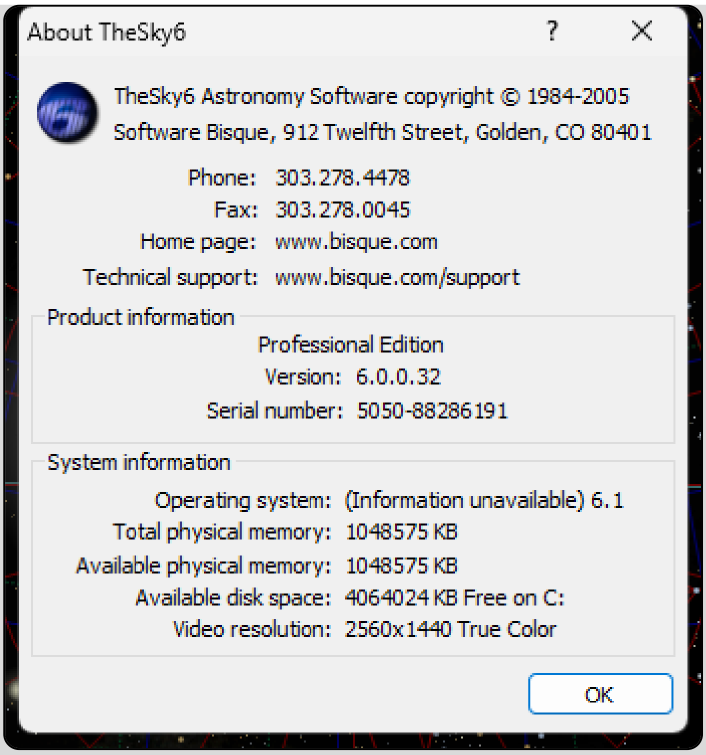

到 AstroSoft\TheSky6pro 中找到並執行 TheSkyV6.0.0.65Update.exe 之後即可

更新後版本會升至 6.0.0.65，此時再使用 Move To 功能 J2000 就有效了。

weij reported at 2023-12-27

Solution:

3、MaxIm DL 5 Load先前W10的設定檔Load進來濾鏡設定全沒，但MaxIm DL 6沒問題

重設即可

weij reported at 2023-12-27

Solution:

4、FocusMax無法透過MaxIm DL 6 找到CCD，只能回去用MaxIm DL 5

我試的時候是可以的，也許只是單純沒設定好

weij reported at 2023-12-27

C.22 LOT 使用光譜儀時會有 RA 方向跳動 (尚未解決)

LOT 使用光譜儀時會有 RA 方向跳動

Tags: mount autoslew lot uvex lisa

Problem:

去年(2022) 11 月時，立晴在鹿林會議上提到使用LISA時，在guiding camera上看到星點在RA方向來回跳動。
當時永欣說可能是因為LOT目前的配重比較適合 imager，而不適合LISA這種較輕的儀器。

20230914 使用 UVEX 觀測時也有發現這個問題，而且非常頻繁。

Solution:

若有發現星點來回跳動，可以試試看先將高精度追蹤關掉，然後馬上再按一次追蹤

今日發生了幾次都用這個方法解決。

weij reported at 2023-09-15

Problem:

20230919 觀測時 (Imager) 發現 tracking 非常不準，沒有 tracking rate 拍出來星點也是橢圓。

打開 autoslew 的 time setting 發現 NTP scatter graph 有斷層，導致回歸線斜率非常高
也許是這個原因才導致赤道儀 RA 方向有問題。

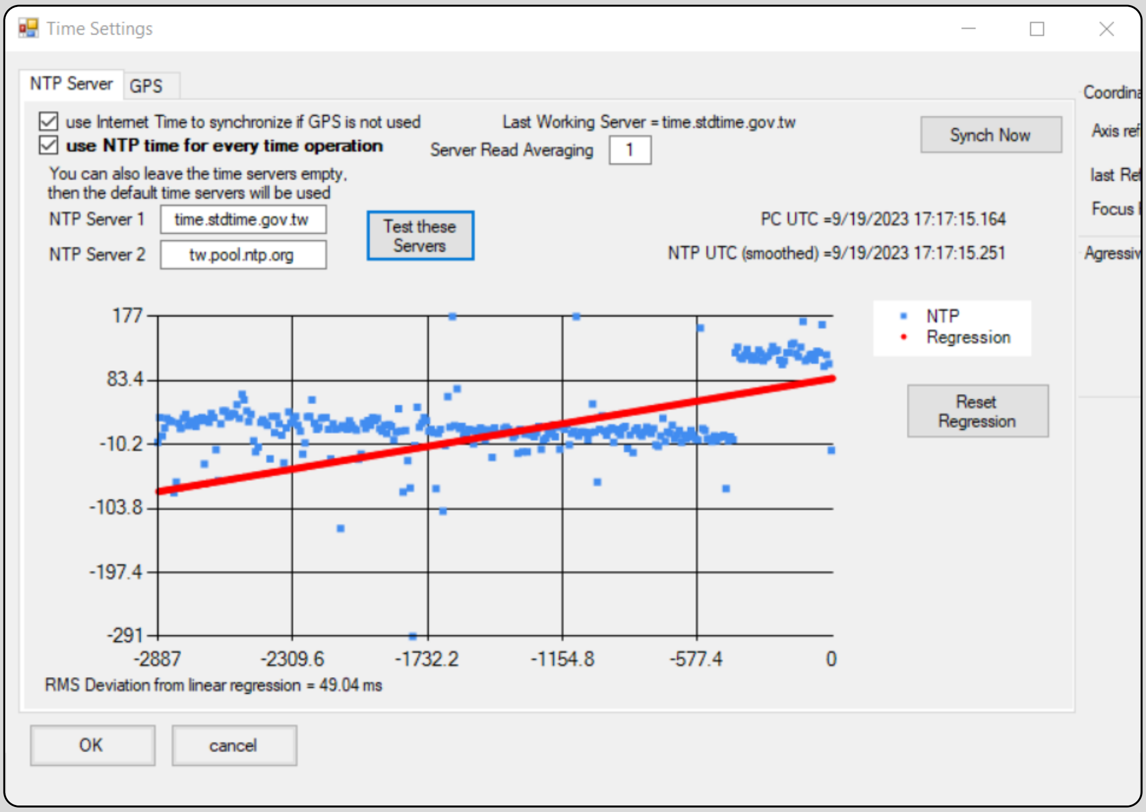

Solution:

本來按了旁邊的 "Reset Regression" 按鈕，讓他重新做回歸分析
但後來 NTP scatter 還是出現斷層

目前是用 SiTech 來幫電腦校時，而 Autoslew 的 NTP 與 GPS 都關掉。
需要再觀察看看是否有問題。

weij reported at 2023-09-20

Problem:

20230922

宇棋把AutoSlew跟CCD PC的SiTech也關掉，但依舊跳動

durian reported at 2023-09-23

Problem:

9/30 利用 LISA 的 guiding cam 做 pointing model 時發生了幾次，好像有多次出現在 HA ~ 2 附近，但也不太能確定是否都出現在 HA ~ 2 時。

另外在 Imager 時沒有發生，與台長討論是否可能是望遠鏡平衡問題，台長說可以拿掉前端配重試試看。

weij reported at 2023-10-04

Problem:

宇棋的光譜觀測時又出現，檢查 HA 大約是 2 hr。

後來在天氣變不好時，趕緊與翔耀一同將望遠鏡前端配重片拿了兩塊 3kg (西北、東南) 下來。前端-不動點：不動點-相機~3:1，所以拿了共 6 kg 下來，相機端力矩約減少 18 kg。

然後簡單測試了一下，繞著 alt 45 度 slew 了一圈，沒有看到有晃動發生。後來等天氣穩定後宇棋觀測也說沒有再遇到此狀況。

因為測試量較少，所以可能未來還是需要再測試看看。

weij reported at 2023-10-12

Problem:

到目前為止還是不知道問題出在哪，所以還是將矛頭指向平衡問題。

如20231012回報所述，將配重片卸下兩塊 3kg，今後幾天測試看看是否還會出現晃動問題。

weij reported at 2023-11-29

Problem:

開關鏡蓋時若赤道儀正在追蹤，就會出現晃動問題。
拿三用電表量 mirror cover 的 24V 電源供應器電壓，大概有 0.01 的變化
但這樣好像也無法確定平常觀測時出現的晃動問題就是電壓波動造成的。

weij reported at 2024-01-08

C.23 Moving object 的追蹤參數太小以至於 ACP 報錯 (尚未解決)

Moving object 的追蹤參數太小以至於 ACP 報錯

Tags: acp

Problem:

Moving object 的追蹤參數太小以至於 ACP 出現以下錯誤

```
16:04:22   Start slew to e6520...
16:04:24   (wait for slew to complete)
16:04:35   (slew complete)
16:04:35   Target is now centered.
16:04:36   MP elements for e6520 --> RA=04:12:26 Dec=28  18' 31" (J2000)
16:04:36   (doing orbital tracking. RA 0.0010 "/sec, Dec 0.0035 "/sec)
16:04:36 **Script Error (Tracking has been stopped)**
16:04:36 Source:   ASCOM.AlpacaClientLocalServer
16:04:36 Message:  GetMethodParameter - Cannot convert value
'6.44558161990406E-05' for parameter 'RightAscensionRate' to double
16:04:37 Location: line 1828 column 29.
ACP console log closed 28-Sep-2023 16:04:38 UTC
```

Solution:

編輯 "C:\Program File (x86)\ACP Obs Control\AquireSupport.wsc" 這個檔案

將這行 (~ 4449 行)

```
Util.ScriptTelescope.RightAscensionRate = RightAscensionRate *
SIDRATE ' ASCOM needs sec/sidereal-sec
```

改成以下即可

```
Util.ScriptTelescope.RightAscensionRate =
Util.FormatVar(RightAscensionRate * SIDRATE, "0.0000") ' ASCOM
needs sec/sidereal-sec
```

weij reported at 2023-09-29

Problem:

後來發現觀測需要 orbital tracking 時，如果 tracking rate 太小還是會遇到。

可能是當追蹤參數<0.0001時， ACP 將資料傳給 Alpaca 的 data 會轉換成 exponent notation string。
而 Alpaca 無法解讀 exponent notation string。

Solution:

目前還沒找到解決方法。
已經到 DC-3 論壇與 ASCOMTalk 詢問是否能更改ACP設置來解決。

目前若遇到此問題需要將 TRACKON 取消。
然後用Autoslew直接輸入 mpc 提供的參數。

weij reported at 2024-03-17

C.24 LWT 圓頂常卡住

LWT 圓頂常卡住

Tags: lwt dome

Problem:

LWT 在觀測時常常突然停住，沒有跟到望遠鏡位置，最常停在 Az270 位置。

Solution:

發生時最簡單的方法是利用網路電源將控制盒重啟，但重啟後Az讀數重置，需要再Find Home。

但到Home後常常又卡住，只能試到正常才能罷休。

weij reported at 2023-11-23

Problem:

26 日將問題轉述台長，並詢問是否要去換舊的DDW圓頂控制器。

到現場時發現 Dome 因為門沒辦法卡緊(會凸出一塊)而造成 Dome 在 Az=90, 270 (Home與Home的對角)時，常會卡住。

Solution:

在圓頂與牆面之間的縫隙噴潤滑油，並旋轉幾圈有改善，但還是卡卡的。

weij reported at 2023-11-26

Problem:

造成門凸出的元兇為門栓彎曲

Solution:

將門栓拆下折平

裝上後門較不凸出了

試轉圓頂後發現情況改善，不會卡住。

但需要再觀測時再注意是否還有出現圓頂停止且需要重啟電源的問題，判定是否為控制箱損壞。

weij reported at 2023-11-27

Problem:

12/7 觀測當天又遇到幾次，且控制盒斷電重開後亦無法轉動。

Solution:

當天先到現場將圓頂稍微轉向，然後就正常了

隔天又至現場將門閂再次整形，8~10日沒有再發生。

weij reported at 2023-12-10

Problem:

12/17的狀況是電腦跟圓頂斷線，然後就連不上，即使電源重開也無法

Solution:

現場將圓頂稍微轉向，然後就正常了

18號把感應磁鐵放正用膠黏住，現場試沒問題，需要再觀察

durian reported at 2023-12-22

C.25 LOT 指向錯亂之處理方式

LOT指向錯亂之處理方式

Tags: autoslew lot sync

Problem:

Autoslew 目前 FindHome 功能異常，若誤按 Home 會導致 pointing 錯亂。

Solution:

1. 得知望遠鏡目前指向座標：兩種方法擇一即可

方法一、plate-solve

拍一張照上傳至 https://nova.astrometry.net/upload，若解星成功記下影像中心的 RA, Dec

方法二、找亮星

手動移動望遠鏡找亮星移至影像中，確認亮星之 RA, Dec

2. 校正望遠鏡位置

步驟一、Autoslew 找到 Select Object，輸入RA,Dec 後 select as target

步驟二、synch Telescope on current object position!

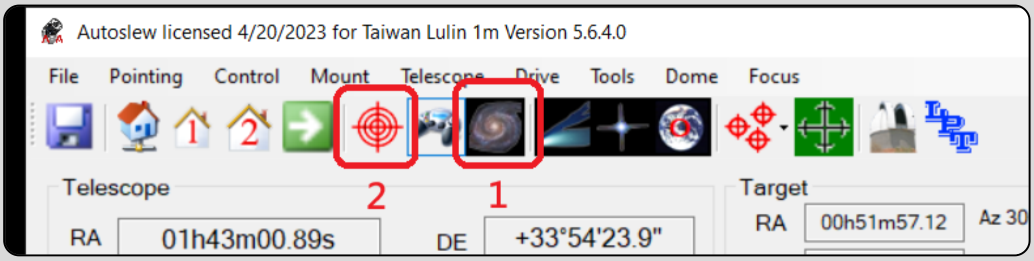

weij reported at 2023-11-29

C.26 RoLIFE Na 濾鏡拆裝

RoLIFE Na濾鏡拆裝

Tags: rolife

Problem:

Na 濾鏡與 QHY174 相機拆裝方法

Solution:

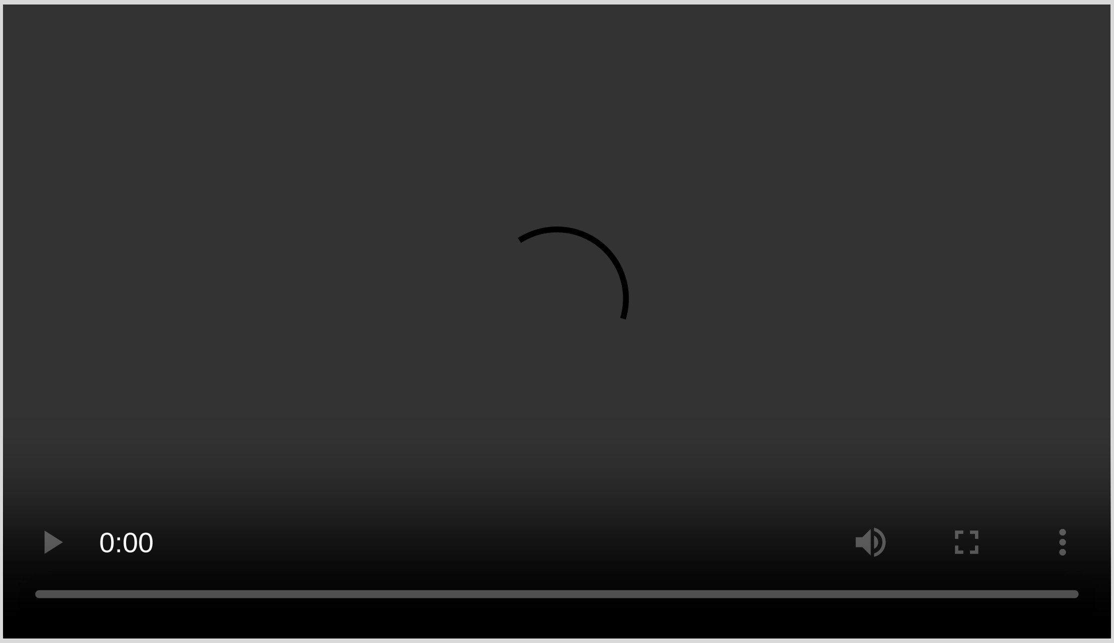

C.27 Problem Report 使用方式

Problem Report 使用方式

Tags:

Problem:

- 如何新增 Report
- 文章輸入欄位說明
- 如何編輯修改

weij reported at 2023-12-10

Problem:

如何新增 Report

Solution:

一、登入後，到 Problem Report 頁面，點選「新增」

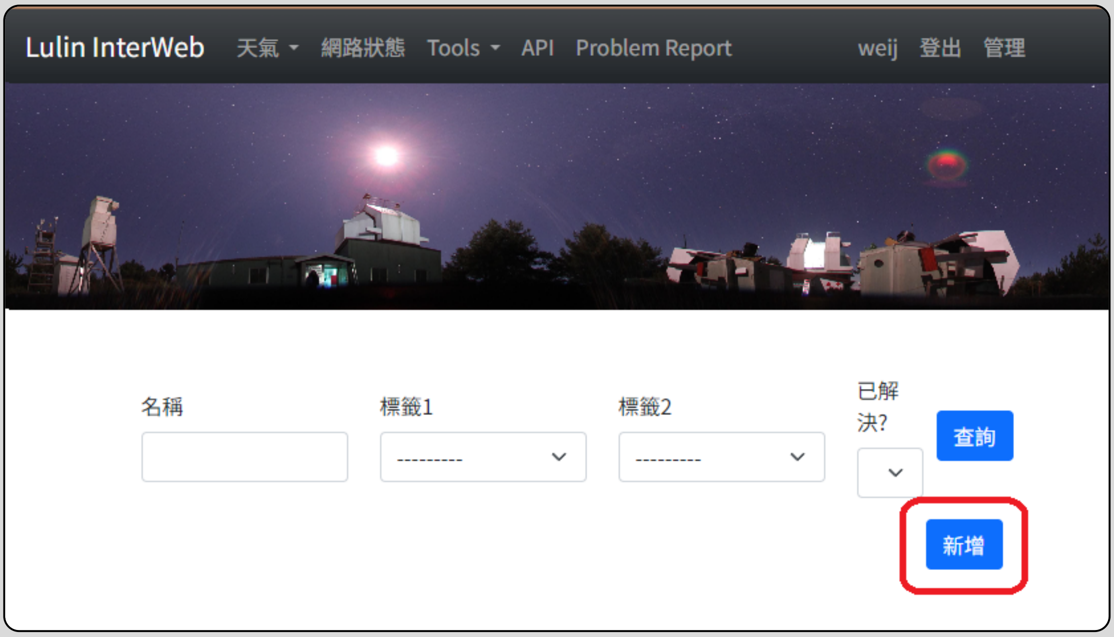

二、打上標題、標籤，然後按新增

不同的標籤用逗號 "," 分開，以便之後查詢

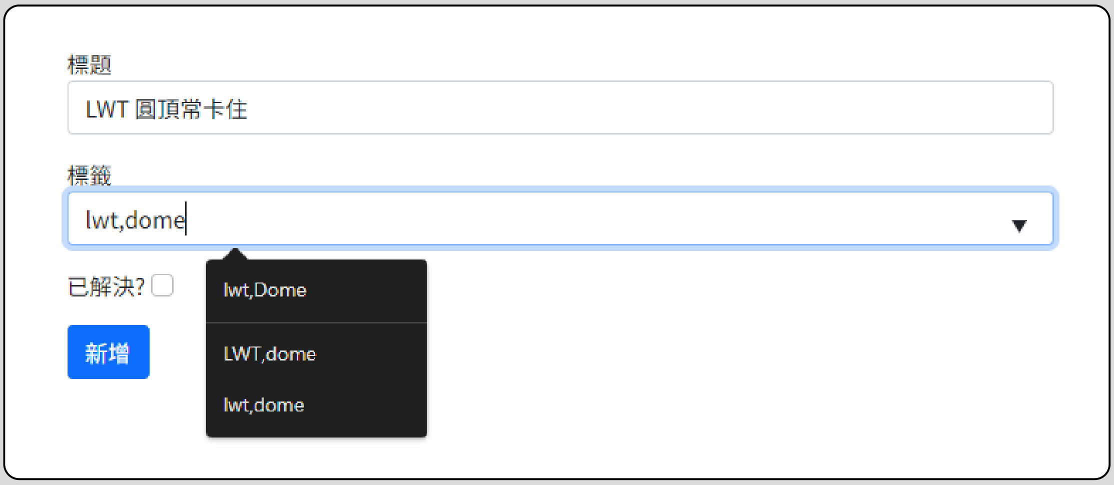

三、新增後會看到新頁面，有"Add Report" 按鈕，按下後就會出現欄位可以輸入「問題描述」與「解決方法」

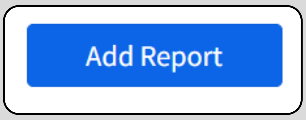

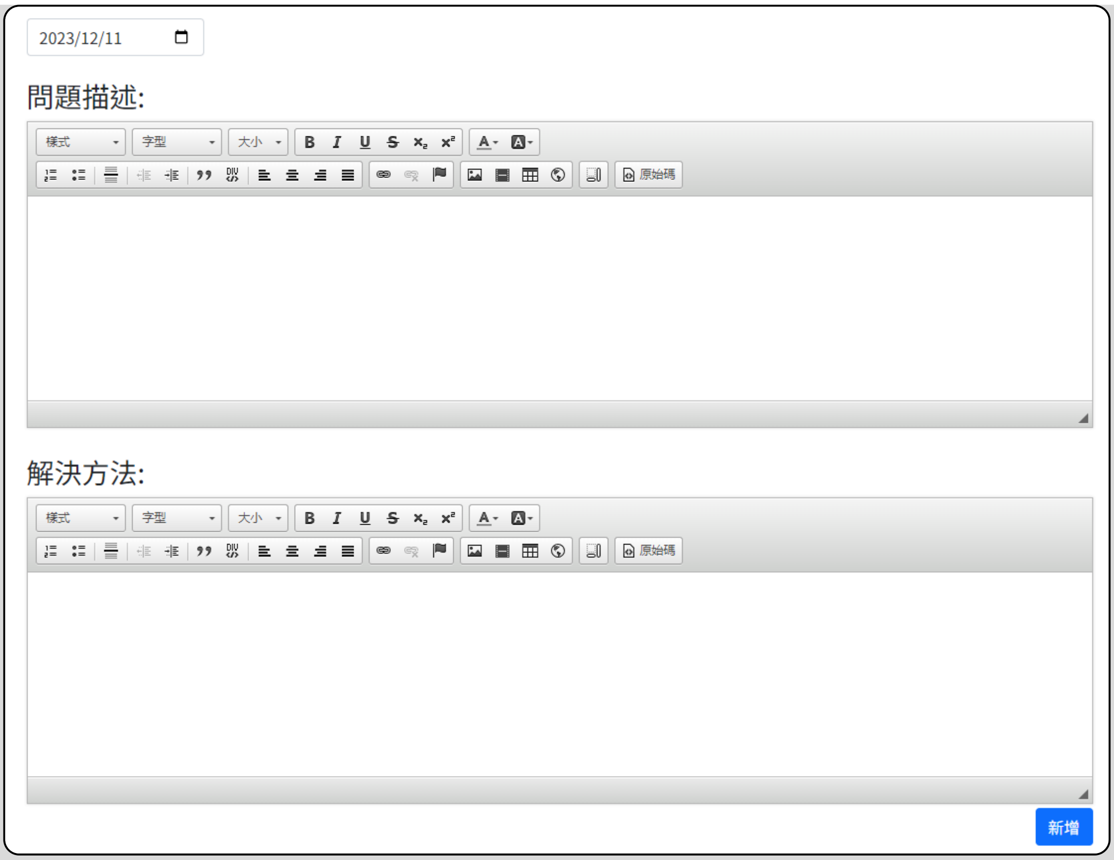

weij reported at 2023-12-11

Problem:

文章輸入欄位說明

Solution:

文字樣式：

文字顏色與文字背景：

段落：

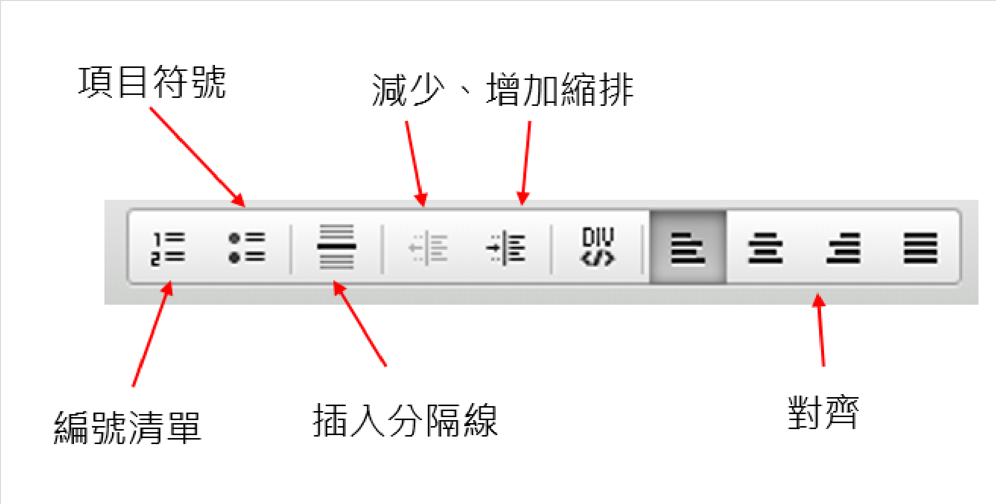
項目符號
減少、增加縮排
編號清單
插入分隔線
對齊

連結：


連結
連結資訊
目標
上傳
進階
輸入連結顯示的文字
顯示文字
連結類型
網址
通訊協定
URL
http://
瀏覽伺服器
輸入連結網址
按確定
確定
取消

插入圖片：

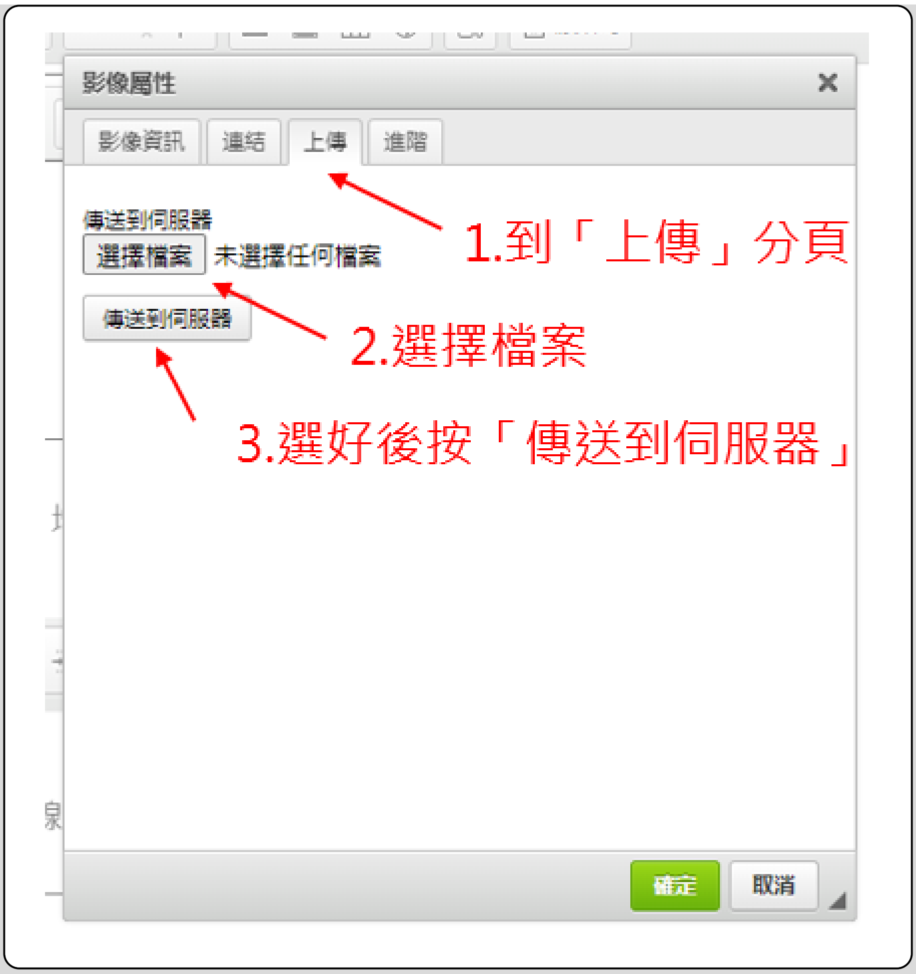
影像屬性
影像資訊
連結
上傳
進階
傳送到伺服器
選擇檔案
未選擇任何檔案
傳送到伺服器
1.到「上傳」分頁
2.選擇檔案
3.選好後按「傳送到伺服器」
確定
取消

或是可以直接把圖片「拖曳」到此視窗，會自己上傳。

若是使用windows截圖功能，可以直接 ctrl+V 貼上

插入影片： 

先使用「插入圖片 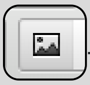 」的1~4步驟，出現網址後將網址複製。

點選插入影片，並貼上網址。

weij reported at 2023-12-11

Problem:

- 如何編輯修改

Solution:

修改標題、標籤、是否解決請點選標題底下的 "Edit" 。

修改回報內容請點區塊右下角的 "Edit"

weij reported at 2023-12-11

C.28 ALLSKY 結露

ALLSKY結露

Tags: allsky

Problem:

12/17傍晚開始發現全天魚眼裡結露，加熱已開但無法消散

Solution:

站長21號打開清理露水後更換O Ring

durian reported at 2023-12-21

C.29 SLT 圓頂天窗無法開啟

SLT 圓頂天窗無法開啟

Tags: slt dome

Problem:

23/12/22 準備拍 duskflat 時 SLT 圓頂天窗無法使用程式開啟，但按天窗控制盒是可以控制的。

重開程式無效、重開 Dome控制盒(牆上的) 無效、拔掉USB線重差也無效

Solution:

可能是 「Dome 控制盒」 與 「Slit 控制盒」的連線有問題

將「Slit 控制盒(圓頂上)」斷電重開再重新連線後就OK。
Slit 控制盒因有 UPS ，所以需要拔線斷電才能重開

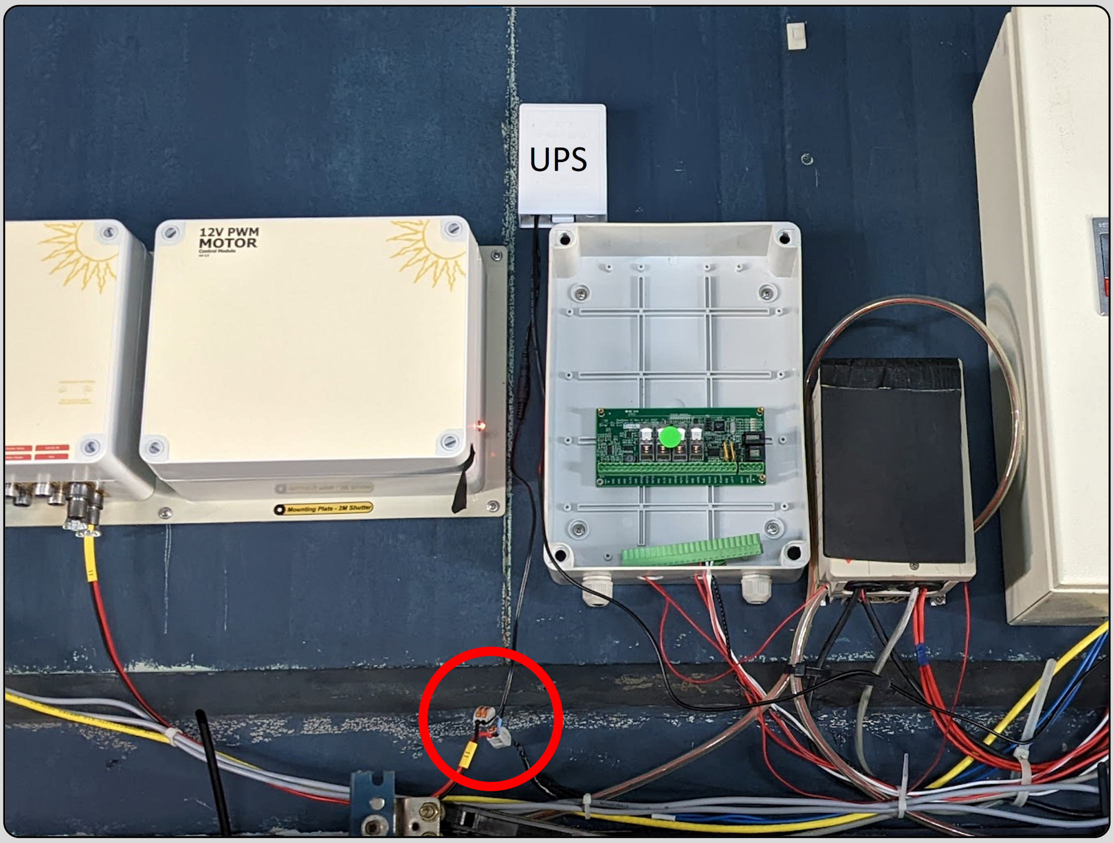

weij reported at 2023-12-22

C.30 LWT 無法 slew

LWT 無法 slew

Tags: lwt thesky

Problem:

25日觀測時，目標已達可觀測仰角，但ACP一直沒有動作。
查看了 LOG 發現ACP 指令 slew 至目標，但望遠鏡沒動就繼續執行下一個目標。

到 TheSkyX 發現 Status 顯示 mount cannot slew 訊息
選目標後 slew 會出現下圖錯誤。

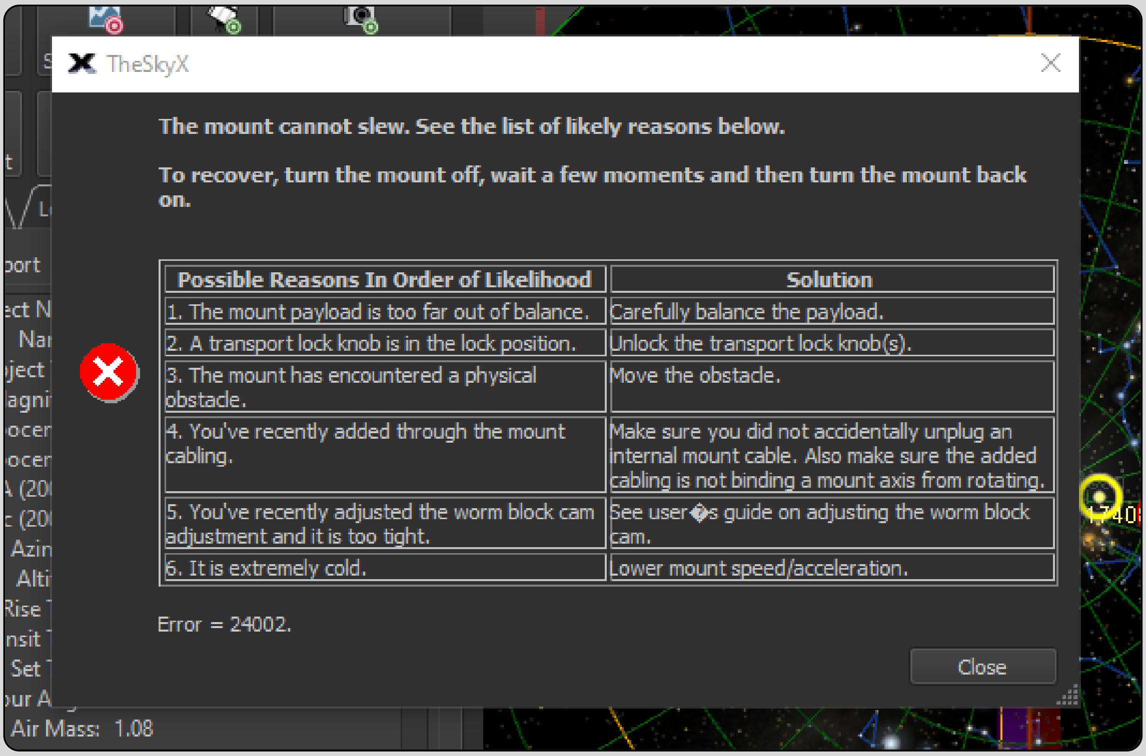

Solution:

重開 TheSkyX 無法復原。

網路電源將赤道儀斷電重開，在試一樣不行

最後到現場將將電源關掉，檢查平衡，但平衡沒問題所以沒調整。
再開電源後，重新連線後就沒問題了。

weij reported at 2023-12-25

C.31 SLT MaxIm DL 出現 Filter wheel error (-4)(尚未解決)

SLT MaxIm DL 出現 Filter wheel error (-4)

Tags: slt maximdl filterwheel

Problem:

ACP 有時會出現 Filter wheel error (-4) 錯誤，且 ACP 不會停止觀測，僅會一直跳下一個目標，需要特別注意。

Solution:

解決方式是要將MaximDL CCD 斷線重連才行。

weij reported at 2023-07-02

Problem:

從發現問題至今還是一直有出現這個問題。

本來想可能是 MaximDL 連線到 FilterWheel 的方式需要改，但 FLI 的 FilterWheel 只能使用 FLI driver 進行連線，也無法選擇 com port。

Solution:

目前將 FilterWheel 換了一條 USB cable 試試看。

需要繼續觀察是否還會出現這個問題。

若未來沒有發生表示可能之前用的線有問題，可以將線拆掉。(白線上面寫CCD 那條)

weij reported at 2024-03-03

Problem:

換了 USB Cable 之後各位助理還是有觀察到這個現象發生。
所以應該不是 USB Cable 的問題。

也許要將 FLI 驅動重裝，甚至是換掉 FilterWheel。

weij reported at 2024-03-18